Clouds and the Earth's Radiant Energy System (CERES)

Data Management System

Single Satellite Footprint TOA/Surface Fluxes and Clouds (SSF) Collection Document

Release2
Version 1

Primary Authors

Erika B. Geier, Richard N. Green,
David P. Kratz, Patrick Minnis
NASA Langley Research Center
Climate Science Branch
Science Directorate
Hampton, VA 23681-2199

Walt F. Miller, Sandra K. Nolan, Carla B. Franklin
Science Applications International Corporation (SAIC)
One Enterprise Parkway, Suite 300
Hampton, VA 23666

NASA Langley Research Center
Climate Science Branch
Science Directorate
21 Langley Boulevard
Hampton, VA 23681-2199

March 2003

Document Revision Record

The Document Revision Record contains information pertaining to approved document changes. The table lists the date the Software Configuration Change Request (SCCR) was approved, the Release and Version Number, the SCCR number, a short description of the revision, and the revised sections. The document authors are listed on the cover. The Head of the CERES Data Management Team approves or disapproves the requested changes based on recommendations of the Configuration Control Board.

Document Revision Record

SCCR Approval Date	Release/ Version Number	DCCR Number	Description of Revision	Section(s) Affected
06/19/99	R1V1	xxxx	• Initial draft document release for team review.	All
01/09/01	R1V2	xxxx	• Draft Document release for TRMM Edition1 SSF.	All
xxxx	R1V3	xxxx	• Modifications of these versions were not recorded in the Document Revision Record.	
xxxx	R1V4	xxxx	• Modifications of these versions were not recorded in the Document Revision Record.	
xxxx	R1V5	xxxx	• Modifications of these versions were not recorded in the Document Revision Record.	
10/19/01	R1V6	302	• Switched from Edition1 to Edition2A parameter/ product definitions and updated parameter definitions based on Science inputs. • Updated format to comply with standards.	1.5, 4.2, 4.3, 5.2, 8, & 15 All
03/28/02	R2V1	332	• Description of MODIS aerosol parameters added to Terra and Aqua SSF. • Updated format to comply with standards.	4.3, 5.2, App B., Index All
3/28/02	R2V1	332	• The CERES Top Level Data Flow Diagram was modified (5/29/03).	1.4

Preface

The Clouds and the Earth's Radiant Energy System (CERES) Data Management System supports the data processing needs of the CERES Science Team research to increase understanding of the Earth's climate and radiant environment. The CERES Data Management Team works with the CERES Science Team to develop the software necessary to implement the science algorithms. This software, being developed to operate at the Langley Distributed Active Archive Center (DAAC), produces an extensive set of science data products.

The Data Management System consists of 12 subsystems; each subsystem represents one or more stand-alone executable programs. Each subsystem executes when all of its required input data sets are available and produces one or more archival science products.

This Collection Guide is intended to give an overview of the science product along with definitions of each of the parameters included within the product. The document has been reviewed by the CERES Working Group teams responsible for producing the product and by the Working Group Teams who use the product.

Acknowledgment is given to Waldena Banks and Carol J. Tolson of Science Applications International Corporation (SAIC) for their support in the preparation of this document.

TABLE OF CONTENTS

TABLE OF CONTENTS

TABLE OF CONTENTS

LIST OF TABLES

LIST OF FIGURES

Single Scanner Footprint TOA/Surface Fluxes and Clouds (SSF) Collection Document

Summary

The Clouds and the Earth's Radiant Energy System (CERES) is a key component of the Earth Observing System (EOS) program. The CERES instrument provides radiometric measurements of the Earth's atmosphere from three broadband channels: a shortwave channel (0.3 - 5 µm), a total channel (0.3 - 200 µm), and an infrared window channel (8 - 12 µm). The CERES instruments are improved models of the Earth Radiation Budget Experiment (ERBE) scanner instruments, which operated from 1984 through 1990 on the National Aeronautics and Space Administration's (NASA) Earth Radiation Budget Satellite (ERBS) and on the National Oceanic and Atmospheric Administration's (NOAA) operational weather satellites NOAA-9 and NOAA-10. The strategy of flying instruments on Sun-synchronous, polar orbiting satellites, such as NOAA-9 and NOAA-10, simultaneously with instruments on satellites that have precessing orbits in lower inclinations, such as ERBS, was successfully developed in ERBE to reduce time sampling errors. CERES continues that strategy by flying instruments on the polar orbiting EOS platforms simultaneously with an instrument on the Tropical Rainfall Measuring Mission (TRMM) spacecraft, which has an orbital inclination of 35 degrees. The TRMM satellite carries one CERES instrument while the EOS satellites carry two CERES instruments, one operating in a fixed azimuth plane scanning mode (FAPS) for continuous Earth sampling and the other operating in a rotating azimuth plane scan mode (RAPS) for improved angular sampling.

To preserve historical continuity, some parts of the CERES data reduction use algorithms identical with the algorithms used in ERBE. At the same time, many of the algorithms on CERES are new. To reduce the uncertainty in data interpretation and to improve the consistency between the cloud parameters and the radiation fields, CERES includes cloud imager data and other atmospheric parameters. The CERES investigation is designed to monitor the top-of-atmosphere radiation budget as defined by ERBE, to define the physical properties of clouds, to define the surface radiation budget, and to determine the divergence of energy throughout the atmosphere. The CERES Data Management System produces products which support research to increase understanding of the Earth's climate and radiant environment.

The Single Scanner Footprint TOA/Surface Fluxes and Clouds (SSF) product is produced from the cloud identification, convolution, inversion, and surface processing for CERES. It combines CERES measurements with scene information from a higher-resolution imager such as VIRS on TRMM and MODIS on Terra and Aqua. Each SSF contains footprints, or CERES Fields-of-View (FOV), from a single hour and a single CERES scanner (3 channels) mounted on one satellite. The major categories of data on the SSF are CERES FOV geometry and viewing angles, radiance and flux (TOA and Surface), area statistics and imager viewing angles, clear area statistics, cloudy area statistics for two cloud height layers, cloud overlap conditions (4 conditions), imager radiance statistics (5 imager channels) over the CERES FOV, and, for some Terra and Aqua data sets, MODIS aerosols. The SSF provides data needed to produce a production-quality set of CERES Angular Distribution Models (CADMs). At a later time, the SSF product will be reprocessed using the production CADMs.

1.0 Collection Overview

1.1 Collection Identification

The SSF filename is

CER_SSF_Sampling-Strategy_Production-Strategy_XXXXXX.YYYYMMDDHH where

CER	Investigation designation for CERES,
SSF	Product-ID for the primary science data product (external distribution),
Sampling-Strategy	Platform, instrument, and imager (e.g., TRMM-PFM-VIRS),
Production-Strategy	Edition or campaign (e.g., At-launch, ValidationR1, Edition1),
XXXXXX	Configuration Code (CC#) for file and software version management,
YYYY	4-digit integer defining data acquisition year,
MM	2-digit integer defining data acquisition month,
DD	2-digit integer defining the data acquisition day,
HH	2-digit hour integer defining the data acquisition hour.

1.2 Collection Introduction

The SSF is an hourly level 1-b data product. It contains full and partial Earth-view measurements, or footprints, which are located in colatitude and longitude at a surface reference level. The SSF is a unique product for studying the role of cloud/aerosol/radiation in climate. Each footprint includes reflected shortwave (SW), emitted longwave (LW) and window (WN) radiances from CERES with temporally and spatially coincident imager-based radiances and cloud properties.

1.3 Objective/Purpose

The overall science objectives of the CERES investigation are
1. For climate change research, provide a continuation of the ERBE radiative fluxes at the top of the atmosphere (TOA) that are analyzed using the same techniques used with existing ERBE data.
2. Double the accuracy of estimates of radiative fluxes at the TOA and the Earth's surface from existing ERBE data.
3. Provide the first long-term global estimates of the radiative fluxes within the Earth's atmosphere.
4. Provide cloud property estimates which are consistent with the radiative fluxes from surface to TOA.

SSF science objectives include
1. Derive surface and cloud properties sufficient to classify a unique set of targets with distinctly different anisotropic radiation fields.
2. Provide a set of cloud properties optimally designed for studies of the role of clouds in the Earth's radiation budget.

3. Develop and apply a next generation of angular distribution models which greatly improve flux estimation.
4. Produce SW and LW flux components of the surface radiation budget based on the empirical relationships between TOA fluxes and measured surface radiation budget components.

The CERES Data Management System (DMS) is a software management and processing system which processes CERES instrument measurements and associated engineering data to produce archival science and other data products. The DMS is executed at the Langley Atmospheric Sciences Data Center (ASDC), which is also responsible for distributing the data products. A high-level view of the CERES DMS is illustrated by the CERES Top Level Data Flow Diagram shown in Figure 1-1.

Circles in the diagram represent algorithm processes called subsystems. Subsystems are a logical collection of algorithms which together convert input data products into output data products. Boxes represent archival, internal, or ancillary data products. Boxes with arrows entering a circle are input data sources for the subsystem, while boxes with arrows exiting the circles are output data products.

1.4 Summary of Parameters

An SSF granule (See Term-19) is saved in Hierarchical Data Format (HDF) structures (See Section 5.0) which contain hourly header parameters, granule metadata and FOV parameters. The hourly header parameters are saved in a Vertex Data (Vdata) structure (See Table 5-14). Each header parameter is saved in a Vdata field which has the same name as the parameter. The granule metadata parameters are saved on an hourly basis (See Table 5-15).

Each FOV parameter is saved in a Scientific Data Set (SDS) which has the same name as the parameter. For easier access and understanding, the FOV parameters are divided into the following categories which map to Vgroups (See Term-43) of the same name:
- Time and Position
- Viewing Angles
- Surface Map
- Scene Type
- Filtered Radiances
- Unfiltered Radiances
- TOA and Surface Fluxes
- Full Footprint Area
- Clear Footprint Area
- Cloudy Footprint Area
- Footprint Imager Radiance Statistics

For greater organizational detail, refer to Section 5.0.
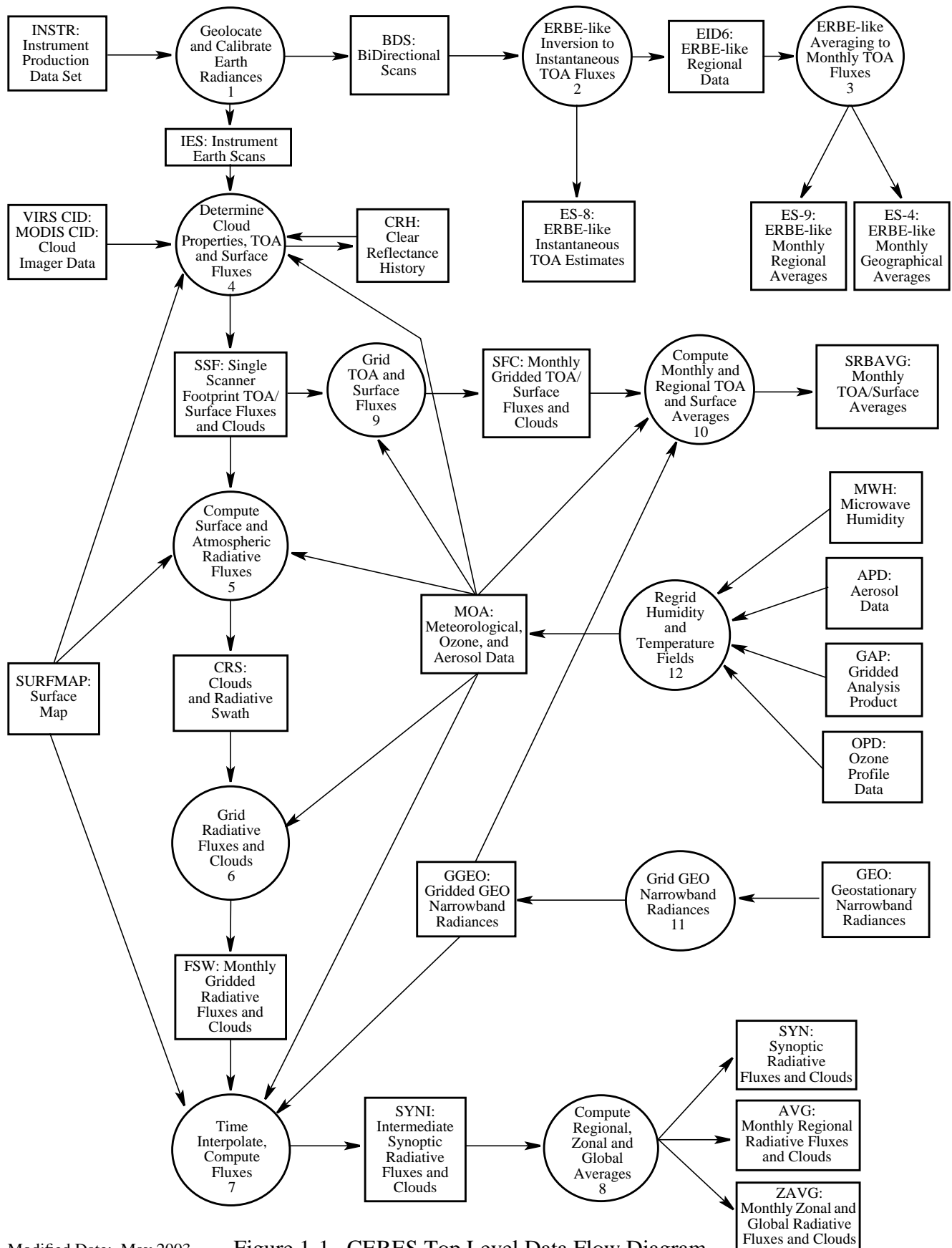
Figure 1-1. CERES Top Level Data Flow Diagram

1.5 Discussion

The SSF is created by a collection of subsystems that make up CERES "Determine Cloud Properties, TOA and Surface Fluxes". These subsystems are jointly referred to as SS 4.0 and span four major functions: Cloud Retrieval, Convolution, Inversion, and Surface Estimation. An overview of SS 4.0 can be found in the CERES ATBD Subsystem 4.0 (See Reference 15). The subsystems that comprise SS 4.0 correspond to the CERES ATBD Subsystems 4.1 through 4.6 (See References 16-24). Philosophy and algorithm discussions can be found in the individual subsystem ATBDs.

The SSF is an hourly data product. Each of the FOVs saved in an SSF granule (See Term-19) is self contained and stands alone; no additional information can be obtained from the FOVs which precede or follow it. This is because FOVs which are sequential in the granule are not ordered in time or space (See SSF-18). All the FOVs within the hour are ordered along the ground track and may not be in chronological order. This ground track, or along-track, ordering is necessary because the CERES scanner may be operating in a Rotating Azimuth Plane Scan (RAPS) mode (See Reference 14). Since the imager scans are always crosstrack, an along-track ordering of CERES FOVs requires less imager data to be resident in memory during processing. The along-track ordering also simplifies locating radiance pairs for the validation process and simplifies locating FOVs in particular regions of the Earth. All SSF geolocation assumes geodetic coordinates.

The SSF is a subset of CERES measurements. Users seeking CERES radiances for all FOVs should look to the BDS or ES-8 data products. An SSF granule (See Term-19) contains only those FOVs which are geolocated within the imager swath of data and can be convolved with some imager pixels (See SSF-54). These FOVs may have one or more CERES radiances flagged bad. Alternately stated, most SSF FOVs contain basic cloud information; some SSF FOVs may have all CERES radiance values flagged bad; and FOVs which are geolocated outside the imager swath are never included on an SSF.

The FOVs saved on the SSF may be full Earth view or partial Earth view. A partial Earth view contains some amount of space, but is still geolocated on the Earth surface (See Term-9).

Each FOV may contain cloud information for up to two cloud layers. The cloud layers are floating and will vary from one FOV to another. Regardless of its actual height, the first layer is defined to always be the lowest layer. When only one layer can be determined for a particular FOV, that layer is defined as the lowest layer. A second, or upper layer, is defined only when an FOV contains two statistically unique layers. Within an SSF granule (See Term-19), it is possible for the lowest layer of one FOV to be much higher than the highest layer of another FOV.

1.6 Related Collections

See the CERES Data Products Catalog (See Reference 13) for a complete product listing.

The CERES ES-8 product is, in some ways, similar to the SSF. The ES-8 contains similar instantaneous parameters, but these parameters are produced using traditional ERBE algorithms.

Users of both the ES-8 and SSF should be aware of the following differences before attempting to combine, compare, or supplement one of these products with the other:

- SSF geolocation is geodetic and at the surface; ES-8 is geocentric and at TOA
- Radiance to flux inversion algorithms and ADMs differ
- Maps to determine underlying surface types differ
- Methods of determining cloud amount within FOV differ

An expanded list of differences can be found in Section C.1 of APPENDIX C.

2.0 Investigators

Dr. Bruce A. Wielicki, CERES Principal Investigator
E-mail: b.a.wielicki@larc.nasa.gov
Telephone: (757) 864-5683

Mail Stop 420
Atmospheric Sciences Research
Building 1250
21 Langley Boulevard
NASA Langley Research Center
Hampton, Virginia 23681-2199
FAX: (757) 864-7996

2.1 Title of Investigation

Clouds and the Earth's Radiant Energy System (CERES)
Determine Cloud Properties, TOA and Surface Fluxes

2.2 Contact Information

Patrick Minnis, Imager & Cloud Retrieval
Telephone: (757) 864-5671
E-mail: p.minnis@larc.nasa.gov

Norman G. Loeb, TOA Radiances & Fluxes
Telephone: (757) 864-5688
E-mail: n.g.loeb@larc.nasa.gov

David P. Kratz, Surface Fluxes
Telephone: (757) 864-5669
E-mail: d.p.kratz@larc.nasa.gov

Mail Stop 420
Atmospheric Sciences Research
Building 1250
21 Langley Boulevard
NASA Langley Research Center
Hampton, Virginia 23681-2199
FAX: (757) 864-7996

3.0 Origination

The CERES data originate from CERES instruments on-board either the TRMM or the EOS Earth-orbiting spacecrafts. Table 3-1 lists the CERES instruments and their host satellites.

Table 3-1. CERES Instruments

Satellite	CERES Instruments	
TRMM	ProtoFlight Model (PFM)	
Terra	Flight Model 1 (FM1)	Flight Model 2 (FM2)
Aqua	Flight Model 3 (FM3)	Flight Model 4 (FM4)

The CERES instrument contains three scanning thermistor bolometer radiometers that measure the radiation in the near-visible through far-infrared spectral region. The shortwave detector measures Earth-reflected and Earth-emitted solar radiation and the window detector measures Earth-emitted longwave radiation in the water vapor window. The total detector measures total Earth-reflected and Earth-emitted radiation. The detectors are coaligned and mounted on a spindle that rotates about the instrument elevation axis. The resolution of the CERES radiometers is usually referenced to the optical FOV.

The CERES instrument has an operational scanning cycle of 6.6 seconds and various scan elevation profiles. Radiometric measurements are sampled from the detectors every 0.01 seconds in all scanning profiles. The instrument makes Earth-viewing science measurements while the detectors rotate in the vertical (elevation scan) plane, and while the instrument horizontal (azimuth scan) plane is either fixed or rotating. The instrument has built-in calibration sources for performing in-flight calibrations, and can also be calibrated by measuring solar radiances reflected by a solar diffuser plate into the instrument field of view. See the In-flight Measurement Analysis document, DRL 64, provided by the CERES instrument builder TRW (See Reference 56), and the CERES Algorithm Theoretical Basis Document (ATBD) for Subsystem 1.0 (See Reference 14).

The CERES data and the imager data used by CERES must come from instruments which are located on the same satellite. Table 3-2 lists the imagers and their host satellites.

Table 3-2. Imager Instruments

Satellite	Imager Instruments
TRMM	VIRS
Terra	MODIS
Aqua	MODIS

The Visible and Infrared Scanner (VIRS) instrument is a five-channel imaging spectroradiometer that measures the radiation in distinct visible through infrared spectral bands. The two visible shortwave channels, 0.63 and 1.61 μm, measure Earth-reflected and Earth-emitted solar radiation and the three infrared channels, 3.78, 10.8, and 12.0 μm, measure Earth-emitted longwave radiation. VIRS is similar to the Advanced Very High Resolution Radiometer (AVHRR), but there are a few notable exceptions. VIRS has a 2.11-km resolution at nadir, the VIRS 0.63 μm

channel replaces the AVHRR 0.83 μm channel, and VIRS has an onboard solar diffuser for visible channel calibration.

VIRS has an operational scanning cycle of 183.7 ms and is limited to cross-track scans, with a 45 degrees scan range. Radiometric measurements are sampled from the detectors every 292 μs. There are five detectors in the focal plan, each with its own spectral filter. A double-sided paddle wheel scan mirror is used to view the ground. The instrument has an on-board blackbody for thermal channel calibration. The visible channels are calibrated by measuring the solar radiances reflected by a solar diffuser plate into the instrument field of view (See Reference 2).

All five VIRS channels are used for CERES cloud retrieval. Imager radiance statistics for all five VIRS channels are also included in the SSF.

The Moderate-Resolution Imaging Spectroradiometer (MODIS) instrument contains thirty-six spectral bands at three different spatial resolutions. Scene energy reflects into the afocal telescope from the double-sided Scan Mirror over a scan range of 55 degrees. A series of three beamsplitter separate the scene energy into four spectral regions which are directed to separate focal plane assemblies. There are 10 detector elements along track for each of the 29 1-km bands, 20 detector elements for each of the five 500 meter bands, and 40 detector elements for each of the two 250 meter bands. This allows for a 10 km along-track swath to be observed during a single scan.

The MODIS instrument has an operational scanning cycle of 1.477 s. Radiometric measurements are sampled every 333 μs with the first 10 μs used to read the previous measurement and reset the detector. MODIS has a full complement of calibration sources that generate various stimuli to provide radiometric, spectral and spatial calibration of the MODIS instrument including the standard blackbody and solar diffuser. (See Reference 3)

CERES receives a subset containing only 19 of the 36 MODIS channels for cloud retrieval. The central wavelengths of the channels included in the CERES subset are recorded in the SSF header (See SSF-H7). For each channel, CERES receives data at one kilometer resolution. In addition to the aggregated one kilometer resolution data, the 0.645 spectral band is also provided at the observed 250 meter resolution. For a given CERES FOV, Convolution selects 5 of these imager channels and generates imager radiance statistics for them.

4.0 Data Description

4.1 Spatial Characteristics

4.1.1 Spatial Coverage

The SSF collection is a global data set whose spatial coverage depends on the satellite orbit as shown in Table 4-1. Each SSF granule (See Term-19) contains one hour of data, which is approximately two-thirds of an orbit, from a single CERES instrument. The width of the SSF swath is limited to the width of the imager swath with which the CERES data was convolved. FOVs on the SSF are ordered by along-track angle.

Table 4-1. SSF Spatial Coverage at Surface

Spacecraft: Instrument(s)	Minimum Latitude (deg)	Maximum Latitude (deg)	Minimum Longitude (deg)	Maximum Longitude (deg)	Spacecraft Altitude (km)
TRMM: PFM	-40	40	-180	180	350
Terra: FM1 & FM2	-90	90	-180	180	705
Aqua: FM3 & FM4	-90	90	-180	180	705

4.1.2 Spatial Resolution

An SSF granule (See Term-19) contains instantaneous scanner measurements. The spatial scale of each measurement FOV is dependent on the satellite height and the viewing zenith (See Term-11). FOVs may be full or partial Earth views.

4.2 Temporal Characteristics

4.2.1 Temporal Coverage

The SSF temporal coverage begins after the spacecraft is launched, the scan covers are opened, and the early in-orbit calibration check-out is completed (See Table 4-2). Each SSF product contains 1 hour of data.

Table 4-2. SSF Temporal Coverage

Spacecraft	Instrument	Launch Date	Start Date	End Date
TRMM	PFM	11/27/1997	12/27/1997	8/31/1998*
Terra	FM1 & FM2	12/18/1999	02/25/2000	TBD
Aqua	FM3 & FM4	05/04/2002	06/19/2002	TBD

* The CERES instrument on TRMM has operated only occasionally since 9/1/98 due to a power converter anomaly. SSF have been created from 9/01/1998 until a yet to be determined date that use a simulated TRMM CERES scan pattern with actual VIRS imager data.

4.2.2 Temporal Resolution

Each SSF FOV represents one scanner measurement. Measurements are taken every 0.01 seconds. However, only those FOVs which can be convolved with some imager pixels (See SSF-54) are included on an SSF granule (See Term-19). Two FOVs which are adjacent in time will have about an 80% overlap.

4.3 Parameter Definitions

The SSF data product is documented with several different elements. Acronyms and Units are explained in Section 16.0. Some acronyms are linked to glossary "Terms" in Section 15.0 which expand the description to a paragraph length. The formal definitions of the SSF parameters are in Section 4.3 and begin with a short statement of the parameter followed by the units, range, and a link to a table which gives data type and dimension information. Following the short definition is a more complete definition, which may include additional information of less interest to some. When necessary, "Notes" in Section 8.0 are given to expand on subjects that will help in the use and understanding of the SSF product. Notes are generally characterized by more details and longer length.

SSF parameters are computed using a geodetic coordinate system (See Term-18) and are located at the Earth's surface (See Term-9), unless otherwise noted. All header parameters are stored in the SSF_Header Vdata. FOV parameters are stored in SDSs which have the same name as the parameter. For details about SSF granule (See Term-19) organization, refer to Section 5.0.

For convenience when searching for a particular parameter, the parameters are divided into subgroups. These subgroups are arbitrary. Each FOV parameter subgroup corresponds to a Vgroup (See Term-43) of the same name.

4.3.1 SSF Header Definitions

Header parameters are recorded once per granule (See Term-19)

SSF-H1   SSF ID

SSF ID is a number which identifies this file as an SSF data product made up of a given set of parameters. (N/A) [112 .. 200] (See Table 5-14)

It is written in the header by the software which created the file and will increase whenever the SSF header parameters or the SSF FOV parameters change. An SSF ID change corresponds only to file format changes. It does not correspond to algorithm changes. For example, if additional parameters are added to the SSF product, then the SSF ID will increase to denote this change. This document describes the SSF structure(s) denoted by the numbers 117 and beyond. Earlier versions with SSF ID values below 117 were not released to the public and are not included in the baseline documentation. ♠

SSF-H2   Character name of CERES instrument

This parameter is an acronym that describes the particular instrument for the data that follows. For example, some valid CERES instrument names are PFM (Proto-flight Model on TRMM), FM1 (Flight Model 1 on Terra), FM2 (Flight Model 2 on Terra), FM3 (Flight Model 3 on Aqua), and FM4 (Flight Model 4).   An instrument name of SIM is used when CERES FOV geometry is simulated for a particular satellite. (See Table 5-14) ♠

SSF-H3   Day and Time at hour start

An SSF granule (See Term-19) contains data for a one hour time period based on Universal time or time at the Greenwich meridian. The start of the current hour is given in Coordinated Universal Time (UTC) and is denoted as an ASCII string of the form YYYY-MM-DDThh:mm:ss.dddddZ. For example, "2002-02-23T14:00:00.000000Z" denotes February 23, 2002 at 14 hours, 0 minutes, and 0.0 seconds past Greenwich midnight. (See Table 5-14)

All FOVs in an SSF data file are observed during a one hour period starting with the SSF-H3 time. However, the earliest data in the file may be later than the start time due to data dropout. Also, the earliest data may not appear at the start of the file since the FOVs are organized spatially along the groundtrack and not chronologically. (See SSF-18) ♠

SSF-H4   Character name of satellite

This parameter describes the satellite on which the CERES instrument (See SSF-H2) is mounted. For example, some valid values are TRMM, AM-1 (Terra platform), and PM-1 (Aqua platform). (See Table 5-14) ♠

SSF-H5   Character name of high resolution imager instrument

This parameter describes the on-board, narrowband imager whose data are used in the analysis of the CERES data. For example, some valid imager names are VIRS, MODISam (MODIS imager on Terra platform), and MODISpm (MODIS imager on Aqua platform). (See Table 5-14) ♠

SSF-H6   Number of imager channels

This parameter is the number of imager (See SSF-H5) channels available for the analysis of the CERES data. The central wavelengths of the available channels are recorded as SSF-H7.
 (N/A) [1 .. 20] (See Table 5-14) ♠

SSF-H7   Central wavelengths of imager channels

This parameter lists the central wavelengths of the narrowband imager (See SSF-H5) channels available for the analysis of CERES data. The number of imager channels available is recorded as SSF-H6. (μm) [0.4 .. 15.0] (See Table 5-14) ♠

SSF-H8   Earth-Sun distance at hour start

This parameter is the distance from the Earth to the Sun in astronomical units (AU) at the beginning of the hour (See SSF-H3).   (AU) [0.98 .. 1.02] (See Table 5-14)

The ToolKit (See Term-41) call PGS_CBP_Earth_CB_Vector (See Reference 47) computes the Earth-Centered Inertial (ECI) frame vector to the Sun. The ToolKit call PGS_CSC_ECIto ECR transforms the position vector to the Earth-Centered Rotating (ECR) or Earth equator, Greenwich meridian system (See Term-7). The magnitude of the position vector is then computed and converted from meters to AU. ♠

SSF-H9   Beta Angle

The beta angle, β, is the angle between the Sun vector and the satellite orbital plane for the first FOV in the granule (See Term-19). It is positive when the Sun and the angular momentum vector are on the same side of the orbital plane.   (deg) [-90 .. 90] (See Table 5-14)

When β = 0, the Sun is in the orbital plane. The beta angle varies slowly with time. Therefore, the beta angle determined for the first FOV is an adequate estimate of the beta angle for the entire hour.   ♠

SSF-H10   Colatitude of subsatellite point at surface at hour start

This is the geodetic colatitude of the geodetic subsatellite point (See Term-38) at Earth surface (See Term-9) at hour start (See SSF-H3) in the Earth equator, Greenwich meridian system (See Term-7). (deg) [0 .. 180] (See Table 5-14) ♠

SSF-H11   Longitude of subsatellite point at surface at hour start

This is the longitude of the geodetic subsatellite point (See Term-38) at Earth surface (See Term-9) at hour start (See SSF-H3) in the Earth equator, Greenwich meridian system (See Term-7). (deg) [0 .. 360] (See Table 5-14) ♠

SSF-H12   Colatitude of subsatellite point at surface at hour end

This is the geodetic colatitude of the geodetic subsatellite point (See Term-38) at Earth surface (See Term-9) at hour end in the Earth equator, Greenwich meridian system (See Term-7). (deg) [0 .. 180] (See Table 5-14)

Hour end is hour start (See SSF-H3) plus one hour. Hour end is the same time as hour start on the next hour's SSF file. ♠

SSF-H13   Longitude of subsatellite point at surface at hour end

This is the longitude of the geodetic subsatellite point (See Term-38) at Earth surface (See Term-9) at hour end in the Earth equator, Greenwich meridian system (See Term-7). (deg) [0 .. 360] (See Table 5-14)

Hour end is hour start (See SSF-H3) plus one hour. Hour end is the same time as hour start on the next hour's SSF file. ♠

SSF-H14   Along-track angle of satellite at hour end

This is the angle at the center of the Earth, through which the satellite traveled from hour start to hour end. (deg) [0 .. 330] (See Table 5-14)

A vector is defined from the center of the Earth to the satellite at the start of the hour. Another vector is defined from the center of the Earth to the satellite at the end of the hour. The along-track angle is the angle (See SSF-18), at the center of the Earth, from the satellite vector at hour start to the satellite vector at hour end in the plane of the orbit and along the path of travel. The along-track angle of the satellite at hour start is defined as 0.0. ♠

SSF-H15   Number of Footprints in SSF product

This is the number of FOVs in the SSF granule (See Term-19). Each FOV contains the radiometric measurements, geometry, and cloud parameters for a single FOV. Footprint and FOV are synonymous. (N/A) (0 .. 360000] (See Table 5-14)

The upper limit on number of footprints is defined by the CERES data rate of 100 measurements per second or 360,000 measurements per hour. Since the SSF product contains only FOVs which can be convolved with some imager pixels (See SSF-54), a reasonable upper limit is 245,475 (See Note-1).

Full and partial Earth views are recorded on the SSF. However, the SSF product does not contain all the CERES radiometric data. If the view vector is unknown, the location of the FOV is unknown and the footprint is not recorded. If the Point Spread Function (PSF) is unknown (as in the short scan mode during rapid retrace (See Term-32)), the size of the footprint is unknown and the footprint is not recorded.

The main purpose of the SSF is to characterize the clouds over the CERES footprint, and then to use this information to define the TOA and surface fluxes. The ES-8 (ERBE-like Instantaneous TOA Estimates) product contains all the CERES radiometric data. When the footprint can be convolved with some imager pixels (See SSF-54), it is recorded on the SSF whether the CERES radiances are known or unknown. ♠

SSF-H16   Subsystem 4.1 identification string

The Subsystem 4.1 identification string is an ASCII string which includes all information necessary for Subsystem 4.1 (See Reference 16) processing code to be rerun in exactly the same fashion. The identification string is free form and may include input identification, algorithm identification, software version numbers, or anything which may be of interest and apply to the entire hour of data. The fields within this string are variable to meet different situations. (See Table 5-14)

The current contents of this string are as follows:

"CRH Albedo YYYY-MM-DDTHH:MM:SS" identifies the time the Clear Sky Reflectance albedo file was created, and, therefore, uniquely identifies this input file.

"CRH BTemp YYYY-MM-DDTHH:MM:SS" identifies the time the Clear Sky Reflective brightness temperature file was created, and, therefore, uniquely identifies this input file.

"Imager xx y.y YYYY-MM-DDTHH:MM:SS" identifies the input imager data and output Cloud Retrieval product, also known as cookiedough (See Term-6). For the VIRS imager, "xx" is the product version and "y.y" is the science algorithm version number of the VIRS level 1-b input file. Since the VIRS data is grouped by orbit rather than by hour, an hour of cookiedough may be

based upon a single VIRS input file or two VIRS input files. In the case of two VIRS input files, the VIRS version information corresponds to that of the earlier orbit. YYYY-MM-DDTHH:MM:SS is the time at which the cookiedough output was created, and, indirectly, indicates the cookiedough version information. For MODIS, this portion of the string is undefined. ♠

SSF-H17   Subsystem 4.2 identification string

The Subsystem 4.2 identification string is an ASCII string which includes all information necessary for Subsystem 4.2 (See Reference 17) processing code to be rerun in exactly the same fashion. The identification string is free form and may include input identification, algorithm identification, software version numbers, or anything which may be of interest and apply to the entire hour of data. The fields within this string are variable to meet different situations. (See Table 5-14)

The current contents of this string are as follows:

"ELVxxxxx" identifies the input elevation map. "xxxxx" are the last five digits of the elevation map configuration number.

"H20xxxxx" identifies the input water content map. "xxxxx" are the last five digits of the water content map configuration number.

"SNOWxxxxx" identifies the input daily snow map. "xxxxx" are the last five digits of the daily snow map configuration number.

"ICExxxxx" identifies the input daily ice map. "xxxxx" are the last five digits of the daily ice map configuration number.

"IGBPxxxxx" identifies the input International Geosphere-Biosphere Programme (IGBP) landcover map. "xxxxx" are the last five digits of the IGBP landcover map configuration number.

"TERRxxxxx" identifies the input terrain map. "xxxxx" are the last five digits of the terrain map configuration number.

"IDxxxxx" identifies a database which is no longer used. Will be removed in a future software delivery.

"EM0375xxxxx" identifies the input 3.75 μm emittance map. "xxxxx" are the last five digits of the emittance map configuration number.

"EM1080xxxxx" identifies the input 10.8 μm emittance map. "xxxxx" are the last five digits of the emittance map configuration number.

"EM1190xxxxx" identifies the input 11.9 μm emittance map. "xxxxx" are the last five digits of the emittance map configuration number. ♠

SSF-H18   Subsystem 4.3 identification string

The Subsystem 4.3 identification string is an ASCII string which includes all information necessary for Subsystem 4.3 (See Reference 18) processing code to be rerun in exactly the same fashion. The identification string is free form and may include input identification, algorithm

identification, software version numbers, or anything which may be of interest and apply to the entire hour of data. The fields within this string are variable to meet different situations. (See Table 5-14)

The current contents of this string are as follows:

"Dxxxxx" identifies the input directional model. "xxxxx" are the last five digits of the directional model configuration number.

"EBIxxxxx" identifies the input ERBE bidirectional model. "xxxxx" are the last five digits of the ERBE bidirectional model configuration number. May be replaced with an imager bidirectional model in a future software delivery.

"BIxxxxx" identifies the input bidirectional model. "xxxxx" are the last five digits of the bidirectional model configuration number.

"PHIxxxxx" identifies the input CERES Phi table. "xxxxx" are the last five digits of the CERES Phi table configuration number. This table contains the CERCAA cirrus algorithm thresholds.

"Txxxxx" identifies the input CERES threshold table. "xxxxx" are the last five digits of the CERES threshold table configuration number.

"ODxxxxx yyyyy" identifies the input clean air aerosol data tables. "xxxxx" are the last five digits of the 0.63 µm data table configuration number. "yyyyy" are the last five digits of the 1.6 µm data table configuration number.

"VINTRAYBREF BDNNREF MODELSNEW NNEL3 NNEL4 NNEL5" identify the 6 inputs to the VIST algorithm. The six inputs files, in the order in which they are listed, are VINTraybref, VINTbdnnref, VINTmodelsnew, VINTchannel3, VINTchannel4, and VINTchannel5. At this time there are no configuration numbers associated with these files. ♠

SSF-H19   Subsystem 4.4 identification string

The Subsystem 4.4 identification string is an ASCII string which includes all information necessary for Subsystem 4.4 (See Reference 19) processing code to be rerun in exactly the same fashion. The identification string is free form and may include input identification, algorithm identification, software version numbers, or anything which may be of interest and apply to the entire hour of data. The fields within this string are variable to meet different situations. (See Table 5-14)

The current contents of this string are as follows:

"SCCR# xxxx YYYYMMDD" identifies the CERES System Configuration Change Request (SCCR) which corresponds to the Clouds/Convolution software. "xxxx" is the actual change request number and "YYYYMMDD" is the date the software was delivered.

"Param YYYYMMDD" identifies the input parameter file. "YYYYMMDD" is the date the file was last modified.

CERESxx" names the point spread function used to convolve imager data with the CERES FOV. "xx" is the number of PSF grid boxes, or bins, in the along scan direction.

"PSF YYYYMMDD" identifies the input point spread function used to convolve imager data with the CERES FOV. "YYYYMMDD" is the date the point spread function was last modified.

"SARB xxxxxx" identifies the input reflectance file provided by the SARB working group. "xxxxxx" are the last six digits of the reflectance file configuration number. ♠

SSF-H20   Subsystem 4.5 identification string

The Subsystem 4.5 identification string is an ASCII string which includes all information necessary for Subsystem 4.5 (See Reference 20) processing code to be rerun in exactly the same fashion. The identification string is free form and may include input identification, algorithm identification, software version numbers, or anything which may be of interest and apply to the entire hour of data. The fields within this string are variable to meet different situations. (See Table 5-14)

The current contents of this string are as follows:

"xxx%RAPS" indicates the amount of Rotating Azimuth Plane Scan (RAPS) data. "xxx" is the percentage of the FOVs in the granule (See Term-19) which were acquired while CERES was in RAPS mode.

"SCC_xxx_YYYYMMDD" identifies the Spectral Correction Coefficient (SCC) file used to unfilter the CERES radiance data (See Term-36). "xxx" identifies the CERES instrument. Valid values are TRM, FM1, and FM2, where TRM corresponds to CERES PFM instrument mounted on the TRMM satellite and FM1 and FM2 correspond to the CERES FM1 and FM2 instruments mounted on the Terra satellite. "YYYYMMDD" identifies the date that these coefficients were assembled into a file.

"CADM_cc_YYYYMMDD" identifies the CERES Angular Distribution Model (CADM) coefficients file used to invert the radiance data. "cc" identifies the model coefficients as SW (shortwave), LW (longwave), or WN (window). "YYYYMMDD" identifies the date that these coefficients were assembled into a file.♠

SSF-H21   Subsystem 4.6 identification string

The Subsystem 4.6 identification string is an ASCII string which includes all information necessary for Subsystem 4.6 (See References 21-24) processing code to be rerun in exactly the same fashion. The identification string is free form and may include input identification, algorithm identification, software version numbers, or anything which may be of interest and apply to the entire hour of data. The fields within this string are variable to meet different situations. (See Table 5-14)

The current contents of this string are as follows:

"MOA Production Date = YYYY-MM-DDThh:mm:ss" identifies the MOA input file by its production date and time. This should be identical to SSF-H23. ♠

SSF-H22   IES production date and time

The IES production date and time identifies the IES data granule (See Term-19) used as input when the current SSF was processed. (See Table 5-14)

The IES date and time is stored as a 24 byte ASCII string of the form
"YYYY-MM-DDThh:mm:ss" [Example: 2002-02-23T14:04:57] followed by 5 blanks. ♠

SSF-H23   MOA production date and time

The MOA production date and time identifies the MOA data file used as input to all of Subsystem
4 when the current SSF was processed. (See Table 5-14)

The MOA date and time is stored as a 24 byte ASCII string of the form
"YYYY-MM-DDThh:mm:ss" [Example: 2002-02-23T14:04:57] followed by 5 blanks. ♠

SSF-H24   SSF production date and time

The SSF production date and time identifies when the current SSF was processed.
(See Table 5-14)

The SSF date is stored as a 24 byte ASCII string of the form "YYYY-MM-DDThh:mm:ss"
[Example: 200-02-23T14:04:57] followed by 5 blanks. ♠

4.3.2 Time and Position Definitions

These parameters identify the time and position information associated with each CERES FOV.

SSF-1   Time of Observation

The Julian Date (See Term-22) at which the radiances (SSF-31 to SSF-33) are measured. (day)
[2440000 .. 2480000] (See Table 5-1)

Note that the Julian day changes at Greenwich noon rather than midnight. The calendar date at
hour start is given by SSF-H3. The time of observation is a 64 bit floating point number
(Example: 2450753.859432137 days).   ♠

SSF-2   Radius of satellite from center of Earth at observation

The distance from the center of the Earth to the satellite at the time of observation (See SSF-1).
The position of the satellite is defined on the SSF by its radius (See SSF-2), colatitude
(See SSF-6), and longitude (See SSF-7). (km) [6000 .. 8000] (See Table 5-1)

The ToolKit (See Term-41) call PGS_EPH_Earth_EphemAttit (See Reference 47) computes the
satellite position vector in Earth-Centered Inertial coordinates. A second ToolKit call,
PGS_CSC_ECIto ECR, transforms the position vector to the Earth-Centered Rotating (ECR) or
Earth equator, Greenwich meridian system (See Term-7). Meters are then converted to
kilometers and the magnitude of the position vector is taken. ♠

SSF-3   X component of satellite inertial velocity

The X component of the satellite inertial velocity at the time of observation (See SSF-1) in the
Earth equator, Greenwich meridian system (See Term-7). (km sec^{-1}) [-10 .. 10] (See Table 5-1)

The ToolKit (See Term-41) call PGS_EPH_EphemAttit (See Reference 47) computes the satellite
velocity vector in Earth-Centered Inertial coordinates. A second ToolKit call, PGS_CSC_ECIto

ECR, transforms the velocity vector to the Earth-Centered Rotating (ECR) or Earth equator, Greenwich meridian system. Then meters second^{-1} are converted to kilometers second^{-1}. ♠

SSF-4   Y component of satellite inertial velocity

The Y component of the satellite inertial velocity at the time of observation (See SSF-1) in the Earth equator, Greenwich meridian system (See Term-7).   (km sec^{-1}) [-10 .. 10] (See Table 5-1)

The satellite inertial velocity components are determined from ToolKit calls (See SSF-3). ♠

SSF-5   Z component of satellite inertial velocity

The Z component of the satellite inertial velocity at the time of observation (See SSF-1) in the Earth equator, Greenwich meridian system (See Term-7). (km sec^{-1}) [-10 .. 10] (See Table 5-1)

The satellite inertial velocity components are determined from ToolKit calls (See SSF-3). ♠

SSF-6   Colatitude of subsatellite point at surface at observation
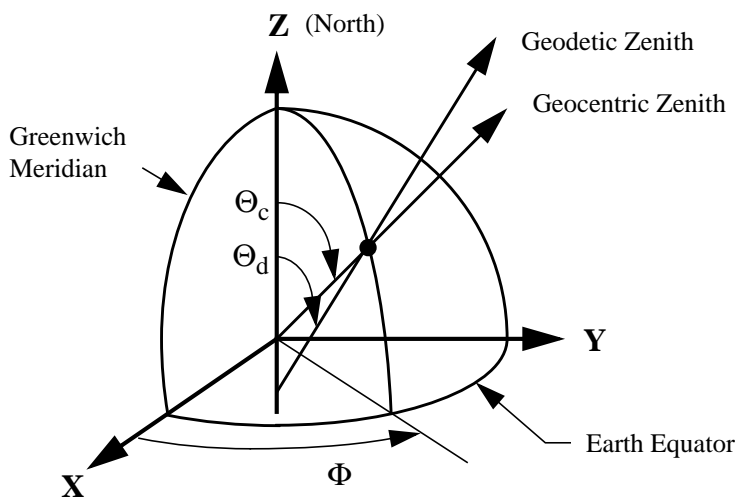
This parameter is the geodetic colatitude angle Θ_d (See Figure 4-1.) of the geodetic subsatellite point (See Term-38). (deg) [0 .. 180] (See Table 5-1)

The geodetic colatitude is the angle between the geodetic zenith (See Term-18) to the satellite and a vector normal to the Earth equator toward the North pole as defined in the Earth equator, Greenwich meridian system (See Term-7). ♠

Figure 4-1. Geocentric and Geodetic Colatitude/Longitude

SSF-7   Longitude of subsatellite point at surface at observation

This parameter is the longitude angle Φ (See Figure 4-1) of the geodetic subsatellite point (See Term-38). (deg) [0 .. 360] (See Table 5-1)

The longitude is the angle in the Earth equator plane from the Greenwich meridian (See Term-7) to the Earth point (See Term-8) meridian, rotating East. The geocentric longitude and geodetic longitude are the same. ♠

SSF-8   Colatitude of subsolar point at surface at observation

This parameter is the geodetic colatitude angle Θ_d (See Figure 4-1) of the geodetic subsolar point (See Term-17) on the Earth surface (See Term-9). (deg) [0 .. 180] (See Table 5-1)

The geodetic colatitude is the angle between the geodetic zenith (See Term-18) to the Sun and a vector normal to the Earth equator toward the North pole as defined in the Earth equator, Greenwich meridian system (See Term-7). ♠

SSF-9   Longitude of subsolar point at surface at observation

This parameter is the longitude angle Φ (See Figure 4-1) of the geodetic subsolar point (See Term-17) on the Earth surface (See Term-9). (deg) [0 .. 360] (See Table 5-1)

The longitude is the angle in the Earth equator plane from the Greenwich meridian (See Term-7) to the geodetic subsolar point meridian, rotating East. The geocentric longitude and geodetic longitude are the same. ♠

SSF-10   Colatitude of CERES FOV at surface

This parameter is the geodetic colatitude angle Θ_d (See Figure 4-1) of the Earth point (See Term-8). (deg) [0 .. 180] (See Table 5-1)

The geodetic colatitude is the angle between the geodetic zenith (See Term-18) at the Earth point and a vector normal to the Earth equator toward the North pole as defined in the Earth equator, Greenwich meridian system (See Term-7). ♠

SSF-11   Longitude of CERES FOV at surface

This parameter is the longitude angle Φ (See Figure 4-1.) of the Earth point (See Term-8). (deg) [0 .. 360]   (See Table 5-1)

The longitude is the angle in the Earth equator plane from the Greenwich meridian (See Term-7) to the Earth point meridian, rotating East. The geocentric longitude and geodetic longitude are the same. ♠

SSF-12   Scan sample number

This parameter defines the order in which the CERES radiances (See SSF-35) were collected by the instrument during the 6.6 second scan cycle (See Figure 15-3). Every scan cycle begins with sample 1. The last radiance in the cycle is sample 660 at 6.59 seconds after sample 1. (N/A) [1 .. 660] (See Table 5-1) ♠

SSF-13   Packet number

This parameter defines the order of the 6.6 seconds scan cycles (See Figure 15-3) within a day. Every CERES radiance has a sample scan number (See SSF-12) to denote its order within the scan cycle and a packet number (See SSF-13) to denote its scan cycle order within the day. (N/A) [0 .. 13100] (See Table 5-1)

FOVs are assigned a relative packet number based on the day in which they fall. If the first hour of a day contains FOVs from a packet which started the previous day, that packet will have two numbers associated with it. Those FOVs which fall before midnight are assigned a packet number for the previous day and included with the previous day data. The remaining FOVs, those which fall after midnight, are assigned a packet number of 0. If there is no packet straddling midnight,

the first packet containing a full scan cycle has a packet number of 1. In this case, data dropout at the beginning of the day does not effect packet number, and the first full scan cycle packet received is numbered on data not time. Once the first full or partial packet of the day has been established, the packet number is incremented on time and not data. ♠

SSF-14 Cone angle of CERES FOV at satellite

The cone angle (See Figure 4-2) is the angle between a vector from the satellite to the center of the Earth and the instrument view vector from the satellite to the Earth point (See Term-8). (deg) [0 .. 90] (See Table 5-1)

The cone angle, along with the clock angle, (See Figure 4-3 and SSF-15) define the direction of the instrument view vector to the Earth point.

The ToolKit (See Term-41) call PGS_CSC_SCtoORB (See Reference 47) transforms the instrument view vector in spacecraft coordinates to (x,y,z) orbital coordinates (See SSF-15) and the cone angle is defined by $z = \cos\alpha$. ♠
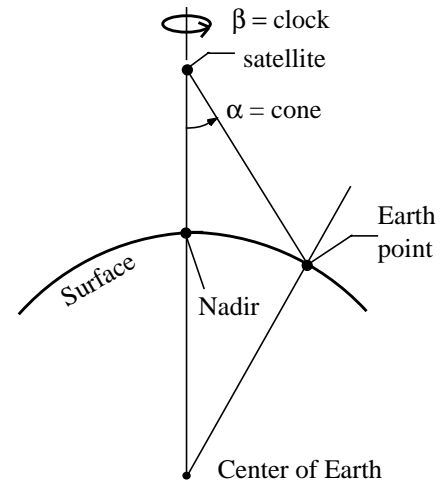
Figure 4-2. Cone and Clock Angles

SSF-15 Clock angle of CERES FOV at satellite wrt inertial velocity
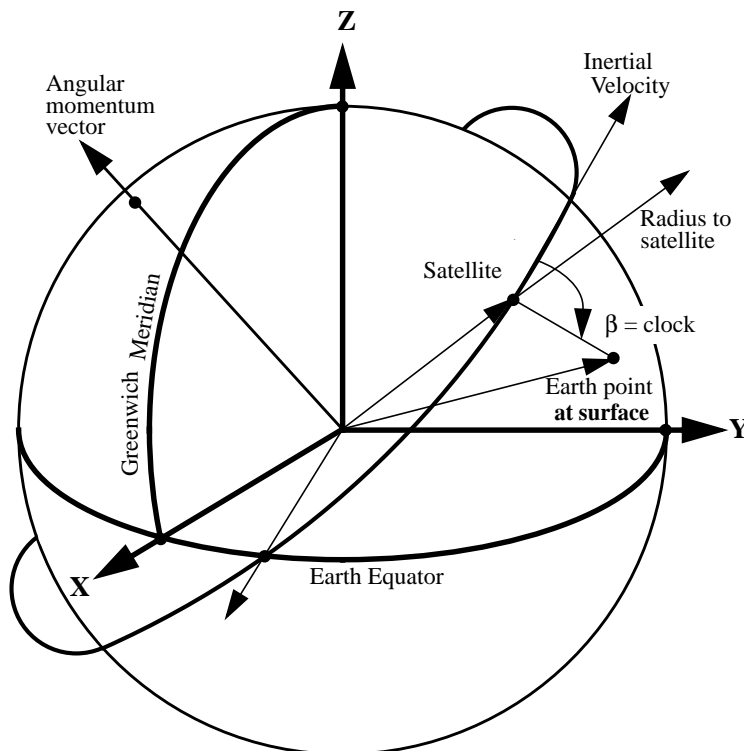
Figure 4-3. Clock Angle

The clock angle (See Figure 4-2 and Figure 4-3) is the azimuth angle of the instrument view vector from the satellite to the Earth point (See Term-8) relative to the inertial velocity vector. (deg) [0 .. 360] (See Table 5-1)

The clock angle, along with the cone angle (See Figure 4-2 and SSF-14) define the direction of the instrument view vector to the Earth point.

The clock angle β is defined in a right-handed coordinate system centered at the satellite where z is toward the center of the Earth, x is in the direction of the inertial velocity vector, and y completes the triad.

When $\beta = 270^o$, the Earth point is on the same side of the orbit as the

orbital angular momentum vector (See Figure 4-3). When $\beta = 0^o$, the Earth point is directly ahead of the satellite.

The ToolKit (See Term-41) call PGS_CSC_SCtoORB (See Reference 47) transforms the instrument view vector in spacecraft coordinates to (x,y,z) orbital coordinates and the clock angle is defined by $x/d = \cos\beta$ and $y/d = \sin\beta$ and $d = \sqrt{x^2 + y^2}$. ♠

SSF-16   Rate of change of cone angle

This parameter is the angular velocity of the cone angle (See SSF-14).
(deg sec^{-1}) [-300 .. 300] (See Table 5-1)

The cone rate is negative when scanning toward nadir, positive when scanning away from nadir, and zero when the cone angle is constant (See Figure 4-2). The cone rate is not measured but approximated with two consecutive cone angle positions. The nominal cone rate is ± 63 deg sec^{-1} and is approximated to within ± 2 deg sec^{-1}.   ♠

SSF-17   Rate of change of clock angle

This parameter is the angular velocity of the clock angle (See SSF-15).
(deg sec^{-1}) [-20 .. 20] (See Table 5-1)

The RAPS mode starts with the scan plane in the along-track orientation and rotates through 180° of clock angle until the scan plane is again in the along-track orientation. The process is then reversed. When the Sun is close to the orbital plane, however, the RAPS mode starts with the scan plane rotated 20° from the along-track orientation and rotates through 140° of clock angle until the scan plane is again 20° from the along-track orientation. This process is then reversed. The clock rate is not measured but approximated with two consecutive clock angle positions.

The nominal magnitude of the clock rate is the absolute value of 6.042 ± 1.098 deg sec^{-1}. The clock rate is negative when the azimuth angle moves toward the velocity vector, positive when the azimuth angle moves away from the velocity vector, and zero when the clock angle is constant. However, when changing azimuth direction the magnitude of the clock rate will approach 0 deg sec^{-1} and then increase to almost 14 deg sec^{-1} before settling back to the nominal magnitude. When the instrument is operating in the FAPS mode, the clock rate is set to zero.   ♠

SSF-18   Along-track angle of CERES FOV at surface

This parameter is the in-orbit angle from hour start (See SSF-H3) to the Earth point (See Term-8). CERES data are ordered on the SSF product by their along-track angle and not on time.
(deg) [-30 .. 330] (See Table 5-1)

The FOV is located with respect to the satellite orbit by the along-track and cross-track angles. We define a vector $\hat{X}_o$ (See Figure 4-4) from the center of the Earth to the satellite at the start of the hour (See SSF-H10). We define another vector $\hat{X}_p$ from the center of the Earth to the Earth

point. The along-track angle γ_{at} is the angle, at the center of the Earth from the satellite start vector to the projection of the Earth point vector onto the orbit plane. The along-track angle is measured along the arc traveled by the spacecraft and can exceed 180°. The angle is based on a right-handed coordinate system with the origin at the center of the Earth, the Z axis along the angular momentum vector, and the X axis at the satellite start vector.

All data associated with a footprint are recorded in the hourly SSF granule (See Term-19) that contains its observation time (See SSF-1). If the instrument is in the RAPS mode, then the footprint could be prior to the start position and yield a negative along-track angle. Likewise, at hour end, the footprint could fall past the end position and yield an along-track angle greater than the angle at the end position. ♠

SSF-19   Cross-track angle of CERES FOV at surface

The FOV is located with respect to the satellite orbit by the along-track and cross-track angles. The cross-track angle is the out-of-orbit-plane angle of the Earth point (See Term-8). The cross-track angle is the angle at the center of the Earth between a vector from the center of the Earth to the Earth point vector and its projection onto the instantaneous orbit plane (see Figure 4-4). The angle is positive if the Earth point is on the same side of the orbit as the angular momentum vector. Otherwise, it is negative. (deg) [-90 .. 90] (See Table 5-1) ♠

$\hat{N}$: Angular momentum vector

$\hat{X}_p$: CERES Earth point

γ_{ct}

γ_{at}

Orbit plane

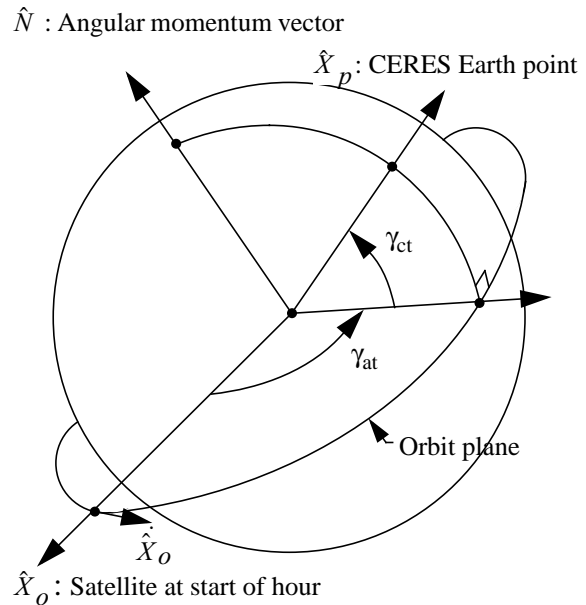$\hat{X}_o$

$\hat{X}_o$: Satellite at start of hour

Figure 4-4. Along-track Angle

4.3.3 Viewing Angles Definitions

These parameters provide the viewing geometry for each CERES FOV.

SSF-20   CERES viewing zenith at surface

This parameter is the geodetic angle θ (See Figure 4-5.) at the Earth point (See Term-8) of the satellite. (deg) [0 .. 90] (See Table 5-2)

The geodetic viewing zenith is the angle between the geodetic zenith (See Term-18) vector and a vector from the Earth point to the satellite. ♠

SSF-21   CERES solar zenith at surface

This parameter is the geodetic zenith angle θ_o (See Figure 4-5.) at the Earth point (See Term-8) of the Sun. (deg) [0 .. 180] (See Table 5-2)
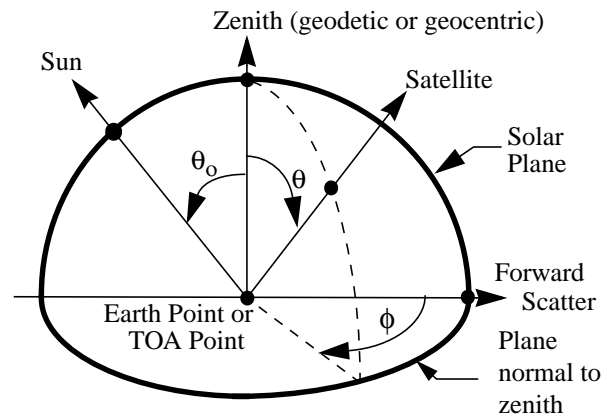
Figure 4-5. Viewing Angles at Surface or TOA

The geodetic solar zenith is the angle between the geodetic zenith (See Term-18) vector and a vector from the Earth point to the Sun. ♠

SSF-22   CERES relative azimuth at surface

This parameter is the geodetic azimuth angle ϕ (See Figure 4-5) at the Earth point (See Term-8) of the satellite relative to the solar plane. (deg) [0 .. 360]   (See Table 5-2)

The relative azimuth is measured clockwise in the plane normal to the geodetic zenith (See Term-18) so that the relative azimuth of the Sun is always 180°. The solar plane is the plane which contains the geodetic zenith vector and a vector from the Earth point to the Sun. If the Earth point is North of the geodetic subsolar point (See Term-17) on the same meridian, then an azimuth of 90° would imply the satellite is East of the Earth point. ♠

SSF-23   CERES viewing azimuth at surface wrt North

This parameter is the geodetic azimuth angle at the Earth point (See Term-8) of the satellite relative to North. (deg) [0 .. 360] (See Table 5-2)

It is similar to the relative azimuth (See SSF-22) except the $\phi \; = \; 0$ reference (See Figure 4-5) is toward North instead of in the solar plane and the forward scatter direction. ♠

4.3.4 Surface Map Definitions

These parameters describe the Earth's surface conditions for each CERES FOV. They are obtained from ancillary databases, which are sometimes referred to as Surface Maps.

SSF-24   Altitude of surface above sea level

This parameter is the PSF-weighted mean (See Term-30) altitude within the CERES FOV based on the altitude at each imager pixel (See Term-27) within the FOV. (m) [-1000 .. 10000] (See Table 5-3)

The surface altitude at the imager pixels are retrieved from a 10 minute (~20 km) static elevation map. This elevation map was created for NASA Langley from the Navy 10 minute database. It is not known if this map is geodetic, geocentric, or other. The Earth model upon which this map is based is also unknown.

For SSF data sets with CC# 014011 or greater, all imager pixels within the FOV are used to compute this parameter. Alternately stated, clear, cloudy and unknown pixels (See Note-7) are used.

For SSF data sets prior to CC# 014011, only imager pixels which could be identified as clear or cloudy are used to compute this parameter.   ♠

SSF-25   Surface type index

This array is a list of the 8 most prominent surface types within the CERES FOV.
(N/A) [0 .. 20] (See Table 5-3)

SSF-26 contains the corresponding PSF-weighted (See Term-29) area coverages. The possible surface type indices are:
1. Evergreen Needleleaf Forest
2. Evergreen Broadleaf Forest
3. Deciduous Needleleaf Forest
4. Deciduous Broadleaf Forest
5. Mixed Forest
6. Closed Shrublands
7. Open Shrublands
8. Woody Savannas
9. Savannas
10. Grasslands
11. Permanent Wetlands
12. Croplands
13. Urban and Built-up
14. Cropland Mosaics
15. Snow and Ice (permanent)
16. Bare Soil and Rocks
17. Water Bodies
18. Tundra
19. Fresh Snow
20. Sea Ice

The 8 surface type indices are ordered on area coverage with the largest being first. If there are fewer than 8 surface types falling within a CERES FOV, all the remaining indice locations will be filled with the 2-byte CERES default (See Table 4-5).

Surface types 1 - 17 correspond to those defined by IGBP. The last 3 surface types were defined for CERES. Surface type 18, Tundra, occurs when a location has an IGBP surface type of 16 (bare soil and rocks) and the Olson vegetation map identifies the same location as Tundra. Fresh snow, number 19, and sea ice, number 20, are not permanent surface types. They are obtained daily from the National Snow and Ice Data Center. The IGBP surface type for snow and ice,

number 15, is for permanent snow and ice. It does not change with time. None of the snow and ice surface types defined above are related to the Cloud-mask snow/ice percent coverage defined in SSF-69.

Every imager pixel (See Term-27) within the FOV is identified as one of surface types 1 - 18. Next, the "Fresh Snow and Sea Ice" maps are examined to determine if any pixel is type 19 or 20. These types take precedence over the 1 - 18 types. All surface maps used by CERES are 10 minute, equal angle. It is not known if these maps are geodetic, geocentric, or other. The Earth model upon which they are based is also unknown.

For SSF data sets with CC# 019015 or greater, all imager pixels within the FOV are used to compute this parameter. Alternately stated, clear, cloudy and unknown pixels (See Note-7) are used.

For SSF data sets with CC# 014011 through 018014, all imager pixels within the FOV are used to compute this parameter. Alternately stated, clear, cloudy and unknown pixels (See Note-7) are used. However, due to a software error, the entire array may be set to CERES default (See Table 4-5) when Unknown cloud-mask (See SSF-64-A) is greater than 0 and there are more than 2 surface types.

For SSF data sets prior to CC# 014011, only imager pixels which could be identified as clear or cloudy are used to compute this parameter. ♠

SSF-26 Surface type percent coverage

This array contains the integer percentage coverage for the 8 most prominent surface types in SSF-25. The coverages are PSF-weighted (See Term-29) over the CERES FOV (See Term-11). (percent) [0 .. 100] (See Table 5-3)

Because the surface types are arranged by prominence, the percent coverage will always be decreasing. If a surface type has a percent less than 0.5%, then the percent is rounded off to 0 and the surface type index remains in SSF-27. If there are fewer than 8 surface types present, then the remaining percentages are set to the 2-byte CERES default (See Table 4-5) and the non default percentages sum to 100. If there are more than 8 surface types present, then the sum of percent coverage may be less than 100.

For SSF data sets with CC# 016013 and CC# 019015 or greater, all imager pixels within the FOV are used to compute this parameter. Alternately stated, clear, cloudy and unknown pixels (See Note-7) are used.

For SSF data sets with CC# 014011 and 018014, all imager pixels within the FOV are used to compute this parameter. Alternately stated, clear, cloudy and unknown pixels (See Note-7) are used. However, due to a software error, the entire array may be set to CERES default (See Table 4-5) when "Unknown cloud-mask" (See SSF-64-A) is greater than 0 and there are more than 2 surface types.

For SSF data sets prior to CC# 014011, only imager pixels which could be identified as clear or cloudy are used to compute this parameter. ♠

4.3.5 Scene Type Definitions

These parameters identify the Angular Distribution Model types, historically called Scene types, used to invert the CERES radiances to fluxes.

SSF-27   CERES SW ADM type for inversion process

This parameter denotes the ADM (See Note-13) type used to invert SW radiance (See SSF-35) to flux (See SSF-38). (N/A) [0 .. 5000]   (See Table 5-4)

The ADM is a function of the scene over the FOV where the scene is defined by various parameters, depending on the set.

SET 2: This set of SW ADMs is referred to as Beta2_TRMM (See Note-12**)** and was developed from the Edition1 SSF data set. Beta2_TRMM ADMs are used on SSF data sets beginning with CC# 013010.

SET 1: This set of SW ADMs is referred to as VIRS12B (See Note-11) and is based on the 12 ERBE scene types listed below. VIRS12B is based on CERES/TRMM data and the ADMs were constructed with the SAB method (See Reference 55). The ADMs for clear snow and all 3 land-ocean mix scenes are exceptions and are based on Nimbus-7 data and constructed with the RPM method (See Reference 30). VIRS12B ADMs are used on SSF data sets prior to CC# 013010.
  0.   unknown
  1.   clear ocean
  2.   clear land
  3.   clear snow
  4.   clear desert
  5.   clear land-ocean mix (or coastal)
  6.   partly cloudy ocean
  7.   partly cloudy land or desert
  8.   partly cloudy land-ocean mix
  9.   mostly cloudy ocean
  10.   mostly cloudy land or desert
  11.   mostly cloudy land-ocean mix
  12.   overcast over any surface ♠

SSF-28   CERES LW ADM type for inversion process

This parameter denotes the ADM (See Note-13) type used to invert LW radiance (See SSF-36) to flux (See SSF-39).   (N/A) [0 .. 5000]   (See Table 5-4)

The ADM is a function of the scene over the FOV where the scene is defined by various parameters, depending on the set.

SET 2: This set of LW ADMs is referred to as Beta2_TRMM (See Note-12**)** and was developed from the Edition1 SSF data set. The LW ADM types are different from the SW ADM types. Beta2_TRMM ADMs are used on SSF data sets beginning with CC# 013010.

SET 1: This set of LW ADMs is referred to as VIRS12B (See Note-11) and is based on the 12 ERBE scene types (See SSF-27). VIRS12B is based on CERES/TRMM data and the ADMs were

constructed with the SAB method (See Reference 55). The ADMs for clear snow scenes are exceptions and are based on Nimbus-7 data and constructed with the RPM method (See Reference 30). VIRS12B ADMs are used on SSF data sets prior to CC# 012009.
   0 - 12 Same as SW ADM types (See SSF-27) ♠

SSF-29   CERES WN ADM type for inversion process

This parameter denotes the ADM (See Note-13) type used to invert WN radiance (See SSF-37) to flux (See SSF-40).   (N/A) [0 .. 5000] (See Table 5-4)

The ADM is a function of the scene over the FOV where the scene is defined by the surface type (See SSF-25) and the mean cloud parameters (See SSF-66 to SSF-114).

SET 2: This set of WN ADMs is referred to as Beta2_TRMM (See Note-12) and was developed from the TRMM Edition1 SSF data set. The WN ADM types are same as the LW ADM types and different from the SW ADM types. Beta2_TRMM ADMs are used on SSF data sets beginning with CC# 013010.

SET 1: This set of WN ADMs is referred to as VIRS12B (See Note-11) and is based on the 12 ERBE scene types (See SSF-27). VIRS12B is based on CERES TRMM data and the ADMs were constructed with the SAB method (See Reference 55). The ADMs for clear snow scenes are exceptions and are based on LW Nimbus-7 data and constructed with the RPM method (See Reference 30). VIRS12B ADMs are used on SSF data sets prior to CC# 012009.
   0 - 12 Same as SW ADM types (See SSF-27)   ♠

SSF-30   ADM geo

This parameter has not yet been defined. (N/A) [-32767 .. 32766]   (See Table 5-4)   ♠

4.3.6 Filtered Radiances Definitions

This parameter group contains the CERES radiances obtained directly from the instrument counts and the associated flags.

SSF-31   CERES TOT filtered radiance - upwards

This parameter is the measured, spectrally integrated radiance emerging from the TOA, where the spectral integration is weighted by the spectral throughput of the TOT channel. It is the "raw" measurement from the TOT channel after count conversion (See Term-2) and is spectrally corrected (See Term-36) to yield the unfiltered LW radiance (See SSF-41) at night. The TOT and SW filtered radiances are spectrally corrected together to yield the LW radiance during the day. (W m^{-2} sr^{-1}) [0 .. 700]   (See Table 5-5)

The value of the filtered TOT radiance is defined as either "good" or "bad" by the quality flag (See SSF-34-B). If the value is "bad", for any reason, the TOT filtered radiance is set to a default value (See Table 4-5). If the value is "good", the measured value is retained.

The TOT filtered radiance is a measure of all radiance that passes through the TOT channel. The spectral weighting produced by the TOT channel throughput is the product of the primary mirror reflectance, the secondary mirror reflectance, and the absorptance of the detector flake. The TOT

spectral throughput passes about 90% of the radiant power with wavelengths longer than 5 μm and about 85% of the power with shorter wavelengths. ♠

SSF-32   CERES SW filtered radiance - upwards

This parameter is the measured, spectrally integrated radiance emerging from the TOA, where the spectral integration is weighted by the spectral throughput of the SW channel. It is the "raw" measurement from the SW channel after count conversion (See Term-2) and is spectrally corrected (See Term-36) to yield the unfiltered SW radiance (See SSF-35). (W m^{-2} sr^{-1}) [-10 .. 510]   (See Table 5-5)

The value of the SW filtered radiance is defined as either "good" or "bad" by the quality flag (See SSF-34-B). If the value is "bad", for any reason, the SW filtered radiance is set to a default value (See Table 4-5). If the value is "good" the measured value is retained.

The SW filtered radiance is a measure of all radiance that passes through the SW channel. The spectral weighting produced by the SW channel throughput is the product of the SW filter throughput and the TOT channel throughput (See SSF-31). The SW spectral throughput passes about 75% of the radiant power with wavelengths shorter than 5 μm and cuts off rather sharply at about 5 μm. Wavelengths longer than this wavelength contribute a very small fraction of this measurement. ♠

SSF-33   CERES WN filtered radiance - upwards

This parameter is the measured, spectrally integrated radiance emerging from the TOA, where the spectral integration is weighted by the spectral throughput of the WN channel. It has a bandpass from approximately 8 to 12 μm. It is the "raw" measurement from the window channel after count conversion (See Term-2) and is spectrally corrected (See Term-36) to yield the unfiltered WN radiance (See SSF-37). (W m^{-2} sr^{-1}μm^{-1}) [0 .. 15]   (See Table 5-5)

Note, to obtain an integrated filtered WN radiance (W m^{-2} sr^{-1}), multiply the filtered WN radiance by the width of the WN band (3.7 μm^{-1}).

The filtered WN radiance is defined as either "good" or "bad" by the quality flag (See SSF-34-B). If the value is "bad", for any reason, the WN filtered radiance is set to a default value (See Table 4-5). If the value is "good", the measured value is retained.

The WN filtered radiance is a measure of all radiance that passes through the WN channel. The spectral weighting produced by the WN channel throughput is the product of the WN filter throughput and the TOT channel throughput (See SSF-31). The WN spectral throughput passes about 67% of the radiant power between 8 to 12 μm. ♠

SSF-34   Radiance and Mode flags

This parameter contains the filtered radiance quality flags (good or bad) and instrument mode flags. It is a 32-bit word where the individual bits contain the flag information. The word bit ordering is shown in Figure 4-6, where bit zero identifies the least significant bit. The individual flags are defined in Table 4-3 followed by their descriptions. (N/A) [See Figure 4-6] (See Table 5-5)

32-Bit Word

Figure 4-6. Radiance and Mode Flags

Table 4-3. Radiance and Mode Quality Flags Definition (Sheet 1 of 2)

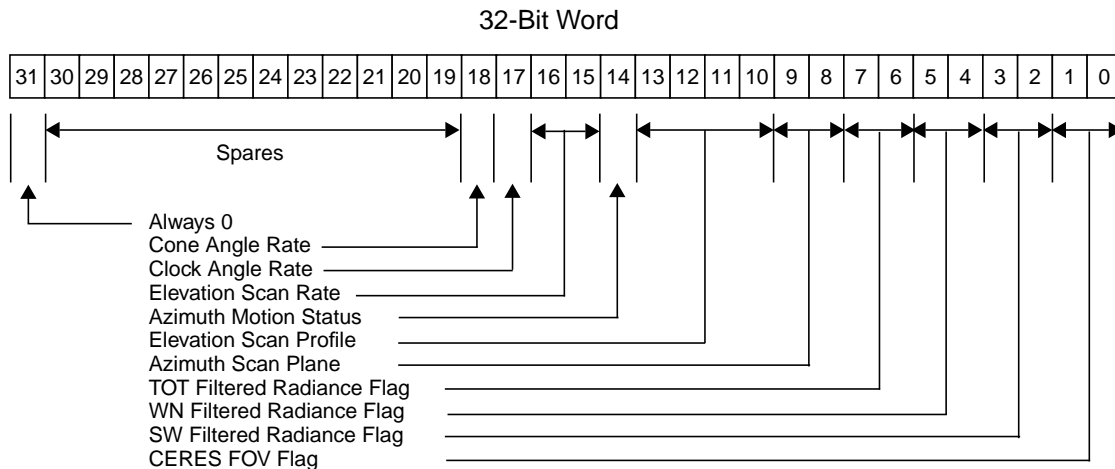| Flag Parameter	Bits	Detail Description	Flag Description
CERES FOV	0..1	SSF-34-A	00 Full Earth view 01 Partial Earth view 10 Partial TOA view 11 Space or unknown
SW filtered radiance WN filtered radiance TOT filtered radiance	2..3 4..5 6..7	SSF-34-B	00 Good radiance 10 Bad radiance 01, 11 Not used
Azimuth scan plane	8..9	SSF-34-C	00 Cross-track (fixed, $\pm 45^o$) 01 RAPS (rotating) 10 Along-track (fixed, not $\pm 45^o$) 11 Transitional or unknown
Elevation scan plane	10..13	SSF-34-D	0000 Normal-earth scan 0001 Short-earth scan 0010 MAM scan 0011 Nadir scan 0100 Stowed Profile others Not used
Azimuth motion status	14	SSF-34-E	0 Azimuth fixed 1 Azimuth in motion
Elevation scan rate	15..16	SSF-34-F	00 Nominal (63.14 ± 2.5 deg sec^{-1}) 01 Fast (>65.64 deg sec^{-1}) 10 Slow/stopped (<60.64 deg sec^{-1}) 11 Transition or unknown
Clock angle rate cone angle rate	17 18	SSF-34-G	0 Good computed rate 1 Bad computed rate

Table 4-3. Radiance and Mode Quality Flags Definition (Sheet 2 of 2)

Flag Parameter	Bits	Detail Description	Flag Description
Spares	19..30		0 Set to zero
Sign	31		0 Always

SSF-34-A CERES FOV Flag:

This flag is set for each CERES science measurement and is used to identify where the CERES footprint is viewing. The footprint FOV used by the geolocation calculations is based on the centroid of the detector point-spread-function, not on the optical line-of-sight. (See Reference 14 or Term-28). FOV calculations use the Earth surface model (WGS-84) and the CERES TOA model (30km above the WGS-84 model) provided by the ECS ToolKit (See Term-41).

    00 = "Full Earth view" set if
       - The FOV PSF centroid pierces both the Earth surface and the TOA surface, and
       - The footprint viewing area is determined to be completely on the Earth surface.
    01 = "Partial Earth view" set if
       - The FOV PSF centroid pierces both the Earth and TOA surface, and
       - The FOV footprint area includes part of the Earth's surface (i.e., straddling the Earth limb).
    10 = "Partial TOA view" set if
       - The FOV PSF centroid pierces TOA surface, but not the Earth's surface, and
       - The FOV footprint area may include part of the Earth's surface (i.e., straddling the Earth limb).
    11 = "Space or unknown" set if
       - The FOV PSF centroid for this measurement does not pierce either the Earth's surface or the TOA surface (e.g., the FOV is looking at a cold space above the TOA). Though the centroid does not pierce the TOA surface, the FOV footprint area may partially overlap this surface.

SSF-34-B SW/WN/TOT Filtered Radiance Flags:

These status flags are set for each CERES science measurement.

    00 = Good: All of the following conditions are met:
       - All values of instrument parameters, which are used for count conversion (bias voltage, detector voltages, heatsink temperatures), passed edit limit and rate limit checks, and the overall state of the instrument is nominal for making radiometric measurements. The spaceclamp value has been computed, and passed edit and rate limit checks.
       - The instrument spurious slow mode has been corrected
       - None of the detectors were saturated at the time the measurements were taken.
       - Final radiance values passed edit checks.
       - There were no computational or numerical errors resulting from the count conversion process.
    10 = Bad: Failed one or more of the above conditions. The CERES default fill value (See Table 4-5) is output instead of the actual computed radiance value.
    01, 11 = Reserved - Not used.

SSF-34-C Azimuth Scan Plane:

This flag is derived from scan level information and is used to define the azimuth gimbal scan plane for each measurement. Individual bit patterns are defined as follows:

    00 = Cross-track
       - This flag is set when the azimuth gimbal is in a fixed position with the elevation scanning plane within 45 degrees of the normal to the spacecraft velocity vector. Typically, this means the gimbal is at the 180 (or 0) degree azimuth position as defined by the instrument coordinate system. This azimuth position allows the elevation scan to sweep across the ground track in a side-to-side motion. This scan plane flag is a special case of the FAPS.
    01 = RAPS (Biaxial)

- This flag is set when the azimuth gimbal is rotating between two defined azimuth end points for the measurement.

10 = Along-track
- This flag is set when the azimuth gimbal is in a fixed position at any position other than crosstrack for the measurement. For example, the instrument may be in the along-track scan plane where the elevation scan plane is oriented parallel to the spacecraft velocity vector (e.g., the azimuth position = 90 or 270 degrees).

11 = Transitional
- Defined as anything not covered above. Typically, this flag is set when the instrument is changing between the crosstrack and biaxial modes while the elevation gimbal is stowed.

SSF-34-D Elevation Scan Profile:

This flag is derived from scan level information that is duplicated for each measurement within the entire packet. Individual bit patterns are defined as follows:

0000 = Normal-Earth Scan (See Figure 15-3)
0001 = Short-Earth Scan (See Figure 15-3)
0010 = MAM Scan
0011 = Nadir Scan
0100 = Stowed Profile
0101 = Other Profile (Anything not classified above.)

SSF-34-E Azimuth Motion Status:

This flag is derived from scan level information that is duplicated for each measurement. Individual bit patterns are defined as follows:

0 = Fixed: The azimuth gimbal is stopped at a fixed position for the entire packet.
1 = In Motion: The azimuth gimbal is moving during all or part of the packet. Motions can include biaxial scans or transitions between azimuth modes.

SSF-34-F Elevation Scan Rate:

This flag is used to identify the elevation gimbal scan rate for the current measurement. The scan rate is derived by taking the absolute value of the elevation gimbal position difference in degrees between the current and previous measurements, and dividing by the sample time interval (0.01 seconds) to obtain a two point instantaneous scan rate. The scan rate for the current sample is then categorized according to the following flag definitions.

00 = Nominal:
- The elevation gimbal for this measurement is moving at a nominal rate of 63.14 ± 2.5 deg sec^{-1}.

01 = Fast:
- The elevation gimbal is moving faster than $63.14 + 2.5$ deg sec^{-1} for this measurement. Typically, this condition occurs when the gimbal is in the fast retrace (See Term-32) portion of the short-earth scan profile or when slewing to the internal calibration position. However, during scan inflection points (when the gimbal changes motion speed or direction) normal servomechanical ringing can occur which could indicate fast rates while the gimbal settles out (which can take up to ten samples).

10 = Slow/Stopped:
- The elevation gimbal is not moving or is moving at a slow rate (i.e., $< 63.14 - 2.5$ deg sec^{-1}) for this measurement. Slow rates are usually identified when the gimbal is ramping up to speed from a stopped position (e.g., from spacelook position). Due to the backward two point scan rate algorithm, the first sample in a scan will be set to stopped since there are no profiles that have the elevation moving at the very beginning of a scan.

11 = Other:
- The elevation gimbal scan rate could not be classified into one of the above categories for this measurement. This would be typical of measurements during gimbal transitions between stop and go conditions.)

SSF-34-G Clock Angle Rate/Cone Angle Rate:

These flags are used to indicate whether an angular rate could be computed from valid angles. No edit checks are performed. (See SSF-16 and SSF-17)

> 0 = Good: The angular rate for this measurement is computed from valid angles for current and previous measurements.
>
> 1 = Bad: The angular rate for this measurement could not be computed. Consequently, the CERES default fill value is output to the BDS rate field. ♠

4.3.7 Unfiltered Radiances Definitions

This parameter group contains the CERES unfiltered radiances obtained by taking into account the instrument-specific spectral response

SSF-35   CERES SW radiance - upwards

This parameter is an estimate of the solar radiance at all wavelengths reflected back into space and contains no thermal radiance. (W m^{-2} sr^{-1}) [-10 .. 510] (See Table 5-6)

It is a spectrally integrated radiance that is intended to represent the radiance of reflected sunlight. In other words, the SW unfiltered radiance is the radiance we would observe if we had a spectrally flat channel that passed all the reflected sunlight and that removed any thermal emission from the Earth and the Earth's atmosphere. Frequently, in informal discussion, we incorrectly refer to the SW unfiltered radiance as a broadband radiance covering the spectral interval from 0 to 5 µm. Each SW unfiltered radiance is a weighted spatial average over the FOV where the weighting is the CERES Point Spread Function.

At night the SW radiance is set to zero where night is defined as a solar zenith angle (See SSF-21) greater than 90° at the Earth point (See Term-8). During the day, the SW radiance, I^{SW}, is defined by $I^{SW} = a_0 + a_1 (m_f^{SWsolar}) + a_2 (m_f^{SWsolar})^2$ where $m_f^{SWsolar} = m_f^{SW} - \text{SW}^{thermal}$ and where a_0, a_1, a_2 are from a set of spectral correction coefficients(See Term-36), m_f^{SW} is the filtered shortwave measurement (See SSF-32), and $\text{SW}^{thermal}$ is an estimate of the thermal radiation in the shortwave measurement. The thermal shortwave is derived from the filtered window radiance (See SSF-33) and is less that 0.5%. If the filtered window radiance is not "good" (See SSF-34), then a constant is used for all scenes, or $\text{SW}^{thermal} = 0.36\ W m^{-2} sr^{-1}$. See Note-5 on the Spectral Correction Algorithm for details.

Under normal conditions the thermal shortwave is derived from the filtered window radiance (See SSF-33) and is given by

$$\mathrm{SW}^{thermal} = A_0 + A_1 x + A_2 x^2$$

$$x = m_f^{WN} * \mathrm{WNchan\_width}$$

$$A_0 = 0.120800$$

$$A_1 = -0.001697$$

$$A_2 = 0.0006875$$

The unfiltered SW radiance is "good" if it contains a non-default value. If the filtered SW radiance is flagged "bad" (See SSF-34), then the unfiltered SW radiance is set to default (See Table 4-5). If the filtered SW radiance is out of range, then the unfiltered SW radiance is set to default. If the unfiltered SW radiance is out of range, then it is also set to default. No other condition will cause the unfiltered SW radiance on the SSF to be set to default. ♠

SSF-36   CERES LW radiance - upwards

This parameter is an estimate of the thermal radiance at all wavelengths emitted to space including shortwave thermal radiance. (W m^{-2} sr^{-1}) [0 .. 200] (See Table 5-6)

It is a spectrally integrated radiance that is intended to represent the radiance from emission of the atmosphere and the Earth that emerges from the top of the atmosphere. In other words, the LW unfiltered radiance is the radiance that we would observe if we had a spectrally flat channel that passed all the emitted radiance and that removed any reflected sunlight. Frequently, in informal discussion, we incorrectly refer to the LW unfiltered radiance as a broadband radiance covering wavelengths longer than 5 μm. Each LW unfiltered radiance is a weighted spatial average over the FOV where the weighting is the CERES Point Spread Function.

At night the LW radiance I^{LW} is defined by $I^{LW}(N) = d_0 + d_1 m_f^{TOT} + d_2 m_f^{WN}$ where d_0, d_1, d_2 are from a set of spectral correction coefficients (See Term-36), m_f^{TOT} is the filtered total measurement (See SSF-31), m_f^{WN} is the filtered window measurement (See SSF-33) and where night is defined as a solar zenith angle (See SSF-21) greater than 90$^{\mathrm{o}}$ at the Earth point (See Term-8). During the day, the LW radiance is basically the TOT radiance minus the SW radiance with the appropriate spectral correction coefficients, or

$I^{LW}(D) = c_0 + c_1 (m_f^{SW} - \mathrm{SW}^{thermal}) + c_2 m_f^{TOT} + c_3 m_f^{WN}$ where c_0, c_1, c_2, c_3 are from a set of spectral correction coefficients, m_f^{TOT} is the filtered total measurement (See SSF-31), m_f^{WN} is the filtered window measurement (See SSF-33) , m_f^{SW} is the filtered shortwave measurement (See SSF-32), and $\mathrm{SW}^{thermal}$ is an estimate of the thermal radiation in the shortwave measurement (See SSF-35). The unfiltered LW radiance is "good" if it contains a non-default value. If the filtered TOT radiance is flagged "bad" (See SSF-34), then the unfiltered LW radiance is set to default (See Table 4-5). If the filtered TOT radiance is out of range (See SSF-31), then the

unfiltered LW radiance is set to default. During the day, the unfiltered LW radiance is set to default if the filtered SW radiance is flagged "bad." During the day, the unfiltered LW radiance is set to default if the filtered SW radiance is out of range (See SSF-32). The unfiltered LW radiance is also set to default if it is out of range. No other condition will cause the unfiltered LW radiance on the SSF to be set to default. ♠

SSF-37   CERES WN radiance - upwards

This parameter is an estimate of the average radiance per micrometer in the spectral window from 8.0 to 12.0 microns (See Note-6). This radiance is dominated by emission from the Earth's surface when the scene is clear. (W m^{-2} sr^{-1}) [0 .. 60] (See Table 5-6)

For SSF data sets prior to CC# 013010, this parameter had the units W m^{-2} sr^{-1}µm^{-1} and a range of 0 .. 15.

Each WN unfiltered radiance is a weighted spatial average over the FOV where the weighting is the CERES Point Spread Function.

The unfiltered WN radiance is defined by $I^{WN} = b_0 + b_1 (m_f^{WN}) + b_2 (m_f^{WN})^2$ where b_0, b_1, b_2 are from a set of spectral correction coefficients (See Term-36), and m_f^{WN} is the filtered window measurement (See SSF-33). The unfiltered WN radiance is "good" if it contains a non-default value. If the filtered WN radiance is flagged "bad" (See SSF-34), then the unfiltered WN radiance is set to default (See Table 4-5). If the filtered WN radiance is out of range (See SSF-33), then the unfiltered WN radiance is set to default. The unfiltered WN radiance is also set to default if it is out of range. No other condition will cause the unfiltered WN radiance on the SSF to be set to default. ♠

4.3.8 TOA and Surface Fluxes Definitions

This parameter group contains CERES surface and TOA fluxes. Also included are albedo and emissivity parameters associated with the CERES channels.

SSF-38   CERES SW TOA flux - upwards

This parameter is an estimate of the instantaneous reflected solar flux from the Earth-atmosphere at the colatitude (See SSF-10) and longitude (See SSF-11) position of the CERES footprint. (Note that colatitude and longitude are defined at the surface.) (W m^{-2}) [0 .. 1400] (See Table 5-7)

At night, the SW TOA flux is set to zero. Night is defined as solar zenith angles (See SSF-21) greater than 90° at the Earth point (See Term-8). The SW TOA flux is set to default (See Table 4-5) when the solar zenith angle is between 86.5^o and 90.0^o. When the solar zenith is less than or equal to 86.5^o, the SW TOA flux is determined by applying an empirical Angular Distribution Model (or ADM see Note-10) anisotropic correction factor to the shortwave radiance (See SSF-35). The anisotropic correction factor is evaluated at the footprint's viewing zenith angle θ

(See SSF-20), relative azimuth angle ϕ (See SSF-22), and solar zenith angle θ_o (See SSF-21). The ADMs are a function of scene type (See SSF-27).

The SW TOA flux is set to default if the SW radiance (See SSF-35) is default, or if the SW scene type (See SSF-27) is unknown. If the instantaneous albedo derived from the SW TOA flux is greater than 1.0, the SW TOA flux is set to default. The SW TOA flux is also set to default for geometric conditions that lead to inaccurate flux estimates. For example, $\theta > 70^o$,

$86.5^o < \theta_o \leq 90^o$,or when in sunglint for clear ocean scenes. ♦

SSF-39   CERES LW TOA flux - upwards

This parameter is an estimate of the instantaneous thermal flux emitted from the Earth-atmosphere at the colatitude (See SSF-10) and longitude (See SSF-11) position of the CERES footprint. (Note that colatitude and longitude are defined at the surface.) (W m^{-2}) [0 .. 500] (See Table 5-7)

The LW TOA flux is determined by applying an empirical Angular Distribution Model (or ADM see Note-10) anisotropic correction factor to the longwave radiance (See SSF-36). The anisotropic correction factor is evaluated at the footprint's viewing zenith angle θ (See SSF-20). The ADMs are a function of scene type (See SSF-28).

The LW TOA flux is set to default (See Table 4-5) if the LW radiance (See SSF-36) is default, or if the LW scene type (See SSF-28) is unknown. The LW TOA flux is also set to default for geometric conditions that lead to inaccurate flux estimates. For example, $\theta > 70^o$. ♦

SSF-40   CERES WN TOA flux - upwards

This parameter is an estimate of the instantaneous thermal flux emitted in the 8.0 to 12.0 μm window from the Earth-atmosphere at the colatitude (See SSF-10) and longitude (See SSF-11) position of the CERES footprint. (Note that colatitude and longitude are defined at the surface.) (W m^{-2}) [0 .. 200] (See Table 5-7)

For SSF data sets prior to CC# 013010, this parameter had the units W m^{-2} μm^{-1} and a range of 2 .. 50.

The WN TOA flux is determined by applying an empirical Angular Distribution Model (or ADM see Note-10) anisotropic correction factor to the window radiance (See SSF-37). The anisotropic correction factor is evaluated at the footprint's viewing zenith angle θ (See SSF-20). The ADMs are a function of scene type (See SSF-29).

The WN TOA flux is set to default (See Table 4-5) if the WN radiance (See SSF-37) is default, or if the WN scene type (See SSF-33) is unknown. The WN TOA flux is also set to default for geometric conditions that lead to inaccurate flux estimates. For example, $\theta > 70^o$. ♦

SSF-41   CERES downward SW surface flux - Model A

This parameter is the estimated downward shortwave flux at the surface based on the Li-Leighton net with Li-Garand surface albedo models. (ATBD 4.6). (W m^{-2}) [0 .. 1400]   (See Table 5-7)

These models are valid only for clear sky, and will be set to CERES default (See Table 4-5) when the FOV is not clear.

For CC# 019015 and later, clear sky is defined as "Clear area percent coverage at subpixel resolution," (See SSF-66), greater than 99.9%.

For CC# 018014 and earlier, clear sky is defined as "Clear area percent coverage at subpixel resolution," (See SSF-66), greater than 95%.

For CC# 13010 through 018014, this parameter should not be used when "Imager percent coverage," (See SSF-54), is less than 60%. These fluxes are incorrect and should have been set to CERES default (See Table 4-5). ♠

SSF-42   CERES downward LW surface flux - Model A

This parameter is the estimated downward longwave flux at the surface based on the Ramanathan-Inamdar model (ATBD 4.6).   (W m^{-2}) [0 .. 700]   (See Table 5-7)

Currently, this value can only be computed for cloud-free and ice-free ocean surfaces and cloud-free tropical land surfaces. It requires CERES LW (See SSF-36) and WN (See SSF-37) unfiltered radiances and surface emissivities (See SSF-51, SSF-52) as inputs and cannot, otherwise, be computed. Algorithms which support cloud forcing and extra-tropical land are expected at a later time.

For CC# 019015 and later, cloud-free is defined as "Clear area percent coverage at subpixel resolution," (See SSF-66), greater than 99.9%.

For CC# 018014 and earlier, cloud-free is defined as "Clear area percent coverage at subpixel resolution," (See SSF-66), greater than 95%.

For CC# 13010 through 018014, this parameter should not be used when "Imager percent coverage," (See SSF-54), is less than 60%. These fluxes are incorrect and should have been set to CERES default (See Table 4-5). ´

SSF-43   CERES downward WN surface flux - Model A

This parameter is the estimated downward window flux at the surface based on the Ramanathan-Inamdar model (ATBD 4.6).   (W m^{-2}) [0 .. 250]   (See Table 5-7)

Currently, this value can only be computed for cloud-free and ice-free ocean surfaces and cloud-free tropical land surfaces. When combined with the downward nonWN surface flux component, one gets the downward LW surface flux (See SSF-42). Algorithms which support cloud forcing and extra-tropical land are expected at a later time.

For CC# 019015 and later, cloud-free is defined as "Clear area percent coverage at subpixel resolution," (See SSF-66), greater than 99.9%.

For CC# 018014 and earlier, cloud-free is defined as "Clear area percent coverage at subpixel resolution," (See SSF-66), greater than 95%.

For CC# 13010 through 018014, this parameter should not be used when "Imager percent coverage," (See SSF-54), is less than 60%. These fluxes are incorrect and should have been set to CERES default (See Table 4-5).

For SSF data sets prior to CC# 013010, this parameter had the units W m^{-2} µm^{-1} and a range of 0 .. 65. ♠

SSF-44   CERES net SW surface flux - Model A

This parameter is the estimated net shortwave flux at the surface based on the Li-Leighton model (ATBD 4.6). Net flux is defined as downwelling flux minus upwelling flux. (W m^{-2}) [0 .. 1400] (See Table 5-7)

The Li-Leighton model is valid only for clear sky, and will be set to CERES default (See Table 4-5) when the FOV is not clear.

For CC# 019015 and later, clear sky is defined as "Clear area percent coverage at subpixel resolution," (See SSF-66), greater than 99.9%.

For CC# 018014 and earlier, clear sky is defined as "Clear area percent coverage at subpixel resolution," (See SSF-66), greater than 95%.

For CC# 13010 through 018014, this parameter should not be used when "Imager percent coverage," (See SSF-54), is less than 60%. These fluxes are incorrect and should have been set to CERES default (See Table 4-5). ♠

SSF-45   CERES net LW surface flux - Model A

The CERES net LW surface flux - Model A is the estimated net longwave flux at the surface based on the Ramanathan-Inamdar model (ATBD 4.6). (W m^{-2}) [-250 .. 50] (See Table 5-7)

This parameter is computed by subtracting the surface emission from the CERES LW flux at surface, downwards (See SSF-42). The surface emission is computed by multiplying the surface emissivity by the Planck radiation associated with the surface temperature. The CERES net LW surface flux can only be computed when a valid CERES LW flux at surface, downwards exists.

For CC# 13010 through 018014, this parameter should not be used when "Imager percent coverage," (See SSF-54), is less than 60%. These fluxes are incorrect and should have been set to CERES default (See Table 4-5). ´

SSF-46   CERES downward SW surface flux - Model B

This parameter is the estimated downward shortwave flux at the surface based on the Langley Parameterized Shortwave Algorithm (LPSA). The downward Model B flux is based on the LPSA net with LPSA surface albedo models. (W m^{-2}) [0 .. 1400] (See Table 5-7)

Beginning with CC# 013010, this parameter contains a downward SW surface flux for all FOVs, regardless of cloud cover.

For CC# 13010 through 018014, this parameter should not be used when "Imager percent coverage," (See SSF-54), is less than 60%. These fluxes are incorrect and should have been set to CERES default (See Table 4-5).

For CC# 012009 and earlier, this parameter is restricted to clear-sky, where clear-sky is defined as "Clear area percent coverage at subpixel resolution," (See SSF-66), greater than 95%. Otherwise, this parameter is set to CERES default (See Table 4-5). ♠

SSF-47 CERES downward LW surface flux - Model B

This parameter is the estimated downward longwave flux at the surface based on the Langley Parameterized Longwave Algorithm (LPLA) (ATBD 4.6). (W m^{-2}) [0 .. 700] (See Table 5-7)

For CC# 013010 through 018014, this parameter should not be used when "Imager percent coverage," (See SSF-54), is less than 60%. These fluxes are incorrect and should have been set to CERES default (See Table 4-5).

This value is computed globally. ♠

SSF-48 CERES net SW surface flux - Model B

This parameter is the estimated net shortwave flux at the surface. Net flux is defined as downwelling flux minus upwelling flux. (W m^{-2}) [0 .. 1400] (See Table 5-7)

For CC# 013010 and later, this parameter is based on the Langley Parameterized Shortwave Algorithm (LPSA).

For CC# 013010 through 018014, this parameter should not be used when "Imager percent coverage," (See SSF-54), is less than 60%. These fluxes are incorrect and should have been set to CERES default (See Table 4-5).

For CC# 012009 and earlier, this parameter is based on the Li-Leighton model (ATBD 4.6) and restricted to clear-sky, where clear-sky is defined as "Clear area percent coverage at subpixel resolution," (See SSF-66), greater than 95%. Otherwise, this parameter is set to CERES default (See Table 4-5). This means that both net SW surface fluxes, Model A (See SSF-44) and Model B are identically defined.

For CC# 012009 and 011008, the downward Model B flux (See SSF-46) is based on the Langley Parameterized Shortwave Algorithm (LPSA) net and not this parameter. ♠

SSF-49 CERES net LW surface flux - Model B

The CERES net LW surface flux - Model B is the estimated net longwave flux at the surface based on the Langley Parameterized Longwave Algorithm (LPLA) (ATBD 4.6). (W m^{-2}) [-250 .. 50] (See Table 5-7)

This parameter is computed globally by subtracting the surface emission from the CERES LW flux at surface, downwards. The surface emission is computed by multiplying the surface emissivity by the Planck radiation associated with the surface temperature.

For CC# 013010 through 018014, this parameter should not be used when "Imager percent coverage," (See SSF-54), is less than 60%. These fluxes are incorrect and should have been set to CERES default (See Table 4-5). ♠

SSF-50   CERES broadband surface albedo

This parameter is the estimated broadband surface albedo for the CERES FOV. It is based on broadband albedo table lookups for each of the IGBP surface types recorded in the surface type index (See SSF-25). Values are scaled by the PSF-weighted (See Term-29) percent coverage of the corresponding IGBP type (See SSF-26) and summed. (N/A) [0 .. 1] (See Table 5-7)

The albedo tables are based on field observations. See <http://tanalo.larc.nasa.gov:8080/ surf_htmls/SARB_surf.html> for references. ♠

SSF-51   CERES LW surface emissivity

This parameter is the estimated LW surface emissivity for the CERES FOV. It is based on LW emissivity lookups for each of the IGBP surface types recorded in the surface type index (See SSF-25). Values are scaled by the PSF-weighted (See Term-29) percent coverage of the corresponding IGBP type (See SSF-26) and summed. (N/A) [0 .. 1] (See Table 5-7)

The emissivity tables are based on lab observations. See <http://tanalo.larc.nasa.gov:8080/ surf_htmls/emis_new> for maps and references. ♠

SSF-52   CERES WN surface emissivity

This parameter is the estimated WN surface emissivity for the CERES FOV. It is based on WN emissivity lookups for each of the IGBP surface types recorded in the surface type index (See SSF-25). Values are scaled by the PSF-weighted (See Term-29) percent coverage of the corresponding IGBP type (See SSF-26) and summed. (N/A) [0 .. 1] (See Table 5-7)

The emissivity tables are based on lab observations. See <http://tanalo.larc.nasa.gov:8080/ surf_htmls/emis_new> for maps and references. ♠

4.3.9 Full Footprint Area Definitions

These diverse parameters apply to the entire CERES FOV. Many are obtained from imager information and the remainder are obtained from MOA.

SSF-53   Number of imager pixels in CERES FOV

This parameter is a count of the actual number of imager pixels (See Term-27) which are within the CERES FOV and could be identified as clear or cloudy (See Note-7). (N/A) [0 .. 32766] (See Table 5-8)

For SSF data sets with CC# 014011 or greater, all full and partial Earth view FOVs containing at least one imager pixel are recorded on the SSF. Since this parameter includes only clear and cloudy pixels, it will be set to 0 when all the imager pixels within the CERES FOV are defined as unknown.

For SSF data sets prior to CC# 014011, this parameter is never set to 0.

For an example, refer to equation (26) in Note-2. The CERES FOV is a rectangular grid that approximates the 95% energy area with respect to the PSF. There is no PSF weighting associated with this variable. ♠

SSF-54   Imager percent coverage

This parameter is the effective area of the CERES FOV observed by the imager which could be identified as clear or cloudy (See Note-7). (percent) [0 .. 100] (See Table 5-8)

For SSF data sets with CC# 014011 or greater, all full and partial Earth view FOVs containing at least one imager pixel are recorded on the SSF. Therefore, this parameter alone no longer determines whether or not a FOV is included on the SSF. To estimate the total amount of imager coverage for clear, cloudy and unknown pixels (See Note-7), this parameter must be combined with the unknown cloud-mask coverage (See SSF-64). Since "imager percent coverage" is obtained by rounding the real percent coverage to the nearest integer, it may be zero even though the number of imager pixels is non-zero. **Users should monitor "imager percent coverage" to determine which FOVs have adequate coverage for their application!**

For SSF data sets prior to CC# 014011, only full Earth view FOVs with at least 60% coverage and partial Earth view FOVs (See SSF-34-A) with at least 60% coverage are recorded on the SSF. Therefore, these older SSF data sets contain fewer FOVs.

An angular bin (See Term-2) within the FOV is considered "observed" if 1 or more imager pixels (See Term-27) are in the angular bin. All observed angular bins are PSF weighted to derive the percent coverage.

The "imager percent coverage" is computed as follows:

$$f^i_{known} = \frac{n^i_{known}}{n^i}$$

$$C_{imag} = \left(\frac{\sum\limits_{S_i} \omega_i f^i_{known}}{\sum\limits_{all\ bins} \omega_i} \right) \times 100$$

where

n^i is the total number of pixels in angular bin i (See Term-2)

n^i_{known} is the number of pixels identified as clear or cloudy

ω_i is the weight of the integral of the PSF over angular bin i (See Note-3.4)

S_i is the set of indices for clear/cloudy observed bins. ♠

SSF-55   Imager viewing zenith over CERES FOV

This parameter is the estimated viewing zenith angle of the imager pixels (See Term-27) that fall within this CERES FOV. The imager viewing zenith angle is computed at the surface. (deg) [0 .. 90] (See Table 5-8)

When the imager data get convolved with the CERES FOV, a pixel is randomly selected from all the pixels that fall within the four angular bins (See Term-2) surrounding the PSF centroid and for which a clear or cloudy determination could be made. The surface viewing zenith angle from that pixel is placed on the FOV. If there are no clear or cloudy pixels within these four angular bins, a clear or cloudy pixel is randomly selected from the twelve angular bins which are one bin removed from the PSF centroid, and the surface viewing zenith angle from that pixel is placed on the FOV. ♠

SSF-56   Imager relative azimuth angle over CERES FOV

This parameter is the estimated relative azimuth angle of the imager pixels (See Term-27) that fall within this CERES FOV. (deg) [0 .. 360]   (See Table 5-8)

When the imager data get convolved with the CERES FOV, a pixel is randomly selected from all the pixels that fall within the four angular bins (See Term-2) surrounding the PSF centroid and for which a clear or cloudy determination could be made. The surface relative azimuth angle from that pixel is placed on the FOV. If there are no pixels within these four angular bins, a clear or cloudy pixel is randomly selected from the twelve angular bins which are one bin removed from the PSF centroid, and the surface relative azimuth angle from that pixel is placed on the FOV.

When operating in a crosstrack scanning mode, the imager relative azimuth angle should be close to the CERES relative azimuth at surface (See SSF-20). ♠

SSF-57   Surface wind - U-vector

This parameter is the surface wind speed vector positive to the East.
(m sec^{-1}) [-100 .. 100] (See Table 5-8)

The surface wind speed vector value is obtained from the one degree, equal angle, MOA region containing the colatitude (See SSF-10) and longitude (See SSF-11) of CERES FOV at surface. A linear interpolation in the temporal domain produces the hourly MOA values from the six-hourly input data samples.

If the primary meteorological input data source for MOA is DAO GEOS-3, then this parameter is located at 10 meters above surface altitude.

If the primary meteorological input data source for MOA is ECMWF, then this parameter corresponds to the lowest level altitude in the ECMWF wind speed profile that has a valid wind speed. ECMWF wind speeds are provided for up to 31, 50, or 60 pressure levels depending on the model used. For the 31 level model, the bottom layer is at about 30 meters. For the 50 and 60 level models, the bottom level is at about 10 meters. ECMWF changes level models at various times. ♠

SSF-58   Surface wind - V-vector

This parameter is the surface wind speed vector positive to the North.
(m sec^{-1}) [-100 .. 100]   (See Table 5-8)

The surface wind speed vector value is obtained from the one degree, equal angle, MOA region containing the colatitude (See SSF-10✉ and longitude (See SSF-11✉ of CERES FOV at surface. A linear interpolation in the temporal domain produces the hourly MOA values from the six-hourly input data samples. A discussion of wind speed location as a function of meteorological input data source is given in SSF-57.♠

SSF-59   Surface skin temperature

This parameter is the MOA surface skin temperature. (K) [175 .. 375] (See Table 5-8)

For SSFs with CC# 011008, this parameter may be incorrect.

The surface skin temperature is the radiating temperature of the surface and has also been defined as the temperature 2 cm into the surface. Over Ocean, the MOA surface skin temperature corresponds to the Reynold's SST. It is different than the Imager-based surface skin temperature (See SSF-79), although the two should be similar. The surface skin temperature value is obtained from the MOA region containing the colatitude (See SSF-10) and longitude (See SSF-11) of CERES FOV at surface. ♠

SSF-60   Column averaged relative humidity

This parameter is the MOA column averaged relative humidity. (N/A) [0 .. 100] (See Table 5-8)

The column averaged relative humidity is obtained from the MOA region containing the colatitude (See SSF-10) and longitude (See SSF-11) of CERES FOV at surface. ♠

SSF-61   Precipitable water

This parameter is the water vapor burden from the surface to TOA in cm or, equivalently, g/cm^2. (cm) [0.001 .. 10] (See Table 5-8)

When the surface type is water (See SSF-25), microwave precipitable water is expected to be available. The microwave precipitable water source is the instantaneous SSM/I data. However, if microwave precipitable water is unavailable, meteorological precipitable water is used. FOVs with a surface type other than water will always have meteorological precipitable water.

MOA precipitable water will be at the same resolution as the source grid from where it was obtained; precipitable water does not get regrid to the CERES grid nor are the meteorological precipitable water and the microwave precipitable water necessarily on the same grid. Microwave precipitable water is currently on a 0.5 degree grid. The meteorological precipitable water grid is included in the source flag (See SSF-62).

This precipitable water value is used to compute the Model A LW and WN Surface fluxes (See SSF-42 and SSF-43) and may be needed to develop new ADMs. It is NOT used to compute the Model B LW Surface fluxes (See SSF-47). (The Model B LW surface algorithm always uses the meteorological precipitable water.) ♠

SSF-62   Flag - Source of precipitable water

This parameter indicates the source of the precipitable water value copied from MOA.
N/A) [0 .. 120] (See Table 5-8)

Possible values for this parameter are:

0 -	No precipitable water available	
1 -	meteorological precipitable water;	DAO on 2 x 2.5 grid
2 -	meteorological precipitable water;	DAO on 1 x 1 grid
3 -	meteorological precipitable water;	DAO on 1 x 1.25 grid
4 -	meteorological precipitable water;	NCEP on 94 x 192 grid
5 -	meteorological precipitable water;	ECMWF (31-levels) on nested CERES grid
6 -	meteorological precipitable water;	ECMWF (50-levels) on nested CERES grid
7 -	meteorological precipitable water;	DAO (1 x 1) on nested CERES grid
8 -	meteorological precipitable water;	ECMWF (60+ levels) on nested CERES grid
9 -	meteorological precipitable water;	DAO (1 x 1.25) on nested CERES grid
101 -	microwave precipitable water;	SSM/I data

If microwave precipitable water is used, 100 is added to the MOA Flag, Source Microwave
Column Precipitable Water and copied into this slot. If meteorological precipitable water is used,
the MOA Flag, Source Meteorological Profiles is directly copied into this slot. A flag value of 0
indicates no available source. Therefore, if this flag is 0 then precipitable water (See SSF-61) will
be set to the CERES default (See Table 4-5).

This parameter is based on MOA Flag, Source Microwave Column Precipitable Water and MOA
Flag, Source Meteorological Profiles. ♠

SSF-63   Cloud property extrapolation over cloudy area

This parameter is the percentage of the cloudy area which was lacking the basic cloud properties
required to determine cloud layer. (Percent) [0 .. 100] (See Table 5-8)

When "Cloud property extrapolation over cloudy area" is set to 0%, the CERES FOV does not
contain a mathematically significant amount of imager pixel (See Term-27) data for which cloud
properties and layers could not be determined. FOVs which contain only clear imager pixels
always have "Cloud property extrapolation over cloudy area" set to 0%. When the cloudy area
without cloud properties and layers is more than ten times larger than the cloudy area with layers
(See Note-8) or when the FOV contains only unknown pixels, this parameter is set to CERES
default (See Table 4-5) and the layer and overlap percent coverages (See SSF-81), as well as all
the cloud properties (See SSF-82 to SSF-114) are also set to CERES default. Otherwise, "Cloud
property extrapolation over cloudy area" is set to 1% or greater.

For a discussion of the types of pixels which may occur within a FOV see Note-8. "Cloud
property extrapolation over cloudy area" is computed as follows:

$$f_{cld}^{i} = \frac{n_{cld}^{i}}{n^{i}}$$

$$f_{nolayer}^i = \frac{n_{nolayer}^i}{n^i}$$

$$\text{Extrapolated Percentage} = \left(\frac{\sum\limits_{C_i} \omega_i f_{nolayer}^i}{\sum\limits_{C_i} \omega_i f_{cld}^i} \right) \times 100$$

where:

n^i is the number of pixels in angular bin i (See Term-2)

$n_{nolayer}^i$ is the number of cloudy pixels lacking cloud properties necessary for layering

n_{cld}^i is the number of cloudy pixels

ω_i is the integral of the PSF over bin i

C_i is the set of indices for observed bins containing one or more cloudy pixels ♠

SSF-64   Notes on general procedures

Prior to CC# 014011, no notes are defined.

This parameter is a collection of notes which are defined by single digits. The digits, from right to left, correspond to unknown cloud-mask (See SSF-64-A), 3 reserved digits, and aerosol A algorithm (See SSF-64-E). Unknown cloud-mask is referenced to the full FOV and derived from pixel level flags set by Cloud retrieval. (N/A) [0 .. 32766](See Table 5-8)
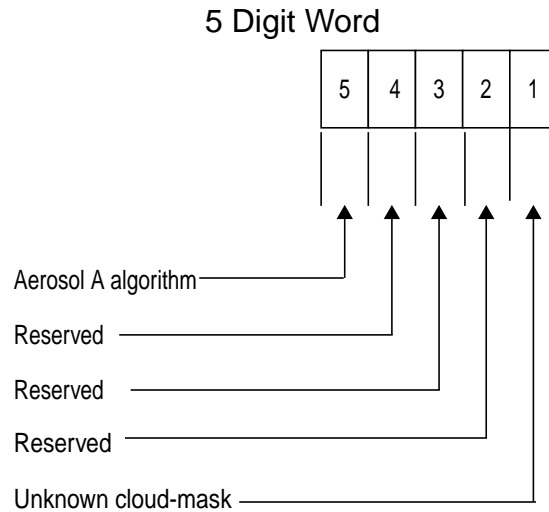
5 Digit Word

Figure 4-7. Notes on general procedures

Table 4-4. Mapping of percent coverage to digit

Digit Value	Range of actual PSF-weighted (See Term-29) percentage
0	0.0%
1	$0.0 < \% < 5.0$
2	$5.0 \leq \% < 20.0$
3	$20.0 \leq \% < 35.0$
4	$35.0 \leq \% < 50.0$
5	$50.0 \leq \% < 65.0$
6	$65.0 \leq \% < 80.0$
7	$80.0 \leq \% < 95.0$
8	$95.0 \leq \% < 100.0$
9	100.0%

SSF-64-A Unknown cloud-mask

If a pixel cannot be classified as clear or cloudy, it is classified as unknown (See Note-7). Unknown percent coverage combined with imager percent coverage (See SSF-54) provides total imager pixel coverage, which must be greater than 0 for the FOV to be included on the SSF. The unknown cloud-mask imager coverage is computed as follows and digitized according to Table 4-4:

$$f_k^i = \frac{n_k^i}{n^i}$$

$$\text{Percent Coverage} \quad = \left(\frac{\sum\limits_{S_i} \omega_i f_k^i}{\sum\limits_{S_i} \omega_i} \right) \times 100$$

where:

n^i is the number of pixels in angular bin i (See Term-2)

n_k^i is the number of pixels identified as unknown cloud-mask (k=1)

ω_i is the integral of the PSF over bin i

S_i is the set of indices for all observed bins

SSF-64-B Reserved

SSF-64-C Reserved

SSF-64-D Reserved

SSF-64-E Aerosol A algorithm
This parameter indicates which algorithm was used to compute the Aerosol A parameters SSF-73 through SSF-78. Aerosol A algorithm is set to 1 when the 2nd generation single channel NOAA/NESDIS retrieval algorithm is used. It is set to 0 when the 3rd generation two channel NOAA/NESDIS retrieval algorithm is used. If any other aerosol A algorithm is used, this digit is set to 2.

♠

SSF-65   Notes on cloud algorithms

For SSFs prior to CC# 014011, this parameter is incorrect and should not be used.

This parameter is a collection of cloud parameters which are defined by single digits. The digits, from right to left, correspond to saturated 3.7 μm imager radiance (See SSF-65-A), potential overlap (See SSF-65-B), cloud-strong (See SSF-65-C), cloud-weak/glint (See SSF-65-D), and reclassified clear (See SSF-65-E). All are referenced to the full FOV, and most are derived from pixel level flags set by Cloud retrieval. (N/A) [0 .. 32766] (See Table 5-8)

5 Digit Word

5	4	3	2	1

Reclassified clear
Cloud-weak/glint
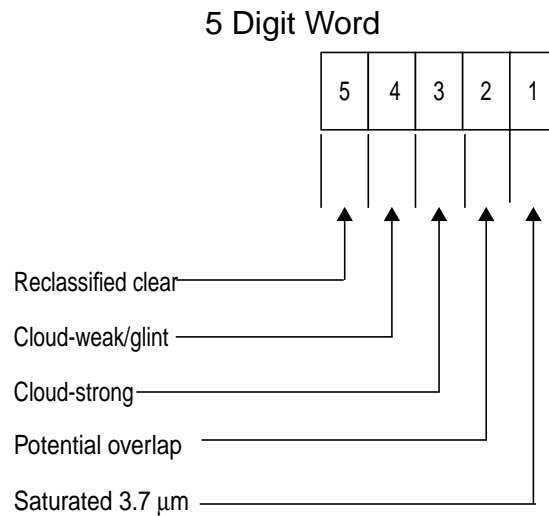Cloud-strong
Potential overlap
Saturated 3.7 μm

Figure 4-8. Notes on Cloud algorithms

SSF-65-A Saturated 3.7 μm
For MODIS, saturated 3.7 μm is set to 0.

For VIRS, there are cases when the imager 3.7 μm channel radiance is set to a default value and the processing algorithm can determine, by looking at the imager 10.8 μm channel radiance, that the 3.7 μm channel is saturated. In these cases, a maximum 3.7 μm radiance value is used internally, but it is not included in the imager radiance statistics (See SSF-118 through SSF-131). The saturated imager coverage is computed as follows and digitized according to Table 4-4:

$$f_k^i = \frac{n_k^i}{n^i}$$

$$\text{Percent Coverage} = \left(\frac{\sum\limits_{S_i} \omega_i f_k^i}{\sum\limits_{S_i} \omega_i} \right) \times 100$$

where:

n^i is the number of pixels in angular bin i (See Term-2)

n_k^i is the number of pixels identified as saturated (k=1), potential overlap (k=2), cloud-strong (k=3), or
    cloud-weak or glint-cloud (k=4)

ω_i is the integral of the PSF over bin i

S_i is the set of indices for clear/cloudy observed bins

SSF-65-B Potential overlap

Potential overlap is used to indicate what percentage of the full FOV contains overlap clouds for which only a single layer of cloud properties could be identified. A cloudy imager pixel (See Term-27) found to contain two cloud layers is said to contain overlap and the cloud properties are recorded in "Overlap condition weighted area percentage" (See SSF-81). Potential overlap pixels are processed as single layer pixels and their coverage is computed and recorded similar to saturated 3.7 µm above (See SSF-65-A). Potential overlap is computed using the 0.63 µm imager channel.

SSF-65-C Cloud-strong

Cloud-strong indicates what percentage range of the full FOV contains cloudy imager pixels (See Term-27) for which the subcategory was identified as cloudy-strong(See Note-7). Alternately stated, this digit represents the cloud-strong coverage normalized by the imager percent coverage area (See SSF-54). A second cloud-strong parameter is computed for those imager pixels which can be placed in a cloud layer (See SSF-82-A). Cloud-strong coverage is computed and recorded similar to saturated 3.7 µm above (See SSF-65-A).

SSF-65-D Cloud-weak/glint

Cloud-weak/glint indicates what percentage range of the full FOV contains cloudy imager pixels (See Term-27) for which the subcategory was identified either cloudy-weak or glint cloud(See Note-7). Alternately stated, this digit represents the combined cloud-weak and glint-cloud coverage normalized by the imager percent coverage area (See SSF-54). It differs from the individual cloud-weak (See SSF-82-B) and glint cloud (See SSF-82-C) parameters which are only computed for those imager pixels that can be placed in a cloud layer.
Cloud-weak/glint coverage is computed and recorded similar to saturated 3.7 µm above (See SSF-65-A).

SSF-65-E Reclassified Clear

Reclassified clear is set to 1 to indicate that the FOV contains one or more reclassified imager pixels. Otherwise, reclassified clear is set to 0. Reclassified clear pixels are those which could not be identified as clear or cloudy by the imager, but since the FOV is over land or desert (no snow) and the CERES WN channel radiance exceeds its threshold, these pixels are reclassified as clear. However, no subcategory information (See Note-7) can be associated with these pixels.

♠

4.3.10 Clear Footprint Area Definitions

The parameters in this group apply only to the clear (See Note-7) portion of the CERES FOV.

SSF-66 Clear area percent coverage at subpixel resolution

This parameter is computed from the highest resolution imager data available.
(percent) [0 .. 100]   (See Table 5-9)

When the number of clear or cloudy imager pixels (See SSF-53) is 0, this clear area percent coverage is set to CERES default (See Table 4-5).

For MODIS, a cloud mask will be derived from the 250m resolution visible channel data. This cloud mask is at a higher resolution than the cloud mask derived from the 1km MODIS channels (hence the term subpixel). The clear area percent coverage at subpixel (See Term-37) resolution is based upon the 250m cloud mask, whenever it is available. At night the 250m cloud mask is unavailable, and the clear area percent coverage at subpixel resolution is based on the 1km, or imager pixel (See Term-27) resolution, cloud mask.

For TRMM, the VIRS imager has only one resolution, 2km. Therefore, the clear area percent coverage at subpixel resolution is always based on the 2km, or imager pixel resolution, cloud mask.

From the cloud mask a cloud fraction is computed. See Note-2 for a complete description. The clear area percent coverage at subpixel resolution is based on the subpixel resolution cloud fraction and should not be confused with the clear area percent coverage at imager resolution (See Term-22). When the imager data are available at only one resolution, SSF-66 and SSF-116 will contain the same value. The clear area percent coverage is PSF-weighted (See Term-29). This variable will be set to 0 when the percent coverage is less than 0.5%.

Clear area percent coverage at subpixel resolution is computed as follows:

$$F_{cld} \;=\; \text{cloud fraction at subpixel resolution} \;=\; \left(\sum_{S_i} \omega_i f^{i}_{cld} \right) \Big/ \left(\sum_{S_i} \omega_i \right)$$

$$C^{*}_{clr} \;=\; (1 - F_{cld}) \times 100$$

where

ω_i is the weight of the integral of the PSF over angular bin i (See Term-2)

S_i is the set of indices for clear/cloudy observed bins

f^{i}_{cld} is the cloud fraction, at subpixel resolution, in bin i. ♠

SSF-67   Cloud-mask clear-strong percent coverage

This parameter is the PSF-weighted (See Term-29) percent of clear-strong (See Note-7) within the CERES FOV. (percent) [0 .. 100]   (See Table 5-8)

If all the pixels with in the FOV are identified as unknown or reclassified clear (See Note-7), this parameter is set to CERES default. The CERES cloud mask (See Note-7) identifies some clear pixels as clear-strong and their coverage is computed. If there are no clear-strong pixels in the FOV, then the coverage is set to 0. If there are clear-strong pixels in the FOV, the coverage is set to 1% or greater.

Clear-strong coverage is computed as follows:

$$f^{i}_{k} \;=\; \frac{n^{i}_{k}}{n^{i}}$$

$$\text{Percent Coverage} \;=\; \left(\frac{\displaystyle\sum_{S_i} \omega_i f^{i}_{k}}{\displaystyle\sum_{S_i} \omega_i} \right) \times 100$$

where:

n^i is the number of pixels in angular bin i (See Term-2)

n_k^i is the number of clear pixels identified as having the defined property

ω_i is the integral of the PSF over bin i

S_i is the set of indices for clear/cloudy observed bins ♠

SSF-68   Cloud-mask clear-weak percent coverage

This parameter is the PSF-weighted (See Term-29) percent of clear-weak (See Note-7) within the CERES FOV. (percent) [0 .. 100] (See Table 5-8)

If all the pixels with in the FOV are identified as unknown or reclassified clear (See Note-7), this parameter is set to CERES default. The CERES cloud mask (See Note-7) identifies some clear pixels as clear-weak and their coverage is computed and recorded similarly to clear-strong (See SSF-67). If there are no clear-weak pixels in the FOV, then the coverage is set to 0. Otherwise, the coverage is set to 1% or greater. ♠

SSF-69   Cloud-mask snow/ice percent coverage

This parameter is the PSF-weighted (See Term-29) percent of snow/ice (See Note-7) within the CERES FOV. This snow/ice coverage is different from the snow and ice surface types discussed in SSF-25. (percent) [0 .. 100] (See Table 5-8)

If all the pixels with in the FOV are identified as unknown or reclassified clear (See Note-7✉, this parameter is set to CERES default. The CERES cloud mask (See Note-7✉ identifies some clear pixels as snow/ice and their coverage is computed and recorded similarly to clear-strong (See SSF-67✉.   A determination of snow/ice is not attempted on cloudy pixels even though the parameter is based on the whole CERES FOV. To make this snow/ice assessment, a microwave snow/ice database is used, but not required. If there are no snow/ice pixels in the FOV, then the coverage is set to 0. Otherwise, the coverage is set to 1% or greater.   ♠

SSF-70   Cloud-mask aerosol B percent coverage

This parameter is the PSF-weighted (See Term-29) percent of aerosol (See Note-7) within the CERES FOV. The detected aerosol B types are defined in SSF-71. Aerosol B is different than aerosol A (See SSF-73 and SSF-74). (percent) [0 .. 100] (See Table 5-8)

If all the pixels with in the FOV are identified as unknown or reclassified clear (See Note-7), this parameter is set to CERES default. The CERES cloud mask (See Note-7) identifies some clear pixels as aerosol. These pixels are referred to as aerosol B pixels and their coverage is computed and recorded similarly to clear-strong (See SSF-67). If there are no aerosol B pixels in the FOV, then the coverage is set to 0. Otherwise, the coverage is set to 1% or greater.   ♠

SSF-71   Flag - Type of aerosol B

This parameter indicates the types of aerosol B which were detected in the CERES FOV and whose coverage was recorded in SSF-70. Aerosol B is different than aerosol A (See SSF-73 and SSF-74). (N/A) [0 .. 9999] (See Table 5-8)

This flag contains the aerosol type for the 4 most prevalent aerosol B types. The right most digit corresponds to the aerosol B type with the largest weighted percent coverage. The second right most digit identifies the second most prevalent aerosol B type, etc.

The defined aerosol B types are:
>   1 - smoke
>   2 - dust (blowing sand)
>   3 - ash (volcanic)
>   4 - oceanic haze
>   5 through 8 - reserved for future use
>   9 - other (not defined as one of the above)

Example:
>   Aerosol B percent coverage (See SSF-70) = 90
>   Flag - type of aerosol B = 12

Dust and smoke cover 90% of the CERES FOV. There is more dust (2) than smoke(1) in the CERES FOV.

If no aerosol B is identified within the CERES FOV, this parameter is set to default (See Table 4-5). The aerosol B type 9,"other", may be used when a combination of aerosols is detected in a single imager observation or when algorithms can't distinguish between two or more aerosol B types. For example, if dust and/or oceanic haze are detected at imager pixel (See Term-27) resolution, then the "other" aerosol B type is used. "Other" can also be used when the aerosol B type is unidentified, unknown, or undefined. These aerosols are different than aerosol A for which total aerosol optical depths are computed in SSF-73 and SSF-74. ♠

SSF-72   Cloud-mask percent coverage supplement

This parameter contains FOV information which is derived from the pixel level CERES cloud mask (See Note-7) determined by Cloud retrieval. The cloud-mask information includes the percentages of fire (See SSF-72-A), glint clear (See SSF-72-B), and cloud shadow (See SSF-72-C). Fire, glint clear and cloud shadow are referenced to the full FOV. (N/A) [0 .. 32766]   (See Table 5-9)

When the number of imager pixels (See SSF-53) is set to 0, fire, glint clear and cloud shadow coverages are unavailable. Since there is no default value associated with a single digit, 0 is also used to denote that coverage is unavailable. Users can determine when clear cloud-mask subcategory information is unavailable by examining those cloud-mask percent coverages which are saved as an integer (See SSF-67 through SSF-70). When those parameters contain a CERES default value, all subcategory coverages are unavailable.

5 Digit Word

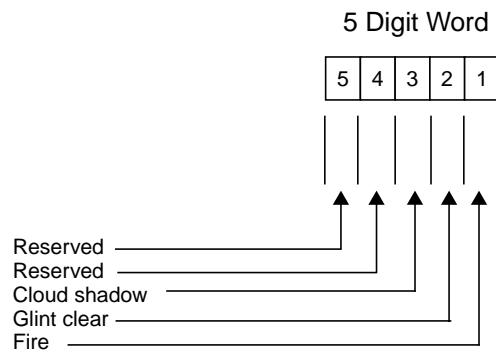| 5	4	3	2	1

Reserved
Reserved
Cloud shadow
Glint clear
Fire

Figure 4-9. Cloud-mask percent coverage supplement

SSF-72-A Fire

Fire coverage is computed similarly to clear-strong (See SSF-67) and digitized according to Table 4-4.

SSF-72-B Glint clear

Imager pixels (See Term-27) are defined as glint clear if the cloud-mask (See Note-7) algorithms determine the probability of sunglint to be greater than or equal to 10%. This is not CERES FOV sunglint. Glint clear is determined for imager pixels and pixel viewing geometry may differ from that of CERES. In crosstrack, the imager and CERES have the same observation geometry and imager sunglint is representative of CERES sunglint. For oblique FAPS observations and for RAPS observations, the imager observation geometry and the CERES observation geometry are different. Glint clear coverage is computed similarly to clear-strong (See SSF-67) and digitized according to Table 4-4.

SSF-72-C Cloud shadow

Cloud shadow coverage is computed similarly to clear-strong (See SSF-67) and digitized according to Table 4-4. ♠

SSF-73   Total aerosol A optical depth - visible

This parameter is a visible optical depth and is defined differently for each satellite. Aerosol A is different than aerosol B (See SSF-70 and SSF-71). (N/A) [-1..5] (See Table 5-9)

For TRMM, this parameter is the PSF-weighted (See Term-29) mean aerosol optical depth at 0.63 μm. Aerosol optical depths are computed over ocean for all aerosol A imager pixels (See Term-27) within the CERES FOV using the NOAA/NESDIS algorithm (See Reference 52). Aerosol A pixels are defined by the CERES Cloud Mask (See Note-7) as "clear-strong", "clear-weak", "clear-glint", or "aerosol". Cloudy pixels with a channel 3 reflectance less than 0.03 are also defined as aerosol A pixels. All aerosol A pixels must pass a 2 by 2 pixel homogeneous test on the 0.63 μm imager radiance. If the variance from the 4 neighboring pixels is greater than a threshold value, the scene is considered cloud contaminated and not used in the aerosol determination. If none of the aerosol A pixels within a CERES FOV have a valid optical depth, this parameter is set to the CERES default (See Table 4-5).

For TRMM, the PSF-weighted (See Term-29) mean aerosol optical depth, $\bar{\tau}_a$, area fraction, f_a, (See SSF-75 and SSF-76), and mean associated imager radiance, $\bar{I}_a$, (See SSF-77 and SSF-78) are computed as follows:

$$f_a^i = \frac{n_a^i}{n^i}$$

$$\bar{\tau}_a = \frac{\displaystyle\sum_{S_i} \omega_i f_a^i \bar{\tau}_a^i}{\displaystyle\sum_{S_i} \omega_i f_a^i}$$

$$f_a = \frac{\displaystyle\sum_{S_i} \omega_i f_a^i}{\displaystyle\sum_{S_i} \omega_i}$$

$$\bar{I}_a = \frac{\displaystyle\sum_{S_i} \omega_i f_a^i \bar{I}_a^i}{\displaystyle\sum_{S_i} \omega_i f_a^i}$$

$$\bar{\theta}_a = \frac{\displaystyle\sum_{S_i} \omega_i f_a^i \bar{\theta}_a^i}{\displaystyle\sum_{S_i} \omega_i f_a^i}$$

where

n^i is the total number of pixels in angular bin i (See Term-2)

n_a^i is the number of aerosol A pixels in bin i

f_a^i is the fraction of aerosol A pixels in bin i

$\bar{\tau}_a^i$ is the average optical depth of the aerosol A pixels in bin i

ω_i is the integral of the PSF over bin i

$\bar{\tau}_a$ is the PSF-weighted mean optical depth over the observed FOV

S_i is the set of indices for clear/cloudy observed bins

f_a is the PSF-weighted fraction of aerosol A pixels over the observed FOV

$\bar{I}_a^i$ is the average imager radiance of the aerosol A pixels in bin i

$\bar{I}_a$ is the PSF-weighted mean imager radiance over the observed FOV

$\bar{\theta}_a$ is the PSF-weighted mean imager viewing zenith angle over the observed FOV

For Terra the source of the mean visible optical depth is TBD. ♠

SSF-74   Total aerosol A optical depth - near IR

This parameter is a near IR optical depth and is defined differently for each satellite. Aerosol A is different than aerosol B (See SSF-70 and SSF-71). (N/A) [-1..5] (See Table 5-9)

For TRMM, this parameter is the PSF-weighted (See Term-29) mean aerosol optical depth at 1.61 μm. Aerosol optical depths are computed over ocean for all aerosol A imager pixels (See Term-27) within the CERES FOV using the NOAA/NESDIS algorithm (See Reference 52). Aerosol A pixels are defined by the CERES Cloud Mask (See Note-7) as "clear-strong", "clear-weak", "clear-glint", or "aerosol". Cloudy pixels with a channel 3 reflectance less than 0.03 are also defined as aerosol A pixels. All aerosol A pixels must pass a 2 by 2 pixel homogeneous test on the 0.63 μm imager radiance. If the variance from the 4 neighboring pixels is greater than a threshold value, the scene is considered cloud contaminated and not used in the aerosol determination. If none of the aerosol A pixels within a CERES FOV have a valid optical depth, this parameter is set to the CERES default (See Table 4-5).

For TRMM, the equations for the PSF-weighted mean aerosol optical depth, $\bar{\tau}_a$, area fraction, f_a, (See SSF-75 and SSF-76), and mean associated imager radiance, $\bar{I}_a$, (See SSF-77 and SSF-78) are given under SSF-73.

For Terra, the mean near IR optical depth is derived from the MOA product. TBD ♠

SSF-75   Aerosol A supplement 1

This parameter is a supplement to the aerosol A optical depth parameters (See SSF-73 and SSF-74) and is defined differently for each satellite. Aerosol A is different than aerosol B (See SSF-70 and SSF-71). (N/A) [-1000..1000] (See Table 5-9)

For TRMM this parameter is the PSF-weighted (See Term-29) area fraction in percent over the CERES FOV associated with the mean aerosol optical depth at 0.63 μm (See SSF-73). See SSF-73 for the equations.

For Terra this parameter is derived from the MOA product. TBD ♠

SSF-76   Aerosol A supplement 2

This parameter is a supplement to the aerosol A optical depth parameters (See SSF-73 and SSF-74) and is defined differently for each satellite. Aerosol A is different than aerosol B (See SSF-70 and SSF-71). (N/A) [-1000..1000] (See Table 5-9)

For TRMM this parameter is the PSF-weighted mean (See Term-30) imager radiance associated with the mean aerosol optical depth at 0.63 μm (See SSF-73). See SSF-73 for the equations.

For Terra this parameter is derived from the MOA product. TBD ♠

SSF-77   Aerosol A supplement 3

This parameter is a supplement to the aerosol A optical depth parameters (See SSF-73 and SSF-74) and is defined differently for each satellite. Aerosol A is different than aerosol B (See SSF-70 and SSF-71). (N/A) [-1000..1000] (See Table 5-9)

For TRMM this parameter is the PSF-weighted mean (See Term-30) imager viewing zenith angle at surface associated with the mean aerosol optical depth at 0.63 µm (See SSF-74). See SSF-73 for the equations.

For Terra this parameter is derived from the MOA product. TBD ♠

SSF-78   Aerosol A supplement 4

This parameter is a supplement to the aerosol A optical depth parameters (See SSF-73 and SSF-74) and is defined differently for each satellite. Aerosol A is different than aerosol B (See SSF-70 and SSF-71). (N/A) [-1000..1000] (See Table 5-9)

For TRMM this parameter is the PSF-weighted mean (See Term-30) imager radiance associated with the mean aerosol optical depth at 1.61 µm (See SSF-74). See SSF-73 for the equations.

For Terra this parameter is derived from the MOA product. TBD ♠

SSF-79   Imager-based surface skin temperature

This parameter is estimated from the clear-sky 11 µm radiance using a narrowband radiative transfer algorithm that requires MOA temperature and humidity profile inputs.
(K) [175 .. 375] (See Table 5-9)

Subsystem 4.1 selects only those imager pixels (See Term-27) which are clear (See Note-7) and computes a surface skin temperature using the MOA temperature/humidity profile associated with the clear-sky imager pixels and Dave Kratz's correlated-K technique (See References 10 and Reference 12). In Subsystem 4.4, the derived surface skin temperatures are PSF-weighted (See Term-30) and averaged to compute a mean skin temperature. If none of the clear imager pixels have a valid surface skin temperature or if there are no clear imager pixels within the FOV, this variable is set to CERES default (See Table 4-5). The imager-based surface skin temperature is different than the MOA surface skin temperature (See SSF-59). ♠

SSF-80   Vertical temperature change

This parameter is computed by subtracting the air temperature at the pressure level 300 hPa below the surface pressure (surface pressure minus 300 hPa) from the Imager-based surface skin temperature (See SSF-79).   (K) [-30 .. 90] (See Table 5-9)

Since Imager-based surface skin temperature is defined only for the clear (See Note-7) portion of the CERES FOV, the vertical temperature change is defined only for the clear portion of the CERES FOV. The air temperature at surface pressure minus 300 hPa will be computed by interpolating the MOA temperature profile. This parameter may be used to develop new LW ADMs for clear sky conditions. ♠

4.3.11 Cloudy Footprint Area Definitions

The parameters in this group describe cloud coverages and the cloudy portion of the CERES FOV. The first parameter in the group contains coverage for four possible cloud conditions within a FOV: clear (See Note-7), lower layer cloud only, upper layer cloud only, and overlapping cloud layers. The conditions are reflected in the last SDS dimension, which is 4. The remaining parameters describe cloud properties for up to two distinct cloud layers within the cloudy portion of the CERES FOV. The cloud layers are reflected in the last SDS dimension, which is 2. The lowest cloud layer parameter value is always recorded before the upper layer value.

SSF-81   Clear/layer/overlap condition percent coverages

This parameter is the PSF-weighted (See Term-29) portion of the CERES FOV, at the imager resolution of the pixel (See Term-27), for clear sky and up to two cloud layer combinations (See Figure 4-10). (percent) [0 .. 100] (See Table 5-11)

The 4 coverages (See Figure 4-10) are:
1. clear (See Note-7)
2. lower cloud only
3. upper cloud only
4. upper over lower cloud

When the number of clear or cloudy imager pixels (See SSF-53) is 0, the entire array is set to CERES default (See Table 4-5).

Lower cloud layer coverage is obtained by adding the lower cloud only (2) percent coverage to the upper over lower cloud (4) percent coverage. **Likewise, upper cloud layer coverage is obtained by adding the upper cloud only(3) percent coverage to the upper over lower cloud (4) percent coverage**. The cloud layer parameters that follow (See SSF-82 thru SSF-114) are based on cloud cover for the entire corresponding layer, which includes overlap. Layer 1 corresponds to the layer lowest in height and layer 2, if it exists, is above layer 1. When a cloud layer percent coverage is 0 or CERES default (See Table 4-5), all the variables associated with that layer will be filled in with the CERES default (See Table 4-5).

If none of the 4 coverages for a given FOV are set to CERES default (See Table 4-5), their sum is 100 ± round off error. If there is only one cloud layer, its weighted area percentage is always recorded as the lower cloud coverage. Any of the conditions which are known not to exist within the CERES FOV have a weighted area percentage of 0. For example, if there is only one cloud layer, the upper cloud percent coverage and the upper over lower cloud percent coverage are set to 0. Similarly, if there are no clouds, the lower, upper, and upper over lower percent coverages are set to 0.

When layer and overlap coverage are not known, they are set to CERES default (See Table 4-5). For example, layer and overlap coverage are set to CERES default when the "Cloud property extrapolation over cloudy area" (See SSF-63) is set to CERES default. For a discussion about when layer information is estimated or determined to be unknown, refer to Note-8. Clear, layer, and overlap percent coverages are all set to CERES default when "Number of imager pixels in CERES FOV" (See SSF-53) is set to 0.

For a complete discussion about how cloud layers are detected and defined, refer to Note-2.

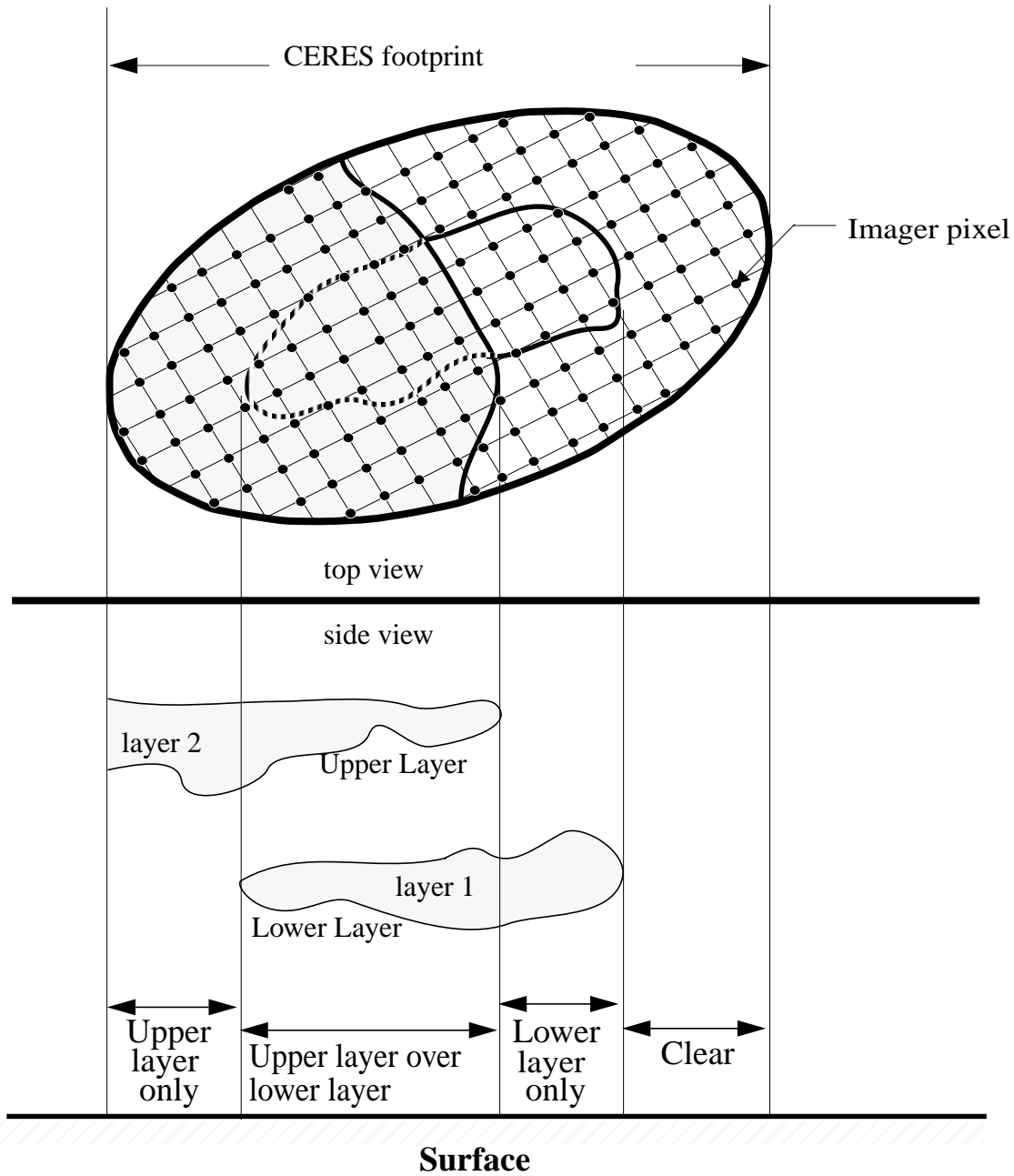Figure 4-10. CERES Clear/layer/overlap illustration

Clear area percent coverage is computed as follows:

$$C_{clr} = \left(\frac{\sum\limits_{S_i} \omega_i f_{clr}^i}{\sum\limits_{S_i} \omega_i} \right) \times 100$$

Lower cloud only area percent coverage is computed as follows:

$$C_{L1} = \left(\frac{\sum\limits_{S_i} \omega_i f^i_{L1}}{\sum\limits_{S_i} \omega_i} \right) \times 100$$

Upper cloud only area percent coverage is computed as follows:

$$C_{L2} = \left(\frac{\sum\limits_{S_i} \omega_i f^i_{L2}}{\sum\limits_{S_i} \omega_i} \right) \times 100$$

Upper over lower cloud overlap area percent coverage is computed as follows:

$$C_{L1/L2} = \left(\frac{\sum\limits_{S_i} \omega_i f^i_{L1/L2}}{\sum\limits_{S_i} \omega_i} \right) \times 100$$

where

ω_i is the weight of the integral of the PSF over angular bin i (See Term-2)

S_i is the set of indices for clear/cloudy observed bins

f^i_{clr} is the fraction of pixels which are clear in bin i

f^i_{L1} is the fraction of pixels which contain only lower cloud in bin i

f^i_{L2} is the fraction of pixels which contain only upper cloud in bin i

$f^i_{L1/L2}$ is the fraction of pixels containing upper cloud over lower cloud in bin i. ♠

SSF-82   Note for cloud layer

This parameter contains notes and supplemental cloud layer information. The right most digits represent coverage of cloud-strong (See SSF-82-A), cloud-weak (See SSF-82-B) and glint cloud (See SSF-82-C), as defined by the CERES cloud mask (See Note-7) and referenced to the cloud layer. This parameter is set to CERES default (See Table 4-5) when the corresponding cloud layer coverage is 0 or CERES default. (N/A) $[0 .. 2^{31-1}]$ (See Table 5-10)

10 Digit Word

10	9	8	7	6	5	4	3	2	1

Reserved

Reserved

Reserved

Reserved

Reserved

Reserved

Reserved

Glint cloud

Cloud-weak
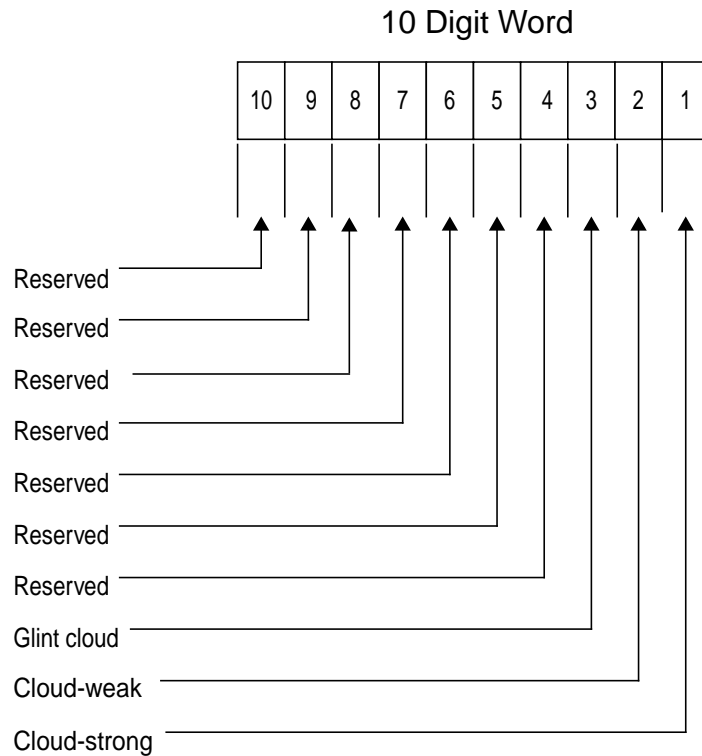
Cloud-strong

Figure 4-11. Cloud Layer Note

The CERES Cloud Mask (See Note-7) identifies a cloudy pixel (See Term-27) as cloud-strong, cloud-weak, or glint cloud. The coverages are computed as follows and digitized according to Table 4-4 :

$$ f_k^i = \frac{n_k^i}{n_{layer}^i} $$

$$ \text{Percent Coverage} = \left(\frac{\sum\limits_{C_i} \omega_i f_k^i}{\sum\limits_{C_i} \omega_i} \right) \times 100 $$

where:

n_{layer}^i is the number of cloud layer pixels in angular bin i (See Term-2)

n_k^i is the number of cloud layer pixels identified as cloud-strong (k=1), cloud-weak (k=2),

    and glint cloud (k=3) in the layer

ω_i is the integral of the PSF over bin i

C_i is the set of indices for observed bins containing cloud layer

layer is either 1, the lower layer, or 2, the higher layer

SSF-82-A Cloud-strong
Cloud-strong indicates the percentage of the layer for which cloud properties (SSF-83 to SSF-114) correspond to strong cloud pixels. A second cloud-strong parameter (See SSF-65-C) is also computed for all cloudy imager pixels within the FOV.

SSF-82-B Cloud-weak
Cloud-weak indicates the percentage of the layer for which cloud properties (SSF-83 to SSF-114) correspond to weak cloud pixels. A second parameter, which combines cloud-weak and glint cloud for all cloudy imager pixels within the FOV, is also computed (See SSF-65-D).

SSF-82-C Glint -cloud
Glint cloud indicates the percentage of the layer for which cloud properties (SSF-83 to SSF-114) correspond to pixels with a high likelihood of sunglint. A second parameter, which combines cloud-weak and glint cloud for all cloudy imager pixels within the FOV, is also computed (See SSF-65-D).

    ♠

SSF-83   Mean visible optical depth for cloud layer

This parameter is a PSF-weighted mean (See Term-30) of the visible optical depth values associated with imager pixels (See Term-27) which fall within the current CERES FOV and have a cloud at the corresponding height layer. (N/A) [0 .. 400] (See Table 5-10)

The bin-averaged values are weighted by the imager pixel fraction of corresponding layer imager pixels to total imager pixels and PSF. See Note-2, equation (32) for an example and complete definition. If there are no imager pixels with valid optical depth values or if the corresponding cloud layer area percent coverage is set to 0 or CERES default (See Table 4-5), this variable is set to CERES default. At night the mean visible optical depth for cloud layer is always set to CERES default.

Mean cloud layer parameters are computed as follows:

$$\bar{p}_{layer} = \frac{\sum\limits_{S_i} \omega_i f_{layer}^i \bar{p}_{layer}^i}{\sum\limits_{S_i} \omega_i f_{layer}^i}$$

where

    ω_i is the weight of the integral of the PSF over angular bin i (See Term-2)

    S_i is the set of indices for clear/cloudy observed bins

    f_{layer}^i is the cloud layer fraction in bin i

$\bar{p}^i_{layer}$ is the cloud layer parameter value in bin i

layer is either 1, the lower layer, or 2, the higher layer
For each imager pixel, visible optical depth is determined iteratively.

If the cloud algorithm was unable to determine an optical depth for an optically thick pixel, a fill value of 128.0 is written to the cookiedough. Likewise, if the cloud algorithm was unable to determine an optical depth for an optically thin pixel, a fill value of 0.05 is written. ♠

SSF-84   Stddev of visible optical depth for cloud layer

This parameter is a PSF-weighted standard deviation (See Term-31) of the bin-averaged visible optical depth values associated with imager pixels (See Term-27) which fall within the current CERES FOV and have a cloud at the corresponding height layer.
(N/A) [0 .. 300] (See Table 5-10)

The bin-averaged values are weighted by the imager pixel fraction of corresponding layer imager pixels to total imager pixels and PSF. See Note-2 for an example and complete definition. If there are no imager pixels with valid optical depth values or if the corresponding cloud layer area percent coverage is set to 0 or CERES default (See Table 4-5), this variable is set to CERES default.

Stddev of cloud layer parameters are computed as follows:

$$S_{layer} = \left[\left(\frac{\sum\limits_{S_i} \omega_i f^i_{layer} (\bar{p}^i_{layer})^2}{\sum\limits_{S_i} \omega_i f^i_{layer}} \right) - (\bar{p}_{layer})^2 \right]^{\frac{1}{2}}$$

where
ω_i is the weight of the integral of the PSF over angular bin i (See Term-2)

S_i is the set of indices for clear/cloudy observed bins

f^i_{layer} is the cloud layer fraction in bin i

$\bar{p}^i_{layer}$ is the cloud layer parameter value in bin i

layer is either 1, the lower layer, or 2, the higher layer. ♠

SSF-85   Mean logarithm of visible optical depth for cloud layer

This parameter is the PSF-weighted mean (See Term-30) of the bin-averaged natural logarithms of the visible optical depth values associated with imager pixels (See Term-27) which fall within the current CERES FOV and have a cloud at the corresponding height layer.
(N/A) [-6 .. 6] (See Table 5-10)

See SSF-83 and Note-2 for an example and complete definition of a PSF-weighted mean. If there are no imager pixels with valid optical depth values or if the corresponding cloud layer area

percent coverage is set to 0 or CERES default (See Table 4-5), this variable is set to CERES default. ♠

SSF-86   Stddev of logarithm of visible optical depth for cloud layer

This parameter is a PSF-weighted standard deviation (See Term-31) of the bin-averaged natural logarithm of visible optical depth values associated with imager pixels (See Term-27) which fall within the current CERES FOV and have a cloud at the corresponding height layer.
(N/A) [0 .. 6]   (See Table 5-10)

See SSF-84 and Note-2 for an example and complete definition of a PSF-weighted standard deviation. If there are no imager pixels with valid optical depth values or if the corresponding cloud layer area percent coverage is set to 0 or CERES default (See Table 4-5), this variable is set to CERES default.   ♠

SSF-87   Mean cloud infrared emissivity for cloud layer

This parameter is a PSF-weighted mean (See Term-30) of the effective infrared emittance values associated with imager pixels (See Term-27) that fall within the current CERES FOV and have a cloud at the corresponding height layer. Effective emissivity is defined as the ratio of the difference between the observed and clear-sky radiance to the difference between the cloud emission radiance and the clear-sky radiance. Both infrared scattering and emission are included in this parameter. Because scattering tends to block radiation from the warmer, lower portions of the cloud, the observed radiance can be less than cloud emission radiance (i.e., the cloud appears colder than it really is). By definition, the effective emissivity in these cases will be greater than one. This condition occurs most often for optically thick clouds at large imager viewing zenith angles (See SSF-55), and for FOVs containing optically thick clouds that have an equivalent blackbody temperature that is within a few degrees of the clear-sky temperature.
(N/A) [0 .. 2] (See Table 5-10)

Nighttime IR emissivities were not recorded on the SSF data product prior to CC# 012009. Also, prior to CC# 012009, the range on IR emissivities was set to 0 .. 1, and imager pixels outside this range were not included in the PSF-weighted mean.

The bin-averaged values are weighted by the imager pixel fraction of corresponding layer imager pixels to total imager pixels and PSF. See SSF-83 and Note-2, equation (32) for an example and complete definition. If there are no imager pixels with valid infrared emissivity values or if the corresponding cloud layer area percent coverage is set to 0 or CERES default (See Table 4-5), this variable is set to CERES default. ♠

SSF-88   Stddev of cloud infrared emissivity for cloud layer

This parameter is a PSF-weighted standard deviation (See Term-31) of the bin-averaged infrared emissivity values associated with imager pixels (See Term-27) which fall within the current CERES FOV and have a cloud at the corresponding height layer.
(N/A) [0 .. 2]   (See Table 5-10)

Nighttime IR emissivities were not recorded on the SSF data product prior to CC# 012009. Also, prior to CC# 012009, the range on IR emissivities was set to 0 .. 1, and imager pixels outside this range were not included in the PSF-weighted mean.

The bin-averaged values are weighted by the imager pixel fraction of corresponding layer imager pixels to total imager pixels and PSF. See SSF-84 and Note-2, equation (34) for an example and complete definition. If there are no imager pixels with valid infrared emissivity values or if the corresponding cloud layer area percent coverage is set to 0 or CERES default (See Table 4-5), this variable is set to CERES default. ♠

SSF-89 Mean liquid water path for cloud layer (3.7)

This parameter is a PSF-weighted mean (See Term-30) of the water path values associated with imager pixels (See Term-27) which fall within the current CERES FOV and have a water particle phase (See SSF-107) for the cloud at the corresponding height layer. (g m^{-2}) [0 .. 10000] (See Table 5-10)

The bin-averaged values are weighted by the imager pixel fraction of corresponding layer imager pixels to total imager pixels and PSF. See SSF-83 and Note-2, equation (32) for an example and complete definition. If there are no imager pixels with valid liquid water path values or if the corresponding cloud layer area percent coverage is set to 0 or CERES default (See Table 4-5), this variable is set to CERES default.

Cloud retrieval computes the pixel liquid water path as a function of the optical depth and effective droplet radius. The extinction coefficient used in the equation is a function of the effective radius. The liquid water density is 1.0 g cm^{-1}. ♠

SSF-90 Stddev of liquid water path for cloud layer (3.7)

This parameter is a PSF-weighted standard deviation (See Term-31) of the bin-averaged water path values associated with imager pixels (See Term-27) which fall within the current CERES FOV and have a water particle phase (See SSF-107) for the cloud at the corresponding height layer.(g m^{-2}) [0 .. 8000] (See Table 5-10)

The bin-averaged values are weighted by the imager pixel fraction of corresponding layer imager pixels to total imager pixels and PSF. See SSF-84 and Note-2, equation (34) for an example and complete definition. If there are no imager pixels with valid liquid water path values or if the corresponding cloud layer area percent coverage is set to 0 or CERES default (See Table 4-5), this variable is set to CERES default. ♠

SSF-91 Mean ice water path for cloud layer (3.7)

This parameter is a PSF-weighted mean (See Term-30) of the ice water path values associated with imager pixels (See Term-27) which fall within the current CERES FOV and have an ice particle phase (See SSF-107) for the cloud at the corresponding height layer. (g m^{-2}) [0 .. 10000] (See Table 5-10)

The bin-averaged values are weighted by the imager pixel fraction of corresponding layer imager pixels to total imager pixels and PSF. See SSF-83 and Note-2, equation (32) for an example and

complete definition.   If there are no imager pixels with valid ice water path values or if the corresponding cloud layer area percent coverage is set to 0 or CERES default (See Table 4-5), this variable is set to CERES default.

Cloud retrieval computes the pixel ice water path W_{ice} from the effective diameter of ice particle D_e using the following regression formula, which is an update from Reference 44.

$$W_{ice} = A_0 D_e + A_1 D_e^2 + A_2 D_e^3 + \tau$$

$$A_0 = 0.259$$

$$A_1 = 8.19 \times 10^{-4}$$

$$A_2 = -8.8 \times 10^{-7}$$

and τ is the optical depth.

♠

SSF-92   Stddev of ice water path for cloud layer (3.7)

This parameter is a PSF-weighted standard deviation (See Term-31) of the bin-averaged water path values associated with imager pixels (See Term-27) which fall within the current CERES FOV and have an ice particle phase (See SSF-107) for the cloud at the corresponding height layer. $(g\ m^{-2})$ [0 .. 8000]   (See Table 5-10)

The bin-averaged values are weighted by the imager pixel fraction of corresponding layer imager pixels to total imager pixels and PSF. See SSF-84 and Note-2, equation (34) for an example and complete definition. If there are no imager pixels with valid ice water path values or if the corresponding cloud layer area percent coverage is set to 0 or CERES default (See Table 4-5), this variable is set to CERES default. ♠

SSF-93   Mean cloud top pressure for cloud layer

This parameter is a PSF-weighted mean (See Term-30) of the top pressure values associated with imager pixels (See Term-27) which fall within the current CERES FOV and have a cloud at the corresponding height layer. (hPa) [0 .. 1100]   (See Table 5-10)

The bin-averaged values are weighted by the imager pixel fraction of corresponding layer imager pixels to total imager pixels and PSF. See SSF-83 and Note-2, equation (32) for an example and complete definition. If there are no imager pixels with valid cloud top pressure values or if the corresponding cloud layer area percent coverage is set to 0 or CERES default (See Table 4-5), this variable is set to CERES default.

Based on the phase, effective cloud temperature, and the cloud emissivity, cloud retrieval uses a set of empirical formulae to compute the emissivity relative to the physical top of the cloud rather than to the effective height of the cloud. This cloud-top emissivity is used to compute an estimate of cloud-top radiance using the clear-sky and observed radiances. Cloud-top radiance is converted to cloud-top temperature using the inverse Planck function. The MOA temperature and height profiles are linearly interpolated, and the height value that corresponds to the cloud-top

temperature is selected. The tops of clouds with large emissivities (> 0.99) are assumed to be the same as the cloud effective height. The cloud-top pressure is obtained from the cloud height using the interpolated MOA profiles. Cloud top pressure is not calculated at night. ♠

SSF-94   Stddev of cloud top pressure for cloud layer

This parameter is a PSF-weighted standard deviation (See Term-31) of the bin-averaged top pressure values associated with imager pixels (See Term-27) which fall within the current CERES FOV and have a cloud at the corresponding height layer. (hPa) [0 .. 600]   (See Table 5-10)

The bin-averaged values are weighted by the imager pixel fraction of corresponding layer imager pixels to total imager pixels and PSF. See SSF-84 and Note-2, equation (34) for an example and complete definition. If there are no imager pixels with valid cloud top pressure values or if the corresponding cloud layer area percent coverage is set to 0 or CERES default (See Table 4-5), this variable is set to CERES default. ♠

SSF-95   Mean cloud effective pressure for cloud layer

This parameter is a PSF-weighted mean (See Term-30) of the effective pressure values associated with imager pixels (See Term-27) which fall within the current CERES FOV and have a cloud at the corresponding height layer. (hPa) [0 .. 1100]   (See Table 5-10)

The bin-averaged values are weighted by the imager pixel fraction of corresponding layer imager pixels to total imager pixels and PSF. See SSF-83 and Note-2, equation (32) for an example and complete definition. If there are no imager pixels with valid cloud effective pressure values or if the corresponding cloud layer area percent coverage is set to 0, or CERES default (See Table 4-5), this variable is set to CERES default.

Cloud retrieval determines the pixel cloud effective pressure after obtaining the cloud effective height (See SSF-99). A linear interpolation of the natural logarithm of pressures from the MOA profile levels that bracket the cloud effective height is performed. The logarithm of pressure is then converted back. A linear regression for each layer of the MOA profile is performed producing a slope and intercept. ♠

SSF-96   Stddev of cloud effective pressure for cloud layer

This parameter is a PSF-weighted standard deviation (See Term-31) of the bin-averaged effective pressure values associated with imager pixels (See Term-27) which fall within the current CERES FOV and have a cloud at the corresponding height layer. (hPa) [0 .. 500]   (See Table 5-10)

The bin-averaged values are weighted by the imager pixel fraction of corresponding layer imager pixels to total imager pixels and PSF. See SSF-84 and Note-2, equation (34) for an example and complete definition. If there are no imager pixels with valid cloud effective pressure values or if the corresponding cloud layer area percent coverage is set to 0 or CERES default (See Table 4-5), this variable is set to CERES default. ♠

SSF-97   Mean cloud effective temperature for cloud layer

This parameter is a PSF-weighted mean (See Term-30) of the effective temperature values associated with imager pixels (See Term-27) which fall within the current CERES FOV and have a cloud at the corresponding height layer. (K) [100 .. 350]   (See Table 5-10)

The bin-averaged values are weighted by the imager pixel fraction of corresponding layer imager pixels to total imager pixels and PSF. See SSF-83 and Note-2, equation (32) for an example and complete definition. If there are no imager pixels with valid cloud effective temperature values or if the corresponding cloud layer area percent coverage is set to 0 or CERES default (See Table 4-5), this variable is set to CERES default.

Cloud effective temperature is the equivalent blackbody temperature of the cloud as seen from above. The temperature of the cloud generally decreases with increasing (decreasing) height (pressure). Thus, the radiation intensity from different layers of a cloud varies with temperature. An integration of that radiation over the cloud thickness, including the attentuation of radiation from lower parts of the cloud by the upper layers, defines the effective temperature. That temperature corresponds to some location between the cloud base and top. Cloud retrieval obtains cloud effective temperature for each pixel first by removing the effects of the atmosphere and any contribution of the surface to the observed 10.8-µm radiance and then using the inverse Planck function to convert the adjusted radiance to temperature. ♠

SSF-98   Stddev of cloud effective temperature for cloud layer

This parameter is a PSF-weighted standard deviation (See Term-31) of the bin-averaged effective temperature values associated with imager pixels (See Term-27) which fall within the current CERES FOV and have a cloud at the corresponding height layer. (K) [0 .. 150]   (See Table 5-10)

The bin-averaged values are weighted by the imager pixel fraction of corresponding layer imager pixels to total imager pixels and PSF. See SSF-84 and Note-2, equation (34) for an example and complete definition. If there are no imager pixels with valid cloud effective temperature values or if the corresponding cloud layer area percent coverage is set to 0 or CERES default (See Table 4-5), this variable is set to CERES default. ♠

SSF-99   Mean cloud effective height for cloud layer

This parameter is a PSF-weighted mean (See Term-30) of the effective height values associated with imager pixels (See Term-27) which fall within the current CERES FOV and have a cloud at the corresponding height layer. (km) [0 .. 20]   (See Table 5-10)

The bin-averaged values are weighted by the imager pixel fraction of corresponding layer imager pixels to total imager pixels and PSF. See SSF-83 and Note-2, equation (32) for an example and complete definition. If there are no imager pixels with valid cloud effective height values or if the corresponding cloud layer area percent coverage is set to 0 or CERES default (See Table 4-5), this variable is set to CERES default.

Cloud retrieval assigns cloud effective height to each cloudy imager pixels by linearly interpolating to the calculated cloud effective temperature (See SSF-97) using the MOA profiles of temperature and height. ♠

SSF-100   Stddev of cloud effective height for cloud layer

This parameter is a PSF-weighted standard deviation (See Term-31) of the bin-averaged effective height values associated with imager pixels (See Term-27) which fall within the current CERES FOV and have a cloud at the corresponding height layer. (km) [0 .. 12] (See Table 5-10)

The bin-averaged values are weighted by the imager pixel fraction of corresponding layer imager pixels to total imager pixels and PSF. See SSF-84 and Note-2, equation (34) for an example and complete definition. If there are no imager pixels with valid cloud effective height values or if the corresponding cloud layer area percent coverage is set to 0 or CERES default (See Table 4-5), this variable is set to CERES default. ♠

SSF-101   Mean cloud base pressure for cloud layer

This parameter is a PSF-weighted mean (See Term-30) of the base pressure values associated with imager pixels (See Term-27) which fall within the current CERES FOV and have a cloud at the corresponding height layer. (hPa) [0 .. 1100] (See Table 5-10)

The bin-averaged values are weighted by the imager pixel fraction of corresponding layer imager pixels to total imager pixels and PSF. See SSF-83 and Note-2, equation (32) for an example and complete definition. If there are no imager pixels with valid cloud base pressure values or if the corresponding cloud layer area percent coverage is set to 0 or CERES default (See Table 4-5), this variable is set to CERES default.

Cloud retrieval obtains cloud thickness from the effective temperature and the logarithm of the optical depth for clouds colder than 245 K. For warm clouds (temperature greater than 275 K), the thickness is related to the square root of the optical depth. For clouds between these temperatures, a linear interpolation between the thickness at the two extremes is performed. The minimum cloud thickness is 100 meters. The thickest cloud is limited by the maximum cloud height. Clouds must be a minimum of 100 meters above the surface. The cloud base height is obtained by subtracting the cloud thickness from the cloud height. The cloud bottom pressure is obtained from the cloud base height. This parameter is not calculated at night. ♠

SSF-102   Stddev of cloud base pressure for cloud layer

This parameter is a PSF-weighted standard deviation (See Term-31) of the bin-averaged base pressure values associated with imager pixels (See Term-27) which fall within the current CERES FOV and have a cloud at the corresponding height layer. (hPa) [0 .. 600] (See Table 5-10)

The bin-averaged values are weighted by the imager pixel fraction of corresponding layer imager pixels to total imager pixels and PSF. See SSF-84 and Note-2, equation (34) for an example and complete definition. If there are no imager pixels with valid cloud base pressure values or if the corresponding cloud layer area percent coverage is set to 0 or CERES default (See Table 4-5), this variable is set to CERES default. ♠

SSF-103   Mean water particle radius for cloud layer (3.7)

This parameter is a PSF-weighted mean (See Term-30) of bin-averaged spherical water droplet model particle radius values based on the 3.7 μm imager channel. It is associated with the imager

pixels (See Term-27) which fall within the current CERES FOV and have a cloud with water particle phase (See SSF-107) at the corresponding height layer. (µm) [0 .. 40] (See Table 5-10)

The bin-averaged values are weighted by the imager pixel fraction of corresponding layer imager pixels to total imager pixels and PSF. See SSF-83 and Note-2, equation (32) for an example and complete definition. If there are no imager pixels with valid water particle radius values or if the corresponding cloud layer area percent coverage is set to 0 or CERES default (See Table 4-5), this variable is set to CERES default.

Cloud retrieval computes water particle radius for each pixel iteratively. This parameter differs from the mean water particle radius based on the 1.6 µm imager channel (See SSF-108). ♠

SSF-104   Stddev of water particle radius for cloud layer (3.7)

This parameter is a PSF-weighted standard deviation (See Term-31) of bin-averaged spherical water droplet particle radius values based on the 3.7 µm imager channel. It is associated with the imager pixels (See Term-27) which fall within the current CERES FOV and have a cloud with water particle phase (See SSF-107) at the corresponding height layer. (µm) [0 .. 20] (See Table 5-10)

The bin-averaged values are weighted by the imager pixel fraction of corresponding layer imager pixels to total imager pixels and PSF. See SSF-84 and Note-2, equation (34) for an example and complete definition. If there are no imager pixels with valid water particle radius values or if the corresponding cloud layer area percent coverage is set to 0 or CERES default (See Table 4-5), this variable is set to CERES default. ♠

SSF-105   Mean ice particle effective diameter for cloud layer (3.7)

This parameter is a PSF-weighted mean (See Term-30) of the effective particle diameter values based on the 3.7 µm imager channel. It is associated with imager pixels (See Term-27) which fall within the current CERES FOV and have a cloud with ice particle phase (See SSF-107) at the corresponding height layer. (µm) [0 .. 300] (See Table 5-10)

The bin-averaged values are weighted by the imager pixel fraction of corresponding layer imager pixels to total imager pixels and PSF. See SSF-83 and Note-2, equation (32) for an example and complete definition. If there are no imager pixels with valid ice particle effective diameter values or if the corresponding cloud layer area percent coverage is set to 0 or CERES default (See Table 4-5), this variable is set to CERES default.

Cloud retrieval computes ice particle radius iteratively. This parameter differs from the mean ice particle diameter based on the 1.6 µm imager channel (See SSF-109). ♠

SSF-106   Stddev of ice particle effective diameter for cloud layer (3.7)

This parameter is a PSF-weighted standard deviation (See Term-31) of the bin-averaged effective particle diameter values based on the 3.7 µm imager channel. It is associated with imager pixels (See Term-27) which fall within the current CERES FOV and have a cloud with ice particle phase (See SSF-107) at the corresponding height layer.
(µm) [0 .. 200] (See Table 5-10)

The bin-averaged values are weighted by the imager pixel fraction of corresponding layer imager pixels to total imager pixels and PSF. See SSF-84 and Note-2, equation (34) for an example and complete definition. If there are no imager pixels with valid ice particle effective diameter values or if the corresponding cloud layer area percent coverage is set to 0 or CERES default (See Table 4-5), this variable is set to CERES default. ♠

SSF-107   Mean cloud particle phase for cloud layer (3.7)

This parameter is a PSF-weighted mean (See Term-30) of the particle phase values based on the 3.7 µm imager channel. It is associated with imager pixels (See Term-27) which fall within the current CERES FOV and have a cloud at the corresponding height layer. (N/A) [1 .. 2] (See Table 5-10)

A particle phase of 1.0 means the entire cloud is water. A particle phase of 2.0 means the entire cloud is ice. The bin-averaged values are weighted by the imager pixel fraction of corresponding layer imager pixels to total imager pixels and PSF. See SSF-83 and Note-2, equation (32) for an example and complete definition. If there are no imager pixels with valid cloud particle phase values or if the corresponding cloud layer area percent coverage is set to 0 or CERES default (See Table 4-5), this variable is set to CERES default.

During cloud retrieval, the particle radius and optical depth are iteratively solved to obtain water and ice model solutions that provide the difference between the 3.7 µm and 10.8 µm brightness temperatures that matches the observations. A set of tests are applied to select the ice or water solution. These tests depend on the availability of a particular solution, the effective cloud temperature, the location of the pixel radiances in a two-dimensional visible-infrared histogram, and the consistency of the solution with a comparison of the observed values to a corresponding set of model results for the 10.8 and 12.0 µm temperature difference. At night, when only infrared channels are available, the cloud retrieval algorithm selects the model (ice or water) result that best matches the 3.7, 10.8, and 12.0 µm observations. No pixel having an effective temperature above 273 K can be designated as an ice cloud pixel. Similarly, no pixel with a cloud temperature below 233 K can be assigned a phase of liquid water.

This parameter differs from the mean cloud particle phase based on the 1.6 µm imager channel (See SSF-110). ♠

SSF-108   Mean water particle radius for cloud layer (1.6)

This parameter is a PSF-weighted mean (See Term-30) of bin-averaged spherical water droplet model particle radius values based on the 1.6 µm imager channel. It is associated with the imager pixels (See Term-27) which fall within the current CERES FOV and have a cloud with water particle phase (See SSF-110) at the corresponding height layer. (µm) [0 .. 40] (See Table 5-10)

The bin-averaged values are weighted by the imager pixel fraction of corresponding layer imager pixels to total imager pixels and PSF. See SSF-83 and Note-2, equation (32) for an example and complete definition. If there are no imager pixels with valid water particle radius values or if the corresponding cloud layer area percent coverage is set to 0 or CERES default (See Table 4-5), this variable is set to CERES default.

This parameter differs from the mean water particle radius based on the 3.7 µm imager channel (See SSF-103). ♠

SSF-109 Mean ice particle effective diameter for cloud layer (1.6)

This parameter is a PSF-weighted mean (See Term-30) of the effective particle diameter values based on the 1.6 µm imager channel. It is associated with imager pixels (See Term-27) which fall within the current CERES FOV and have a cloud with ice particle phase (See SSF-110) at the corresponding height layer. (µm) [0 .. 300] (See Table 5-10)

The bin-averaged values are weighted by the imager pixel fraction of corresponding layer imager pixels to total imager pixels and PSF. See SSF-83 and Note-2, equation (32) for an example and complete definition. If there are no imager pixels with valid ice particle effective diameter values or if the corresponding cloud layer area percent coverage is set to 0 or CERES default (See Table 4-5), this variable is set to CERES default.

This parameter differs from the mean ice particle diameter based on the 3.7 µm imager channel (See SSF-105). ♠

SSF-110 Mean cloud particle phase for cloud layer (1.6)

This parameter is a PSF-weighted mean (See Term-30) of the particle phase values based on the 1.6 µm imager channel. It associated with imager pixels (See Term-27) which fall within the current CERES FOV and have a cloud at the corresponding height layer. (N/A) [1 .. 2] (See Table 5-10)

A particle phase of 1.0 means the entire cloud is water. A particle phase of 2.0 means the entire cloud is ice. The bin-averaged values are weighted by the imager pixel fraction of corresponding layer imager pixels to total imager pixels and PSF. See SSF-83 and Note-2, equation (32) for an example and complete definition. If there are no imager pixels with valid cloud particle phase values or if the corresponding cloud layer area percent coverage is set to 0 or CERES default (See Table 4-5), this variable is set to CERES default.

This parameter differs from the mean cloud particle phase based on the 3.7 µm imager channel (See SSF-107) and is not used in the algorithm which determines layers. ♠

SSF-111 Mean vertical aspect ratio for cloud layer

This parameter is a PSF-weighted mean (See Term-30) of the vertical aspect ratio values associated with imager pixels (See Term-27) which fall within the current CERES FOV and have a cloud at the corresponding height layer. (N/A) [0 .. 20] (See Table 5-10)

The bin-averaged values are weighted by the imager pixel fraction of corresponding layer imager pixels to total imager pixels and PSF. See SSF-83 and Note-2, equation (32) for an example and complete definition. If there are no imager pixels with valid vertical aspect ratio values or if the corresponding cloud layer area percent coverage is set to 0 or CERES default (See Table 4-5), this variable is set to CERES default.

Cloud retrieval currently has no algorithm to calculate cloud vertical aspect ratio. ♠

SSF-112   Stddev of vertical aspect ratio for cloud layer

This parameter is a PSF-weighted standard deviation (See Term-31) of the bin-averaged vertical aspect ratio values associated with imager pixels (See Term-27) which fall within the current CERES FOV and have a cloud at the corresponding height layer.
(N/A) [0 .. 15] (See Table 5-10)

The bin-averaged values are weighted by the imager pixel fraction of corresponding layer imager pixels to total imager pixels and PSF. See SSF-84 and Note-2, equation (34) for an example and complete definition. If there are no imager pixels with valid vertical aspect ratio values or if the corresponding cloud layer area percent coverage is set to 0 or CERES default (See Table 4-5), this variable is set to CERES default. ♠

SSF-113   Percentiles of visible optical depth for cloud layer (13)

This parameter contains the 1, 5, 10, 20, 30, 40, 50, 60, 70, 80, 90, 95, 99 percentiles, for the associated CERES FOV and cloud layer, of the visible optical depth. The percentiles are computed by ordering the visible optical depths from smallest to largest and picking off the values most representative of the designated percentiles. (N/A) [0 .. 400] (See Table 5-10)

When there are 100 or more imager pixels (See Term-27) falling within the cloud layer of the CERES FOV, the visible optical depths closest to the desired percentiles are most representative of the designated percentiles. For example, if there are 150 imager pixels then the 1st percentile is the smallest visible optical depth, the 5th percentile is the 7th smallest visible optical depth, the 10th percentile is the 15th smallest visible optical depth, and so on.

When there are fewer than 100 imager pixels falling within the cloud layer of the CERES FOV, the visible optical depths are evenly distributed and selected at the desired percentiles. For example, if there are 25 pixels, then the smallest visible optical depth corresponds to the 1st through 4th percentiles, second smallest visible optical depth corresponds to the 5th through 8th percentiles, the third smallest visible optical depth corresponds to the 9th through 12th percentiles, and so on.

If there are no imager pixels with valid optical depth values or if the corresponding cloud layer area percent coverage is set to 0 or CERES default (See Table 4-5⊠, this variable is set to CERES default. ♠

SSF-114   Percentiles of IR emissivity for cloud layer (13)

This parameter contains the 1, 5, 10, 20, 30, 40, 50, 60, 70, 80, 90, 95, 99 percentiles, for the associated CERES FOV and cloud layer, of the 11 μm effective emittance. Infrared scattering is included in this parameter. Therefore, at large imager viewing zenith angles (See SSF-55), an imager pixel containing an optically thick cloud with a low temperature contrast between the cloud and the surface may have effective IR emittance value greater than one. The percentiles are computed by ordering the IR emissivities from smallest to largest and picking off the values most representative of the designated percentiles. This is done in the manner described in SSF-113.
(N/A) [0 .. 2] (See Table 5-10).

Nighttime IR emissivities were not recorded on the SSF data product prior to CC# 012009. Also, prior to CC# 012009, the range on IR emissivities was set to 0 .. 1, and imager pixels outside this range were ignored. ♠

4.3.12 Footprint Imager Radiance Statistics Definitions

This parameter group contains imager radiance statistics over the CERES FOV for five imager channels and cloud cover at imager resolution for the FOV. Parameters which apply to each of the five imager channels have an SDS dimension of n x 5. Imager channel statistics are in the same order as the list of central wavelengths (See SSF-115).

SSF-115   Imager channel central wavelength

This parameter is an array of the 5 imager channel central wavelengths, in the order in which the footprint imager radiance statistics are recorded. (µm) [0.4 .. 15] (See Table 5-11)

The imager channel wavelengths for which radiance statistics are recorded can vary between footprints. The array location where the radiance statistics for a particular imager channel are recorded can also vary between footprints.

On an imager pixel (See Term-27) level, radiance values for all imager channels of possible interest are saved. Convolution then determines which 5 imager channels are of interest for this CERES FOV and records those imager channel central wavelengths, in order, in this array.   ♠

SSF-116   All subpixel clear area percent coverage

This parameter is discussed at length in Note-2. This parameter should not be confused with the clear percent coverage in SSF-81 or the clear area percent coverage at subpixel resolution (See SSF-66). However, when subpixel (See Term-37) resolution is unavailable, this parameter value will be equivalent to both SSF-66 and SSF-81 . (percent) [0 .. 100] (See Table 5-11)

When the number of clear or cloudy imager pixels (See SSF-53) is 0, this clear area percent coverage is set to CERES default (See Table 4-5).

An all subpixel clear pixel is defined as an imager pixel (See Term-27) that does not contain a single cloudy subpixel(See Term-37). All subpixel clear area percent coverage is computed as follows:

$$f^i_{clr} \ = \ n^i_{clr}/n^i$$

$$C_{clr} \ = \ \left(\frac{\sum\limits_{S_i} \omega_i f^i_{clr}}{\sum\limits_{S_i} \omega_i} \right) \times 100$$

Where:

   f^i_{clr} is the fraction of pixels which are all subpixel clear in bin i

   n^i_{clr} is the number of all subpixel clear pixels in bin i

n^i is the total number of pixels in bin i

ω_i is the integral of the PSF over the angular bin i (See Term-2)

S_i is the set of indices for clear/cloudy observed bins.

If this parameter is set to 0, then the clear footprint imager radiance statistics parameters (See SSF-118 and SSF-119) will be set to CERES default (See Table 4-5). ♠

SSF-117   All subpixel overcast cloud area percent coverage

This parameter is discussed at length in Note-2.   (percent) [0 .. 100] (See Table 5-11)

When the number of clear or cloudy imager pixels (See SSF-53) is 0, this overcast area percent coverage is set to CERES default (See Table 4-5).

An all subpixel overcast pixel is defined as an imager pixel (See Term-27) that does not contain a single clear subpixel(See Term-37). The all subpixel overcast area percent coverage is computed as follows:

$$f^i_{ov} = n^i_{ov}/n^i$$

$$C_{ov} = \left(\frac{\sum_{S_i} \omega_i f^i_{ov}}{\sum_{S_i} \omega_i} \right) \times 100$$

Where:

f^i_{ov} is the fraction of pixels which are all subpixel overcast in bin i

n^i_{ov} is the number of all subpixel overcast pixels in bin i

n^i is the total number of pixels in bin i

ω_i is the integral of the PSF over the angular bin i (See Term-2)

S_i is the set of indices for clear/cloudy observed bins.

If this parameter is set to 0, then the overcast footprint imager radiance statistics parameters (See SSF-120 and SSF-121) will be set to CERES default (See Table 4-5). ´

SSF-118   Mean imager radiances over clear area

This parameter is a PSF-weighted mean (See Term-30) of the radiance associated with all subpixel (See Term-37) clear area (See SSF-116) imager pixels (See Term-27) for each of the five channels used in processing the footprint (See SSF-115). The order in which the radiances are stored is specified in SSF-115. (W m^{-2} sr^{-1} μm^{-1}) [-1000 .. 1000] (See Table 5-11)

Most adjustments made to the imager pixel radiance values before they are used to determine clear/cloudy scenes (See Note-7) and any associated cloud properties, will be reflected in the all the imager radiance statistics (SSF-118 through SSF-131) recorded on the SSF. There is a 4 μm thermal leak in the VIRS 1.6 μm channel and the adjustment for this leak is reflected in all the VIRS 1.6 μm channel radiance statistics. The magnitude of this thermal leak is approximately the

same as low albedo scenes, such as over oceans. However, when the VIRS 3.75 μm channel imager pixel radiance is determined to be saturated, a maximum reflectance is used to compute cloud properties, but it is not included in any imager radiance statistics.

An arithmetic mean is taken of all imager pixels in the angular bin (See Term-2) before they are weighted by the imager pixel fraction of clear to total imager pixels and PSF. See Equation 41 in Note-2. If there are no clear imager pixels or if there are no imager pixels with valid imager radiance values, this variable is set to CERES default (See Table 4-5). Missing radiances will be filled by like values in the angular bin if available or by using the footprint arithmetic average.

Mean imager radiances over clear area for a given imager channel is computed as follows:

$$f^i_{clr} = n^i_{clr}/n^i$$

$$\bar{I}_{clr} = \frac{\sum\limits_{S_i} \omega_i f^i_{clr} \bar{I}^i_{clr}}{\sum\limits_{S_i} \omega_i f^i_{clr}}$$

Where:

f^i_{clr} is the fraction of pixels which are all subpixel clear (See SSF-116) in bin i

n^i_{clr} is the number of clear pixels in bin i

n^i is the total number of pixels in bin i

ω_i is the integral of the PSF over the angular bin i

S_i is the set of indices for clear/cloudy observed bins

$\bar{I}^i_{clr}$ is the average imager radiance of the clear pixels in bin i ♠

SSF-119   Stddev of imager radiances over clear area

This parameter is a PSF-weighted standard deviation (See Term-31) of the radiance associated with clear (See Note-7) imager pixels (See Term-27) for each of the five channels used in processing the footprint (See SSF-115). The order in which the radiances are stored is specified in SSF-115. (W m^{-2} sr^{-1} μm^{-1}) [0 .. 1000] (See Table 5-11)

Most adjustments made to the imager pixel radiances are reflected in the SSF imager radiance statistics. Refer to SSF-118 for a complete explanation and list of adjustments.

An arithmetic mean is taken of all imager pixels in the angular bin (See Term-2) before they are weighted by the imager pixel fraction of clear to total imager pixels and PSF. See Equation 42 in Note-2. If there are any clear imager pixels with valid imager radiance values within the CERES FOV, this variable will be set to the actual value, even if the clear area percent coverage rounds to 0. If there are no clear imager pixels or if there are no imager pixels with valid imager radiance values, this variable is set to CERES default (See Table 4-5). Missing radiances will be filled by like values in the angular bin if available or by using the footprint arithmetic average.

Stddev of imager radiances over clear area for a given imager channel is computed as follows:

$$f^i_{clr} \;=\; n^i_{clr} / n^i$$

$$S_{clr} \;=\; \left[\left(\frac{\displaystyle\sum_{S_i} \omega_i f^i_{clr} (\bar{I}^i_{clr})^2}{\displaystyle\sum_{S_i} \omega_i f^i_{clr}} \right) - (\bar{I}_{clr})^2 \right]^{1/2}$$

Where:

f^i_{clr} is the fraction of pixels which are clear (See Note-7) in bin i

n^i_{clr} is the number of clear pixels in bin i

n^i is the total number of pixels in bin i

ω_i is the integral of the PSF over the angular bin i

S_i is the set of indices for clear/cloudy observed bins

$\bar{I}^i_{clr}$ is the average imager radiance of the clear pixels in bin i

$\bar{I}_{clr}$ is mean imager radiances over clear area (See SSF-118). ♠

SSF-120   Mean imager radiances over overcast cloud area

This parameter is a PSF-weighted mean (See Term-30) of the radiance associated with overcast imager pixels (See Term-27) (defined as imager pixels with a cloud fraction percentage greater than or equal to 99) for each of the five channels used in processing the footprint (See SSF-115). The order in which the radiances are stored is specified in SSF-115. (W m^{-2} sr^{-1} μm^{-1}) [-1000 .. 1000] (See Table 5-11)

Most adjustments made to the imager pixel radiances are reflected in the SSF imager radiance statistics. Refer to SSF-118 for a complete explanation and list of adjustments.

An arithmetic mean is taken of all imager pixels in the angular bin (See Term-2) before they are weighted by the imager pixel fraction of overcast to total imager pixels and PSF. See Equation 43 in Note-2. If there are any overcast imager pixels with valid imager radiance values within the CERES FOV, this variable will be set to the actual value, even if the overcast area percent coverage rounds to 0. If there are no overcast imager pixels or if there are no imager pixels with valid imager radiance values, this variable is set to CERES default (See Table 4-5). Missing radiances will be filled by like values in the angular bin if available or by using the footprint arithmetic average.

Mean imager radiances over overcast cloud area for a given imager channel is computed as follows:

$$f^i_{ov} \;=\; n^i_{ov} / n^i$$

$$\bar{I}_{ov} = \frac{\sum_{S_i} \omega_i f^i_{ov} \bar{I}^i_{ov}}{\sum_{S_i} \omega_i f^i_{ov}}$$

Where:

f^i_{ov} is the fraction of pixels which are overcast in bin i

n^i_{ov} is the number of overcast pixels in bin i

n^i is the total number of pixels in bin i

ω_i is the integral of the PSF over the angular bin i

S_i is the set of indices for clear/cloudy observed bins

$\bar{I}^i_{ov}$ is the average imager radiance of the overcast pixels in bin i. ♠

SSF-121   Stddev of imager radiances over overcast cloud area

This parameter is a PSF-weighted standard deviation (See Term-31) of the radiance associated with overcast imager pixels (See Term-27) for each of the five channels used in processing the footprint (See SSF-115). The order in which the radiances are stored is specified in SSF-115. (W m^{-2} sr^{-1} μm^{-1}) [0 .. 1000] (See Table 5-11)

Most adjustments made to the imager pixel radiances are reflected in the SSF imager radiance statistics. Refer to SSF-118 for a complete explanation and list of adjustments.

An arithmetic mean is taken of all imager pixels in the angular bin (See Term-2) before they are weighted by the imager pixel fraction of overcast to total imager pixels and PSF. See Equation 44 in Note-2. If there are any overcast imager pixels with valid imager radiance values within the CERES FOV, this variable will be set to the actual value, even if the overcast area percent coverage rounds to 0. If there are no overcast imager pixels or if there are no imager pixels with valid imager radiance values, this variable is set to CERES default (See Table 4-5).

Stddev of imager radiances over overcast cloud area for a given imager channel is computed as follows:

$$f^i_{ov} = n^i_{ov}/n^i$$

$$S_{ov} = \left[\left(\frac{\sum_{S_i} \omega_i f^i_{ov} (\bar{I}^i_{ov})^2}{\sum_{S_i} \omega_i f^i_{ov}}\right) - (\bar{I}_{ov})^2\right]^{1/2}$$

Where:

f^i_{ov} is the fraction of pixels which are overcast in bin i

n^i_{ov} is the number of overcast pixels in bin i

n^i is the total number of pixels in bin i

ω_i is the integral of the PSF over the angular bin i

S_i is the set of indices for clear/cloudy observed bins

$\bar{I}_{ov}^i$ is the average imager radiance of the overcast pixels in bin i

$\bar{I}_{ov}$ is mean imager radiances over overcast area (See SSF-120). ♠

SSF-122   Mean imager radiances over full CERES FOV

This parameter is a PSF-weighted mean (See Term-30) of the radiance associated with all imager pixels (See Term-27) convolved in the current CERES FOV for each of the five channels used in processing the footprint (See SSF-115). The order in which the radiances are stored is specified in SSF-115.   (W m^{-2} sr^{-1} μm^{-1}) [-1000 .. 1000] (See Table 5-11)

Most adjustments made to the imager pixel radiances are reflected in the SSF imager radiance statistics. Refer to SSF-118 for a complete explanation and list of adjustments.

An arithmetic mean is taken of all imager pixels in the angular bin (See Term-2) before they are weighted by the PSF. See Equation 45 in Note-2. If there are any imager pixels with valid imager radiance values within the CERES FOV, this variable will be set to the actual value. If there are no imager pixels with valid imager radiance values, this variable is set to CERES default (See Table 4-5).

Mean imager radiances over full CERES FOV for a given imager channel is computed as follows:

$$\bar{I} = \frac{\sum\limits_{S_i} \omega_i \bar{I}^i}{\sum\limits_{S_i} \omega_i}$$

Where:

ω_i is the integral of the PSF over the angular bin i

S_i is the set of indices for clear/cloudy observed bins

$\bar{I}^i$ is the average imager radiance of the pixels in bin i. ♠

SSF-123   Stddev of imager radiances over full CERES FOV

This parameter is a PSF-weighted standard deviation (See Term-31) of the radiance associated with all imager pixels (See Term-27) convolved in the current CERES FOV for each of the five channels used in processing the footprint (See SSF-115). The order in which the radiances are stored is specified in SSF-115.   (W m^{-2} sr^{-1} μm^{-1}) [0 .. 1000] (See Table 5-11)

Most adjustments made to the imager pixel radiances are reflected in the SSF imager radiance statistics. Refer to SSF-118 for a complete explanation and list of adjustments.

An arithmetic mean is taken of all imager pixels in the angular bin (See Term-2) before they are weighted by the PSF. See Equation 46 in Note-2. If there are any imager pixels with valid imager radiance values within the CERES FOV, this variable will be set to the actual value. If there are

no imager pixels with valid imager radiance values, this variable is set to CERES default (See Table 4-5).

Stddev of imager radiances over full CERES FOV for a given imager channel is computed as follows:

$$
S = \left[\left(\frac{\sum_{S_i} \omega_i (\bar{I}^i)^2}{\sum_{S_i} \omega_i} \right) - \bar{I}^2 \right]^{1/2}
$$

Where:

ω_i is the integral of the PSF over the angular bin i

S_i is the set of indices for clear/cloudy observed bins

$\bar{I}^i$ is the average imager radiance of the pixels in bin i

$\bar{I}$ is mean imager radiances over full CERES FOV (See SSF-122). ♠

SSF-124   5th percentile of imager radiances over full CERES FOV

This parameter contains the 5th percentile of imager radiances for each of five spectral channels over each CERES FOV. The order in which the radiances are stored is specified in SSF-115.   (W m^{-2} sr^{-1} µm^{-1}) [-1000 .. 1000] (See Table 5-11)

Most adjustments made to the imager pixel radiances are reflected in the SSF imager radiance statistics. Refer to SSF-118 for a complete explanation and list of adjustments.

The 5th percentile is defined as the radiance value which is exceeded by 95 percent of the readings from that spectral channel. PSF-weighting is not used in the computation of this number. A minimum of 20 radiances are required to calculate these values. If 20 radiances are not available, this array is set to CERES default (See Table 4-5). ♠

SSF-125   95th percentile of imager radiances over full CERES FOV

This parameter contains the 95th percentile of imager radiances for each of five spectral channels over each CERES FOV. The order in which the radiances are stored is specified in SSF-115.   (W m^{-2} sr^{-1} µm^{-1}) [-1000 .. 1000] (See Table 5-11)

Most adjustments made to the imager pixel radiances are reflected in the SSF imager radiance statistics. Refer to SSF-118 for a complete explanation and list of adjustments.

The 95th percentile is defined as the radiance value exceeded by 5 percent of the readings from that spectral channel. PSF-weighting is not used in the computation of this number. A minimum of 20 radiances is required to calculate these values. If 20 radiances are not available, this array is set to CERES default (See Table 4-5). ♠

SSF-126   Mean imager radiances over cloud layer 1 (no overlap)

This parameter is a PSF-weighted mean (See Term-30) of the radiance associated with cloud layer 1 only imager pixels (See Term-27). The order in which the radiances are stored is specified in SSF-115.   (W m^{-2} sr^{-1} μm^{-1}) [-1000 .. 1000] (See Table 5-11)

Most adjustments made to the imager pixel radiances are reflected in the SSF imager radiance statistics. Refer to SSF-118 for a complete explanation and list of adjustments.

Cloud layer 1 only imager pixels are imager pixels not containing an upper layer corresponding with layer 2. A calculation is done for each of the five channels used in processing the footprint (See SSF-115). An arithmetic mean is taken of all imager pixels in the angular bin (See Term-2) before they are weighted by the imager pixel fraction of layer 1 only to total imager pixels and PSF. See Equation 49 in Note-2. If there are any layer 1 imager pixels with valid imager radiance values within the CERES FOV, this variable will be set to the actual value, even if the lower cloud overlap area percent coverage (See SSF-81) rounds to 0. If there are no cloud layer 1 only imager pixels or if there are no cloud layer 1 only imager pixels with valid imager radiance values, this variable is set to CERES default (See Table 4-5).

Mean imager radiances over cloud layer 1 (no overlap) for a given imager channel is computed as follows:

$$f^i_{L1} \ = \ n^i_{L1} / n^i$$

$$\bar{I}_{L1} \ = \ \frac{\displaystyle\sum_{S_i} \omega_i f^i_{L1} \bar{I}^i_{L1}}{\displaystyle\sum_{S_i} \omega_i f^i_{L1}}$$

Where:

f^i_{L1} is the fraction of pixels which contain only lower cloud in bin i

n^i_{L1} is the number of pixels containing only lower cloud in bin i

n^i is the total number of pixels in bin i

ω_i is the integral of the PSF over the angular bin i

S_i is the set of indices for clear/cloudy observed bins

$\bar{I}^i_{L1}$ is the average imager radiance of the pixels containing only lower cloud in bin i. ♠

SSF-127   Stddev of imager radiances over cloud layer 1 (no overlap)

This parameter is a PSF-weighted standard deviation (See Term-31) of the radiance associated with cloud layer 1 only imager pixels (See Term-27). The order in which the radiances are stored is specified in SSF-115.
(W m^{-2} sr^{-1} μm^{-1}) [0 .. 1000] (See Table 5-11)

Most adjustments made to the imager pixel radiances are reflected in the SSF imager radiance statistics. Refer to SSF-118 for a complete explanation and list of adjustments.

Cloud layer 1 only imager pixels are imager pixels not containing an upper layer corresponding with layer 2. A calculation is done for each of the five channels used in processing the footprint (See SSF-115). An arithmetic mean is taken of all imager pixels in the angular bin (See Term-2) before they are weighted by the imager pixel fraction of layer 1 only to total imager pixels and PSF. See Equation 50 in Note-2. If there are any layer 1 imager pixels with valid imager radiance values within the CERES FOV, this variable will be set to the actual value, even if the lower cloud overlap area percent coverage (See SSF-81) rounds to 0. If there are no cloud layer 1only imager pixels or if there are no cloud layer 1 only imager pixels with valid imager radiance values, this variable is set to CERES default (See Table 4-5).

Stddev of imager radiances over cloud layer 1 (no overlap) for a given imager channel is computed as follows:

$$f_{L1}^i = n_{L1}^i / n^i$$

$$S_{L1} = \left[\left(\frac{\sum\limits_{S_i} \omega_i f_{L1}^i (\bar{I}_{L1}^i)^2}{\sum\limits_{S_i} \omega_i f_{L1}^i} \right) - (\bar{I}_{L1})^2 \right]^{1/2}$$

Where:

f_{L1}^i is the fraction of pixels which contain only lower cloud in bin i

n_{L1}^i is the number of pixels containing only lower cloud in bin i

n^i is the total number of pixels in bin i

ω_i is the integral of the PSF over the angular bin i

S_i is the set of indices for clear/cloudy observed bins

$\bar{I}_{L1}^i$ is the average imager radiance of the pixels containing only lower cloud in bin i

$\bar{I}_{L1}$ is mean imager radiance over cloud layer 1 (no overlap) (See SSF-126). ♠

SSF-128 Mean imager radiances over cloud layer 2 (no overlap)

This parameter is a PSF-weighted mean (See Term-30) of the radiance associated with cloud layer 2 only imager pixels (See Term-27). The order in which the radiances are stored is specified in SSF-115. (W m^{-2} sr^{-1} μm^{-1}) [-1000 .. 1000] (See Table 5-11)

Most adjustments made to the imager pixel radiances are reflected in the SSF imager radiance statistics. Refer to SSF-118 for a complete explanation and list of adjustments.

Cloud layer 2 only imager pixels are imager pixels not containing a lower layer corresponding with layer 1. A calculation is done for each of the five channels used in processing the footprint (See SSF-115). An arithmetic mean is taken of all imager pixels in the angular bin (See Term-2) before they are weighted by the imager pixel fraction of layer 2 only to total imager pixels and PSF. See Equation 51 in Note-2. If there are any layer 2 imager pixels with valid imager radiance values within the CERES FOV, this variable will be set to the actual value, even if the upper cloud

overlap area percent coverage (See SSF-81) rounds to 0. If there are no cloud layer 2 only imager pixels or if there are no layer 2 only imager pixels with valid imager radiance values, this variable is set to CERES default (See Table 4-5).

Mean imager radiances over cloud layer 2 (no overlap) for a given imager channel is computed as follows:

$$f_{L2}^i \ = \ n_{L2}^i \big/ n^i$$

$$\bar{I}_{layer2} \ = \ \frac{\sum\limits_{S_i} \omega_i f_{L2}^i \bar{I}_{L2}^i}{\sum\limits_{S_i} \omega_i f_{L2}^i}$$

Where:

f^i_{L2} is the fraction of pixels which contain only upper cloud in bin i

n^i_{L2} is the number of pixels containing only upper cloud in bin i

n^i is the total number of pixels in bin i
ω_i is the integral of the PSF over the angular bin i
S_i is the set of indices for clear/cloudy observed bins

$\bar{I}^i_{L2}$ is the average imager radiance of the pixels containing only upper cloud in bin i. ♠

SSF-129   Stddev of imager radiances over cloud layer 2 (no overlap)

This parameter is a PSF-weighted standard deviation (See Term-31) of the radiance associated with cloud layer 2 only imager pixels (See Term-27). The order in which the radiances are stored is specified in SSF-115.
(W m^{-2} sr^{-1} µm^{-1}) [0 .. 1000] (See Table 5-11)

Most adjustments made to the imager pixel radiances are reflected in the SSF imager radiance statistics. Refer to SSF-118 for a complete explanation and list of adjustments.

Cloud layer 2 only imager pixels are imager pixels not containing a lower layer corresponding with layer 1. A calculation is done for each of the five channels used in processing the footprint (See SSF-115). An arithmetic mean is taken of all imager pixels in the angular bin (See Term-2) before they are weighted by the imager pixel fraction of layer 2 only to total imager pixels and PSF. See Equation 52 in Note-2. If there are any layer 2 imager pixels with valid imager radiance values within the CERES FOV, this variable will be set to the actual value, even if the upper cloud overlap area percent coverage (See SSF-81) rounds to 0. If there are no cloud layer 2 only imager pixels or if there are no cloud layer 2 only imager pixels with valid imager radiance values, this variable is set to CERES default (See Table 4-5).

Stddev of imager radiances over cloud layer 2 (no overlap) for a given imager channel is computed as follows:

$$f_{L2}^i \ = \ n_{L2}^i \big/ n^i$$

$$S_{L2} = \left[\left(\frac{\sum\limits_{S_i} \omega_i f^i_{L2}(\bar{I}^i_{L2})^2}{\sum\limits_{S_i} \omega_i f^i_{L2}}\right) - (\bar{I}_{L2})^2\right]^{1/2}$$

Where:

f^i_{L2} is the fraction of pixels which contain only upper cloud in bin i

n^i_{L2} is the number of pixels containing only upper cloud in bin i

n^i is the total number of pixels in bin i

ω_i is the integral of the PSF over the angular bin i

S_i is the set of indices for clear/cloudy observed bins

$\bar{I}^i_{L2}$ is the average imager radiance of the pixels containing only upper cloud in bin i

$\bar{I}_{L2}$ is mean imager radiance over cloud layer 2 (no overlap) (See SSF-128). ♠

SSF-130   Mean imager radiances over cloud layer 1 and 2 overlap

This parameter is a PSF-weighted mean (See Term-30) of the radiance associated with cloud imager pixels (See Term-27) that have two layers which correspond to layer 1 and 2 for each of five channels. The order of the five spectral channels is specified in SSF-115. (W m^{-2} sr^{-1} µm^{-1}) [-1000 .. 1000] (See Table 5-11)

Most adjustments made to the imager pixel radiances are reflected in the SSF imager radiance statistics. Refer to SSF-118 for a complete explanation and list of adjustments.

A calculation is done for each of the five channels used in processing the footprint (See SSF-115). An arithmetic mean is taken of all imager pixels in the angular bin (See Term-2) before they are weighted by the imager pixel fraction of overlap to total imager pixels and PSF. See Equation 53 in Note-2. If there are any layer 1 and 2 overlap imager pixels with valid imager radiance values within the CERES FOV, this variable will be set to the actual value, even if the upper over lower cloud overlap area percent coverage (See SSF-81) rounds to 0. If there are no overlap imager pixels or if there are no overlap imager pixels with valid imager radiance values, this variable is set to CERES default (See Table 4-5).

Mean imager radiances over cloud layer 1 and 2 overlap for a given imager channel is computed as follows:

$$f^i_{L1/L2} = n^i_{L1/L2}/n^i$$

$$\bar{I}_{L1/L2} = \frac{\sum\limits_{S_i} \omega_i f^i_{L1/L2} \bar{I}^i_{L1/L2}}{\sum\limits_{S_i} \omega_i f^i_{L1/L2}}$$

Where:

$f^i_{L1/L2}$ is the fraction of pixels which contain upper over lower cloud in bin i

$n^i_{L1/L2}$ is the number of pixels containing upper over lower cloud in bin i

n^i is the total number of pixels in bin i

ω_i is the integral of the PSF over the angular bin i

S_i is the set of indices for clear/cloudy observed bins

$\bar{I}^i_{L1/L2}$ is the average imager radiance of the pixels containing upper over lower cloud in bin i. ♠

SSF-131   Stddev of imager radiances over cloud layer 1 and 2 overlap

This parameter is a PSF-weighted standard deviation (See Term-31) of the radiance associated with cloud imager pixels (See Term-27) that have two layers which correspond to layer 1 and 2 for each of five spectral channels. The order of the five spectral channels is specified in SSF-115. (W m^{-2} sr^{-1} μm^{-1}) [0 .. 1000] (See Table 5-11)

Most adjustments made to the imager pixel radiances are reflected in the SSF imager radiance statistics. Refer to SSF-118 for a complete explanation and list of adjustments.

A calculation is done for each of the five channels used in processing the footprint (See SSF-115). An arithmetic mean is taken of all imager pixels in the angular bin (See Term-2) before they are weighted by the imager pixel fraction of overlap to total imager pixels and PSF. See Equation 54 in Note-2. If there are any layer 1 and 2 overlap imager pixels with valid imager radiance values within the CERES FOV, this variable will be set to the actual value, even if the upper over lower cloud overlap area percent coverage (See SSF-81) rounds to 0. If there are no overlap imager pixels or if there are no overlap imager pixels with valid imager radiance values, this variable is set to CERES default (See Table 4-5).

Stddev of imager radiances over cloud layer 1 and 2 overlap for a given imager channel is computed as follows:

$$f^i_{L1/L2} = n^i_{L1/L2}/n^i$$

$$S_{L1/L2} = \left[\left(\frac{\sum\limits_{S_i}\omega_i f^i_{L1/L2}(\bar{I}^i_{L1/L2})^2}{\sum\limits_{S_i}\omega_i f^i_{L1/L2}}\right) - (\bar{I}_{L1/L2})^2\right]^{1/2}$$

Where:

$f^i_{L1/L2}$ is the fraction of pixels which contain upper over lower cloud in bin i

$n^i_{L1/L2}$ is the number of pixels containing upper over lower cloud in bin i

n^i is the total number of pixels in bin i

ω_i is the integral of the PSF over the angular bin i

S_i is the set of indices for clear/cloudy observed bins

$\bar{I}^i_{L1/L2}$ is the average imager radiance of the pixels containing upper over lower cloud
    in bin i

$\bar{I}^i_{L1/L2}$ is mean imager radiance over cloud layer 1 and 2 overlap (See SSF-130). ♠

4.3.13 MODIS Land Aerosols

This parameter group does not exist on TRMM SSF data sets. It contains land aerosol
information from the MODIS MOD04_L2 (Terra) or MYD04_L2 (Aqua) aerosol products.
CERES does not alter the MODIS aerosol values or restrict them in any way. Since CERES does
not have the land and ocean database MODIS uses, the aerosols are assigned to pixels without
regard to the IGBP type, i.e. land aerosols can be assigned to water pixels. The aerosol product is
only available when the scene is illuminated by the sun. CERES only convolves the MODIS land
aerosol values with the CERES FOV. Users should, therefore, consult MODIS Atmosphere
documentation (http://modis-atmos.gsfc.nasa.gov/MOD04_L2/index.html) for parameter
definitions and known problems.

SSF-132   Percentage of CERES FOV with MODIS land aerosol

This parameter is the PSF-weighted (See Term-29) percent of   MODIS land aerosol coverage
within the CERES FOV. (percent) [0 .. 100] (See Table 5-12)

This parameter is referenced to the full FOV. If one or more MODIS pixels within the CERES
FOV contain land aerosol values, the percentage is set to 1% or greater.

In the cookiedough (See Term-6), all MODIS imager pixels which fall within the 10x10 km
spatial resolution of the MODIS aerosol product are assigned the MODIS land aerosol values
which apply to that region regardless of IGBP type. This allows the MODIS pixels to be treated
individually and allows the PSF-weighted aerosol parameters to be computed in a manner
consistent with the other SSF parameters.

Percentage of CERES FOV with MODIS land aerosol is computed as follows:

$$f^i_k = \frac{n^i_k}{n^i}$$

$$\text{Percent Coverage} = \left(\frac{\sum\limits_{S_i} \omega_i f^i_k}{\sum\limits_{S_i} \omega_i} \right) \times 100$$

where:

n^i is the number of pixels in angular bin i (See Term-2)

n_k^i is the number of pixels identified as having land/ocean aerosol values

ω_i is the integral of the PSF over bin i

S_i is the set of indices for observed bins ♠

SSF-133   PSF-wtd MOD04 cloud fraction land

This parameter is the PSF-weighted mean (See Term-30) of the MODIS Cloud_Fraction_Land within the current CERES FOV based on the value assigned to each imager pixel (See Term-27) within the FOV. (percent) [0 .. 100] (See Table 5-12)

An arithmetic mean is taken of all imager pixels in the angular bin (See Term-2) before they are weighted by the PSF. See Equation 45 in Note-2. If there are any imager pixels with valid MODIS Cloud_Fraction_Land values within the CERES FOV, this variable is set to the actual value. If there are no imager pixels with valid MODIS Cloud_Fraction_Land values, this variable is set to CERES default (See Table 4-5.).

Cloud fraction land is a mean aerosol property. Mean aerosol property over full CERES FOV is computed as follows:

$$\bar{\tau} = \frac{\sum_{S_i} \omega_i \bar{\tau}^i}{\sum_{S_i} \omega_i}$$

Where:

ω_i is the integral of the PSF over the angular bin i

S_i is the set of indices for the observed bins

$\bar{\tau}^i$ is the average aerosol property of the pixels in bin i.

In the cookiedough (See Term-6), all MODIS imager pixels which fall within the 10x10 km spatial resolution of the MODIS aerosol product are assigned the MODIS land aerosol values which apply to that region regardless of IGBP type. This allows the MODIS pixels to be treated individually and allows the PSF-weighted aerosol parameters to be computed in a manner consistent with the other SSF parameters. ♠

SSF-134   PSF-wtd MOD04 aerosol types land

This parameter contains FOV information which is derived from the pixel level MODIS Aerosol_Land_Type parameter. It includes the percentages of mixed, dust, sulfate, and smoke from right to left. These PSF-weighted percent coverages are referenced to the full FOV. (N/A) [0 .. 9999]   (See Table 5-12)

If no MODIS aerosol type land information is available for the footprint, this variable is set to CERES default (See Table 4-5.)
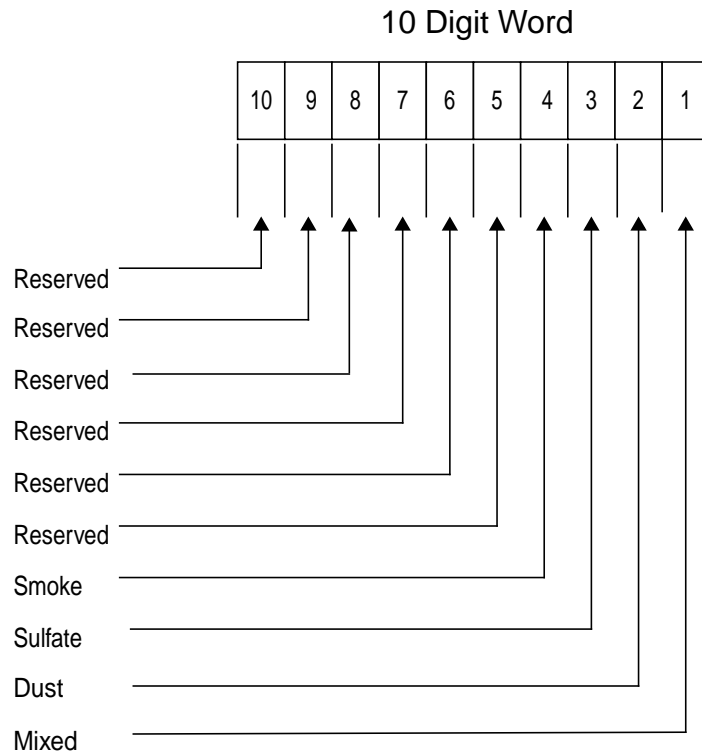
Figure 4-12. PSF-wtd MOD04 aerosol types land

The PSF-weighted percentage of CERES FOV of each aerosol type is separately calculated as the percentage of CERES FOV as shown in (See SSF-132). Each aerosol coverages is digitized according to Table 4-4. ♠

SSF-135   PSF-wtd MOD04 dust weighting factor land

This parameter is the PSF-weighted mean (See Term-30) of the MODIS Dust_Weighting_Factor_Land associated with all imager pixels (See Term-27) convolved in the current CERES FOV. (N/A) [0 .. 1] (See Table 5-12)

An arithmetic mean is taken of all imager pixels in the angular bin (See Term-2) before they are weighted by the PSF. The dust weighting factor land is a mean aerosol property. It is computed in the same manner as (See SSF-133). If there are any imager pixels with valid MODIS Dust_Weighting_Factor_Land values within the CERES FOV, this variable is set to the actual value. If there are no imager pixels with valid MODIS Dust_Weighting_Factor_Land values, this variable is set to CERES default (See Table 4-5.)♠

SSF-136   PSF-wtd MOD04 corrected optical depth land (0.470)

This parameter is the PSF-weighted mean (See Term-30) of the MODIS Corrected_Optical_Depth_Land at 0.470 μm associated with all imager pixels (See Term-27) convolved in the current CERES FOV. (N/A) [0 .. 3] (See Table 5-12)

An arithmetic mean is taken of all imager pixels in the angular bin (See Term-2) before they are weighted by the PSF. Corrected optical depth land at 0.470 μm is a mean aerosol property. It is computed in the same manner as (See SSF-133).   If there are any imager pixels with valid MODIS Corrected_Optical_Depth_Land at 0.470 μm values within the CERES FOV, this variable is set to the actual value. If there are no imager pixels with valid MODIS Corrected_Optical_Depth_Land at 0.470 μm values, this variable is set to CERES default (See Table 4-5.)♠

SSF-137   PSF-wtd MOD04 corrected optical depth land (0.550)

This parameter is the PSF-weighted mean (See Term-30) of the MODIS Corrected_Optical_Depth_Land at 0.550 μm associated with all imager pixels (See Term-27) convolved in the current CERES FOV. (N/A) [0 .. 3] (See Table 5-12)

An arithmetic mean is taken of all imager pixels in the angular bin (See Term-2) before they are weighted by the PSF. Corrected optical depth land at 0.550 μm is a mean aerosol property. It is computed in the same manner as (See SSF-133). If there are any imager pixels with valid MODIS Corrected_Optical_Depth_Land at 0.550 μm values within the CERES FOV, this variable is set to the actual value. If there are no imager pixels with valid MODIS Corrected_Optical_Depth_Land at 0.550 μm values, this variable is set to CERES default (See Table 4-5.)♠

SSF-138   PSF-wtd MOD04 corrected optical depth land (0.659)

This parameter is the PSF-weighted mean (See Term-30) of the MODIS Corrected_Optical_Depth_Land at 0.659 μm associated with all imager pixels (See Term-27) convolved in the current CERES FOV. (N/A) [0 .. 3] (See Table 5-12)

An arithmetic mean is taken of all imager pixels in the angular bin (See Term-2) before they are weighted by the PSF. Corrected optical depth land at 0.659 μm is a mean aerosol property. It is computed in the same manner as (See SSF-133). If there are any imager pixels with valid MODIS Corrected_Optical_Depth_Land at 0.659 μm values within the CERES FOV, this variable is set to the actual value. If there are no imager pixels with valid MODIS Corrected_Optical_Depth_Land at 0.659 μm values, this variable is set to CERES default (See Table 4-5.)♠

SSF-139   MOD04 number pixels percentile land (0.659) in CERES FOV

This parameter is the sum of the MODIS Number_Pixels_Percentile_Land at 0.659 μm associated with all imager pixels (See Term-27) in the current CERES FOV. (N/A) [0 .. 2147483647] (See Table 5-12)

A sum is calculated from all imager pixels in the CERES FOV that have valid Number_Pixels_Percentile_Land at 0.659 μm. If there are any imager pixels with valid MODIS Number_Pixels_Percentile_Land at 0.659 μm values within the CERES FOV, this variable is set to the actual value. If there are no imager pixels with valid MODIS

Number_Pixels_Percentile_Land at 0.659 µm values, this variable is set to CERES default (See Table 4-5.)

In the cookiedough (See Term-6), all MODIS imager pixels which fall within the 10x10 km spatial resolution of the MODISaerosol product are assigned the MODIS land aerosol values which apply to that region regardless of IGBP type. This allows the MODIS pixels to be treated individually.♠

SSF-140   PSF-wtd MOD04 mean reflectance land (0.470)

This parameter is the PSF-weighted mean (See Term-30) of the MODIS Mean_Reflectance_Land at 0.470 µm associated with all imager pixels (See Term-27) convolved in the current CERES FOV. (N/A) [0 .. 1] (See Table 5-12)

An arithmetic mean is taken of all imager pixels in the angular bin (See Term-2) before they are weighted by the PSF. Mean reflectance land at 0.470 µm is a mean aerosol property. It is computed in the same manner as (See SSF-133). If there are any imager pixels with valid MODIS Mean_Reflectance_Land at 0.470 µm values within the CERES FOV, this variable is set to the actual value. If there are no imager pixels with valid MODIS Mean_Reflectance_Land at 0.470 µm values, this variable is set to CERES default (See Table 4-5.)♠

SSF-141   PSF-wtd MOD04 mean reflectance land   (0.659)

This parameter is the PSF-weighted mean (See Term-30) of the MODIS Mean_Reflectance_Land at 0.659 µm associated with all imager pixels (See Term-27) convolved in the current CERES FOV. (N/A) [0 .. 1] (See Table 5-12)

An arithmetic mean is taken of all imager pixels in the angular bin (See Term-2) before they are weighted by the PSF. Mean reflectance land at 0.659 µm is a mean aerosol property. It is computed in the same manner as (See SSF-133). If there are any imager pixels with valid MODIS Mean_Reflectance_Land at 0.659 µm values within the CERES FOV, this variable is set to the actual value. If there are no imager pixels with valid MODIS Mean_Reflectance_Land at 0.659 µm values, this variable is set to CERES default (See Table 4-5.)♠

SSF-142   PSF-wtd MOD04 mean reflectance land (0.865)

This parameter is the PSF-weighted mean (See Term-30) of the MODIS Mean_Reflectance_Land at 0.865 µm associated with all imager pixels (See Term-27) convolved in the current CERES FOV. (N/A) [0 .. 1] (See Table 5-12)

An arithmetic mean is taken of all imager pixels in the angular bin (See Term-2) before they are weighted by the PSF. Mean reflectance land at 0.865 µm is a mean aerosol property. It is computed in the same manner as (See SSF-133). If there are any imager pixels with valid MODIS Mean_Reflectance_Land at 0.865 µm values within the CERES FOV, this variable is set to the actual value. If there are no imager pixels with valid MODIS Mean_Reflectance_Land at 0.865 µm values, this variable is set to CERES default (See Table 4-5.)♠

SSF-143   PSF-wtd MOD04 mean reflectance land (2.130)

This parameter is the PSF-weighted mean (See Term-30) of the MODIS MOD04 Mean_Reflectance_Land at 2.130 µm associated with all imager pixels (See Term-27) convolved in the current CERES FOV. (N/A) [0 .. 1] (See Table 5-12).

An arithmetic mean is taken of all imager pixels in the angular bin (See Term-2) before they are weighted by the PSF. Mean reflectance land at 2.130 µm is a mean aerosol property. It is computed in the same manner as (See SSF-133). If there are any imager pixels with valid MODIS Mean_Reflectance_Land at 2.130 µm values within the CERES FOV, this variable is set to the actual value. If there are no imager pixels with valid MODIS Mean_Reflectance_Land at 2.130 µm values, this variable is set to CERES default (See Table 4-5.)♠

SSF-144   PSF-wtd MOD04 mean reflectance land (3.750)

This parameter is the PSF-weighted mean (See Term-30) of the MODIS MOD04 Mean_Reflectance_Land at 3.750 µm associated with all imager pixels (See Term-27) convolved in the current CERES FOV. (N/A) [0 .. 1] (See Table 5-12)

An arithmetic mean is taken of all imager pixels in the angular bin (See Term-2) before they are weighted by the PSF. Mean reflectance land at 3.750 µm is a mean aerosol property. It is computed in the same manner as (See SSF-133). If there are any imager pixels with valid MODIS Mean_Reflectance_Land at 3.750 µm values within the CERES FOV, this variable is set to the actual value. If there are no imager pixels with valid MODIS Mean_Reflectance_Land at 3.750 µm values, this variable is set to CERES default (See Table 4-5.)♠

SSF-145   PSF-wtd MOD04 std reflectance land (0.470)

This parameter is the PSF-weighted mean (See Term-30) of the MODIS MOD04 STD_Reflectance_Land at 0.470 µm associated with all imager pixels (See Term-27) convolved in the current CERES FOV. (N/A) [0 .. 2] (See Table 5-12)

An arithmetic mean is taken of all imager pixels in the angular bin (See Term-2) before they are weighted by the PSF.   Standard deviation reflectance land at 0.470 µm is a mean aerosol property. It is computed in the same manner as (See SSF-133). If there are any imager pixels with valid MODIS STD_Reflectance_Land at 0.470 µm values within the CERES FOV, this variable is set to the actual value. If there are no imager pixels with valid MODIS STD_Reflectance_Land at 0.470 µm values, this variable is set to CERES default (See Table 4-5.)♠

4.3.14 MODIS Ocean Aerosols

This parameter group does not exist on TRMM SSF data sets. It contains ocean aerosol information from the MODIS MOD04_L2 (Terra) or MYD04_L2 (Aqua) aerosol products. CERES does not alter the MODIS aerosol values or restrict them in any way. Since CERES does not have the land and ocean database MODIS uses, the aerosols are assigned to pixels without regard to the IGBP type, i.e. ocean aerosols can be assigned to land pixels. This should be less likely then the reverse. MODIS only calculates ocean aerosols when there are no land pixels within the 10x10 km box. CERES only convolves the MODIS ocean aerosol values with the

CERES FOV. Users should, therefore, consult MODIS Atmosphere documentation (http://modis-atmos.gsfc.nasa.gov/MOD04_L2/index.html) for parameter definitions and known problems.

SSF-146   Percentage of CERES FOV with MODIS ocean aerosol

This parameter is the PSF-weighted (See Term-29) percent of   MODIS ocean aerosol coverage within the CERES FOV. (percent) [0 .. 100] (See Table 5-12)

This parameter is referenced to the full FOV. If one or more MODIS pixels within the CERES FOV contain ocean aerosol values, the percentage is set to 1% or greater. The percentage of CERES FOV for ocean aerosol is calculated as the percentage of CERES FOV as shown in (See SSF-132). ♠

SSF-147   PSF-wtd MOD04 cloud fraction ocean

This parameter is the PSF-weighted mean (See Term-30) of the MODIS Cloud_Fraction_Ocean within the current CERES FOV based on the value assigned to each imager pixel (See Term-27) within the FOV. (percent) [0 .. 100] (See Table 5-12)

An arithmetic mean is taken of all imager pixels in the angular bin (See Term-2) before they are weighted by the PSF. Cloud fraction ocean is a mean aerosol property. It is computed in the same manner as (See SSF-133).   If there are any imager pixels with valid MODIS Cloud_Fraction_Ocean values within the CERES FOV, this variable is set to the actual value. If there are no imager pixels with valid MODIS Cloud_Fraction_Ocean values, this variable is set to CERES default (See Table 4-5.) ♠

SSF-148   PSF-wtd MOD04 solution indices ocean small, average

This parameter contains CERES FOV information which is derived from the pixel level MODIS Solution_Index_Ocean_Small parameter. It includes the percentages that the five aerosol models are used (S_A - S_E). Using mean radius and standard deviation of the size distribution, they are 0.035, 0.40; 0.07, 0.40; 0.06, 0.60; 0.08, 0.60; and 1.00, 0.60 from right (A) to left (E). These PSF-weighted percent coverages are referenced to the full CERES FOV. (N/A) [0 .. 99999]   (See Table 5-12)

If no MODIS Solution_Index_Ocean_Small information is available for the footprint, this variable is set to CERES default (See Table 4-5.).

10 Digit Word
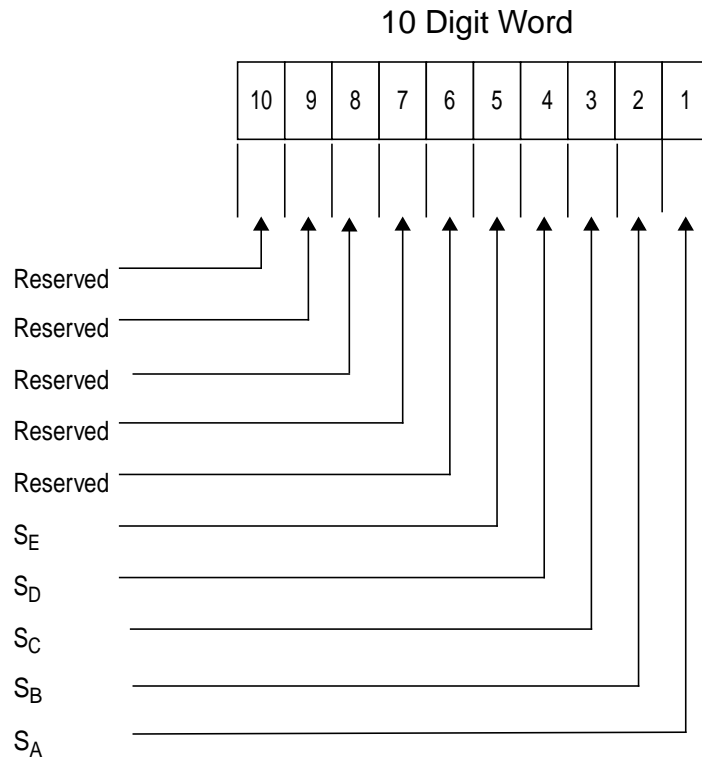
Figure 4-13. PSF-wtd MOD04 Solution Indices Ocean Small, Average

The percentage of CERES FOV for each model solution used is separately calculated as the percentage of CERES FOV as shown in (See SSF-132). Each aerosol coverages is digitized according to Table 4-4. ♠Each aerosol model used is separately calculated as other percentage of CERES FOV as shown in (See SSF-132). Each aerosol coverages is digitized according to Table 4-4. ♠

SSF-149   PSF-wtd MOD04 solution indices ocean large, average

This parameter contains CERES FOV information which is derived from the pixel level MODIS Solution_Index_Ocean_Large parameter. It includes the percentages that the six aerosol models are used (L_A - L_F). Using mean radius and standard deviation of the size distribution, they are 0.040, 0.60; 0.60, 0.60; 0.80, 0.60; 0.40, 0.60; 0.50, 0.80; and 1.00, 0.80 from right (A) to left (F). These PSF-weighted percent coverages are referenced to the full CERES FOV. (N/A) [0 .. 999999]   (See Table 5-12)

If no MODIS Solution_Index_Ocean_Large information is available for the footprint, this variable is set to CERES default (See Table 4-5.)

10 Digit Word
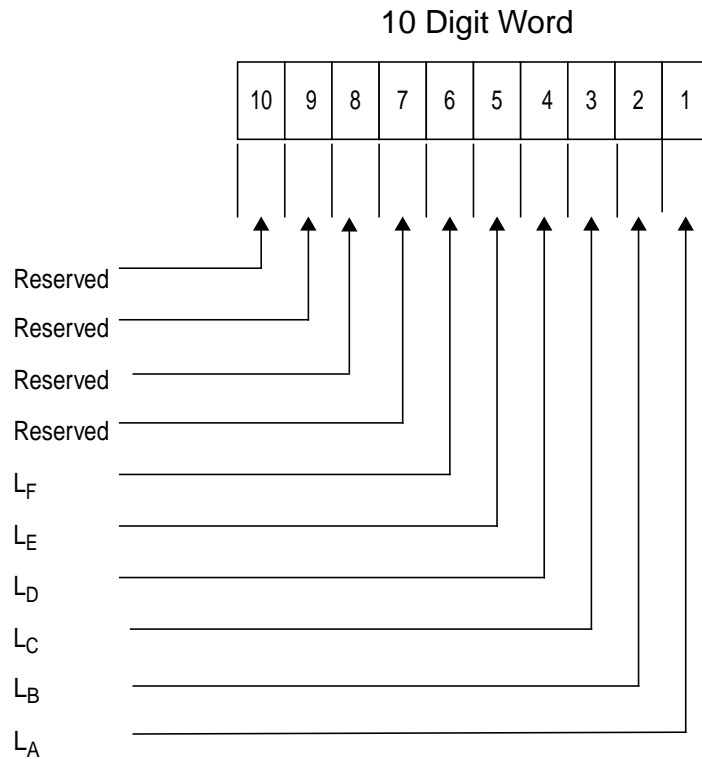
Figure 4-14. PSF-wtd MOD04 Solution Indices Ocean Large, Average

The percentage of CERES FOV for each model used is separately calculated as the percentage of CERES FOV as shown in (See SSF-132). Each aerosol coverages is digitized according to Table 4-4. ♠

SSF-150   PSF-wtd MOD04 effective optical depth average ocean (0.470)

This parameter is the PSF-weighted mean (See Term-30) of the MODIS MOD04 Effective_Optical_Depth_Average_Ocean at 0.470 µm associated with all imager pixels (See Term-27) convolved in the current CERES FOV. (N/A) [0 .. 3] (See Table 5-12)

An arithmetic mean is taken of all imager pixels in the angular bin (See Term-2) before they are weighted by the PSF. Effective optical depth average ocean at 0.470 µm is a mean aerosol property. It is computed in the same manner as (See SSF-133). If there are any imager pixels with valid MODIS Effective_Optical_Depth_Average_Ocean at 0.470 µm values within the CERES FOV, this variable is set to the actual value. If there are no imager pixels with valid MODIS Effective_Optical_Depth_Average_Ocean at 0.470 µm values, this variable is set to CERES default (See Table 4-5.) ♠

SSF-151   PSF-wtd MOD04 effective optical depth average ocean (0.550)

This parameter is the PSF-weighted mean (See Term-30) of the MODIS MOD04 Effective_Optical_Depth_Average_Ocean at 0.550 µm associated with all imager pixels (See Term-27) convolved in the current CERES FOV. (N/A) [0 .. 3] (See Table 5-12)

An arithmetic mean is taken of all imager pixels in the angular bin (See Term-2) before they are weighted by the PSF. Effective optical depth average ocean at 0.550 µm is a mean aerosol property. It is computed in the same manner as (See SSF-133).   If there are any imager pixels with valid MODIS Effective_Optical_Depth_Average_Ocean at 0.550 µm values within the CERES FOV, this variable will be set to the actual value. If there are no imager pixels with valid MODIS Effective_Optical_Depth_Average_Ocean at 0.550 µm values, this variable is set to CERES default (See Table 4-5.) ♠

SSF-152   PSF-wtd MOD04 effective optical depth average ocean (0.659)

This parameter is the PSF-weighted mean (See Term-30) of the MODIS MOD04 Effective_Optical_Depth_Average_Ocean at 0.659 µm associated with all imager pixels (See Term-27) convolved in the current CERES FOV. (N/A) [0 .. 3] (See Table 5-12)

An arithmetic mean is taken of all imager pixels in the angular bin (See Term-2) before they are weighted by the PSF. Effective optical depth average ocean at 0.659 µm is a mean aerosol property. It is computed in the same manner as (See SSF-133).   If there are any imager pixels with valid MODIS Effective_Optical_Depth_Average_Ocean at 0.659 µm values within the CERES FOV, this variable will be set to the actual value. If there are no imager pixels with valid MODIS Effective_Optical_Depth_Average_Ocean at 0.659 µm values, this variable is set to CERES default (See Table 4-5.) ♠

SSF-153   PSF-wtd MOD04 effective optical depth average ocean (0.865)

This parameter is the PSF-weighted mean (See Term-30) of the MODIS MOD04 Effective_Optical_Depth_Average_Ocean at 0.865 µm associated with all imager pixels (See Term-27) convolved in the current CERES FOV. (N/A) [0 .. 3] (See Table 5-12)

An arithmetic mean is taken of all imager pixels in the angular bin (See Term-2) before they are weighted by the PSF. Effective optical depth average ocean at 0.865 µm is a mean aerosol property. It is computed in the same manner as (See SSF-133). If there are any imager pixels with valid MODIS Effective_Optical_Depth_Average_Ocean at 0.865 µm values within the CERES FOV, this variable will be set to the actual value. If there are no imager pixels with valid MODIS Effective_Optical_Depth_Average_Ocean at 0.865 µm values, this variable is set to CERES default (See Table 4-5.) ♠

SSF-154   PSF-wtd MOD04 effective optical depth average ocean (1.240)

This parameter is the PSF-weighted mean (See Term-30) of the MODIS MOD04 Effective_Optical_Depth_Average_Ocean at 1.240 µm associated with all imager pixels (See Term-27) convolved in the current CERES FOV. (N/A) [0 .. 3] (See Table 5-12)

An arithmetic mean is taken of all imager pixels in the angular bin (See Term-2) before they are weighted by the PSF. Effective optical depth average ocean at 1.240 µm is a mean aerosol

property. It is computed in the same manner as (See SSF-133). If there are any imager pixels with valid MODIS Effective_Optical_Depth_Average_Ocean at 1.240 µm values within the CERES FOV, this variable will be set to the actual value. If there are no imager pixels with valid MODIS Effective_Optical_Depth_Average_Ocean at 1.240 µm values, this variable is set to CERES default (See Table 4-5.) ♠

SSF-155   PSF-wtd MOD04 effective optical depth average ocean (1.640)

This parameter is the PSF-weighted mean (See Term-30) of the MODIS MOD04 Effective_Optical_Depth_Average_Ocean at 1.640 µm associated with all imager pixels (See Term-27) convolved in the current CERES FOV. (N/A) [0 .. 3] (See Table 5-12)

An arithmetic mean is taken of all imager pixels in the angular bin (See Term-2) before they are weighted by the PSF. Effective optical depth average ocean at 1.640 µm is a mean aerosol property. It is computed in the same manner as (See SSF-133). If there are any imager pixels with valid MODIS Effective_Optical_Depth_Average_Ocean at 1.640 µm values within the CERES FOV, this variable will be set to the actual value. If there are no imager pixels with valid MODIS Effective_Optical_Depth_Average_Ocean at 1.640 µm values, this variable is set to CERES default (See Table 4-5.) ♠

SSF-156   PSF-wtd MOD04 effective optical depth average ocean (2.130)

This parameter is the PSF-weighted mean (See Term-30) of the MODIS MOD04 Effective_Optical_Depth_Average_Ocean at 2.130 µm associated with all imager pixels (See Term-27) convolved in the current CERES FOV. (N/A) [0 .. 3] (See Table 5-12)

An arithmetic mean is taken of all imager pixels in the angular bin (See Term-2) before they are weighted by the PSF. Effective optical depth average ocean at 2.130 µm is a mean aerosol property. It is computed in the same manner as (See SSF-133). If there are any imager pixels with valid MODIS Effective_Optical_Depth_Average_Ocean at 2.130 µm values within the CERES FOV, this variable will be set to the actual value. If there are no imager pixels with valid MODIS Effective_Optical_Depth_Average_Ocean at 2.130 µm values, this variable is set to CERES default (See Table 4-5.) ♠

SSF-157   PSF-wtd MOD04 optical depth small average ocean (0.550)

This parameter is the PSF-weighted mean (See Term-30) of the MODIS MOD04 Optical_Depth_Small_Average_Ocean at 0.550 µm associated with all imager pixels (See Term-27) convolved in the current CERES FOV. (N/A) [0 .. 3] (See Table 5-12)

An arithmetic mean is taken of all imager pixels in the angular bin (See Term-2) before they are weighted by the PSF. Optical depth small average ocean at 0.550 µm is a mean aerosol property. It is computed in the same manner as (See SSF-133). If there are any imager pixels with valid MODIS Optical_Depth_Small_Average_Ocean at 0.550 µm values within the CERES FOV, this variable will be set to the actual value. If there are no imager pixels with valid MODIS Optical_Depth_Small_Average_Ocean at 0.550 µm values, this variable is set to CERES default (See Table 4-5.) ♠

SSF-158   PSF-wtd MOD04 optical depth small average ocean (0.865)

This parameter is the PSF-weighted mean (See Term-30) of the MODIS MOD04
Optical_Depth_Small_Average_Ocean at 0.865 µm associated with all imager pixels (See Term-27) convolved
in the current CERES FOV. (N/A) [0 .. 3] (See Table 5-12)

An arithmetic mean is taken of all imager pixels in the angular bin (See Term-2) before they are weighted by the
PSF. Optical depth small average ocean at 0.865 µm is a mean aerosol property. It is computed in the same
manner as (See SSF-133). If there are any imager pixels with valid MODIS
Optical_Depth_Small_Average_Ocean at 0.865 µm values within the CERES FOV, this variable will be set to
the actual value. If there are no imager pixels with valid MODIS Optical_Depth_Small_Average_Ocean at 0.865
µm values, this variable is set to CERES default (See Table 4-5.) ♠

SSF-159   PSF-wtd MOD04 optical depth small average ocean (2.130)

This parameter is the PSF-weighted mean (See Term-30) of the MODIS MOD04
Optical_Depth_Small_Average_Ocean at 2.130 µm associated with all imager pixels (See Term-27) convolved
in the current CERES FOV. (N/A) [0 .. 3] (See Table 5-12)

An arithmetic mean is taken of all imager pixels in the angular bin (See Term-2) before they are weighted by the
PSF. Optical depth small average ocean at 2.130 µm is a mean aerosol property. It is computed in the same
manner as (See SSF-133). If there are any imager pixels with valid MODIS
Optical_Depth_Small_Average_Ocean at 2.130 µm values within the CERES FOV, this variable will be set to
the actual value. If there are no imager pixels with valid MODIS Optical_Depth_Small_Average_Ocean at 2.130
µm values, this variable is set to CERES default (See Table 4-5.) ♠

SSF-160   PSF-wtd MOD04 cloud condensation nuclei ocean, average

This parameter is the PSF-weighted mean (See Term-30) of the MODIS MOD04
Cloud_Condensation_Nuclei_Ocean associated with all imager pixels (See Term-27) convolved in the current
CERES FOV. (N/A) [0 .. 10^{10}] (See Table 5-12)

An arithmetic mean is taken of all imager pixels in the angular bin (See Term-2) before they are weighted by the
PSF. Cloud condensation nuclei ocean, average is a mean aerosol property. It is computed in the same manner
as (See SSF-133). If there are any imager pixels with valid MODIS Cloud_Condensation_Nuclei_Ocean values
within the CERES FOV, this variable will be set to the actual value. If there are no imager pixels with valid
MODIS Cloud_Condensation_Nuclei_Ocean values, this variable is set to CERES default (See Table 4-5.) ♠

4.4 Fill Values

Table 4-5 lists the smallest default CERES Fill Values. All values greater than or equal to these values are
considered to be default CERES fill values. They are used when data are missing, when there is insufficient data
to make a calculation, or the data are suspect and there is no quality flag associated with the parameter. A value
which has a corresponding flag need not be set to a CERES default value when the data value is suspect. Suspect

values are values that were calculated but failed edit checks. The smallest CERES default fill values are defined as follows:

Table 4-5. CERES Default Fill Values

Fill Value Name	Value	Fill Value Description
INT1_DFLT	127	default value for a 1-byte integer
INT2_DFLT	32767	default value for a 2-byte integer
INT4_DFLT	2147483647	default value for a 4-byte integer
REAL4_DFLT	3.402823E+38	smallest default value for a 4-byte real
REAL8_DFLT	1.797693134862315E+308	smallest default value for a 8-byte real

4.5 Sample Data File

A sample data granule (See Term-19) containing 5 SSF FOVs is part of a package which also includes sample read software (in C), a Readme file, a postscript file describing granule contents, and an ASCII listing of the data in the sample granule (data dump). The sample SSF package can be ordered from the Langley ASDC (See Section 12.0). It is available from the Langley Web Ordering Tool and has the name format: CERES_Test_SSF_versioninformation.

5.0 Data Organization

This section discusses the organization of the SSF structures as written to the output data file. All SSF granules (See Term-19) are stored in the Hierarchical Data Format (HDF) developed by the National Center for Supercomputing Applications (NCSA). The HDF permits aggregation of commonly used data structures within a single file, and a common, platform independent Application Programming Interface (API). The SSF product contains HDF SDSs and Vdata structures. The SSF Vdata structures contain those parameters which are only recorded once per granule. The SSF SDSs contain the parameters which are recorded for each FOV. See the HDF User's Guide for additional information (See Reference 33). SSF Metadata is implemented using the ECS ToolKit (See Term-41) metadata routines (See Reference 47), which are based on HDF Annotations.

5.1 Data Granularity

All SSF data granules are hourly HDF files.

5.2 SSF HDF Scientific Data Sets (SDS)

The TRMM SSF contains 126 SDSs which correspond to the 126 parameters recorded for each FOV. The Terra and Aqua SSF contains an addtional 34 SDS for a total of 160 SDSs. This corresponds to the 160 parameters recorded for each FOV. The additional 34 parameters are based on the MODIS MOD04 or MYD04 aerosol product. The SDSs within the SSF are 1, 2, or 3 dimensional, depending on the parameter. Each FOV on the SSF has a value, or multiple values in the case of 2 or 3 dimensional SDSs, for every SDS. The parameter instances contained in each SDS are arranged according to the along-track angle of the FOV with which they are associated. The ordering used by the C programming language and most HDF viewers associates the first dimension to the number of FOVs. In FORTRAN, the dimensions are reversed such that the number of FOVs becomes the last dimension. Table 5-1 through Table 5-11 summarize each parameter, and therefore each SDS, contained within the SSF granule (See Term-19).

This section contains tables of the measurement-level FOV parameters. The FOV parameters are organized into logical subgroups or HDF Vgroups (See Term-43). These subgroups are arbitrary and were generated as a convenience when searching for a particular parameter. Within the tables, each parameter is hyperlinked to a definition from the item number, SSF-i, where i denotes the parameter number. The ranges stated for each parameter are absolute and are never exceeded. If a parameter value exceeds the stated range during processing, it will be replaced with the proper CERES default fill value (See Table 4-5).

5.2.1 Time and Position

These parameters identify the time and position information associated with each CERES FOV.

Table 5-1. Time and Position Table

Item	Parameter Name (SDS Name)	Units	Range	SDS Dimensions	Data Type	Maximum Hourly Size (MB)
SSF-1	Time of observation	day	2440000..2480000	n*	64 bit real	1.87
SSF-2	Radius of satellite from center of Earth at observation	km	6000 .. 8000	n*	64 bit real	1.87
SSF-3	X component of satellite inertial velocity	km sec^{-1}	-10 .. 10	n*	64 bit real	1.87
SSF-4	Y component of satellite inertial velocity	km sec^{-1}	-10 .. 10	n*	64 bit real	1.87
SSF-5	Z component of satellite inertial velocity	km sec^{-1}	-10 .. 10	n*	64 bit real	1.87
SSF-6	Colatitude of subsatellite point at surface at observation	deg	0 .. 180	n*	32 bit real	0.94
SSF-7	Longitude of subsatellite point at surface at observation	deg	0 .. 360	n*	32 bit real	0.94
SSF-8	Colatitude of subsolar point at surface at observation	deg	0 .. 180	n*	32 bit real	0.94
SSF-9	Longitude of subsolar point at surface at observation	deg	0 .. 360	n*	32 bit real	0.94
SSF-10	Colatitude of CERES FOV at surface	deg	0 .. 180	n*	32 bit real	0.94
SSF-11	Longitude of CERES FOV at surface	deg	0 .. 360	n*	32 bit real	0.94
SSF-12	Scan sample number	N/A	1 .. 660	n*	16 bit integer	0.47
SSF-13	Packet number	N/A	0 .. 13100	n*	16 bit integer	0.47
SSF-14	Cone angle of CERES FOV at satellite	deg	0 .. 90	n*	32 bit real	0.94
SSF-15	Clock angle of CERES FOV at satellite wrt inertial velocity	deg	0 .. 360	n*	32 bit real	0.94
SSF-16	Rate of change of cone angle	deg sec^{-1}	-300 .. 300	n*	32 bit real	0.94
SSF-17	Rate of change of clock angle	deg sec^{-1}	-20 .. 20	n*	32 bit real	0.94
SSF-18	Along-track angle of CERES FOV at surface	deg	-30 .. 330	n*	32 bit real	0.94
SSF-19	Cross-track angle of CERES FOV at surface	deg	-90 .. 90	n*	32 bit real	0.94

* n is the number of FOVs processed. For sizing estimates, n is set to 245,475 FOVs.

5.2.2 Viewing Angles

These parameters provide the viewing geometry for each CERES FOV.

Table 5-2. Viewing Angles Table

Item	Parameter Name (SDS Name)	Units	Range	SDS Dimen-sions	Data Type	Maximum Hourly Size (MB)
SSF-20	CERES viewing zenith at surface	deg	0 .. 90	n*	32 bit real	0.94
SSF-21	CERES solar zenith at surface	deg	0 .. 180	n*	32 bit real	0.94
SSF-22	CERES relative azimuth at surface	deg	0 .. 360	n*	32 bit real	0.94
SSF-23	CERES viewing azimuth at surface wrt North	deg	0 .. 360	n*	32 bit real	0.94

* n is the number of FOV processed. For sizing estimates, n is set to 245,475 FOVs.

5.2.3 Surface Map

These parameters describe the Earth's surface conditions for each CERES FOV. They are obtained from ancillary databases, which are sometimes referred to as Surface Maps.

Table 5-3. Surface Map Parameter Table

Item	Parameter Name (SDS Name)	Units	Range	SDS Dimen-sions	Data Type	Maximum Hourly Size (MB)
SSF-24	Altitude of surface above sea level	m	-1000 .. 10000	n*	32 bit real	0.94
SSF-25	Surface type index	N/A	1 .. 20	n* x 8	16 bit integer	3.75
SSF-26	Surface type percent coverage	N/A	0 .. 100	n* x 8	16 bit integer	3.75

* n is the number of FOVs processed. For sizing estimates, n is set to 245,475 FOV.

5.2.4 Scene Type

These parameters identify the Angular Distribution Model types, historically called Scene types, used to invert the CERES radiances to fluxes.

Table 5-4. Scene Type Parameter Table (Sheet 1 of 2)

Item	Parameter Name (SDS Name)	Units	Range	SDS Dimen-sions	Data Type	Maximum Hourly Size (MB)
SSF-27	CERES SW ADM type for inversion process	N/A	0 .. 5000	n*	16 bit integer	0.47
SSF-28	CERES LW ADM type for inversion process	N/A	0 .. 5000	n*	16 bit integer	0.47
SSF-29	CERES WN ADM type for inversion process	N/A	0 .. 5000	n*	16 bit integer	0.47

Table 5-4. Scene Type Parameter Table (Sheet 2 of 2)

Item	Parameter Name (SDS Name)	Units	Range	SDS Dimen-sions	Data Type	Maximum Hourly Size (MB)
SSF-30	ADM geo	N/A	-32767 .. 32766	n*	16 bit integer	0.47

* n is the number of FOV processed. For sizing estimates, n is set to 245,475 FOVs.

5.2.5 Filtered Radiances

This parameter group contains the CERES radiances obtained directly from the instrument counts and the associated flags.

Table 5-5. Filtered Radiances Table

Item	Parameter Name (SDS Name)	Units	Range	SDS Dimen-sions	Data Type	Maximum Hourly Size (MB)
SSF-31	CERES TOT filtered radiance - upwards	W m^{-2} sr^{-1}	0 .. 700	n*	32 bit real	0.94
SSF-32	CERES SW filtered radiance - upwards	W m^{-2} sr^{-1}	-10 .. 510	n*	32 bit real	0.94
SSF-33	CERES WN filtered radiance - upwards	W m^{-2} sr^{-1}μm^{-1}	0 .. 15	n*	32 bit real	0.94
SSF-34	Radiance and Mode flags	N/A	See Figure 4-6	n*	32 bit integer	0.94

* n is the number of FOV processed. For sizing estimates, n is set to 245,475 FOVs.

5.2.6 Unfiltered Radiances

This parameter group contains the CERES unfiltered radiances obtained by taking into account the instrument-specific spectral response.

Table 5-6. Unfiltered Radiances Table

Item	Parameter Name (SDS Name)	Units	Range	SDS Dimen-sions	Data Type	Maximum Hourly Size (MB)
SSF-35	CERES SW radiance - upwards	W m^{-2} sr^{-1}	-10 .. 510	n*	32 bit real	0.94
SSF-36	CERES LW radiance - upwards	W m^{-2} sr^{-1}	0 .. 200	n*	32 bit real	0.94
SSF-37	CERES WN radiance - upwards	W m^{-2} sr^{-1}	0 .. 60	n*	32 bit real	0.94

* n is the number of FOV processed. For sizing estimates, n is set to 245,475 FOVs.

5.2.7 TOA and Surface Fluxes

This parameter group contains CERES surface and TOA fluxes. Also included are albedo and emissivity parameters associated with the CERES channels.

Table 5-7. TOA and Surface Fluxes Table

Item	Parameter Name (SDS Name)	Units	Range	SDS Dimen-sions	Data Type	Maximum Hourly Size (MB)
SSF-38	CERES SW TOA flux - upwards	W m^{-2}	0 .. 1400	n*	32 bit real	0.94
SSF-39	CERES LW TOA flux - upwards	W m^{-2}	0 .. 500	n*	32 bit real	0.94
SSF-40	CERES WN TOA flux - upwards	W m-^{2}	0 .. 200	n*	32 bit real	0.94
SSF-41	CERES downward SW surface flux - Model A	W m^{-2}	0 .. 1400	n*	32 bit real	0.94
SSF-42	CERES downward LW surface flux - Model A	W m^{-2}	0 .. 700	n*	32 bit real	0.94
SSF-43	CERES downward WNsurface flux - Model A	W m^{-2}	0 .. 250	n*	32 bit real	0.94
SSF-44	CERES net SW surface flux - Model A	W m^{-2}	0 .. 1400	n*	32 bit real	0.94
SSF-45	CERES net LW surface flux - Model A	W m^{-2}	-250 .. 50	n*	32 bit real	0.94
SSF-46	CERES downward SW surface flux - Model B	W m^{-2}	0 .. 1400	n*	32 bit real	0.94
SSF-47	CERES downward LW surface flux - Model B	W m^{-2}	0 .. 700	n*	32 bit real	0.94
SSF-48	CERES net SW surface flux - Model B	W m^{-2}	0 .. 1400	n*	32 bit real	0.94
SSF-49	CERES net LW surface flux - Model B	W m^{-2}	-250 .. 50	n*	32 bit real	0.94
SSF-50	CERES broadband surface albedo	N/A	0 .. 1	n*	32 bit real	0.94
SSF-51	CERES LW surface emissivity	N/A	0 .. 1	n*	32 bit real	0.94
SSF-52	CERES WN surface emissivity	N/A	0 .. 1	n*	32 bit real	0.94

* n is the number of FOV processed. For sizing estimates, n is set to 245,475 FOVs.

5.2.8 Full Footprint Area

These diverse parameters apply to the entire CERES FOV. Many are obtained from imager information and the remainder are obtained from MOA, an ancillary gridded meteorological data product.

Table 5-8. Full Footprint Area Table (Sheet 1 of 2)

Item	Parameter Name (SDS Name)	Units	Range	SDS Dimen-sions	Data Type	Maximum Hourly Size (MB)
SSF-53	Number of imager pixels in CERES FOV	N/A	0 .. 32766	n*	16 bit integer	0.47
SSF-54	Imager percent coverage	N/A	0 .. 100	n*	16 bit integer	0.47

Table 5-8. Full Footprint Area Table (Sheet 2 of 2)

Item	Parameter Name (SDS Name)	Units	Range	SDS Dimen- sions	Data Type	Maximum Hourly Size (MB)
SSF-55	Imager viewing zenith over CERES FOV	deg	0 .. 90	n*	32 bit real	0.94
SSF-56	Imager relative azimuth over CERES FOV	deg	0 .. 360	n*	32 bit real	0.94
SSF-57	Surface wind - U-vector	m sec^{-1}	-100 .. 100	n*	32 bit real	0.94
SSF-58	Surface wind - V-vector	m sec^{-1}	-100 .. 100	n*	32 bit real	0.94
SSF-59	Surface skin temperature	K	175 .. 375	n*	32 bit real	0.94
SSF-60	Column averaged relative humidity	N/A	0 .. 100	n*	32 bit real	0.94
SSF-61	Precipitable water	cm	0.001 .. 10	n*	32 bit real	0.94
SSF-62	Flag - Source of precipitable water	N/A	0 .. 120	n*	16 bit integer	0.47
SSF-63	Cloud property extrapolation over cloudy area	N/A	0 .. 100	n*	16 bit integer	0.47
SSF-64	Notes on general procedure	N/A	0 .. 32766	n*	16 bit integer	0.47
SSF-65	Notes on cloud algorithms	N/A	0 .. 32766	n*	16 bit integer	0.47

* n is the number of FOV processed. For sizing estimates, n is set to 245,475 FOVs.

5.2.9 Clear Footprint Area

The parameters in this group apply only to the clear (See Note-7) portion of the CERES FOV.

Table 5-9. Clear Footprint Area Table (Sheet 1 of 2)

Item	Parameter Name (SDS Name)	Units	Range	SDS Dimen- sions	Data Type	Maximum Hourly Size (MB)
SSF-66	Clear area percent coverage at subpixel resolution	N/A	0 .. 100	n*	32 bit real	0.94
SSF-67	Cloud-mask clear-strong percent coverage	N/A	0 .. 100	n*	16 bit integer	0.47
SSF-68	Cloud-mask clear-weak percent coverage	N/A	0 .. 100	n*	16 bit integer	0.47
SSF-69	Cloud-mask snow/ice percent coverage	N/A	0 .. 100	n*	16 bit integer	0.47
SSF-70	Cloud-mask aerosol B percent coverage	N/A	0 .. 100	n*	16 bit integer	0.47
SSF-71	Flag - Type of aerosol B	N/A	0 .. 9999	n*	16 bit integer	0.47
SSF-72	Cloud-mask percent coverage supplement	N/A	0 .. 32766	n*	16 bit integer	0.47
SSF-73	Total aerosol A optical depth - visible	N/A	-1 .. 5	n*	32 bit real	0.94
SSF-74	Total aerosol A optical depth - near IR	N/A	-1 .. 5	n*	32 bit real	0.94
SSF-75	Aerosol A supplement 1	N/A	-1000 .. 1000	n*	32 bit real	0.94
SSF-76	Aerosol A supplement 2	N/A	-1000 .. 1000	n*	32 bit real	0.94

Table 5-9. Clear Footprint Area Table (Sheet 2 of 2)

Item	Parameter Name (SDS Name)	Units	Range	SDS Dimen- sions	Data Type	Maximum Hourly Size (MB)
SSF-77	Aerosol A supplement 3	N/A	-1000 .. 1000	n*	32 bit real	0.94
SSF-78	Aerosol A supplement 4	N/A	-1000 .. 1000	n*	32 bit real	0.94
SSF-79	Imager-based surface skin temperature	K	175 .. 375	n*	32 bit real	0.94
SSF-80	Vertical Temperature change	K	-30 .. 90	n*	32 bit real	0.94

* n is the number of FOV processed. For sizing estimates, n is set to 245,475 FOVs.

5.2.10 Cloudy Footprint Area

The parameters in this group apply to the cloudy (See Note-7) portion and the clear/layer/overlap portion of the CERES FOV. The cloudy portion of the CERES FOV may contain up to two distinct cloud layers. The cloud layers are reflected in the last SDS dimension, which is 2. The lowest cloud layer parameter value is always recorded before the upper layer value. The last parameter in the group contains cloud overlap information for the entire CERES FOV. An FOV contains four cloud overlap conditions: clear, lower layer only, upper layer only, and overlapping cloud layers. The overlap conditions are reflected in the last SDS dimension, which is 4.

Table 5-10. Cloudy Footprint Area Table (Sheet 1 of 3)

Item	Parameter Name (SDS Name)	Units	Range	SDS Dimen- sions	Data Type	Maximum Hourly Size (MB)
SSF-81	Clear/layer/overlap percent coverages	N/A	0 .. 100	n* x 4	32 bit real	13.74
SSF-82	Note for cloud layer	N/A	$0 .. 2^{31-1}$	n* x 2	32 bit integer	1.87
SSF-83	Mean visible optical depth for cloud layer	N/A	0 .. 400	n* x 2	32 bit real	1.87
SSF-84	Stddev of visible optical depth for cloud layer	N/A	0 .. 300	n* x 2	32 bit real	1.87
SSF-85	Mean logarithm of visible optical depth for cloud layer	N/A	-6 .. 6	n* x 2	32 bit real	1.87
SSF-86	Stddev of logarithm of visible optical depth for cloud layer	N/A	0 .. 6	n* x 2	32 bit real	1.87
SSF-87	Mean cloud infrared emissivity for cloud layer	N/A	0 .. 2	n* x 2	32 bit real	1.87
SSF-88	Stddev of cloud infrared emissivity for cloud layer	N/A	0 .. 2	n* x 2	32 bit real	1.87
SSF-89	Mean liquid water path for cloud layer (3.7)	g m^{-2}	0 .. 10000	n* x 2	32 bit real	1.87

Table 5-10. Cloudy Footprint Area Table (Sheet 2 of 3)

Item	Parameter Name (SDS Name)	Units	Range	SDS Dimen-sions	Data Type	Maximum Hourly Size (MB)
SSF-90	Stddev of liquid water path for cloud layer (3.7)	g m^{-2}	0 .. 8000	n* x 2	32 bit real	1.87
SSF-91	Mean ice water path for cloud layer (3.7)	g m^{-2}	0 .. 10000	n* x 2	32 bit real	1.87
SSF-92	Stddev of ice water path for cloud layer (3.7)	g m^{-2}	0 .. 8000	n* x 2	32 bit real	1.87
SSF-93	Mean cloud top pressure for cloud layer	hPa	0 .. 1100	n* x 2	32 bit real	1.87
SSF-94	Stddev of cloud top pressure for cloud layer	hPa	0 .. 600	n* x 2	32 bit real	1.87
SSF-95	Mean cloud effective pressure for cloud layer	hPa	0 .. 1100	n* x 2	32 bit real	1.87
SSF-96	Stddev of cloud effective pressure for cloud layer	hPa	0 .. 350	n* x 2	32 bit real	1.87
SSF-97	Mean cloud effective temperature for cloud layer	K	100 .. 350	n* x 2	32 bit real	1.87
SSF-98	Stddev of cloud effective temperature for cloud layer	K	0 .. 150	n* x 2	32 bit real	1.87
SSF-99	Mean cloud effective height for cloud layer	km	0 .. 20	n* x 2	32 bit real	1.87
SSF-100	Stddev of cloud effective height for cloud layer	km	0 .. 12	n* x 2	32 bit real	1.87
SSF-101	Mean cloud base pressure for cloud layer	hPa	0 .. 1100	n* x 2	32 bit real	1.87
SSF-102	Stddev of cloud base pressure for cloud layer	hPa	0 .. 600	n* x 2	32 bit real	1.87
SSF-103	Mean water particle radius for cloud layer (3.7)	μm	0 .. 40	n* x 2	32 bit real	1.87
SSF-104	Stddev of water particle radius for cloud layer (3.7)	μm	0 .. 20	n* x 2	32 bit real	1.87
SSF-105	Mean ice particle effective diameter for cloud layer (3.7)	μm	0 .. 300	n* x 2	32 bit real	1.87
SSF-106	Stddev of ice particle effective diameter for cloud layer (3.7)	μm	0 .. 200	n* x 2	32 bit real	1.87
SSF-107	Mean cloud particle phase for cloud layer (3.7)	N/A	1 .. 2	n* x 2	32 bit real	1.87
SSF-108	Mean water particle radius for cloud layer (1.6)	μm	0 .. 40	n* x 2	32 bit real	1.87

Table 5-10. Cloudy Footprint Area Table (Sheet 3 of 3)

Item	Parameter Name (SDS Name)	Units	Range	SDS Dimen-sions	Data Type	Maximum Hourly Size (MB)
SSF-109	Mean ice particle effective diameter for cloud layer (1.6)	μm	0 .. 300	n* x 2	32 bit real	1.87
SSF-110	Mean cloud particle phase for cloud layer (1.6)	N/A	1 .. 2	n* x 2	32 bit real	1.87
SSF-111	Mean vertical aspect ratio for cloud layer (TBD)	N/A	0 .. 20	n* x 2	32 bit real	1.87
SSF-112	Stddev of vertical aspect ratio for cloud layer (TBD)	N/A	0 .. 15	n* x 2	32 bit real	1.87
SSF-113	Percentiles of visible optical depth for cloud layer	N/A	0 .. 400	n* x 13 x 2	32 bit real	24.35
SSF-114	Percentiles of IR emissivity for cloud layer	N/A	0 .. 2	n* x 13 x 2	32 bit real	24.35

* n is the number of FOV processed. For sizing estimates, n is set to 245,475 FOVs.

5.2.11 Footprint Imager Radiance Statistics

This parameter group contains imager radiance statistics over the CERES FOV for five imager channels and cloud cover at imager resolution for the FOV. Parameters which apply to each of the five imager channels have an SDS dimension of n* x 5. Imager channel statistics are in the same order as the list of central wavelengths (See SSF-115).

Table 5-11. Footprint Imager Radiance Statistics Table (Sheet 1 of 2)

Item	Parameter Name (SDS Name)	Units	Range	SDS Dimen-sions	Data Type	Maximum Hourly Size (MB)
SSF-115	Imager channel central wavelength	μm	0.4 .. 15.0	n* x 5	32 bit real	4.68
SSF-116	All subpixel clear area percent coverage	N/A	0 .. 100	n*	16 bit integer	0.47
SSF-117	All subpixel overcast cloud area percent coverage	N/A	0 ..100	n*	16 bit integer	0.47
SSF-118	Mean imager radiances over clear area	$W\ m^{-2}\ sr^{-1}\ \mu m^{-1}$	-1000 .. 1000	n* x 5	32 bit real	4.68
SSF-119	Stddev of imager radiances over clear area	$W\ m^{-2}\ sr^{-1}\ \mu m^{-1}$	0 .. 1000	n* x 5	32 bit real	4.68
SSF-120	Mean imager radiances over overcast cloud area	$W\ m^{-2}\ sr^{-1}\ \mu m^{-1}$	-1000 .. 1000	n* x 5	32 bit real	4.68
SSF-121	Stddev of imager radiances over overcast cloud area	$W\ m^{-2}\ sr^{-1}\ \mu m^{-1}$	0 .. 1000	n* x 5	32 bit real	4.68

Table 5-11. Footprint Imager Radiance Statistics Table (Sheet 2 of 2)

Item	Parameter Name (SDS Name)	Units	Range	SDS Dimen-sions	Data Type	Maximum Hourly Size (MB)
SSF-122	Mean imager radiances over full CERES FOV	W m^{-2} sr^{-1} μm^{-1}	-1000 .. 1000	n* x 5	32 bit real	4.68
SSF-123	Stddev of imager radiances over full CERES FOV	W m^{-2} sr^{-1} μm^{-1}	0 .. 1000	n* x 5	32 bit real	4.68
SSF-124	5th percentile of imager radiances over full CERES FOV	W m^{-2} sr^{-1} μm^{-1}	-1000 .. 1000	n* x 5	32 bit real	4.68
SSF-125	95th percentile of imager radiances over full CERES FOV	W m^{-2} sr^{-1} μm^{-1}	-1000 .. 1000	n* x 5	32 bit real	4.68
SSF-126	Mean imager radiances over cloud layer 1 (no overlap)	W m^{-2} sr^{-1} μm^{-1}	-1000 .. 1000	n* x 5	32 bit real	4.68
SSF-127	Stddev of imager radiances over cloud layer 1 (no overlap)	W m^{-2} sr^{-1} μm^{-1}	0 .. 1000	n* x 5	32 bit real	4.68
SSF-128	Mean imager radiances over cloud layer 2 (no overlap)	W m^{-2} sr^{-1} μm^{-1}	-1000 .. 1000	n* x 5	32 bit real	4.68
SSF-129	Stddev of imager radiances over cloud layer 2 (no overlap)	W m^{-2} sr^{-1} μm^{-1}	0 .. 1000	n* x 5	32 bit real	4.68
SSF-130	Mean imager radiances over cloud layer 1 and 2 overlap	W m^{-2} sr^{-1} μm^{-1}	-1000 .. 1000	n* x 5	32 bit real	4.68
SSF-131	Stddev of imager radiances over cloud layer 1 and 2 overlap	W m^{-2} sr^{-1} μm^{-1}	0 .. 1000	n* x 5	32 bit real	4.68

* n is the number of FOV processed. For sizing estimates, n is set to 25,475 FOVs.

5.2.12 MODIS Land Aerosols

This optional parameter group may exist only on Terra or Aqua data sets. It contains MODIS land aerosol values that correspond to the CERES FOV.

Table 5-12. MODIS Land Aerosols Table (Sheet 1 of 2)

Item	Parameter Name (SDS Name)	Units	Range	SDS Dimen-sions	Data Type	Maximum Hourly Size (MB)
SSF-132	Percentage of CERES FOV with MODIS land aerosol	N/A	0 .. 100	n*	16 bit integer	0.47
SSF-133	PSF-wtd MOD04 cloud fraction land	N/A	0 .. 100	n*	16 bit integer	0.47
SSF-134	PSF-wtd MOD04 aerosol types land	N/A	0 .. 9999	n*	32 bit integer	0.94
SSF-135	PSF-wtd MOD04 dust weighting factor land	N/A	0 .. 1	n*	32 bit real	0.94

Table 5-12. MODIS Land Aerosols Table (Sheet 2 of 2)

Item	Parameter Name (SDS Name)	Units	Range	SDS Dimen-sions	Data Type	Maximum Hourly Size (MB)
SSF-135	PSF-wtd MOD04 corrected optical depth land (0.470)	N/A	0 .. 3	n*	32 bit real	0.94
SSF-137	PSF-wtd MOD04 corrected optical depth land (0.550)	N/A	0 - 3	n*	32 bit real	0.94
SSF-138	PSF-wtd MOD04 corrected optical depth land (0.659)	N/A	0 - 3	n*	32 bit real	0.94
SSF-139	MOD04 number pixels percentile land (0.659)	N/A	$0 .. 2^{31}-1$	n*	32 bit real	0.94
SSF-140	PSF-wtd MOD04 mean reflectance land (0.470)	N/A	0 .. 1	n*	32 bit real	0.94
SSF-141	PSF-wtd MOD04 mean reflectance land (0.659)	N/A	0 .. 1	n*	32 bit real	0.94
SSF-142	PSF-wtd MOD04 mean reflectance land (0.865)	N/A	0 .. 1	n*	32 bit real	0.94
SSF-143	PSF-wtd MOD04 mean reflectance land (2.130)	N/A	0 .. 1	n*	32 bit real	0.94
SSF-144	PSF-wtd MOD04 mean reflectance land (3.750)	N/A	0 .. 1	n*	32 bit real	0.94
SSF-145	PSF-wtd MOD04 std reflectance land (0.470)	N/A	0 .. 2	n*	32 bit real	0.94

* n is the number of FOV processed. For sizing estimates, n is set to 25,475 FOVs.

5.2.13 MODIS Ocean Aerosols

This optional parameter group may exist only on Terra or Aqua data sets. It contains MODIS ocean aerosol values that correspond to the CERES FOV.

Table 5-13. MODIS Land Aerosols Table (Sheet 1 of 2)

Item	Parameter Name (SDS Name)	Units	Range	SDS Dimen-sions	Data Type	Maximum Hourly Size (MB)
SSF-146	Percentage of CERES FOV with MODIS ocean aerosol	N/A	0 .. 100	n*	16 bit integer	0.47
SSF-147	PSF-wtd MOD04 cloud fraction ocean	N/A	0 .. 100	n*	16 bit integer	0.47
SSF-148	PSF-wtd MOD04 solution indices ocean small, average	N/A	0 ..9999	n*	32 bit integer	0.94
SSF-149	PSF-wtd MOD04solution indices ocean large, average	N/A	0 .. 9999	n*	32 bit integer	0.94

Table 5-13. MODIS Land Aerosols Table (Sheet 2 of 2)

Item	Parameter Name (SDS Name)	Units	Range	SDS Dimen-sions	Data Type	Maximum Hourly Size (MB)
SSF-150	PSF-wtd MOD04 effective optical depth average ocean (0.470)	N/A	0 .. 1	n*	32 bit real	0.94
SSF-151	PSF-wtd MOD04 effective optical depth average ocean (0.550)	N/A	0 - 3	n*	32 bit real	0.94
SSF-152	PSF-wtd MOD04 effective optical depth average ocean(0.659)	N/A	0 - 3	n*	32 bit real	0.94
SSF-153	PSF-wtd MOD04 effective optical depth average ocean(0.865)	N/A	0 - 3	n*	32 bit real	0.94
SSF-154	PSF-wtd MOD04 effective optical depth average ocean(1.240)	N/A	$0 .. 2^{31}\text{-}1$	n*	32 bit real	0.94
SSF-155	PSF-wtd MOD04 effective optical depth average ocean(1.640)	N/A	0 .. 1	n*	32 bit real	0.94
SSF-156	PSF-wtd MOD04 effective optical depth average ocean(2.130)	N/A	0 .. 1	n*	32 bit real	0.94
SSF-157	PSF-wtd MOD04 optical depth small average ocean (0.550)	N/A	0 .. 1	n*	32 bit real	0.94
SSF-158	PSF-wtd MOD04 optical depth small average ocean (0.865)	N/A	0 .. 1	n*	32 bit real	0.94
SSF-159	PSF-wtd MOD04 optical depth small average ocean (2.130)	N/A	0 .. 2	n*	32 bit real	0.94
SSF-160	PSF-wtd MOD04 cloud condensation nucei ocean, average	CCN cm $^{-2}$	$0 .. 1*10^{10}$	n*	32 bit real	0.94

* n is the number of FOV processed. For sizing estimates, n is set to 25,475 FOVs.

5.3 HDF Vertex Data (Vdata)

A Vdata is an HDF structure that allows record-based storage of multiple parameters and/or multiple data types as shown in the example in Figure 5-1. Vdata records are analogous to records found in relational database systems where a single record comprises one or more data fields, and each data field can be represented by its own data type.

SSF_Header is a Vdata (See Table 5-14) which contains fields that correspond to the header parameters.

Field 1 Unsigned 16 bit Integer	Field 2 32 bit Floats		Field 3 Signed 8 bit Integer
Value	Value 1	Value 2	Value

Figure 5-1. Vdata record example

5.3.1 SSF header parameters

Header parameters are recorded once per granule (See Term-19) in the SSF_Header Vdata..

Table 5-14. SSF_Header

Item	Parameter Name (Field Name)	Units	Range	Dimen-sions	Data Type
SSF-H1	SSF ID	N/A	112 .. 200	1	32 bit integer
SSF-H2	Character name of CERES instrument	N/A	N/A	1	32 bit string
SSF-H3	Day and Time at hour start	N/A	N/A	1	224 bit string
SSF-H4	Character name of satellite	N/A	N/A	1	32 bit string
SSF-H5	Character name of high resolution imager instrument	N/A	N/A	1	64 bit string
SSF-H6	Number of imager channels	N/A	1 .. 20	1	32 bit integer
SSF-H7	Central wavelengths of imager channels	μm	0.4 .. 15.0	20	32 bit real
SSF-H8	Earth-Sun distance at hour start	AU	0.98 .. 1.02	1	32 bit real
SSF-H9	Beta Angle	deg	-90 .. 90	1	32 bit real
SSF-H10	Colatitude of subsatellite point at surface at hour start	deg	0 .. 180	1	32 bit real
SSF-H11	Longitude of subsatellite point at surface at hour start	deg	0 .. 360	1	32 bit real
SSF-H12	Colatitude of subsatellite point at surface at hour end	deg	0 .. 180	1	32 bit real
SSF-H13	Longitude of subsatellite point at surface at hour end	deg	0 .. 360	1	32 bit real
SSF-H14	Along-track angle of satellite at hour end	deg	0 .. 330	1	32 bit real
SSF-H15	Number of Footprints in SSF product	N/A	0 .. 360000	1	32 bit integer
SSF-H16	Subsystem 4.1 identification string	N/A	N/A	1	1024 bit string
SSF-H17	Subsystem 4.2 identification string	N/A	N/A	1	1024 bit string
SSF-H18	Subsystem 4.3 identification string	N/A	N/A	1	1024 bit string
SSF-H19	Subsystem 4.4 identification string	N/A	N/A	1	1024 bit string
SSF-H20	Subsystem 4.5 identification string	N/A	N/A	1	1024 bit string
SSF-H21	Subsystem 4.6 identification string	N/A	N/A	1	1024 bit string
SSF-H22	IES production date and time	N/A	N/A	1	192 bit string
SSF-H23	MOA production date and time	N/A	N/A	1	192 bit string
SSF-H24	SSF production date and time	N/A	N/A	1	192 bit string
		Total Size			1000 bytes

5.4 SSF Metadata

In addition to the header data, the SSF also contains metadata that is recorded once per granule (See Term-19). The types of SSF metadata, summarized in Table 5-15, are listed in Appendix A.

Table 5-15. SSF Metadata Summary

HDF Name	Description Table	records	Number of Fields
CERES Baseline Header Metadata	Table A-1	1	36
CERES_metadata Vdata	Table A-2	1	14
SSF Product-specific Metadata	Table A-3	1	3

6.0 Theory of Measurements and Data Manipulations

6.1 Theory of Measurements

 See References 15-24 for the basic theory of measurements.

6.2 Data Processing Sequence

SS 4.0 is the first data processing unit in the CERES Data Management System that applies new algorithms developed specifically for CERES. There are two primary input data sets to this subsystem; the Instrument Earth Scan (IES) and the Cloud Imager Data from VIRS or MODIS. The IES is an hourly CERES level-1b data product containing along-track ordered FOVs from a single CERES instrument (See Reference 14). The imager data product is also level-1b and contains chronologically-ordered scan lines from the imager instrument mounted on the same satellite as the CERES. Numerous ancillary data sets are also required.

SS 4.0 can be divided into 4 logical groups: Cloud Retrieval, Convolution, Inversion, and Surface Estimation. The actual code is grouped slightly differently. Cloud Retrieval and Convolution are stand-alone programs which are run back to back to minimize file space. Inversion and Surface Estimation reside as separate modules which are called from the same main program.

Cloud Retrieval processes the Cloud Imager Data from VIRS or MODIS and identifies imager pixels (See Term-27) as clear-sky or cloudy (See Note-7). This is accomplished using periodically updated data sets of clear sky albedo, brightness temperature, and standard meteorological data. For each cloudy pixel, the cloud layer pressure, height, temperature, and optical properties are calculated. Similarly, skin temperature, aerosol, and optical properties are calculated for the clear pixels. The processed imager data are saved in a temporary file for convolution.

Convolution combines the processed imager pixels with the CERES FOVs found on the IES. The pixel-level imager data located within a CERES FOV are averaged using weights from the CERES point spread function. These imager-based parameters are then added to the CERES parameters and written to an intermediate SSF granule (See Term-19). CERES FOVs which do not have imager pixel coverage or have less coverage than is thought to be needed are not written to the SSF. Imager pixels which do not overlap CERES FOVs are ignored. When Convolution finishes, the processed imager data are immediately deleted.

Inversion spectrally corrects the CERES radiometric measurements and inverts them to TOA fluxes. Surface Estimation then uses these TOA fluxes to directly estimate surface fluxes using several different algorithms. These additional parameters are added to those already available for each FOV and the SSF granule (See Term-19) is written.

For detailed information see the Subsystem Architectural Design Documents (See References 26-28).

6.3 Special Corrections/Adjustments

Algorithms not discussed in the ATBD are discussed in this section. What should we put here???

7.0 Errors

See Subsystem 4.0 CERES Validation Documents (See References 5-11).

If you have any high level accuracy goals which you would like included here, please send them to Erika Geier.

7.1 Quality Assessment

Quality Assessment (QA) activities are performed at the Science Computing Facility (SCF) by the Data Management Team. Processing reports containing statistics and processing results are examined for anomalies. If the reports show anomalies, data visualization tools are used to examine those products in greater detail to begin the anomaly investigation.

7.2 Data Validation by Source

See Subsystem 4.0 Validation Documents (See References 5-11) for details on the data validation plans.

8.0 Notes

Notes are given to expand on subjects that will help in the use and understanding of the SSF product. These notes are generally characterized by more details and longer length than other definitions (See Section 4.3).

Note-1 How to estimate the number of CERES FOVs per hour

- Estimated maximum number of TRMM FOVs in an SSF file

    Assume:
    CERES operating in Normal elevation scan pattern
    Imager coverage is not an issue (example: along-track scanning)
    FOVs must be geolocated at Earth surface
    Given:
    71.4 deg CERES cone angle at horizon (ATBD 4.4)
    142.8 deg/halfscan is Earth viewing
    0.6314 deg/FOV is scan rate (SS 1)
    3.3 sec/halfscan
    (142.8 deg/halfscan) / 0.6314 deg/FOV = 226 FOV/halfscan
    (226 FOV/halfscan) * (3600 sec/hour) / (3.3 sec/halfscan) = 246545 FOV/hour

- Estimated maximum number of EOS FOVs in an SSF file

    Assume:
    CERES operating in Normal elevation scan pattern
    Imager coverage is not an issue (example: along-track scanning)
    FOVs must be geolocated at Earth surface
    Given:
    64.2 deg CERES cone angle at horizon (ATBD 4.4)
    128.4 deg/halfscan is Earth viewing
    0.6314 deg/FOV is scan rate (SS 1)
    3.3 sec/halfscan
    (128.4 deg/halfscan) / 0.6314 deg/FOV = 203 FOV/halfscan
    (203 FOV/halfscan) * (3600 sec/hour) / (3.3 sec/halfscan) = 221455 FOV/hour

- Estimated number of TRMM FOVs in an SSF during crosstrack scanning

    Assume:
    CERES operating in Normal elevation scan pattern
    FOVs must fall within imager swath
    Given:
    45 deg VIRScone angle at horizon
    90 deg/halfscan is Earth viewing
    0.6314 deg/FOV is scan rate (ATBD 1.0)
    3.3 sec/halfscan

(90 deg/halfscan) / 0.6314 deg/FOV = 142 FOV/halfscan
(142 FOV/halfscan) * (3600 sec/hour) / (3.3 sec/halfscan) = 154909 FOV/hour

- Estimated number of EOS FOV in an SSF during crosstrack scanning

  Assume:
    CERES operating in Normal elevation scan pattern
    FOV must fall within imager swath
  Given:
    55 deg MODIS cone angle at horizon
    110 deg/halfscan is Earth viewing
    0.635 deg/FOV is scan rate (ATBD 1.0)
    3.3 sec/halfscan
    (110 deg/halfscan) / 0.6314 deg/FOV = 174 FOV/halfscan
    (174 FOV/halfscan) * (3600 sec/hour) / (3.3 sec/halfscan) = 189818 FOV/hour

Note-2 CERES Definitions of Clear, Broken, and Overcast Clouds and Cloud Layers

(or it ain't a cloud layer till the cookie cutter says it's a cloud layer)

Richard N. Green October 8, 1996

The layering discussion of this document is out-of-date and needs to be rewritten. It is included here only as a place holder. Also, the tables at the end of this note should be reworked so that they fit in portrait mode.

The CERES processing convolves (cookie cutter) the scanner point spread function (PSF) with the imager pixel data (cookie-dough) to determine cloud properties over the CERES field of view (FOV). Since the imager pixel data can be nonuniform, we divide the 95% energy FOV (footprint) into angular bins, average the pixels in a bin, and integrate over the bins to get footprint averages. These average cloud parameters are recorded on the SSF product. The purpose of this note is to define in detail the cloud parameters and how they are calculated in the presence of data dropout and empty bins. All discussions will assume MODIS imager data at a pixel resolution of 1km and a cloud mask at a subpixel resolution of 250m. Thus, for each imager pixel there is a 4×4=16 point cloud mask.

Note-2.1 Determination of Broken and Overcast Clouds

The cookie-dough for a single pixel is defined in ATBD Table 4.4-3 and is reproduced here as . A single pixel is defined as clear, broken, or overcast by the cloud fraction f_{cld} (#2) which is derived from the subgrid cloud mask of zeroes and ones. If a pixel does not have a cloud fraction for whatever reason, the pixel is disregarded. Each 1km pixel has 16 neighboring points (4 by 4) in the cloud mask and we define the pixel cloud condition as follows:

    clear $f_{cld} = 0/16 = 0$
    broken $1/16 \leq f_{cld} \leq 15/16$
    overcast $f_{cld} = 16/16 = 1$

Overcast cloud is usually defined as a cloud with a cloud fraction greater than 99%. Since 15/16 is 0.9375, we must have all 16 subgrid points classified as cloud (mask = 1) for overcast.

Throughout this note we will use 16^{ths} to illustrate the algorithms. In practice some of the mask points could be missing or unreliable so that we will work with a real valued cloud fraction. This means that broken clouds are defined by $0.01 < f_{cld} < 0.99$.

We also define a clear, broken, and overcast fraction for an angular bin. If the ith angular bin contains n^i pixels, then we define the bin clear fraction as the fraction of single pixels defined as clear or

$$f^i_{clr} = n^i_{clr} / n^i. \qquad (1)$$

The broken and overcast cloud fractions are defined similarly so that $f^i_{clr} + f^i_{bk} + f^i_{ov} = 1$. The "cloud" fraction for the ith bin is defined as the average of the single pixel cloud fractions or

$$c^i_{cld} = \frac{1}{n^i} \sum_{\text{all pixels}} f^{ij}_{cld} \tag{2}$$

where f^{ij}_{cld} is the cloud fraction (#2) for the jth pixel in the ith bin. We have defined four different fractions: clear, broken, overcast, cloud. Note that the clear, broken and overcast cloud fractions are at the pixel resolution of 1km and the cloud fraction (2) is at the subgrid resolution of 250m. A broken cloud pixel at 1km resolution contains clear and overcast at the 250m resolution. The cloud fraction averages the overcast (mask=1) at the subgrid resolution and is not equal to one minus the clear fraction. Neither is the cloud fraction equal to the sum of the broken and overcast cloud fractions.

The mean imager radiance for the ith bin is defined by

$$\bar{I}^i = \frac{1}{n^i} \sum_{\text{all pixel}} I^{ij} \tag{3}$$

and the clear mean radiance for the bin is defined as

$$\bar{I}^i_{clr} = \frac{1}{n^i_{clr}} \sum_{\text{clr pixel}} I^{ij}. \tag{4}$$

The broken and overcast mean radiances are similarly defined so that

$$\bar{I}^i = f^i_{clr}\bar{I}^i_{clr} + f^i_{bk}\bar{I}^i_{bk} + f^i_{ov}\bar{I}^i_c. \tag{5}$$

If a single pixel is missing the imager radiance (bad or no data), then it is filled with the average of the other pixels in the bin with the same cloud condition. If there are no like pixels in the bin with good radiances, then the mean bin radiance for the cloud condition is filled with the weighted average of other like bin averages. This is necessary for mean radiances and fractions to balance as discussed later.

We next define five quantities of area coverage over the footprint: imager data, clear, broken, overcast, cloud. First, let us define S_i as the set of angular bin indices (the i's) that contain pixel data, and ω_i as the integral of the PSF over the ith bin. With these definitions we define the five "PSF weighted" area coverages as:

$$C_{\text{imag}} = \left(\sum_{S_i} \omega_i\right) \Big/ \left(\sum_{\text{all bins}} \omega_i\right) \tag{6}$$

$$C_q = \left(\sum_{S_i} \omega_i f^i_q\right) \Big/ \left(\sum_{S_i} \omega_i\right) \tag{7}$$

where the subscript "q" denotes clr, bk, ov, or cld. It follows that

$$C_{clr} + C_{bk} + C_{ov} = 1$$
$$C_{bk} + C_{ov} \neq C_{cld}$$
(8)

The imager radiance is averaged over the various area types. The mean radiance over the footprint is given by

$$\bar{I} = \left(\sum_{S_i} \omega_i \bar{I}^i\right) \Big/ \left(\sum_{S_i} \omega_i\right).$$
(9)

and

$$\bar{I}_q = \left(\sum_{S_i} \omega_i f_q^i \bar{I}_q^i\right) \Big/ \left(\sum_{S_i} \omega_i f_q^i\right)$$
(10)

where "q" denotes clr, bk, or ov. With these definitions if follows that the area coverages and the mean radiances are in balance, or

$$C_{clr}\bar{I}_{clr} + C_{bk}\bar{I}_{bk} + C_{ov}\bar{I}_{ov} = \bar{I}$$
(11)

Because the area coverages sum to one (8) and the radiances are in balance (11), the SSF product does not record broken cloud quantities since they can be determined from

$$C_{bk} = 1 - (C_{clr} + C_{ov})$$
$$\bar{I}_{bk} = \frac{\bar{I} - (C_{clr}\bar{I}_{clr} + C_{ov}\bar{I}_{ov})}{C_{bk}}.$$
(12)

Moreover, for TRMM and the VIRS imager we do not have a subgrid cloud mask so that the single pixel cloud fraction (#2) will be either 0 or 1 which does not allow for broken pixels.

We can also average a general property "x" over the footprint. However, there are several different cases of general parameters and this discussion is beyond the scope of this paper and will be dealt with later.

Note-2.2 A Numerical Example of Cloud Fraction and Radiance Determination

Now let us examine the numerical example (Example 1) given in Table 2. The numbers are hypothetical and do not represent a realistic case. The purpose is to show how the above definitions and equations are applied and how missing data is handled. We have assumed the footprint has 10 angular bins all of which contain imager pixels except for bin 9. All of the pixels were either clear or had one layer clouds (#1 of). Bin 2 contains one clear pixel and one cloudy pixel. Bin 6 contains 3 pixels. In the "Pixel Data" section we see the subgrid mask data given in 16[ths]. Notice that clear pixels contain no cloud data such as cloud mask or cloud parameters. They do contain, however, the imager radiances. Actually, the cookie-dough contains many narrowband radiances. Only one radiance is given here for illustration.

Below the cookie-dough data are "Calculated Quantities". The PSF weights are dependent on the arrangement of the angular bins and the scanner Point Spread Function. These weights are computed off-line and are applicable to all footprints with the same angular bin structure and PSF. The values of ω_i were arbitrarily chosen to sum to one for numerical convenience. The number of pixels in each bin and the cloud classification fractions are given next. Bin 1 has 1 pixel which is clear or has a clear fraction of 1.0 or 100% clear. Bin 2 contained 2 pixels and is 50% clear and 50% broken cloud. The clear pixel has a "cloud" fraction of 0/16 and the other pixel has one of the 16 points in the cloud mask define as cloud (mask=1) so that its cloud fraction is 1/16. The average bin cloud fraction is thus 1/32.

In bin 2 we see the average imager radiance over the 1 clear pixel is 12. The average over the broken cloud area is 14. And since the fractions are both 50%, the mean radiance over the bin is 13. Bin 6 presents several illustrations. There are two overcast pixels, but only one has a radiance value. As mentioned above we fill the missing radiance value with the average of like pixels which for bin 6 is a radiance of 38 and the average bin overcast radiance is therefore 38. The single broken cloud pixel gives a broken radiance of 32. We weight these radiances with the appropriate fractions of 1/3 and 2/3 and determine the mean bin radiance as 36.

An additional illustration is presented by bin 4 that contains 1 pixel with a missing radiance. In this case we fill the bin radiance with the weighted average of the other like radiances, or

$$\bar{I}_{bk}^4 = \frac{(.03)\left(\frac{1}{2}\right)(14) + (.10)(1)(29) + (.20)\left(\frac{1}{3}\right)(32) + (.15)(1)(34)}{(.03)\left(\frac{1}{2}\right) + (.10)(1) + (.20)\left(\frac{1}{3}\right) + (.15)(1)} = 31.19$$

The mean of a general cloud parameter for a bin is just the arithmetic average of the available data. The mean parameter over the footprint is a weighted average.

We now calculate the footprint parameters:

$$S_i = \text{set of indices for observed bins}$$
$$= \{1,2,3,4,5,6,7,8,10\} \tag{13}$$

$$N = \text{number of imager pixels in FOV} = \sum_{S_i} n^i \tag{14}$$
$$= 1 + 2 + 1 + 1 + 1 + 3 + 1 + 1 + 1 = 12$$

$$C_{\text{imag}} = \text{imager area coverage} = \left(\sum_{S_i} \omega_i\right) \Big/ \left(\sum_{\text{all bins}} \omega_i\right) \tag{15}$$
$$= .02+.03+.10+.15+.20+.20+.15+.10+.02 = 0.97$$

$$C_{clr} = \text{clear area coverage} = \left(\sum_{S_i}\omega_i f^i_{clr}\right)\Big/\left(\sum_{S_i}\omega_i\right) \tag{16}$$

$$= [(.02)(1)+(.03)(1/2)+(.10)(1)+(.02)(1)]\Big/0.97 = 0.16$$

$$C_{bk} = broken \text{ cloud area coverage} = \left(\sum_{S_i}\omega_i f^i_{bk}\right)\Big/\left(\sum_{S_i}\omega_i\right) \tag{17}$$

$$= [(.03)(1/2)+(.10)(1)+(.15)(1)+(.20)(1/3)+(.15)(1)]\Big/0.97 = 0.50$$

$$C_{ov} = overcast \text{ cloud area coverage} = \left(\sum_{S_i}\omega_i f^i_{ov}\right)\Big/\left(\sum_{S_i}\omega_i\right) \tag{18}$$

$$= [(.20)(1)+(.20)(2/3)]\Big/0.97 = 0.34$$

$$C_{cld} = \text{cloud area coverage} = \left(\sum_{S_i}\omega_i f^i_{cld}\right)\Big/\left(\sum_{S_i}\omega_i\right) \tag{19}$$

$$= \left[\begin{array}{c}(.03)(1/32)+(.10)(13/16)+(.15)(15/16)+(.20)(16/16)\\ + (.20)(46/48)+(.15)(14/16)\end{array}\right]\Big/0.97 = 0.72$$

Note that (8) is verified or $0.16 + 0.50 + 0.34 = 1$ and $0.50 + 0.34 \neq 0.72$.

The mean imager radiances are as follows:

$$\bar{I}_{clr} = \text{mean imager radiance over clear area} = \left(\sum_{S_i}\omega_i f^i_{clr}\bar{I}^i_{clr}\right)\Big/\left(\sum_{S_i}\omega_i f^i_{clr}\right) \tag{20}$$

$$= \frac{(.02)(1)(12)+(.03)(1/2)(12)+(.10)(1)(21)+(.02)(1)(17)}{(.02)(1)+(.03)(1/2)+(.10)(1)+(.02)(1)} = 18.45$$

$$\bar{I}_{bk} = \text{mean imager radiance over broken cloud area} = \left(\sum_{S_i}\omega_i f^i_{bk}\bar{I}^i_{bk}\right)\Big/\left(\sum_{S_i}\omega_i f^i_{bk}\right) \tag{21}$$

$$= \frac{(.03)(1/2)(14)+(.10)(1)(29)+(.15)(1)(31.19)+(.20)(1/3)(32)+(.15)(1)(34)}{(.03)(1/2)+(.10)(1)+(.15)(1)+(.20)(1/3)+(.15)(1)} = 31.19$$

$$\bar{I}_{ov} = \text{mean imager radiance over overcast cloud area} = \left(\sum_{S_i}\omega_i f^i_{ov}\bar{I}^i_{ov}\right)\Big/\left(\sum_{S_i}\omega_i f^i_{ov}\right) \tag{22}$$

$$= \frac{(.20)(1)(40)+(.20)(2/3)(38)}{(.20)(1)+(.20)(2/3)} = 39.20$$

$$\bar{I} = \text{mean imager radiance over FOV} = \left(\sum_{S_i} \omega_i \bar{I}^i\right) \Bigg/ \left(\sum_{S_i} \omega_i\right)$$

$$= \frac{\begin{bmatrix}(.02)(12)+(.03)(13)+(.10)(29)+(.15)(31.19)+(.20)(40) \\ +(.20)(36)+(.15)(34)+(.10)(21)+(.02)(17)\end{bmatrix}}{.02+.03+.10+.15+.20+.20+.15+.10+.02} = 31.91 \tag{23}$$

Note that (11) is verified or $(.1598)(18.45)+(.4966)(31.19)+(.3436)(39.20) = 31.91$.

Note-2.3 Determination of Cloud Height Categories A and B

Cloud layers will be defined as being in one of four height categories (Figure 1) by their effective pressure (See , #24 and #35). In general a single footprint can contain clear areas and clouds in all four categories. However, we will restrict clouds within a single footprint to two layers and assign each cloud layer to the height category which contains the layer average pressure. Layer 1 is defined as the lowest layer (or only layer) and we will assign it to category A where A could be 1, 2, 3, or 4. If there is a second layer, then layer 2 is the highest layer and we assign it to category B where B could be 2, 3, or 4, but not the same as category A. The mean cloud data in an angular bin is defined as being in categories A and B. It is possible, however, for the effective pressure of a given angular bin to be outside of categories A and B, but recall we have defined layers and assigned each layer to the category containing its mean.

We now determine the two layers and the two categories A and B from the mean clouds in the bins. The mean cloud effective pressures (#24 and #35) can range over all 4 cloud categories, but we must restrict them to categories A and B for layers 1 and 2 as discussed above. If all bins are clear, then we have no cloud categories. Let us first consider the case where all cloudy bins contain only 1-layer clouds. There is no 2-layer clouds in the footprint. We can determine the mean x and standard deviation S of the effective pressure #24 over the n bins that contain a 1-layer cloud. It is possible that we have not one but two distinct single layers over the footprint. To test this, we order the pressures and determine the increment between increasing pressures. If the maximum increment is greater than 50 hPa, then we divide the pressures into two sets at the

maximum increment and define two layers with $(\bar{x}_1, S_1, n_1)$ and $(\bar{x}_2, S_2, n_2)$ where $\bar{x} = \dfrac{1}{n}\sum_{i=1}^{n} x_i$

and $S^2 = \dfrac{1}{n-1}\sum_{i=1}^{n}(x_i - \bar{x})^2$. If $t_\alpha = |(\bar{x}_1 - \bar{x}_2)| \Big/ \sqrt{S_1^2/n_1 + S_2^2/n_2}$ is greater than 2.13, then we have two distinct layers and define categories A and B with $\bar{x}_1$ and $\bar{x}_2$ so that A<B and category A is the lower cloud layer with the greater pressure. It is possible to have 2 distinct layer and both are in the same category. In this case, we do not divide but stay with one layer containing all $n = n_1 + n_2$ pixels. If t is less than 2.13, then the layers are not distinct and we have one layer and define category A with $\bar{x}$ where $n = n_1 + n_2$. If either n_1 or n_2 is less that 3, then we will not attempt the Student t test to separate the pressures but leave them in one layer.

We will use only one value for $t_\alpha = 2.13$. Since our minimum sample is 6 with 4 degrees of freedom, we can determine that a t_α of 2.13 implies a 90% confidence level. With the maximum sample of 64 for TRMM, we are 96% confident with 2.13.

Next, let us consider the case where all cloudy bins contain 2 cloud layers. We can determine $(\bar{x}, S, n)$ for the higher layer with #35. We can also test #35 for two distinct layers as above. If we have one layer, then we define category B with $\bar{x}$ and define category A with the mean of #24. If we have two distinct layers, then we define category A and B with $\bar{x}_1$ and $\bar{x}_2$ and put all lower layers (#24) into either A or B depending on which is closest.

And finally, if we have within a single footprint some bins with one layer and some bins with two layers, then we combine the first two cases. From the bins with one layer we determine $(\bar{x}, S, n)$ from #24 and also test it for two distinct layers. If #24 yields one layer and defines category A'. We use the notation A' instead of A because it is not clear at this point whether the defined layer is low or high. After A' and B' have been defined, we set A and B such that A<B. Next we determine $(\bar{x}, S, n)$ from #35 for the bins with two layers and determine if #24 from the 1-layer case and #35 from the 2-layer case give distinctly different layers. If they are different, then category B' has been defined (provided A' and B' are not equal) and #24 from the 2-layer bins are put into the closest category. If they are not different, then clouds in the bins with one layer and the top layer of the 2-layer bins are in the same layer and #24 from the 2-layer cases defines category B'. If, however, we find that the bins with one layer define two distinct layers, then all the cloud layers in the two layer bins are put into the closest of these two distinct layers.

Whenever we determine two layers and two height categories A and B, we reexamine. The average pressure corresponding to A and to B are used to define two layers and each pressure from each bin is placed in the closest layer independent of what its designation was on the first pass. It is possible to start with a two layer cloud in a bin and upon reexamination put both layers into the same final layer or category. An example will help to demonstrate this.

Note-2.4 Numerical Examples of Cloud Layer Determination

We now build on Example 1 and work through Example 2 as given in Table 3. The cloud mask and number of cloud layers for each imager pixel are the same as in Example 1. We now add the pixel effective pressure in each cloud layer and determine for the entire footprint if we have one cloud layer (layer A) or two distinct cloud layers (layer A and B) (see Fig. 1). This involves collecting the available data into "cloud layers" as compared to "clear", "broken", and "overcast clouds". All of the bins in example 2 are 100% clear or 100% 1-layer except for bin 2 which is 50% clear and 50% 1-layer. We will make use of these fractions later. The mean "bin" effective pressure is determined in the same way as we determined the general parameters, that is, we assume uniformity over the bin and form the arithmetic average. Bin 6 is an example of this. Since we have the case where all cloudy bins are 1-layer clouds, we just collect the pressures in bins 2, 3, 4, 5, 6, and 7. The mean ordered pressures are {245, 250, 268, 320, 320, 335} and the increments are {5, 18, 52, 0, 15}. Since the largest increment of 52 is greater than 50, we proceed with two sets. The first set is {245, 250, 268} with $n_1 = 3$, $\bar{p}_1 = 254.33$, $S_1 = 12.10$ and the

second set is {320, 320, 335} with $n_2 = 3$, $\bar{p}_2 = 325.00$, $S_2 = 8.66$. We next test for two distinct layers with the t test, or

$$t = \frac{\left|\bar{p}_1 - \bar{p}_2\right|}{\left[\dfrac{S_1^2}{n_1} + \dfrac{S_2^2}{n_2}\right]^{1/2}} = \frac{\left|254.33 - 325.00\right|}{\left[\dfrac{(12.10)^2}{3} + \dfrac{(8.66)^2}{3}\right]^{1/2}} = 8.23 > 2.13. \tag{24}$$

Therefore, there are two layers with layer A with a pressure p_A=325.00 and layer B with pressure p_B=254.33. It will be simpler here to refer to layer 1 in cloud height category A as just layer A. On reexamination, all pressures remain in the same layer.

We now go to Example 3 where we have both 1-layer and 2-layer clouds (see Table 4). Some of the pixel data has changed from Example 2. The clear, 1-layer, and 2-layer fractions are determined as before. Within a bin we determine the mean pressure for clear, 1-layer, and 2-layer pixels. Bin 2 and 6 give examples how this is handled. We start with the 1-layer clouds in bins 2, 3, 4, 6, 10. The ordered pressures are {280, 290, 330, 335, 612} and the increments are {10, 40, 5, 277}. Since the largest increment of 277 is greater than 50, we would normally form two sets. However, since one of the sets has less than 3 pressures and since we require 3 samples to calculate a sample standard deviation, we do not separate the set but form one set (layer A') where $n_{A'} = 5$, $\bar{p}_{A'} = 369.40$, $S_{A'} = 137.74$. We notice that bin 10 with a pressure of 612 has been put into the wrong layer. But, if we separate into two layers at this point, we are establishing a layer with only one observation and then would have to force the other data values to conform to it. Since bin 10 is different, it could be erroneous. It seems best to proceed and reexamine at the end.

Next we collect all the pressures from the high layer of the 2 layer bins or from bins 5, 6, 7, 8 we have the mean pressures {340, 335, 350, 606} with $n = 4$, $\bar{p} = 407.75$, $S = 132.31$. We now test to see if this set is different than the layer A' set, or

$$t_\alpha = \frac{\left|369.40 - 407.75\right|}{\left[\dfrac{(137.74)^2}{5} + \dfrac{(132.31)^2}{4}\right]^{1/2}} = 0.42 < 2.13. \tag{25}$$

Since $t_\alpha < 2.13$ we can not justify two different sets so we combine the two or set $A' = \{280, 290, 330, 335, 612, 340, 335, 350, 606\}$ with $n_{A'} = 9$ and $\bar{p}_{A'} = 386.44$.

Layer B' is given by the lower layers of the 2-layer bins or set $B' = \{620, 638, 664, 710\}$ with $n_{B'} = 4$, $\bar{p}_{B'} = 658.00$. Since we already have two layers, layer A' and B', and we can only have 2 layers over a footprint, it makes no sense to test layer B' for two distinct layers. Besides, layer B' is composed of the lower, less-well-known layers. We prefer to rely on the 1-layer and upper layers. Now, since $\bar{p}_{A'} < \bar{p}_{B'}$ and layer A should have the greater pressure (see Fig. 1), we reverse the layers and define A and B such that $\bar{p}_A = 658.00$ and $\bar{p}_B = 386.44$. The next step is

to use these two mean pressures and reexamine all pressures, putting them into the nearest layer. The new sets are set A = {620, 638, 664, 658, 612} with $n_A = 5$, $\bar{p}_A = 638.40$, $S_A = 22.78$ and set B = {280, 290, 335, 340, 330, 335, 350} with $n_B = 7$, $\bar{p}_B = 322.86$, $S_B = 26.75$. Notice that the layer in bin 10 correctly switched layers and that the two layers in bin 8 were combined into one layer. We will define layer A as height category 2 (lower middle clouds) since $500 < (\bar{p}_A = 638.40) < 700$. We also define layer B as height category 3 (upper middle clouds) since $300 < (\bar{p}_B = 322.86) < 500$. Recall that we restricted clouds to 2 of the 4 cloud height categories over a footprint. Thus, even though bin 2 and 3 have clouds in category 4 (high clouds) defined by $p < 300$, they are combined with a layer whose center is in category 3. The mean pressure, $\bar{p}_B = 322.86$, and the standard deviation, $S_B = 26.75$, indicate that the boundary of 300 is only (322.85-300.00)/26.75 = 0.85 sigma away and that the layer may well contain cloud pressures on both sides of the boundary.

And finally, we determine the layer pressures for each angular bin and the fraction of clear, layer A and layer B in each bin as. We now have enough information to determine the overlap fractions as shown in Table 4. These will be discussed in the next section.

SSF Data Product

The SSF (see Table 6) contains all the footprint data including clear, and overcast fractions (and the information to determine the broken fraction. see (12)) and the cloud layering information along with mean radiances over these areas. Let us use the numbers in Example 3 (Table 4) to numerical define several of the SSF parameters.

SSF-53: Number of imager pixels in CERES FOV

From (13) and (14) we have

$$S_i = \text{set of indices for observed bins}$$
$$= \{1,2,3,4,5,6,7,8,10\} \tag{26}$$

$$N = \text{number of imager pixels in FOV} = \sum_{S_i} n^i$$
$$= 1 + 2 + 1 + 1 + 1 + 3 + 1 + 1 + 1 = 12 \tag{27}$$

SSF-54: Imager percent coverage

From (6) we have

$$C_{\text{imag}} = \text{imager area coverage} = \left(\sum_{S_i} \omega_i\right) / \left(\sum_{\text{all bins}} \omega_i\right)$$
$$= .02+.03+.10+.15+.20+.20+.15+.10+.02 = 0.97 \ (97\%) \tag{28}$$

SSF-66: Clear area percent coverage at subpixel resolution

The clear area coverage is at the highest resolution or at the subgrid resolution and should not be confused with SSF-106, the clear area percent coverage at imager resolution. If we have no subgrid resolution, then SSF-64 and SSF-106 are identical. We determine the clear coverage by calculating the cloud fraction and subtracting it from 1.0, or from (2) and (7) we have

$$C_{cld} = \text{cloud area coverage} = \left(\sum_{S_i} \omega_i f^i_{cld}\right)\Big/\left(\sum_{S_i} \omega_i\right)$$

$$= \left[\begin{array}{c}(.03)(1/32)+(.10)(13/16)+(.15)(15/16)+(.20)(16/16)\\ +(.20)(46/48)+(.15)(14/16)+(.10)(9/16)+(.02)(3/16)\end{array}\right]\Big/ 0.97 = 0.807 \quad (29)$$

$$C^*_{clr} = 1 - C_{cld} = 1 - 0.807 = 0.192 \ (19\%)$$

SSF-82: Note for cloud layer

We have two cloud layers in category A and B. We will denote these simply as layer A and B and their area coverage as C_A and C_B. Similar to (7) we have

$$C_A = \text{cloud layer A area coverage} = \left(\sum_{S_i} \omega_i f^i_A\right)\Big/\left(\sum_{S_i} \omega_i\right)$$

$$= [(.20)(1)+(.20)(2/3)+(.15)(1)+(.10)(1)+(.02)(1)]/0.97 = 0.622 \ (62\%) \quad (30)$$

and

$$C_B = [(.03)(1/2)+(.10)(1)+(.15)(1)+(.20)(1)+(.20)(1)+(.15)(1)]/0.97$$

$$= 0.840 \ (84\%) \quad (31)$$

Notice that because of overlay of layers A and B, $C_{clr} + C_A + C_B > 100\%$.

SSF-95: Mean cloud effective pressure for cloud layer

The mean cloud pressure over the footprint is a weighted average and should not be confused with the arithmetic average pressure used to determine cloud layers A and B. Similar to (10) we have

$$\bar{v}_A = \text{Cloud layer A mean effective pressure} = \left(\sum_{S_i} \omega_i f^i_A \bar{p}^i_A\right)\Big/\left(\sum_{S_i} \omega_i f^i_a\right)$$

$$= \frac{\left[\begin{array}{c}(.20)(1)(620)+(.20)(2/3)(638)+(.15)(1)(664)\\ +(.10)(1)(658)+(.02)(1)(612)\end{array}\right]}{(.20)(1)+(.20)(2/3)+(.15)(1)+(.10)(1)+(.02)(1)} = 640.95 \quad (32)$$

and

$$\bar{p}_B = \frac{\left[\begin{array}{c}(.03)(1/2)(280)+(.10)(1)(290)+(.15)(1)(335)\\ +(.20)(1)(340)+(.20)(1)(333.33)+(.15)(1)(350)\end{array}\right]}{(.03)(1/2)+(.10)(1)+(.15)(1)+(.20)(1)+(.20)(1)+(.15)(1)} = 332.04 \quad (33)$$

SSF-96: Stddev of cloud effective pressure for cloud layer

The standard deviation of the effective pressure for cloud layer A is given by

$$
S_A = \left[\left(\sum_{S_i} \omega_i f^i_A (\bar{p}^i_A)^2 \right) \Big/ \left(\sum_{S_i} \omega_i f^i_a \right) - (\bar{p}_A)^2 \right]^{\frac{1}{2}}
$$

$$
= \left[\frac{\begin{bmatrix} (.20)(1)(620)^2 + (.20)(2/3)(638)^2 + (.15)(1)(664)^2 \\ + (.10)(1)(658)^2 + (.02)(1)(612)^2 \end{bmatrix}}{(.20)(1) + (.20)(2/3) + (.15)(1) + (.10)(1) + (.02)(1)} - (640.95)^2 \right]^{\frac{1}{2}}
\tag{34}
$$

$$
= 18.85
$$

and for layer B

$$
S_B = \left[\frac{\begin{bmatrix} (.03)(1/2)(280)^2 + (.10)(1)(290)^2 + (.15)(1)(335)^2 \\ (.20)(1)(340)^2 + (.20)(1)(333.33)^2 + (.15)(1)(350)^2 \end{bmatrix}}{(.03)(1/2) + (.10)(1) + (.15)(1) + (.20)(1) + (.20)(1) + (.15)(1)} - (332.04)^2 \right]^{\frac{1}{2}}
\tag{35}
$$

$$
= 18.54
$$

SSF-81: Clear/layer/overlap condition percent coverages

The 11 cloud overlap conditions are given in Table 5. However, since we only allow 2 cloud layers in a footprint, only 4 of the 11 overlap conditions are possible for a given footprint. First we determine the two height categories from the mean effective pressures (SSF-86). Recall that the pressure for layer A is 640.95 so that it is category 2 (lower middle cloud) and layer B pressure is 332.04 and is in category 3 (upper middle cloud). Thus, the 4 possible cloud overlap conditions are 1, 3, 4, 9 (see Table 5). The area fractions are from (7) where q = clr, A/O, B/O, B/A for clear, layer A only, layer B only, layer B over layer A, respectively, and where f^i_q are determined in the normal way and recorded in Table 4

$$
C_{clr} = \text{clear area coverage} = \left(\sum_{S_i} \omega_i f^i_{clr} \right) \Big/ \left(\sum_{S_i} \omega_i \right)
\tag{36}
$$

$$
= [(.02)(1) + (.03)(1/2)]/0.97 = 0.036 \ (4\%)
$$

$$
C_{A/O} = \text{lower middle cloud only area coverage} = \left(\sum_{S_i} \omega_i f^i_{A/O} \right) \Big/ \left(\sum_{S_i} \omega_i \right)
\tag{37}
$$

$$
= [(.10)(1) + (.02)(1)]/0.97 = 0.123 \ (12\%)
$$

$$C_{B/O} = upper \text{ middle cloud only area coverage} = \left(\sum_{S_i}\omega_i f^i_{B/O}\right)\Big/\left(\sum_{S_i}\omega_i\right) \tag{38}$$

$$= [(.03)(1/2)+(.10)(1)+(.15)(1)+(.20)(1/3)]/0.97=0.341 \text{ (34\%)}$$

$$C_{B/A} = upper \text{ over lower middle cloud area coverage} = \left(\sum_{S_i}\omega_i f^i_{B/A}\right)\Big/\left(\sum_{S_i}\omega_i\right) \tag{39}$$

$$= [(.20)(1)+(.20)(2/3)+(.15)(1)]/0.97=0.498 \text{ (50\%)}$$

SSF-116: All subpixel clear area percent coverage

Same as C_{clr} for SSF-104.

SSF-117: All subpixel overcast cloud area percent coverage

$$C_{ov} = \left(\sum_{S_i}\omega_i f^i_{ov}\right)\Big/\left(\sum_{S_i}\omega_i\right) \tag{40}$$

$$= [(.20)(1)+(.20)(2/3)]/0.97=0.343 \text{ (34\%)}$$

SSF-118: Mean imager radiances over clear area

$$\bar{I}_{clr} = \text{mean imager radiance over clear area} = \left(\sum_{S_i}\omega_i f^i_{clr}\bar{I}^i_{clr}\right)\Big/\left(\sum_{S_i}\omega_i f^i_{clr}\right) \tag{41}$$

$$= \frac{(.02)(1)(12)+(.03)(1/2)(12)}{(.02)(1)+(.03)(1/2)} = 12.00$$

SSF-119: Stddev of imager radiances over clear area

$$S_{clr} = \left[\frac{(.02)(1)(12)^2+(.03)(1/2)(12)^2}{(.02)(1)+(.03)(1/2)} - (12)^2\right]^{\frac{1}{2}} = 0.00 \tag{42}$$

SSF-120: Mean imager radiances over overcast cloud area

$$\bar{I}_{ov} = \text{mean imager radiance over overcast cloud area} = \left(\sum_{S_i}\omega_i f^i_{ov}\bar{I}^i_{ov}\right)\Big/\left(\sum_{S_i}\omega_i f^i_{ov}\right) \tag{43}$$

$$= \frac{(.20)(1)(40)+(.20)(2/3)(38)}{(.20)(1)+(.20)(2/3)} = 39.20$$

SSF-121: Stddev of imager radiances over overcast cloud area

$$S_{ov} = \left[\frac{(.20)(1)(40)^2 + (.20)(2/3)(38)^2}{(.20)(1) + (.20)(2/3)} - (39.20)^2 \right]^{\frac{1}{2}} = 0.98 \tag{44}$$

SSF-122: Mean imager radiances over full CERES FOV

$$\bar{I} = \text{mean imager radiance over FOV} = \left(\sum_{S_i} \omega_i \bar{I}^i \right) \Big/ \left(\sum_{S_i} \omega_i \right)$$

$$= \frac{\left[\begin{array}{c} (.02)(12) + (.03)(13) + (.10)(29) + (.15)(28.30) + (.20)(40) \\ + (.20)(36) + (.15)(34) + (.10)(21) + (.02)(17) \end{array} \right]}{.02 + .03 + .10 + .15 + .20 + .20 + .15 + .10 + .02} = 31.46 \tag{45}$$

SSF-123: Stddev of imager radiances over full CERES FOV

$$S = \left[\frac{\left[\begin{array}{c} (.02)(12)^2 + (.03)(13)^2 + (.10)(29)^2 + (.15)(28.30)^2 \\ + (.20)(40)^2 + (.20)(36)^2 + (.15)(34)^2 + (.10)(21)^2 + (.02)(17)^2 \end{array} \right]}{.02 + .03 + .10 + .15 + .20 + .20 + .15 + .10 + .02} - (31.46)^2 \right]^{\frac{1}{2}}$$

$$= 7.50 \tag{46}$$

SSF-124: 5th percentile of imager radiances over full CERES FOV

We have 9 bins with mean radiances. The ordered radiances are

$$[\ 12,\ 13,\ 17,\ 21,\ 28.30,\ 29,\ 34,\ 36,\ 40\ ] \tag{47}$$

and their corresponding percentiles are

$$[\ 0,\ 12.5,\ 25,\ 37.5,\ 50,\ 62.5,\ 75,\ 87.5,\ 100] \tag{48}$$

The closest percentile to 5% is 0% with a radiance of 12.

SSF-125: 95th percentile of imager radiances over full CERES FOV

From SSF-114 above we see that the closest percentile to 95% is 100% with a radiance of 40.

SSF-126: Mean imager radiances over cloud layer 1 (no overlap)

$$\bar{I}_{A/O} \;=\; \text{mean imager radiance over cloud layer A} \;=\; \left(\sum_{S_i}\omega_i f^i_{A/O}\bar{I}^i\right)\Big/\left(\sum_{S_i}\omega_i f^i_{A/O}\right) \tag{49}$$

$$=\; \frac{(.10)(1)(21)+(.02)(1)(17)}{(.10)(1)+(.02)(1)} \;=\; 20.33$$

SSF-127: Stddev of imager radiances over cloud layer 1 (no overlap)

$$S_{A/O} \;=\; \left[\frac{(.10)(1)(21)^2+(.02)(1)(17)^2}{(.10)(1)+(.02)(1)} - (20.33)^2\right]^{\frac{1}{2}} \;=\; 1.54 \tag{50}$$

SSF-128: Mean imager radiances over cloud layer 2 (no overlap)

$$\bar{I}_{B/O} \;=\; \text{mean imager radiance over cloud layer B} \;=\; \left(\sum_{S_i}\omega_i f^i_{B/O}\bar{I}^i\right)\Big/\left(\sum_{S_i}\omega_i f^i_{B/O}\right) \tag{51}$$

$$=\; \frac{(.03)(1/2)(13)+(.10)(1)(29)+(.15)(1)(28.30)+(.20)(1/3)(36)}{(.03)(1/2)+(.10)(1)+(.15)(1)+(.20)(1/3)} \;=\; 29.37$$

SSF-129: Stddev of imager radiances over cloud layer 2 (no overlap)

$$S_{B/O} \;=\; \left[\frac{(.03)(1/2)(13)^2+(.10)(1)(29)^2+(.15)(1)(28.30)^2+(.20)(1/3)(36)^2}{(.03)(1/2)+(.10)(1)+(.15)(1)+(.20)(1/3)} - (29.37)^2\right]^{\frac{1}{2}} \tag{52}$$

$$=\; 4.62$$

SSF-130: Mean imager radiances over cloud layer 1 and 2 overlap

$$\bar{I}_{B/A} \;=\; \text{mean imager radiance over cloud layer overlap} \;=\; \left(\sum_{S_i}\omega_i f^i_{B/A}\bar{I}^i\right)\Big/\left(\sum_{S_i}\omega_i f^i_{B/A}\right) \tag{53}$$

$$=\; \frac{(.20)(1)(40)+(.20)(2/3)(36)+(.15)(1)(34)}{(.20)(1)+(.20)(2/3)+(.15)(1)} \;=\; 37.03$$

SSF-131: Stddev of imager radiances over cloud layer 1 and 2 overlap

$$S_{B/A} \;=\; \left[\frac{(.20)(1)(40)^2+(.20)(2/3)(36)^2+(.15)(1)(34)^2}{(.20)(1)+(.20)(2/3)+(.15)(1)} - (37.03)^2\right]^{\frac{1}{2}} \;=\; 2.67 \tag{54}$$

Table 8-1. Imager Pixel Parameters

General	Cloud layer 1 (low)	Cloud layer 2 (high)

1. Number of cloud layers (-1, 0, 1, or 2)
2. Cloud fraction (0-1.0)
3. Time of imager observation
4. Imager colatitude and longitude
5. Altitude of surface above sea level
6. Surface type index
7. Imager viewing zenith angle
8. Imager relative azimuth angle
9. Imager channel identifier (delete??)
10. Imager radiance for #9 (20 items)
11. Sunglint index
12. Snow/Ice index
13. Aerosol index
14. Fire index
15. Shadowed index
16. Total aerosol vis. optical depth, clear
17. Total aerosol effective radius, clear
18. Imager-based surface skin temperature
19. Algorithm notes
	20. Visible optical depth
	21. Infrared emissivity
	22. Water/Ice path
	23. Top pressure
	24. Effective* pressure
	25. Effective temperature
	26. Effective height
	27. base pressure
	28. Particle radius/diameter
	29. Particle phase
	       (0-ice or 1-water)
	30. Vertical Aspect ratio
		31. Visible optical depth
		32. Infrared emissivity
		33. Water/Ice path
		34. Top pressure
		35. Effective* pressure
		36. Effective temperature
		37. Effective height
		38. base pressure
		39. Particle radius/diameter
		40. Particle phase
		       (0-ice or 1-water)
		41. Vertical Aspect ratio

* Effective as viewed from space or cloud top if optically thick and cloud center if optically thin.

Table 8-2.

Bin Index	1	2		3	4	5	6			7	8	9	10	i
Pixel Data														
No. of layers	0	0	1	1	1	1	1	1	1	1	0	*	0	#1 Tab4.4-3
Subgrid mask	-	-	1/16	13/16	15/16	16/16	16/16	16/16	14/16	14/16	-		-	#2
Imager rad.	12	12	14	29	*	40	*	38	32	34	21		17	#11 1st item
General parm	-	-	x_{22}	*	x_4	x_5	x_{16}	x_{26}	x_{36}	x_7	-		-	#21,22,...,etc
Eff. Pressure layer 1(low)	-	-	250	320	245	268	290	330	340	335	-		-	#25
Calculated Quantities														
PSF weight	.02	.03		.10	.15	.20	.20			.15	.10	.03	.02	ω_i
No. pixels	1	2		1	1	1	3			1	1	0	1	n^i
Clear fraction	1	1/2		0	0	0	0			0	1		1	f^i_{clr}
Broken frac	0	1/2		1	1	0	1/3			1	0		0	f^i_{bk}
Overcast frac	0	0		0	0	1	2/3			0	0		0	f^i_{ov}
Cloud frac	0/16	1/32		13/16	15/16	16/16	46/48			14/16	0/16		0/16	f^i_{cld}
Clear radiance	12	12		-	-	-	-			-	21		17	$\bar{I}^i_{clr}$
Broken rad	-	14		29	31.19#	-	32			34	-		-	$\bar{I}^i_{bk}$
Overcast rad	-	-		-	-	40	38			-	-		-	$\bar{I}^i_{ov}$
Mean radiance	12	13		29	31.19#	40	36			34	21		17	$\bar{I}^i$
Mean parm	-	$x_2=x_{22}$		*	x_4	x_5	$x_6=(x_{16}+x_{26}+x_{36})/3$			x_7	-		-	$\bar{x}^i$
clear fraction	1	1/2		0	0	0	0			0	1		1	
1-layer fraction	0	1/2		1	1	1	1			1	0		0	
Mean Pressure layer 1(low)	-	-	250	320	245	268	320			335	-		-	
Cld Category layer A(low)	-	-	-	320	-	-	320			335	-		-	
layer B(high)	-	-	250	-	245	268	-			-	-		-	

* No data, # data fill, - N/A

132

Table 8-3.

	1	2		3	4	5	6			7	8	9	10	i
Bin Index	1	2		3	4	5	6			7	8	9	10	i
Pixel Data														
No. of layers	0	0	1	1	1	2	1	2	2	2	2	*	1	#1 Tab4.4-3
Subgrid mask	-	-	1/16	13/16	15/16	16/16	16/16	16/16	14/16	14/16	9/16		3/16	#2
Imager rad.	12	12	14	29	*	40	*	38	32	34	21		17	#11 1st item
General parm	-	-	x_2	*	x_4	x_5	x_{16}	x_{26}	x_{36}	x_7	x_8		x_{10}	#21,22,...,etc
	-	-	-	-	-	y_5	y_{16}	y_{26}	y_{36}	y_7	y_8		-	#32,33,...,etc
Eff. Pressure layer 1(low)	-	-	280	290	335	620	330	638	*	664	710		612	#25
layer 2(high)	-	-	-	-	-	340	-	325	345	350	606		-	#36
Calculated Quantities														
PSF weight	.02	.03		.10	.15	.20	.20			.15	.10	.03	.02	ω_i
No. pixels	1	2		1	1	1	3			1	1	0	1	n^i
Clear fraction	1	1/2		0	0	0	0			0	0		0	f^i_{clr}
Broken frac	0	1/2		1	1	0	1/3			1	1		1	f^i_{bk}
Overcast frac	0	0		0	0	1	2/3			0	0		0	f^i_{ov}
Cloud frac	0/16	1/32		13/16	15/16	16/16	46/48			14/16	9/16		3/16	f^i_{cld}
Clear radiance	12	12		-	-	-	-			-	-		-	$\bar{I}^i_{clr}$
Broken rad	-	14		29	28.30#	-	32			34	21		17	$\bar{I}^i_{bk}$
Overcast rad	-	-		-	-	40	38			-	-		-	$\bar{I}^l_{ov}$
Mean radiance	12	13		29	28.30#	40	36			34	21		17	$\bar{x}^i$
Mean parm	-	$x_2=x_{22}$		*	x_4	x_5	$x_6=(x_{16}+x_{26}+x_{36})/3$			x_7	-		-	$\bar{I}^i$
Mean Pressure layer 1(low)	-	-	280	290	335	620	330	638		664	710		612	
layer 2(high)	-	-	-	-	-	340	-	335		350	606		-	
Layer Pressure layer A(low)	-	-		-	-	620	638			664	658		612	$\bar{p}_A$
layer B(high)	-	280		290	335	340	333.33			350	-		-	$\bar{p}_B$
Clear fraction	1	1/2		0	0	0	0			0	0		0	f^i_{clr}
Layer A(low) frac	0	0		0	0	1	2/3			1	1		1	f^i_A
Layer B(high) frac	0	1/2		1	1	1	1			1	0		0	f^i_B
Overlap fractions Clear frac	1	1/2		0	0	0	0			0	0		0	f^i_{clr}
Layer A only	0	0		0	0	0	0			0	1		1	$f^i_{A/O}$
Layer B only	0	1/2		1	1	0	1/3			0	0		0	$f^i_{B/O}$
Layer B over A	0	0		0	0	1	2/3			1	0		0	$f^i_{B/A}$

* No data, # data fill, - N/A

133

Table 8-4.

Bin Index	1	2	2	3	4	5	6	6	6	7	8	9	10	i
Pixel Data														
No. of layers	0	0	1	1	1	2	1	2	2	2	2	*	1	#1 Tab4.4-3
Subgrid mask	-	-	1/16	13/16	15/16	16/16	16/16	16/16	14/16	14/16	9/16		3/16	#2
Imager rad.	12	12	14	29	*	40	*	38	32	34	21		17	#11 1st item
General parm	-	-	x_2	*	x_4	x_5	x_{16}	x_{26}	x_{36}	x_7	x_8		x_{10}	#21,22,...,etc
	-	-	-	-	-	y_5	y_{16}	y_{26}	y_{36}	y_7	y_8		-	#32,33,...,etc
Eff. Pressure layer 1(low)	-	-	280	290	335	620	330	638	*	664	710		612	#25
layer 2(high)	-	-	-	-	-	340	-	325	345	350	606		-	#36
Calculated Quantities														
PSF weight	.02	.03		.10	.15	.20	.20			.15	.10	.03	.02	ω_i
No. pixels	1	2		1	1	1	3			1	1	0	1	n^i
Clear fraction	1	1/2		0	0	0	0			0	0		0	f^i_{clr}
Broken frac	0	1/2		1	1	0	1/3			1	1		1	f^i_{bk}
Overcast frac	0	0		0	0	1	2/3			0	0		0	f^i_{ov}
Cloud frac	0/16	1/32		13/16	15/16	16/16	46/48			14/16	9/16		3/16	f^i_{cld}
Clear radiance	12	12		-	-	-	-			-	-		-	$\bar{I}^i_{clr}$
Broken rad	-	14		29	28.30#	-	32			34	21		17	$\bar{I}^i_{bk}$
Overcast rad	-	-		-	-	40	38			-	-		-	$\bar{I}^i_{ov}$
Mean radiance	12	13		29	28.30#	40	36			34	21		17	$\bar{x}^i$
Mean parm	-	$x_2=x_{22}$		*	x_4	x_5	$x_6=(x_{16}+x_{26}+x_{36})/3$			x_7	-		-	$\bar{I}^i$
Mean Pressure layer 1(low)	-	280		290	335	620	330	638		664	710		612	
layer 2(high)	-	-		-	-	340	-	335		350	606		-	
Layer Pressure layer A(low)	-	-		-	-	620	638			664	658		612	$\bar{p}_A$
layer B(high)	-	280		290	335	340	333.33			350	-		-	$\bar{p}_B$
Clear fraction	1	1/2		0	0	0	0			0	0		0	f^i_{clr}
Layer A(low) frac	0	0		0	0	1	2/3			1	1		1	f^i_A
Layer B(high) frac	0	1/2		1	1	1	1			1	0		0	f^i_B
Overlap fractions Clear frac	1	1/2		0	0	0	0			0	0		0	f^i_{clr}
Layer A only	0	0		0	0	0	0			0	1		1	$f^i_{A/O}$
Layer B only	0	1/2		1	1	0	1/3			0	0		0	$f^i_{B/O}$
Layer B over A	0	0		0	0	1	2/3			1	0		0	$f^i_{B/A}$

* No data, # data fill, - N/A

Table 8-5.

Index	Definition	Symbol	
No layer			
1	clear (no clouds)	CLR	0
One layer			
2	low cloud only (cloud effective pressure > 700 hPa)	L	1
3	lower middle cloud only (700 eff. pressure > 500 hPa)	LM	2
4	upper middle cloud only (500 eff. pressure > 300 hPa)	UM	3
5	high cloud only (eff. pressure £ 300 hPa)	++++--+-	4
Two layers		H	
6	high cloud over upper middle cloud		43
7	high cloud over lower middle cloud	H/UM	42
8	high cloud over low cloud	H/LM	41
9	upper middle cloud over lower middle cloud	H/L	32
10	upper middle cloud over low cloud	UM/LM	31
11	lower middle cloud over low cloud	UM/L	21
		LM/L	

CERES footprint

20 km

2 km

Imager pixel

top view

side view

**4 Cloud
Height Categories**

4. high clouds

300 hPa

layer 2

Category B

3. upper middle clouds

500 hPa

layer 1

2. lower middle clouds

Category A

700 hPa

Clear

1. low clouds

Surface
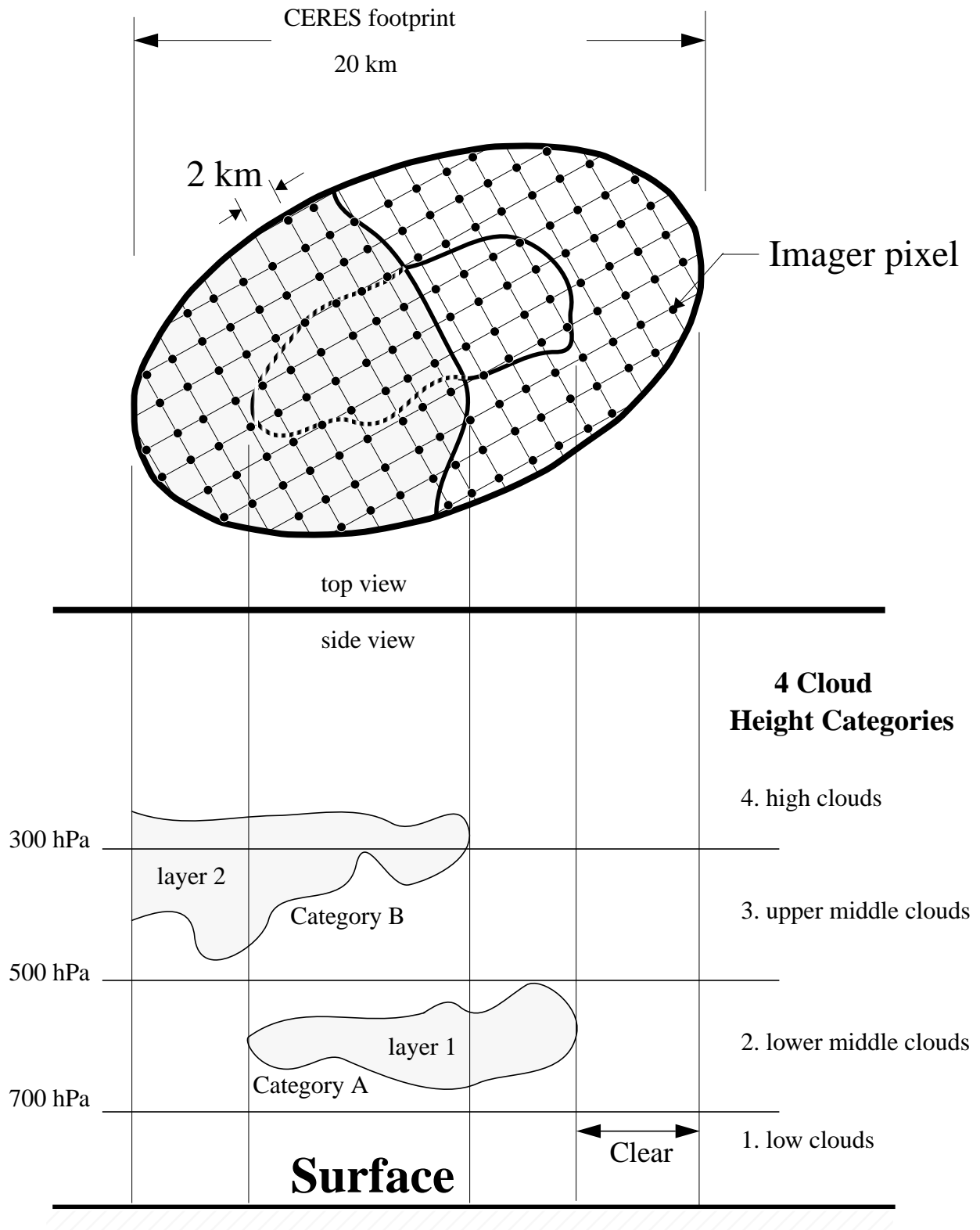
Figure 8-1. CERES Cloud Geometry

Note-3 CERES Point Spread Function

Note-3.1 CERES Point Spread Function

The CERES scanning radiometer is an evolutionary development of the ERBE scanning radiometer. It is desired to increase the resolution as much as possible, using a thermistor bolometer as the detector. As the resolution is increased, the sampling rate must increase to achieve spatial coverage. When the sampling rate becomes comparable to the response time of the detector, the effect of the time response of the detector on the PSF must be considered. Also, the signal is usually filtered electronically prior to sampling in order to attenuate electronic noises and to remove high frequency components of the signal which would cause aliasing errors. The time response of the filter, together with that of the detector causes a lag in the output relative to the input radiance. This time lag causes the centroid of the PSF to be displaced from the centroid of the optical FOV. Thus, the signal as sampled comes not only from where the radiometer is pointed, but includes a "memory" of the input from where it had been looking. Another effect of the time response is to broaden the PSF, which will reduce the resolution of the measurement, increase blurring errors, and decrease aliasing errors.

Note-3.2 Geometry of the Point Spread Function

The scanner footprint geometry is given in Figure 8-2. The optical FOV is a truncated diamond
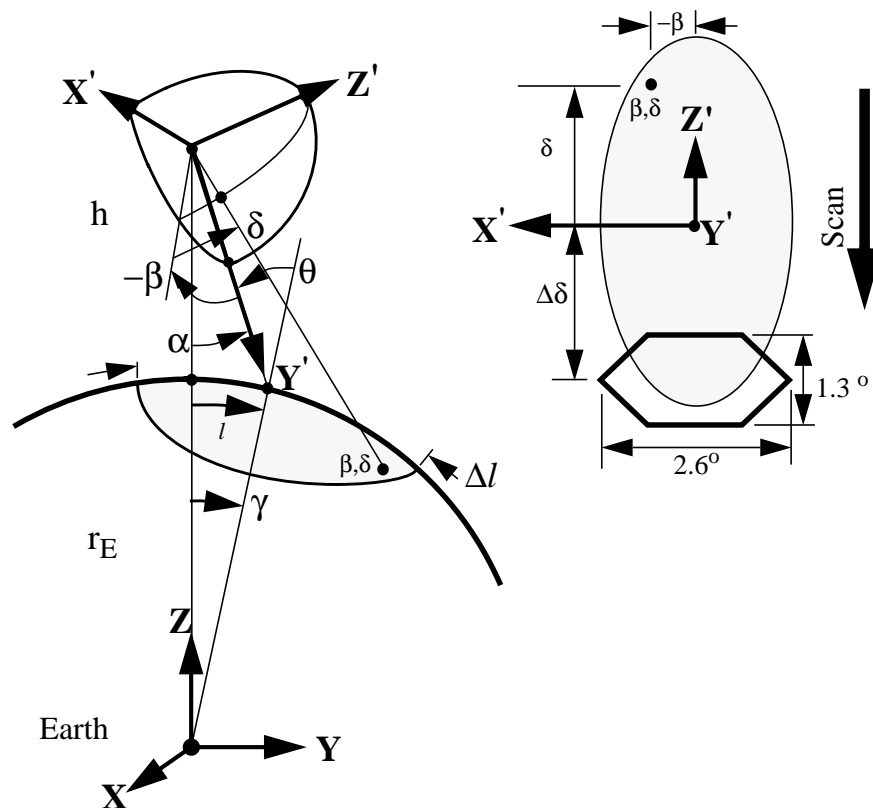
Figure 8-2. Scanner Footprint

(or hexagon) and is 1.3$^{\text{o}}$ in the along-scan direction and 2.6$^{\text{o}}$ in the across-scan direction. The effective FOV (or footprint) is given by the PSF and is shown as an ellipse. A point within the

footprint is located by β and δ. The cone angle α (or nadir angle) determines the location of the footprint centroid on the Earth. If $\alpha = 0$, the footprint is at nadir. The viewing zenith angle θ is a direct result of the satellite altitude h, the Earth radius r_E, and the cone angle α. The surface distance l and the Earth central angle γ between nadir and the centroid are also a result of the viewing geometry. In Figure 8-2 we have denoted the length of the FOV by Δl.

Figure 8-4 gives three CERES FOVs. The shaded area is the optical FOV. Note that only half of the FOV is given since it is symmetrical about the scan line. The origin has been placed at the centroid of the PSF which trails the optical axis by about 1.5 degree. This is the lag that is inherent in the system. About the PSF centroid, the outline has been drawn on the 95-percent energy boundary. An angular grid, also has been drawn over the 95% energy FOV for weighting cloud parameters in a later process. All of the pertinent dimensions are given.

Note-3.3 Analytic form of the Point Spread Function

A full discussion of an analytic model of the point spread function and its development is given in Smith (See Reference 48). From Figure 8-2, we redraw half of the optical FOV in Figure 8-3

$$\delta'_f(\beta) = \begin{cases} -a & 0 \le \beta < a \\ -2a + \beta & a \le \beta < 2a \end{cases}$$

$$\delta'_b(\beta) = \begin{cases} a & 0 \le \beta < a \\ 2a - \beta & a \le \beta < 2a \end{cases}$$
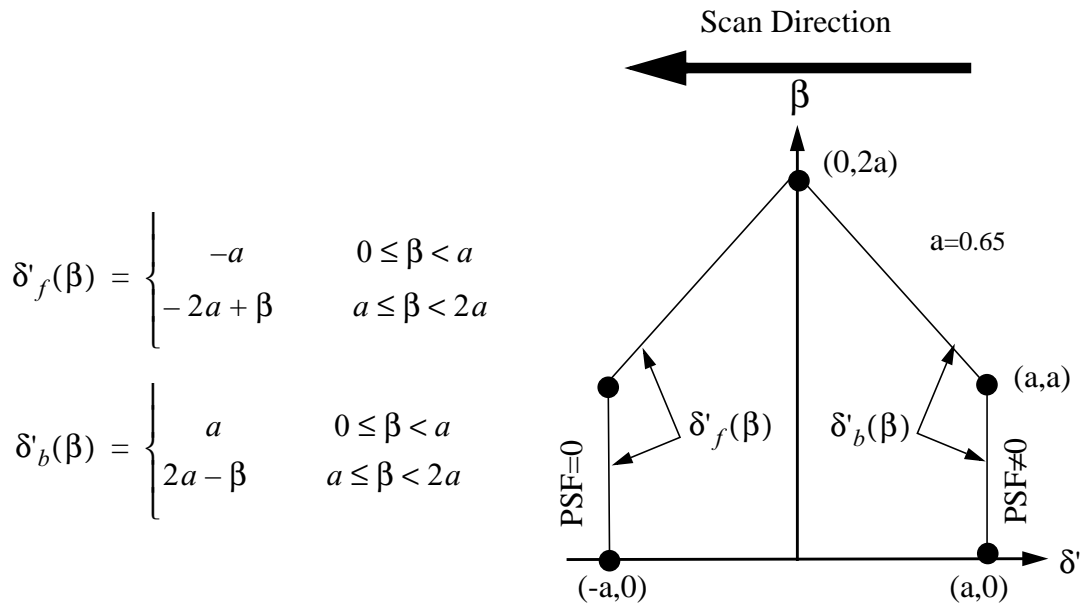
Figure 8-3. Optical FOV

where δ' is the along-scan angle and β is the cross-scan angle. Note that δ' points opposite the scan direction and increases toward the tail of the PSF (See Figure 8-4). The forward and back boundaries are given by $\delta'_f(\beta)$ and $\delta'_b(\beta)$, respectively.

With these definitions the CERES PSF is written as

$$P(\delta', \beta) = \begin{cases} 0 & |\beta| > 2a \\ 0 & \delta' < \delta'_f(\beta) \\ F[\delta' - \delta'_f(\beta)] & \delta'_f(\beta) \le \delta' < \delta'_b(\beta) \\ F[\delta' - \delta'_f(\beta)] - F[\delta' - \delta'_b(\beta)] & (otherwise) \end{cases} \tag{1}$$

where

$$\begin{aligned} F(\xi) = &\ 1 - (1 + a_1 + a_2)e^{-1.78348\xi} \\ &+ e^{-3.04050\xi}[a_1\cos(0.91043\xi) + b_1\sin(0.91043\xi)] \\ &+ e^{-2.20860\xi}[a_2\cos(2.78981\xi) + b_2\sin(2.78981\xi)] \end{aligned} \tag{2}$$

and

$$\begin{aligned} a_1 &= 5.83761 & a_2 &= -0.18956 \\ b_1 &= 2.87362 & b_2 &= 1.02431 \end{aligned}$$

where ξ is in degrees and (0.91043ξ) and (2.78981ξ) are in radians. The centroid of the PSF is derived in Smith (**See** Reference 48) and is 1.51^o from the optical axis. This shift is denoted in Figure 8-4 and a new angle δ is defined relative to the centroid. To evaluate the PSF we determine δ and then set $\delta' = \delta + \delta_0$ where δ_0 is the shift (or offset) from the optical axis to the centroid.

The numerical values given in equation (2) are based on the following prelaunch calibration constants:

$f_c = 10.5263$ hertz   Characteristic frequency of the Bessel Filter

$\tau = 0.0089$ sec   Detector time constant

$\dot{\alpha} = 63.0$ deg/sec   Scan rate

Table must be from BDS - check for any text that goes with

Table 8-6. Detector Time Constant (τ seconds)

Instrument	Detector Channel		
	Total	**Window**	**Shortwave**
PFM	0.00860	0.00830	0.00815
FM1	0.00850	0.00795	0.00825
FM2	0.00800	0.00820	0.00820
FM3	N/A	N/A	N/A
FM4	N/A	N/A	N/A

The general form of equation (2) is given by

$$
\begin{aligned}
F(\xi) = \ &1 - (1 + a_1 + a_2)e^{-\eta t} \\
&+ e^{\mu_1 t}[a_1 \cos(\omega_1 t) + b_1 \sin(\omega_1 t)] \\
&+ e^{\mu_2 t}[a_2 \cos(\omega_2 t) + b_2 \sin(\omega_2 t)]
\end{aligned}
\tag{3}
$$

where

$$
t = \frac{2\pi f_c}{\dot{\alpha}} \xi
$$

and where the complex roots of the 4-pole Bessel filter are

$$
\begin{aligned}
v_1 &= -2.89621 + 0.86723i = \mu_1 + i\omega_1 \\
v_2 &= -2.10379 + 2.65742i = \mu_2 + i\omega_2
\end{aligned}
$$

the residues of the Bessel filter are

$$
\begin{aligned}
u_1 &= +1.66339 - 8.39628i \\
u_2 &= -1.66339 + 2.24408i
\end{aligned}
$$

and

$$
\eta = \frac{1}{2\pi f_c \tau}.
$$

Note that ω_i, η, and t are non-dimensional so that $(\omega_i t)$ is in radians. The cone angle ξ has units of degrees. The complex variables p_i, v_i, u_i define a_i and b_i as

$$p_i = \frac{u_i}{\eta + v_i}, \qquad a_i = 2\eta Re\left(\frac{p_i}{v_i}\right), \qquad b_i = -2\eta Imag\left(\frac{p_i}{v_i}\right), \qquad i = 1, 2$$

The centroid of the PSF can be derived from the analytic expression and is given by

$$\delta_0 = \dot{\alpha}\tau(1 + \eta) \tag{4}$$

Note-3.4 Integration over the CERES FOV

We will need to integrate over the CERES FOV to determine the average cloud properties and area coverage. If we define x as a general cloud parameter over the 95% energy FOV (See Figure 8-4), then the weighted average value of x is given by

$$\bar{x} = \frac{\displaystyle\int_{FOV} P(\delta, \beta)x(\delta, \beta)\cos\delta d\beta d\delta}{\displaystyle\int_{FOV} P(\delta, \beta)\cos\delta d\beta d\delta} \tag{5}$$

where $P(\delta, \beta)$ is the PSF given by (1) and δ and β are the coordinates of a point in the FOV (See Figure 8-2). But, the value of x is known only at discrete imager pixels (See Term-27). We denote the values within the FOV by $x(\delta_k, \beta_k) \equiv x_k$ where k = 1,2, ... ,K. In general these x_k's will not be uniformly spaced over the FOV so that we must average over smaller sections of the FOV or a sub-grid and then integrate. Let us define a δ–β grid that matches the imager sampling at nadir (see sketch). Ideally, this grid would give one imager sample per grid area or angular bin. For TRMM we have h = 350 km and for VIRS Δl = 2 km so that $\Delta\delta = \tan^{-1}\left(\frac{\Delta l}{h}\right) = 0.33$ deg . For
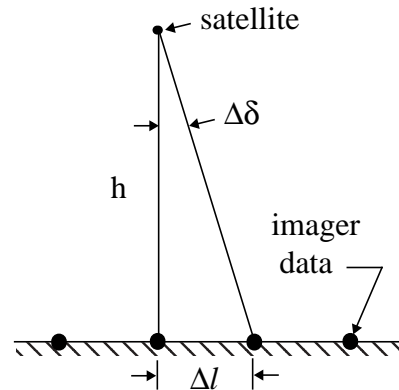
Terra we have h = 705 km and for MODIS Δl = 1 km so that $\Delta\delta$ = 0.08 deg. Thus, for TRMM we define a δ–β grid where the bin size is $\Delta\delta = 0.33$ deg and $\Delta\beta = 0.33$ deg and assume x(δ,β) is constant in a bin. We can now express the average value of x from (5) as

$$\bar{x} = \frac{\displaystyle\sum_{i, j} w_{ij} x_{ij}}{\displaystyle\sum_{i, j} w_{ij}} \tag{6}$$

where the weight w_{ij} is the integral of the PSF over an angular bin or

$$w_{ij} \equiv \int_{\delta = \delta_i}^{\delta = \delta_i + \Delta\delta} \int_{\beta = \beta_i}^{\beta = \beta_i + \Delta\beta} P(\delta, \beta) \cos\delta \, d\beta \, d\delta \tag{7}$$

and x_{ij} is the arithmetic mean of all the $x(\delta_k, \beta_k)$ in the angular bin such that $\delta_i < \delta_k \leq \delta_i + \Delta\delta$ and $\beta_i < \beta_k \leq \beta_i + \Delta\beta$. The δ–β grid and values of w_{ij} are given in Figure 8-4 for half the FOV.

.
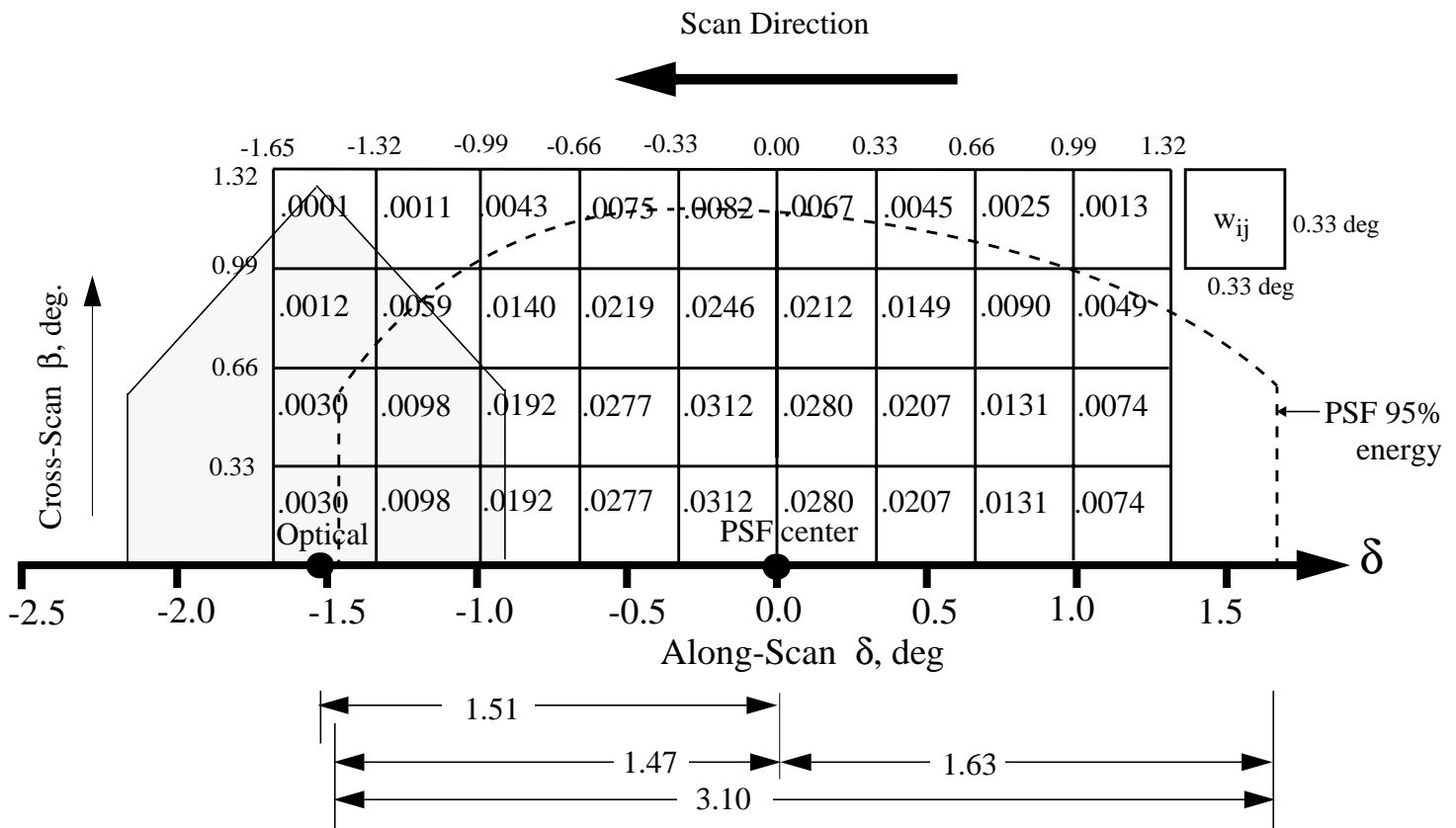
Figure 8-4. TRMM Angular Bin Weights

We have taken the FOV to be defined by $-1.65^o < \delta \leq 1.32^o$ and $-1.32^o < \beta \leq 1.32^o$ which approximates the 95% energy FOV in Figure 8-4. The integral over the FOV is given by $\sum_{ij} w_{ij} = 0.9483$

which is slightly less than 95% energy. So far we have made mention of only the centroid of the PSF. We now consider three measures of the central tendency. For the PSF in (1) the mean (centroid) is 1.51 deg from the optical axis, the mode (maximum P) is 1.35 deg and the median (50 percentile) is 1.44 deg. Since the scanner center location will ultimately be fine tuned with an empirical coastline detector (Hoffman et al., 1987) and alignment with the imager navigation, the

PSF centroid will be used as the center of the PSF and δ and β are referenced to this point. Thus, we consider the optical axis to be located at $\delta = -1.51$.

Note-3.5 Software implementation of the Point Spread Function

There are two PSFs and corresponding FOVs used to process CERES data. The first is the FOV defined in Figure 8-5. It applies only to CERES data with the nominal scan rate of approximately 63 deg sec^{-1}. Therefore, it does not applied to all CERES data. A second FOV, defined from the static PSF (Figure 8-5.), is applied to data with a scan rate near 0 deg sec^{-1}.
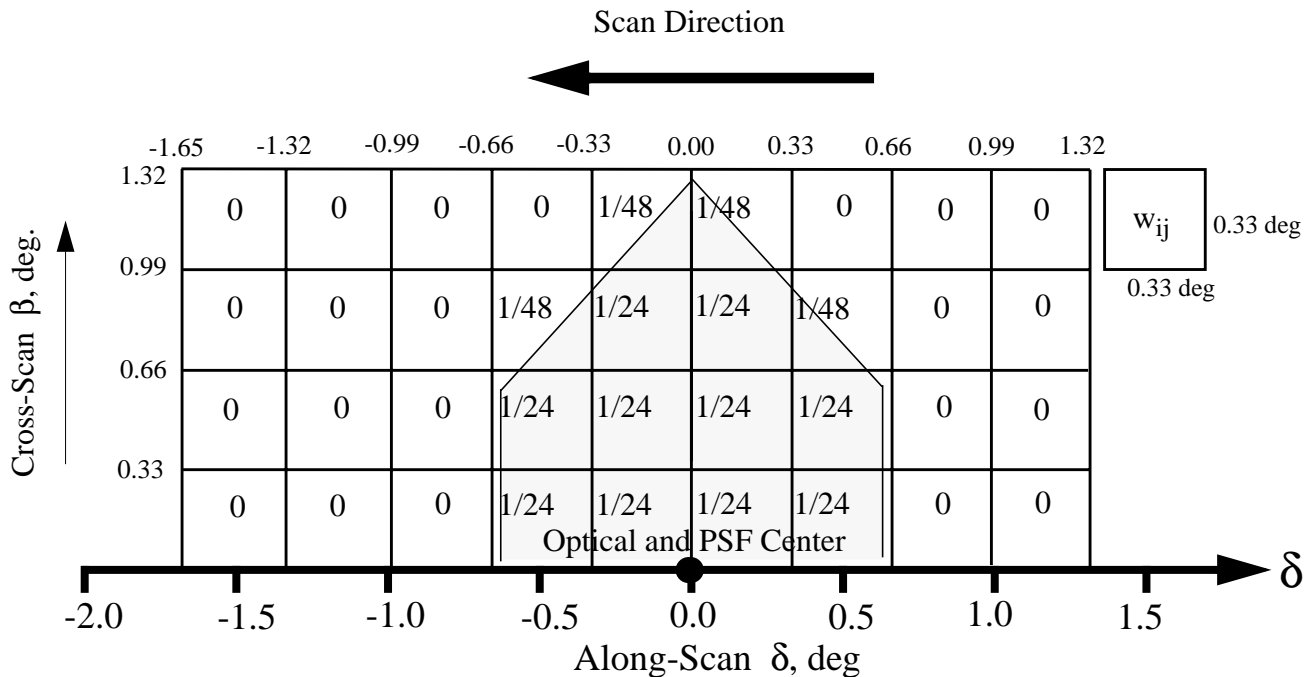
Figure 8-5. Static PSF and Field-of-View

The scan rate for a CERES measurement is given by SSF-16. If the absolute value of the scan rate is between 55 and 70 deg sec^{-1}, the first PSF is used. If the scan rate is between 0 and 5 deg sec^{-1}, the second or static PSF is used. If the CERES measurement has a scan rate outside these two ranges, then the measurement is not processed and not recorded in the SSF. No CERES measurement from the rapid retrace (See Term-32) portion of the short elevation scan will be included in the SSF because they have a nominal scan rate that exceeds 249 deg sec^{-1}.

Note-3.6 Validation of the Point Spread Function

The shape of the PSF is modeled by (1) where the detector time constant was determined in the lab during instrument calibration. The analytic model gives an offset of $\delta_0 = 1.51$ deg.

???The full calibration results give $\delta_0 = 1.56$ deg. (what about different channels and instruments. What about TRW documents as references.

???The light bulb data gives a mode of 1.51 and a centroid offset of $\delta_0 = 1.55$. Other channel modes are ???.

Note-3.7 References related to the Point Spread Function

need to put into reference section or delete

???Bob Lee

???TRW

???Light bulb memo (Pete Spence)

???Priestley thesis

Note-4 Conversion of Julian Date to Calendar Date

The Julian Date is a time system that has been adopted by astronomers and is used in many scientific experiments. The Julian Date or Julian Day is the number of mean solar days since 1200 hours (GMT/UT/UTC/Zulu) on Monday, 24 November 4714 BCE, based on the current Gregorian calendar, or more precisely, the Gregorian Proleptic calendar. In other words, Julian day number 0 (zero) was Monday, 24 November 4714 Before Current Era (BCE), 1200 hours (noon). A new Julian day starts when the mean Sun at noon crosses the Greenwich meridian. This differs from Universal Time (UT) or Greenwich Mean Solar Time by 12 hours since UT changes day at Greenwich midnight. Table 8-7 below provides Julian day numbers which relate Universal Time to Julian Date.

Important facts related to the Gregorian calendar are:
   a) There is no year zero; year -1 is immediately followed by year 1.
   b) A leap year is any year which is divisible by 4, except for those centesimal years (years divisible by 100) which must also be divisible by 400 to be considered a leap year.
   c) A leap year has 366 days, with the month of February containing 29 days.
   d) Year -1 is defined as a leap year, thus being also defined as containing 366 days, and being divisible by 4, 100, and 400.

Information on history, calendars, and Julian day numbers can be found in Blackadar's (See Reference 4) "A Computer Almanac", and on the WWW (See Reference 34).

The Julian day whole number is followed by the fraction of the day that has elapsed since the preceding noon (1200 hours UTC). The Julian Date JDATE can be represented as:

    JDATE = JDay + JFract
    where:
       JDay = the integer Julian Day number and
       JFract = the "fractional" Julian day (0 to 0.99...9)
              (e.g. 245_0814.0 = 1200 or noon, 31 December, 1997 UT)

When the fractional part of the combined Julian Date is .0, it is noon or 1200 hours GMT and when the fraction part is .5, then it is midnight or 0000 hours GMT.

The calculation of GMT (YYYYMMDD-HH:MM:SS.SSS) from Julian Date (JDATE) is performed using the following process.

   1. The YYYYMMDD can be determined using Table 8-7 to find the year and the beginning of the month whose Julian Day occurs before the JDay integer value.
   2. Calculate the number of days past the 0.5 day of the month via Table 8-7 which provides Julian day numbers which relate Universal Time to Julian Date.

The GMT is determined by first computing the number of seconds in the day since midnight:
       if JFract > 0.5,
       thenSeconds = 86400.0 * (JFract-0.5)
       if JFract <= 0.5,
       thenSeconds = 86400.0 * (JFract+0.5)

Then compute HH, MM, and SS where:

HH = Int(Seconds/3600)
MM = Int(Seconds-(HH*3600.0)/60)
SS = Seconds-(HH*60.0 + MM)*60.0

As an example, if JD = 244_5733.5833, then the GMT date is computed using Table 8-7 by finding the closest beginning monthly calendar noon date, which is Feb 0.5, 1984 (UT).

(Feb 0.5)Jday
244_5731 < 244_5733.5833

JD = 244_5733.5833 is 2.5833 days past Feb 0.5, 1984 UT (i.e., past 1984 Jan 31^d 12^h 0^m 0^s)

where 1984 Jan 31^d 12^h 0^m 0^{ss} = (244_5733-244_5731).

Beginning with the whole days portion of 2.5833 (i.e., 2), the GMT Date is 1984 Jan 31^d 12^h 0^m 0^s + 2 = 1984 Feb 2^d 12^h 0^m 0^s.

Next, since JFract (0.5833) is > 0.5, 12^h is added to the GMT Date, yielding: 1984 Feb 2^d 12^h 0^m 0^s + 12^h 0^m 0^s = 1984 Feb 3^d 0^h 0^m 0^s.

Finally, to get the GMT time and since JFract (0.5833) is > 0.5, the number of seconds = 86400 *(0.5833 -0.5) = 7197.12 yielding:
HH = 7197.12 / 3600 = 01.9992 = 01^h
MM = 7197.12 - ((1*3600) / 60) = 59.952 = 59^m
SS = 7197.12 - ((1*60) + 59)*60) = 57.12^s

Therefore, the GMT Date corresponding to the Julian Date 244_5733.5833 = 1984 Feb 3^d 1^h 59^m 57.12^s, which is UT = 1984 Jan 31^d 12^h 0^m 0^s + 2.5833 days.

Table 8-7. Julian Day Number

Year	Jan 0.5[a]	Feb 0.5	Mar. 0.5	Apr. 0.5	May 0.5	June 0.5	July 0.5	Aug 0.5	Sept 0.5	Oct 0.5	Nov 0.5	Dec 0.5
1980t	244_4239	_4270	_4299	_4330	_4360	_4391	_4421	_4452	_4483	_4513	_4544	_4574
1981	_4605	_4636	_4664	_4695	_4725	_4756	_4786	_4817	_4848	_4878	_4909	_4939
1982	_4970	_5001	_5029	_5060	_5090	_5121	_5151	_5182	_5213	_5243	_5274	_5304
1983	_5335	_5366	_5394	_5425	_5455	_5486	_5516	_5547	_5578	_5608	_5639	_5669
1984t	_5700	_5731	_5760	_5791	_5821	_5852	_5882	_5913	_5944	_5974	_6005	_6035
1985	244_6066	_6097	_6125	_6156	_6186	_6217	_6247	_6278	_6309	_6339	_6370	_6400
1986	_6431	_6462	_6490	_6521	_6551	_6582	_6612	_6643	_6674	_6704	_6735	_6765
1987	_6796	_6827	_6855	_6886	_6916	_6947	_6977	_7008	_7039	_7069	_7100	_7130
1988t	_7161	_7192	_7221	_7252	_7282	_7313	_7343	_7374	_7405	_7435	_7466	_7496
1989	_7527	_7558	_7586	_7617	_7647	_7678	_7708	_7739	_7770	_7800	_7831	_7861
1990	244_7892	_7923	_7951	_7982	_8012	_8043	_8073	_8104	_8135	_8165	_8196	_8226
1991	_8257	_8288	_8316	_8347	_8377	_8408	_8438	_8469	_8500	_8530	_8561	_8591
1992t	_8622	_8653	_8682	_8713	_8743	_8774	_8804	_8835	_8866	_8896	_8927	_8957
1993	_8988	_9019	_9047	_9078	_9108	_9139	_9169	_9200	_9231	_9261	_9292	_9322
1994	_9353	_9384	_9412	_9443	_9473	_9504	_9534	_9565	_9596	_9626	_9657	_9687
1995	244_9718	_9749	_9777	_9808	_9838	_9869	_9899	_9930	_9961	_9991	*0022	*0052
1996t	245_0083	_0114	_0143	_0174	_0204	_0235	_0265	_0296	_0327	_0357	_0388	_0418
1997	_0449	_0480	_0508	_0539	_0569	_0600	_0630	_0661	_0692	_0722	_0753	_0783
1998	_0814	_0845	_0873	_0904	_0934	_0965	_0995	_1026	_1057	_1087	_1118	_1148
1999	_1179	_1210	_1238	_1269	_1299	_1330	_1360	_1391	_1422	_1452	_1483	_1513
2000t	245_1544	_1575	_1604	_1635	_1665	_1696	_1726	_1757	_1788	_1818	_1849	_1879
2001	_1910	_1941	_1969	_2000	_2030	_2061	_2091	_2122	_2153	_2183	_2214	_2244
2002	_2275	_2306	_2334	_2365	_2395	_2426	_2456	_2487	_2518	_2548	_2579	_2609
2003	_2640	_2671	_2699	_2730	_2760	_2791	_2821	_2852	_2883	_2913	_2944	_2974
2004t	245_3005	_3036	_3965	_3096	_3126	_3157	_3187	_3218	_3249	_3279	_3310	_3340
2005	_3371	_3402	_3430	_3461	_3491	_3522	_3552	_3583	_3614	_3644	_3675	_3705
2006	_3736	_3767	_3795	_3826	_3856	_3887	_3917	_3948	_3979	_4009	_4040	_4070
2007	_4101	_4132	_4160	_4191	_4221	_4252	_4282	_4313	_4344	_4374	_4405	_4435
2008t	245_4466	_4497	_4526	_4557	_4587	_4618	_4648	_5679	_4710	_4740	_4771	_4801
2009	_4832	_4863	_4891	_4922	_4952	_4983	_5013	_5044	_5075	_5105	_5136	_5166

[a] Jan. 0.5 (UT) is the same as Greenwich noon (12h) UT, Dec. 31.   * These dates begin with 245   † Denotes leap years

Note-5 Spectral Correction Algorithm

The radiances as measured by the CERES instruments are filtered radiances and the spectral correction algorithm unfilters these radiances. The desired unfiltered radiances are defined by

$$I^{SW} = \int_0^\infty I_\lambda^r d\lambda$$

$$I^{LW} = \int_0^\infty I_\lambda^e d\lambda$$

$$I^{WN} = \frac{1}{\lambda_2 - \lambda_1}\int_{\lambda_1}^{\lambda_2} I_\lambda^e d\lambda$$

where λ (μm) is the wavelength, $\lambda_1 = 8.1$ and $\lambda_2 = 11.8$, and I_λ^r and I_λ^e are the reflected and emitted components of the total observed radiance or $I_\lambda = I_\lambda^r + I_\lambda^e$. The filtered measurements are modeled as

$$m_f^i = \int_0^\infty S_\lambda^i I_\lambda d\lambda \qquad i = \text{SW, TOT}$$

$$m_f^i = \frac{1}{\lambda_2 - \lambda_1}\int_0^\infty S_\lambda^i I_\lambda d\lambda \qquad i = WN$$

where S_λ^i is the normalized spectral response function $(0 \le S_\lambda^i \le 1)$. The spectral response function for CERES_ TRMM is shown in the Figure 8-6 and represents the spectral throughput of the individual detector's optical elements determined from laboratory measurements. An estimate of the unfiltered SW and WN radiances are determined from the filtered radiance measurements as follows:

$$\hat{I}^{SW} = a_0 + a_1 \ (m_f^{SW_r}) + a_2 \ (m_f^{SW_r})^2$$

$$\hat{I}^{WN} = b_0 + b_1 \ (m_f^{WN}) + b_2 \ (m_f^{WN})^2$$

where a_0, a_1, a_2, b_0, b_1, and b_2 are theoretically derived regression coefficients that depend on scene type and viewing geometry. $m_f^{SW_r}$ represents the reflected portion of the filtered SW radiance measurement and is given by $m_f^{SW_r} = m_f^{SW} - m_f^{SW_e}$ where $m_f^{SW_e}$ is the emitted thermal portion of m_f^{SW} and is estimated from m_f^{WN} using a pre-determined empirical 2nd order polynomial expression relating nighttime m_f^{SW} and m_f^{WN} measurements. For CERES_ TRMM the least-square fit is given by:

$$m_f^{SW_e} = k_0 + k_1(m_f^{WN}) + k_2(m_f^{WN})^2$$

where $k_0 = 0.1208$, $k_1 = -0.001697$, and $k_2 = 0.0006875$. Since there are no filtered longwave radiance measurements in CERES, the unfiltered emitted LW radiance must be inferred from measurements in the other available channels. An estimate of the daytime (D) and nighttime (N) LW radiance is given by

$$\hat{I}^{LW}(D) = c_0 + c_1 m_f^{SW_r} + c_2 m_f^{TOT} + c_3 m_f^{WN}$$

$$\hat{I}^{LW}(N) = d_0 + d_1 m_f^{TOT} + d_2 m_f^{WN}$$

where the c and d coefficients are theoretically derived regression coefficients. All of the spectral correction coefficients (SCC) are obtained from a regression analysis of theoretically derived filtered and unfiltered radiances in each channel. The simulated radiances are inferred from a spectral radiance database of typical Earth scenes and the spectral response functions. Each CERES instrument has its own set of SCC based on its spectral response. There are different SCC for land, ocean, snow, and cloud. The SCC also vary with solar zenith, viewing zenith, and relative azimuth. Additional details are given in Reference 41.
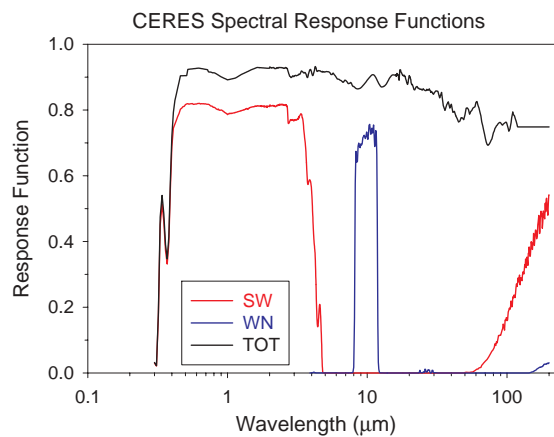
Figure 8-6. CERES_TRMM Spectral Response

Note-6 Bandwidth of the Window Channel

The nominal bandwidth of the CERES window channel is 8 to 12 µm. However, the CERES_TRMM window channel has its half power points of the spectral response are at 8.1 and 11.8 µm (See Figure 8-6). When unfiltering the window channel it is more accurate to estimate the radiance in the 8.1 to 11.8 µm wavelength interval than the 8 to 12 µm interval. For this reason the CERES window channels are unfiltered to 8.1 to 11.8 µm and the result divided by 3.7 µm so that the unfiltered radiance is in units of $W\ m^{-2}\ sr^{-1}\mu m^{-1}$. This 3.7 µm interval is used for all CERES window channels even though the individual instrument responses vary slightly.

Note-7 CERES Cloud Mask

 CERES Cloud Mask operates on imager radiance data and uses a threshold method to determine scene type. Cloudy pixels, for example, occur when one or more of radiances differ significantly from the expected clear-sky radiances. A "clear" imager pixel is any pixel in the clear subcategory. A "cloudy" imager pixel is any pixel in the cloudy subcategory. The result of the cloud mask is a scene type for each imager pixel as given in Table 8-8.

Table 8-8. CERES Cloud Mask Scenes

CERES Cloud Mask: pick one and only one scene type.		
Clear Subcategory:	**Cloudy Subcategory:**	**Unknown Subcategory:**
Clear-strong (See SSF-67) Clear-weak (See SSF-68) Fire (See SSF-72-A) Snow/Ice (See SSF-69) Glint clear (See SSF-72-B) Cloud shadow (See SSF-72-C) Aerosol (See SSF-70 and SSF-71) Reclassified clear (See SSF-65)	Cloudy-strong (See SSF-82) Cloudy-weak (See SSF-82) Glint cloud (See SSF-82)	Bad data

Cloud retrieval attempts to identify every imager pixel as clear or cloudy. For most VIRS cases, this requires a pixel to have associated with it all five radiances. There are 3 exceptions to this rule. The first exception is when VIRS channel 4 is very cold and the pixel is consequently identified as cloudy. The second exception is when VIRS channel 3 radiance is set to default, but from the channel 4 radiance it can the established that the channel 3 was actually saturated. In this case, a saturated value is assigned to the channel 3 radiance for all further Cloud processing (See SSF-65-A). The last exception is when no clear or cloudy determination could be made from the imager data, but the CERES FOV was over land or desert (no snow) and the CERES WN channel radiance exceeded a threshold, allowing the pixel to be reclassified as clear. In all other VIRS cases, where there are missing imager radiances, the imager pixel is identified as unknown due to bad data.

Once cloud retrieval has determined whether a pixel is clear or cloudy, it must determine the associated subcategory. Only a single subcategory can be determined for a pixel. If no subcategory can be determined, the pixel is reclassified as unknown.

The clear subcategory Reclassified clear was added beginning with CC# 014011. Prior to that, these pixels were classified as unknown data.

The cloud mask as implemented and used by Cloud retrieval software is documented on the website http://earth-www.larc.nasa.gov/~cwg/cloudmask/cloudmask.html.

When the cookiecutter attempts to compute the imager-based properties over a CERES FOV, it ignores all imager pixels identified as unknown, treating them as if they did not exist. The remaining pixels are located in the CERES FOV angular bins (See Term-2). Cloudy pixels for which no cloud properties were computed are discussed in NOTE 8.

Note-8 Anomalous Cloudy Areas

Every pixel that falls within a CERES FOV can be identified as:
- Clear
- Cloudy with layer information
- Cloudy no layer information
- Bad Data

Clear pixels are simply those that fall within the clear subcategory (See Note-7). Cloudy with layer information pixels are those that fall within the cloudy subcategory (See Note-7) and have the cloud properties required to identify layers (See Note-2). Conversely, Cloudy no layer information pixels are those that fall within the cloudy subcategory but don't have the cloud properties required to identify layers. They occur when pixels cannot be processed by VIST because they do not fall within a "tile" or when VIST cannot determine cloud properties from the imager radiances. Finally, bad data pixels are those that fall within the unknown subcategory (See Note-7) or, alternately stated, pixels which could not be identified as clear or cloudy. Bad data pixels are ignored and not used. The area of the CERES FOV containing clear pixels or cloudy pixels, regardless of layer information, is recorded in Imager percent coverage (See SSF-54).

Clear and cloudy with layer information pixels can be processed normally. CERES FOVs which are comprised entirely of these two types of pixels require no special treatment. However, FOVS containing cloudy no layer information pixels are considered anomalous. Early analysis has shown that it is important to retain as much data as possible to avoid the bias that results when pixels and or FOVs are selectively ignored. Therefore, pixels that cannot be placed in a cloud layer should not be ignored nor should FOVs containing these pixels be dropped from the SSF. An algorithm that attempts to retain as much information as possible has been developed.

If the cloudy no layer information area covers less than 0.0002% of the FOV, then it is ignored when computing layer/overlap percent coverages (See SSF-81) and cloud properties (See SSF-82 to SSF-114). Such a small area is deemed mathematically insignificant and need not be extrapolated. However, if these cloudy no layer information pixel(s) are considered overcast, they will be included in the overcast footprint imager radiance statistics (See SSF-117, SSF-120, and SSF-121). This scenario rarely occurs.

When a FOVs contains a mathematically significant area of cloudy no layer information pixels, the FOV's cloud layer information can either be inferred from the portion of the FOV that has layer information or all parameters related to layering can be set to CERES default (See Table 4-5) for the entire FOV. As of this writing, the cloudy no layer information cannot be more than a factor of 10 larger than the cloudy with layer information area, if information is to be inferred. The cloudy area without layer information is assumed to be of the same proportion of layer 1, layer 2, and layer 2 over layer 1 areas as the cloudy area with layer information, so Clear/layer/overlap condition percent coverages (See SSF-81) are adjusted accordingly. The cloud properties (See SSF-82 to SSF-114) for the cloudy area with layer information are assumed to be representative of the entire cloudy area. The cloudy area with no layer information as a PSF-weighted (See Term-29) percentage of the entire cloudy area is recorded in Cloud property extrapolation over cloudy area (See SSF-63).

When the cloudy area containing layer information is determined to be too small for information to be inferred (cloudy with layer / cloudy no layer < 0.1), all parameters related to cloud layers are set to CERES default (See Table 4-5). Parameters set to default include layer 1, layer 2, and layer 2 over layer 1 areas stored in the array Clear/layer/overlap condition percent coverages (See SSF-81), all cloud properties for both layers (See SSF-82 to SSF-114), and Cloud property extrapolation over cloudy area (See SSF-63).

Note-9 Cloud Property Retrieval Algorithm

This section will discuss the hierarchy of determining cloud properties within the VIST algorithm.

Note-10 General Angular Distribution Model Discussion

TOA flux parameters include references to an ADM Note.

Note-11 VIRS12B Angular Distribution Models

Introduction

The VIRS12B is a set of SW, LW, and WN ADMs based on the CERES/TRMM data. VIRS12B
is an intermediate set of ADMs between the ERBE production ADMs (See References 53 and
57) and future CERES ADMs based on multiple cloud properties. To construct the VIRS12B, the
CERES/TRMM data was sorted into the 12 ERBE scene types based on the VIRS cloud cover
and the CERES surface map. These 12 scenes use the same names as ERBE, but are different in
concept. For example, overcast for the ERBE MLE means the scene is cold and bright while
overcast for the VIRS cloud mask means the presence of cloud independent of thickness. The
angular bins in viewing zenith, relative azimuth, and solar zenith are also different than for ERBE
production. And finally, VIRS12B has separate LW and WN ADMs for day and night.

The VIRS12B set of ADMs was constructed from 3 months of CERES/TRMM data from January
to March 1998 with the SSF production strategies "ValidationR2" and "ValR2-NL". CERES uses
two sampling modes. The rotating azimuth plane scan mode (RAPS) gives good angular
sampling and the fixed azimuth plane scan mode (FAPS) gives good spatial sampling, but poor
angular sampling. To accommodate both spatial and angular sampling, CERES/TRMM
alternated between FAPS for 2 days and RAPS for 1 day. Thus, only 25 days of RAPS data were
available over the 3 month period from which to construct ADMs. This data set is minimal but
has several advantages over using the ERBE production ADMs based on Nimbus-7 data and the
MLE scene identification. VIRS12B is data consistent since the ADMs were constructed with
CERES data and applied to CERES data. They also use the same VIRS scene identification for
construction and application. Another advantage of VIRS12B over the ERBE production ADMs
is their reference at the Earth surface instead of the TOA. The VIRS12B set was constructed at
the surface (without atmospheric effects) which is closer to the source of radiation than the TOA
and minimizes geometric errors (See Note-13). The WN ADMs are new and did not exist for
ERBE.

TRMM ValidationR2 and earlier SSF production strategies denote ADM type as 0-12 although
they do not use the VIRS12B set. These earlier SSFs used the RPM ADMs (See Reference 30)
for all scene types. The SSF production strategy is denoted in the granule (See Term-19) name.
Also, the header contains the SSF ID (See SSF-H1). This paragraph applies only to SSF ID equal
to 112.

VIRS12B ADM Scene Types

The VIRS12B ADM types below are based upon the ERBE 12 scene types and are the same for
SW, LW, and WN. The scene type is selected based on the ADM cloud amount and the ADM
surface type.
0. unknown
1. clear ocean
2. clear land
3. clear snow
4. clear desert
5. clear land-ocean mix (or coastal)
6. partly cloudy ocean

7. partly cloudy land or desert
8. partly cloudy land-ocean mix
9. mostly cloudy ocean
10. mostly cloudy land or desert
11. mostly cloudy land-ocean mix
12. overcast over any surface

Mapping from CERES Cloud Amount to ADM Cloud Amount

The CERES cloud percentage for an FOV is determined by subtracting the "clear percent coverage at the subpixel resolution" (See SSF-66) from 100. The type of cloud coverage is based on the following mapping:

If $0 \leq$ cloud percentage $\leq 5\%$, then the FOV is "clear".
If $5\% <$ cloud percentage $\leq 50\%$, then the FOV is "partly cloudy".
If $50\% <$ cloud percentage $\leq 95\%$, then the FOV is "mostly cloudy".
If $95\% <$ cloud percentage $\leq 100\%$, then the FOV is "overcast"

Mapping from CERES Surface Types to ADM Surface Types

To determine the proper VIRS12B ADM type, the FOV surface types must be mapped into the ADM surface types and then a single ADM surface type must be assigned to the FOV. The 20 possible CERES surface types (See SSF-25) are mapped into 4 ADM surface types as shown here:

ADM land: CERES surface types 1-6, 8-14, 18
ADM ocean: CERES surface types 17
ADM snow: CERES surface types 15, 19, 20
ADM desert: CERES surface types 7, 16

The corresponding percentages for each CERES surface type (See SSF-26) are summed for each ADM surface type using the above mapping. A single ADM surface type is assigned to the FOV using the following algorithm:

If the % desert > 50%, then the ADM surface type is "desert".
If the % snow > 50%, then the ADM surface type is "snow".
If the % ocean > 67%, then the ADM surface type is "ocean".
If the (% land + % desert +% snow) > 67%, then the ADM surface type is "land".
Otherwise, the ADM surface type is "land-ocean mix"

SW ADM Grid

The SW ADMs are a function of 12 scene types, 9 viewing zenith (See SSF-20) bins, 10 relative azimuth (See SSF-10) bins, and 9 solar zenith (See SSF-21) bins. The zenith angles are defined from 0° to 90° and are divided into 10° bins. The SW ADMs is assumed symmetric in azimuth so that the relative azimuth angle is defined from 0° to 180° and divided into 20° bins except for the first and last bins of 10° each.

With the exception of clear snow and all 3 land-ocean mix scenes, the SW VIRS12B is based on CERES/TRMM data and the ADMs were constructed with the SAB method (See Reference 55). However, for clear snow and all 3 land-ocean mix scenes the SW ADMs are based on Nimbus-7 data and constructed with the RPM method (See Reference 30).

The ADMs are defined as piecewise constant functions over these angular bins. The ADMs are evaluated by linear interpolation in all angles.

LW ADM Grid

The LW ADMs are a function of 12 scene types, 9 viewing zenith (See SSF-20) bins, 10 colatitude (See SSF-10) bins, and 2 solar zenith (See SSF-21) bins. The LW ADMs are not seasonal. The viewing zenith angle is defined from 0° to 90° and is divided into 10° bins. The colatitude angle is defined from 0° to 180° and is divided into 18° bins. The solar zenith angle is defined from 0° to 180° and is divided at 90° into day and night bins.

With the exception of clear snow, the LW VIRS12B is based on CERES/TRMM data and the ADMs were constructed with the SAB method (See Reference 55). However, for clear snow scenes the LW ADMs are based on Nimbus-7 data and constructed with the RPM method (See Reference 30). LW coefficients could not be developed in the colatitude bins which lie outside the TRMM orbit. Therefore, LW ADM coefficients for colatitudinal bin 4 are replicated in colatitudinal bins 1, 2, and 3. Likewise, LW ADM coefficients for colatitudinal bin 7 are replicated in colatitudinal bins 8, 9, and 10.

The ADMs are defined as piecewise constant functions over these angular bins. The ADMs are evaluated by linear interpolation in viewing zenith and colatitude.

WN ADM Grid

The WN ADMs are a function of 12 scene types, 9 viewing zenith (See SSF-20) bins, 10 colatitude (See SSF-10) bins, and 2 solar zenith (See SSF-21) bins. The WN ADMs are not seasonal. The viewing zenith angle is defined from 0° to 90° and is divided into 10° bins. The colatitude angle is defined from 0° to 180° and is divided into 18° bins. The solar zenith angle is defined from 0° to 180° and is divided at 90° into day and night bins.

With the exception of clear snow, the WN VIRS12B is based on CERES/TRMM data and the ADMs were constructed with the SAB method (See Reference 55). However, for clear snow scenes the WN ADMs are based on LW Nimbus-7 data and constructed with the RPM method (See Reference 30). Also, like LW, WN coefficients could not be developed in the colatitude bins which lie outside the TRMM orbit. Therefore, WN ADM coefficients for colatitudinal bin 4 are replicated in colatitudinal bins 1, 2, and 3, and WN ADM coefficients for colatitudinal bin 7 are replicated in colatitudinal bins 8, 9, and 10.

The ADMs are defined as piecewise constant functions over these angular bins. The ADMs are evaluated by linear interpolation in viewing zenith and colatitude.

Note-12 Beta2_TRMM Angular Distribution Models

Introduction

The Beta2_TRMM is a set of SW, LW, and WN ADMs based on the CERES Edition1TRMM data. It is a draft, or beta (See Term-5), set of the CERES TRMM ADMs based on multiple cloud properties.

The Beta2_TRMM set of ADMs was constructed from the 9 months of available CERES/TRMM data with the SSF production strategy "Edition1". The CERES instrument has three scan modes. The Cross-Track scan mode is the same as that used in ERBE; it gives good spatial sampling, but poor angular sampling. The Rotating Azimuth Plane scan (RAPS) mode gives good angular sampling. The Along-Track scan mode is used for the validation of the CERES instantaneous fluxes. To accommodate both spatial and angular sampling, CERES/TRMM alternated between Cross-Track for 2 days and RAPS for 1 day. On nine occasions, the RAPS day was replaced with an Along-Track scan day.

The Beta2_TRMM ADM types differ for SW and LW/ WN.

Beta2_TRMM SW ADM Scene Types

There are 602 SW ADM types.

SW ADM types	Scene	Cloud Phase
1-5	Clear Ocean	N/A
6-10	Clear Ocean - Sunglint	N/A
11	Clear Mod-Hi Tree/Shrub	N/A
12	Clear Lo-Mod Tree/Shrub	N/A
13	Clear Dark Desert	N/A
14	Clear Bright Desert	N/A
15-182	Cloudy Ocean	Liquid
183-350	Cloudy Ocean	Ice
351-380	Cloudy Mod-Hi Tree/Shrub	Liquid
381-410	Cloudy Mod-Hi Tree/Shrub	Ice
411-440	Cloudy Lo-Mod Tree/Shrub	Liquid
441-470	Cloudy Lo-Mod Tree/Shrub	Ice
471-500	Cloudy Dark Desert	Liquid
501-530	Cloudy Dark Desert	Ice
531-560	Cloudy Bright Desert	Liquid
561-590	Cloudy Bright Desert	Ice
591-602	VIRS12B (See Note-11)	

The Clear Ocean and Clear Ocean - Sunglint ADM types are stratified by 5 windspeed classes. The windspeeds were determined from percentiles. For ADM types 6-10, the derivative of the ADM is too large, so the wind speed class mean ADM value is used.

SW ADM Offset 1	Percentile	wind speed range
0	25	< 3.7 m sec^{-1}
1	50	$3.7 - 5.5$ m sec^{-1}
2	75	$5.5 - 7.3$ m sec^{-1}
3	100	> 7.3 m sec^{-1}

4	N/A	unknown wind speed

Within Cloudy Ocean, the ADM types are stratified by 12 CERES cloud percentage ranges.

SW ADM Offset 1	**Cloud Percentage Range**
0	0.1 - 10.0
14	10.0 - 20.0
28	20.0 - 30.0
42	30.0 - 40.0
56	40.0 - 50.0
70	50.0 - 60.0
84	60.0 - 70.0
98	70.0 - 80.0
112	80.0 - 90.0
126	90.0 - 95.0
140	95.0 - 99.9
154	99.9 - 100.0

Within each Cloud percentage range, the Cloudy Ocean ADM types are stratified by 14 optical depth ranges. The adjusted optical depth does not appear on the SSF data product.

SW ADM Offset 2	**Adjusted Optical Depth Range**
0	0.01 - 1.0
1	1.0 - 2.5
2	2.5 - 5.0
3	5.0 - 7.5
4	7.5 - 10.0
5	10.0 - 12.5
6	12.5 - 15.0
7	15.0 - 17.5
8	17.5 - 20.0
9	20.0 - 25.0
10	25.0 - 30.0
11	30.0 - 40.0
12	40.0 - 50.0
13	> 50.0

The Cloudy Land ADM types are stratified by only 5 CERES cloud percentage ranges.

SW ADM Offset 1	**Cloud Percentage Range**
0	0.1 - 25.0
6	25.0 - 50.0
12	50.0 - 75.0
18	75.0 - 99.9
24	99.9 - 100.0

Within each Cloud percentage range, the Cloudy Land ADM types are stratified by only 6 adjusted optical depths. The adjusted optical depth does not appear on the SSF data product

SW ADM Offset 2	**Adjusted Optical Depth Range**
0	0.01 - 2.5
1	2.5 - 6.0

2	6.0 - 10.0
3	10.0 - 18.0
4	18.0 - 40.0
5	> 40.0

Example: ADM type 359 corresponds to a Moderate-High Tree/Shrub scene that is 25% - 50% cloudy. It has a liquid cloud phase and an optical depth range of 6 - 10.

Mapping from CERES Cloud Amount to ADM Cloud Amount

The CERES cloud percentage for an FOV is determined by subtracting the "clear percent coverage at the subpixel resolution" (See SSF-66) from 100. The type of cloud coverage is based on the following mapping:

If $0 \le$ cloud percentage $< 0.1\%$, then the FOV is "clear"
Else the FOV is "cloudy"

SW ADM Grid

The SW ADMs are a function of 590 ADM types, 9 viewing zenith (See SSF-20) bins, 10 relative azimuth (See SSF-10) bins, and 9 solar zenith (See SSF-21) bins. The zenith angles are defined from 0° to 90° and are divided into 10° bins. The SW ADMs is assumed symmetric in azimuth so that the relative azimuth angle is defined from 0° to 180° and divided into 20° bins except for the first and last bins of 10° each.

The ADMs are defined as piecewise constant functions over these angular bins. The ADMs are evaluated by linear interpolation in all angles.

Beta2_TRMM LW ADM Scene Types

New ADMs have also been developed for the LW channels.

LW/WN ADM types	**Scene**
1-12	VIRS12B (See Note-11)
13	Newer ADMs

There are actually 747 ADM types represented by the number 13. They are divided into clear sky (cloud percentage < 0.1), broken cloud (cloud percentage 0.1 - 99.0), and overcast (cloud percentage > 99.0). The clear sky ADMs are stratified by ocean/land/desert, 3 intervals of precipitable water, and 5 intervals of vertical temperature change. The broken cloud ADMs are stratified by ocean/land, 4 intervals of cloud fraction, 3 intervals of precipitable water, 4 intervals of IR emissivity and 6 intervals of surface to cloud temperature differences. The broken cloud ADMs are stratified by 3 intervals of precipitable water, 6 intervals of IR emissivity and 7 intervals of surface to cloud temperature differences.

LW ADM Grid

The LW ADMs are a function of ADM types, and 9 viewing zenith (See SSF-20) bins. The LW ADMs are not seasonal. The viewing zenith angle is defined from 0° to 90° and is divided into 10° bins. The ADMs are defined as piecewise constant functions over the angular bin and are evaluated by linear interpolation in viewing zenith.

Beta2_TRMM WN ADM Scene Types

The WN ADM scene types are defined in the identical fashion as the LW ADM scene types.

WN ADM Grid

The WN ADM grid is identical to the LW ADM grid.

Note-13 Definition of Angular Distribution Models (ADM)

The angular distribution model, $R(\theta, \phi)$, is a function of the viewing zenith angle, θ, and relative azimuth angle, ϕ, (See Figure 4-5) and defines the functional relationship between flux, F, and radiance, I, as

$$I(\theta, \phi) = \pi^{-1} F R(\theta, \phi) \tag{1}$$

Let us integrate radiance I in (1) over the hemisphere to get flux F, or

$$\int_0^{2\pi} \int_0^{\pi/2} I(\theta, \phi) \cos\theta \sin\theta \, d\theta \, d\phi = \pi^{-1} F \int_0^{2\pi} \int_0^{\pi/2} R(\theta, \phi) \cos\theta \sin\theta \, d\theta \, d\phi \tag{2}$$

or

$$\pi^{-1} \int_0^{2\pi} \int_0^{\pi/2} R(\theta, \phi) \cos\theta \sin\theta \, d\theta \, d\phi = 1 \tag{3}$$

which establishes a normalization for $R(\theta, \phi)$. It is common to assume R is independent of azimuth for longwave radiation so that the normalization (3) reduces to

$$2 \int_0^{\pi/2} R(\theta) \cos\theta \sin\theta \, d\theta = 1 \tag{4}$$

The main purpose for modeling anisotropy as $R(\theta, \phi)$ is to estimate flux from measured radiance by (1) as

$$\hat{F} = \frac{\pi^{-1} I(\theta, \phi)}{R(\theta, \phi)} \tag{5}$$

$R(\theta, \phi)$ is also a function of other angles and scene types such as land, ocean, cloud cover, optical depth, etc. For shortwave, $R_i(\theta, \phi; \theta_o)$ denotes R is a function of the solar zenith angle, θ_o, (See Figure 4-5.) and scene type i. When constructing R from data, we sort the data into scene types and assume R is piecewise constant over angular bins. When evaluating R for specific angles $(\theta, \phi; \theta_o)$ we assume R is piecewise linear and use a tri-linear interpolation and a slightly different normalization constant. There is no interpolation between scene types. For longwave, $R_i(\theta; \Theta)$ denotes R is a function of colatitude, Θ, and scene type i. Construction and evaluation is the same as for shortwave.

$R(\theta, \phi)$ is also a function of altitude. Equation (5) converts radiance to flux with R. But, the R that converts radiance to flux at satellite altitude is not the same R that converts the same radiance to flux at the TOA. The altitude dependence of R is illustrated in Figure 8-7. where we assume a

Lambertian Earth (R=1) and construct R to retrieve flux at different altitudes. In general, for Lambertian longwave radiation, we see $R(\theta) = \left(\dfrac{r_e + h}{r_e}\right)^2$ or $R(\theta) = 0$ depending on h and θ.
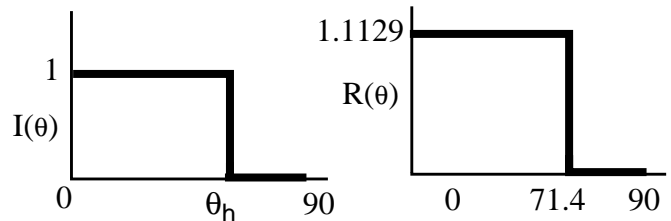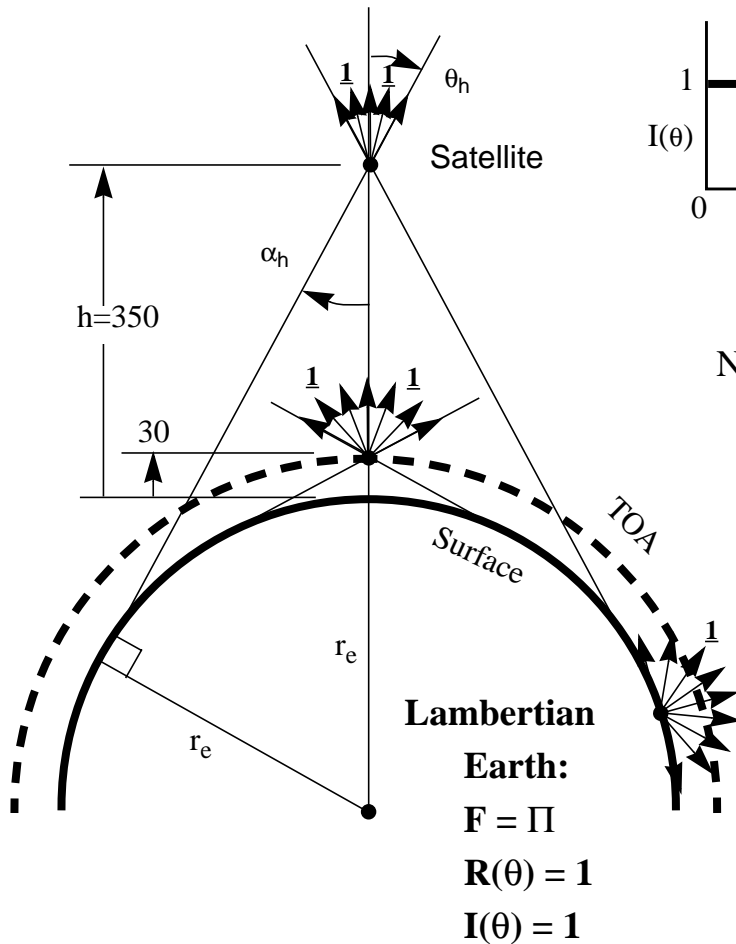
Normalization:

$$2\int_0^{\pi\,\S\,2} R(\theta)\sin(\theta)\cos(\theta)d\theta = 1$$

$$\sin\theta_h = \sin\alpha_h = \frac{r_e}{r_e + h}$$

$$\theta_h = 71.4^o$$

$$F = \int_0^{\theta_h}\int_0^{2\pi} I(\theta)\sin\theta\cos\theta\,d\theta\,d\phi$$

$$F = \pi\sin^2\theta_h = \pi\left(\frac{r_e}{r_e + h}\right)^2$$

$$R(\theta) = \frac{\pi I(\theta)}{F} = \frac{\pi(1)}{\pi\left(\dfrac{r_e}{r_e + h}\right)^2} = \left(\frac{r_e + h}{r_e}\right)^2$$

$$R(\theta) = 1.1129$$

At h=30 km (TOA)

$$R(\theta) = 1.0094 \,, 0^o \le \theta \le 84.4^o$$

Lambertian Earth:

$$\mathbf{F = \Pi}$$

$$\mathbf{R(\theta) = 1}$$

$$\mathbf{I(\theta) = 1}$$

ADM for Lambertian Earth:

$$R(\theta) = \left(\frac{r_e + h}{r_e}\right)^2 \qquad 0^o \le \theta \le \theta_h$$

$$= 0 \qquad \theta_h < \theta \le 90^o$$

Figure 8-7. ADM versus Altitude

Note-14   Conversion of Subsatellite Point from Geodetic to Geocentric
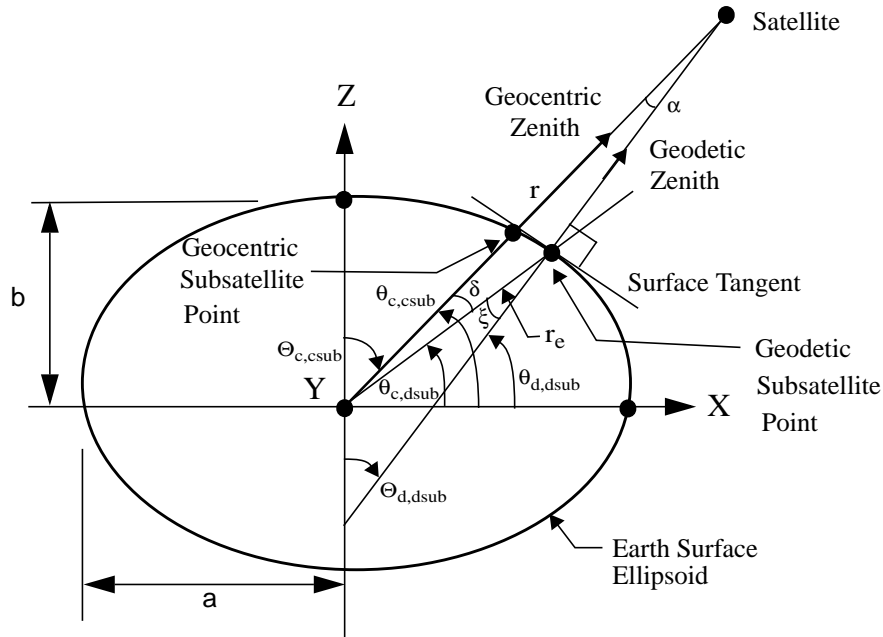
Figure 8-8. Subsatellite Point

The geodetic colatitude of the geodetic subsatellite point at the Earth surface, $\Theta_{d,\,dsub}$, is defined as SSF-6. We can determine the latitude as $\theta_{d,\,dsub} = 90° - \Theta_{d,\,dsub}$ and the geocentric latitude (See Term-12) as

$$\theta_{c,\,dsub} = \tan^{-1}\left[\frac{b^2}{a^2}\tan\theta_{d,\,dsub}\right]$$

where a and b are the axes of the Earth surface model from Term-9. It follows from the Figure that $\xi = \theta_{d,\,dsub} - \theta_{c,\,dsub}$. The radius to the geodetic subsatellite point (See Term-38), r_e, is

$$r_e = \frac{ab}{[a^2\sin^2\theta_{c,\,dsub} + b^2\cos^2\theta_{c,\,dsub}]^{1/2}}.$$

The radius to the satellite, r, is defined by SSF-2. From the Figure and the law of sines, we have

$$\sin\alpha = \frac{r_e}{r}\sin(180° - \xi)$$

and it follows that $\delta = \xi - \alpha$ and $\theta_{c,\,csub} = \theta_{c,\,dsub} + \delta$ and $\Theta_{c,\,csub} = 90° - \theta_{c,\,csub}$

The longitude of the geocentric subsatellite point is the same as the longitude of the geodetic subsatellite point (See Term-38).

Note-15 Determination of the Sun Beta Angle from SSF Parameters

The beta angle, β, is the angle between the Sun vector and the satellite orbital plane and is positive when the Sun and the angular momentum vector are on the same side of the orbital plane. When $\beta = 0$, the Sun is in the orbital plane. The beta angle varies slowly with time so that we will determine an instantaneous β value. The initial beta angle, β, is given by SSF-H9.

The angular momentum vector is the vector cross product of the satellite position vector and the satellite velocity vector. The satellite position unit vector is defined by its geodetic subsatellite point (See Term-38) which is defined by its geodetic colatitude (See SSF-6) and longitude (See SSF-7). We can convert from geodetic to geocentric (See Note-14) so that the satellite position vector is

$$X_{sat} = \sin\Theta_{sat}\cos\Phi_{sat}$$
$$Y_{sat} = \sin\Theta_{sat}\sin\Phi_{sat}$$
$$Z_{sat} = \cos\Theta_{sat}$$

where Θ_{sat} is the geocentric colatitude and Φ_{sat} is longitude. The X, Y, Z components of the satellite velocity are given by SSF-3, SSF-4, SSF-5 and the angular momentum vector, $\vec{H}$, is

$$X_H = Y_{sat}\dot{Z}_{sat} - Z_{sat}\dot{Y}_{sat}$$
$$Y_H = Z_{sat}\dot{X}_{sat} - X_{sat}\dot{Z}_{sat}$$
$$Z_H = X_{sat}\dot{Y}_{sat} - Y_{sat}\dot{X}_{sat}$$

where the magnitude is given by $H = \sqrt{X_H^2 + Y_H^2 + Z_H^2}$. The geodetic subsolar point (See Term-17) is given by SSF-8, SSF-9 and from Figure 15-1 we see that the geodetic and geocentric colatitudes are equal. It follows that the Sun vector is

$$X_{sun} = \sin\Theta_{sun}\cos\Phi_{sun}$$
$$Y_{sun} = \sin\Theta_{sun}\sin\Phi_{sun}$$
$$Z_{sun} = \cos\Theta_{sun}$$

And finally, the angle between the Sun vector and the angular momentum vector is from the vector dot product so that

$$\beta = 90° - \cos^{-1}\left[\frac{X_{sun}X_H + Y_{sun}Y_H + Z_{sun}Z_H}{H}\right].$$

9.0 Application of the Data Set

Help me out here!!!

The SSF data product provides instantaneous, geolocated surface properties, cloud properties, radiances, and fluxes for Subsystem 5.0 (Compute Surface and Atmospheric Radiative Fluxes) and Subsystem 9.0 (Grid TOA and Surface Fluxes). It is intended as a primary level-2 archival CERES data product.

10.0 Future Modifications and Plans

Modifications to the SSF product are driven by validation results and any Terra or Terra related parameters. The Langley ASDC provides users notification of changes.

11.0 Software Description

A sample C read program that interfaces with the HDF libraries and a README file are available from the LaRC ASDC User Services as part of a sample package (See Section 4.5). The program was designed to run on a Unix workstation and can be compiled with a C compiler. *{Pointer to ASDC read program}*

12.0 Contact Data Center/Obtain Data

NASA Langley Atmospheric Sciences Data CenterTelephone:(757) 864-8656
Science, User and Data Service Office   FAX: (757) 864-8807
NASA Langley Research Center   E-mail: larc@eos.nasa.gov
Mail Stop 157D   URL: http://eosweb.larc.nasa.gov/
2 South Wright Street
Hampton, VA 23681-2199
USA

13.0 Output Products and Availability

Several media types are supported by the Langley Web Ordering Tool. Data can be downloaded from the Web or via FTP. Alternatively, data can be ordered on media tapes. The media tapes supported are 4mm 2Gb (90m), 8mm 2Gb (8200), 8mm 5Gb (8500), and 8mm 7Gb (8500c).

Data ordered via the Web or via FTP can be downloaded in either Uncompressed mode or in UNIX Compressed mode. Data written to media tape (in either Uncompressed mode or in UNIX Compressed mode) is in UNIX TAR format.

14.0 References

1. Barnes, R. A., Barnes, W. L., Lyu, C.-H., and Gales, J. M.: An Overview of the Visible and Infrared Scanner Radiometric Calibration Algorithm. Journal of Atmospheric and Oceanic Technology, Vol. 17, No. 4, Apr. 2000, pp. 395-405.

2. Barnes, W. L., Barnes, R. A., and Holmes, A. W.: Characterization and Calibration Results from the Visible and Infrared Scanner (VIRS) for the Tropical Rainfall Measuring Mission (TRMM). SPIE, Vol. 2957, 1996, pp. 266-276.

3. Barnes, W. L., Pagano, T. S., and Salomonson, V. V.: Prelaunch Characteristics of the Moderate Resolution Imaging Spectroradiometer (MODIS) on EOS-AM1. IEEE Transactions on Geoscience and Remote Sensing, Vol. 36, No. 4, July 1998, pp. 1,088-1,100.

4. Blackadar, A.: A Computer Almanac. Weatherwise, Vol. 37, No. 5, Oct. 1984, pp. 257-260.

5. Minnis, P., Nguyen, L., Young, D. F., Trepte, Q. Z., Welch, R. M., and Baum, B. A.: Clouds and the Earth's Radiant Energy System (CERES) Validation Document, Imager Clear-Sky Determination and Cloud Detection (Subsystem 4.1), Release 4.0. August 2000 {URL = http://asd-www.larc.nasa.gov/validation/valid_doc.html}. Accessed Feb. 2001.

6. Minnis, P., Smith, W. L., Jr., Dong, X., Chen, Y., Wielicki, B. A., and Baum, B. A.: Clouds and the Earth's Radiant Energy System (CERES) Validation Document, Imager Cloud-Top Heights and Imager Cloud-Base Heights (Subsystem 4.2), Release 4.0. August 2000 {URL = http://asd-www.larc.nasa.gov/validation/valid_doc.html}. Accessed Feb. 2001.

7. Minnis, P., Young, D. F., Dong, X., and Sun-Mack, S.: Clouds and the Earth's Radiant Energy System (CERES) Validation Document, Validation of Imager Cloud Optical Properties (Subsystem 4.3), Release 4.0. August 2000 {URL = http://asd-www.larc.nasa.gov/validation/valid_doc.html}. Accessed Feb. 2001.

8. Green, R. and Wielicki, B. A.: Clouds and the Earth's Radiant Energy System (CERES) Validation Document, Convolution of Imager Cloud Properties With CERES Footprint Point Spread Function (Subsystem 4.4), Release 4.0. August 2000 {URL = http://asd-www.larc.nasa.gov/validation/valid_doc.html}. Accessed Feb. 2001.

9. Loeb, N. G., Green, R. N., Chambers, L. H., Wielicki, B. A., Hu, Y., Coakley, J. A., III, Stowe, L. L., and Hinton, P. O'R.: Clouds and the Earth's Radiant Energy System (CERES) Validation Document, CERES Inversion to Instantaneous TOA Fluxes (Subsystem 4.5), Release 4.0. August 2000 {URL = http://asd-www.larc.nasa.gov/validation/valid_doc.html}. Accessed Feb. 2001.

10. Kratz, D. P.: The Correlated k-Distribution Technique as Applied to the AVHRR Channels, J. Quant. Spectrosc. Radiat. Transfer, 53, 1995, 501-517.

11. Kratz, D. P., Li, Z., and Gupta, S. K.: Clouds and the Earth's Radiant Energy System (CERES) Validation Document, Validation of CERES Surface Radiation Budget (SRB) (Subsystem 4.6), Release 4.0. August 2000 {URL = http://asd-www.larc.nasa.gov/validation/valid_doc.html}. Accessed Feb. 2001.

12. Kratz, D.P. and F. G. Rose: Accounting for Molecular Absorption within the Spectral Range of the CERES Window Channel, J. Quant. Spectrosc. Radiat. Transfer, 61, 1999, 83-95.

13. Single Scanner Footprint TOA/Surface Fluxes and Clouds (SSF). Clouds and the Earth's Radiant Energy System (CERES) Data Management System Data Products Catalog, Rel. 3, Ver. 2, Nov. 2000 {URL = http://asd-www.larc.nasa.gov/DPC/DPC.html}. Accessed Feb. 2001.

14. Lee, R. B., III, Barkstrom, B. R., Crommelynck, D. A., Smith, G. L., Bolden, W. C., Paden, J., Pandey, D. K., Thomas, S., Thornhill, L., Wilson, R. S., Bush, K. A., Hess, P. C., and Weaver, W. L.: Clouds and the Earth's Radiant Energy System (CERES) Algorithm Theoretical Basis Document, Instrument Geolocate and Calibrate Earth Radiances (Subsystem 1.0), Release 2.2. June 1997 {URL = http://asd-www.larc.nasa.gov/ATBD/ATBD.html}. Accessed Feb. 2001.

15. Wielicki, B. A., Baum, B. A., Coakley, J. A., Jr., Green, R. N., Hu, Y., King, M. D., Lin, B., Kratz, D. P., Minnis, P., and Stowe, L. L.: Clouds and the Earth's Radiant Energy System (CERES) Algorithm Theoretical Basis Document, Overview of Cloud Retrieval and Radiative Flux Inversion (Subsystem 4.0), Release 2.2. June 2, 1997 {URL = http://asd-www.larc.nasa.gov/ATBD/ATBD.html}. Accessed Feb. 2001.

16. Baum, B. A., Welch, R. M., Minnis, P., Stowe, L. L., Coakley, J. A., Jr., Trepte, Q., Heck, P., Dong, X., Doelling, D., Sun-Mack, S., Murray, T., Berendes, T., Kuo, K.-S., and Davis, P.: Clouds and the Earth's Radiant Energy System (CERES) Algorithm Theoretical Basis Document, Imager Clear-Sky Determination and Cloud Detection (Subsystem 4.1), Release 2.2. June 2, 1997 {URL = http://asd-www.larc.nasa.gov/ATBD/ATBD.html}. Accessed Feb. 2001.

17. Baum, B. A., Minnis, P., Coakley, J. A., Jr., Wielicki, B. A., Heck, P., Tovinkere, V., Trepte, Q., Mayor, S., Murray, T., and Sun-Mack, S.: Clouds and the Earth's Radiant Energy System (CERES) Algorithm Theoretical Basis Document, Imager Cloud Layer and Height Determination (Subsystem 4.2), Release 2.2. June 2, 1997 {URL = http://asd-www.larc.nasa.gov/ATBD/ATBD.html}. Accessed Feb. 2001.

18. Minnis, P., Young, D. F., Kratz, D. P., Coakley, J. A., Jr., King, M. D., Garber, D. P., Heck, P. W., Mayor, S., and Arduini, R. F.: Clouds and the Earth's Radiant Energy System (CERES) Algorithm Theoretical Basis Document, Cloud Optical Property Retrieval (Subsystem 4.3), Release 2.2. June 2, 1997 {URL = http://asd-www.larc.nasa.gov/ATBD/ATBD.html}. Accessed Feb. 2001.

19. Green, R. and Wielicki, B. A.: Clouds and the Earth's Radiant Energy System (CERES) Algorithm Theoretical Basis Document, Convolution of Imager Cloud Properties With CERES Footprint Point Spread Function (Subsystem 4.4), Release 2.2. June 2, 1997 {URL = http://asd-www.larc.nasa.gov/ATBD/ATBD.html}. Accessed Feb. 2001.

20. Green, R. N., Wielicki, B. A., Coakley, J. A., III, Stowe, L. L., Hinton, P. O'R., and Hu, Y.: Clouds and the Earth's Radiant Energy System (CERES) Algorithm Theoretical Basis Document, CERES Inversion to Instantaneous TOA Fluxes (Subsystem 4.5), Release 2.2.

June 2, 1997 {URL = http://asd-www.larc.nasa.gov/ATBD/ATBD.html}. Accessed Feb. 2001.

21.   Barkstrom, B. R., Kratz, D. P., Cess, R. D., Li, Z., Inamdar, A. K., Ramanathan, V., and Gupta, S. K.: Clouds and the Earth's Radiant Energy System (CERES) Algorithm Theoretical Basis Document, Empirical Estimates of Shortwave and Longwave Surface Radiation Budget Involving CERES Measurements (Subsystem 4.6.0), Release 2.2. June 2, 1997 {URL = http://asd-www.larc.nasa.gov/ATBD/ATBD.html}. Accessed Feb. 2001.

22.   Li, Z. and Kratz, D. P.: Clouds and the Earth's Radiant Energy System (CERES) Algorithm Theoretical Basis Document, Estimate of Shortwave Surface Radiation Budget From CERES (Subsystem 4.6.1), Release 2.2. June 2, 1997 {URL = http://asd-www.larc.nasa.gov/ATBD/ATBD.html}. Accessed Feb. 2001.

23.   Inamdar, A. K. and Ramanathan, V.: Clouds and the Earth's Radiant Energy System (CERES) Algorithm Theoretical Basis Document, Estimation of Longwave Surface Radiation Budget From CERES (Subsystem 4.6.2), Release 2.2. June 2, 1997 {URL = http://asd-www.larc.nasa.gov/ATBD/ATBD.html}. Accessed Feb. 2001.

24.   Gupta, S. K., Whitlock, C. H., Ritchey, N. A., and Wilber, A. C.: Clouds and the Earth's Radiant Energy System (CERES) Algorithm Theoretical Basis Document, An Algorithm for Longwave Surface Radiation Budget for Total Skies (Subsystem 4.6.3), Release 2.2. June 2, 1997 {URL = http://asd-www.larc.nasa.gov/ATBD/ATBD.html}. Accessed Feb. 2001.

25.   Dong, X., Ackerman, T. P., Clothiaux, E. E., Pilewskie, P., and Han, Y.: Microphysical and Radiative Properties of Stratiform Clouds Deduced from Ground-based Measurements. Journal of Geophysical Research, Vol. 102, 1997, pp. 23,829-23,843.

26.   Currey, C., Fan, A., Murray, T., Sun-Mack, S., and Tolson, C.: Clouds and the Earth's Radiant Energy System (CERES) Data Management System Software Design Document, Cloud Retrieval (Subsystems 4.1-4.3), Architectural Draft, Release 1.0. Mar. 1996 {URL = http://asd-www.larc.nasa.gov/SDD/SDD.html}. Accessed Feb. 2001.

27.   Currey, C. and McKinley, C.: Clouds and the Earth's Radiant Energy System (CERES) Data Management System Software Design Document, Convolution of Imager Cloud Properties with CERES Footprint Point Spread Function (Subsystem 4.4), Architectural Draft, Release 1.0. Mar. 1996 {URL = http://asd-www.larc.nasa.gov/SDD/SDD.html}. Accessed Feb. 2001.

28.   Geier, E., Jimenez, L., Nolan, S., and Robbins, J.: Clouds and the Earth's Radiant Energy System (CERES) Data Management System Software Design Document, CERES Inversion to Instantaneous TOA Fluxes and Empirical Estimates of Surface Radiation Budget (Subsystems 4.5 and 4.6), Architectural Draft, Release 1.0. Mar. 1996 {URL = http://asd-www.larc.nasa.gov/SDD/SDD.html}. Accessed Feb. 2001.

29.   Garreaud, R., Ruttlant, J., Quintana, J., Carrasco, J., and Minnis, P.: CIMAR-5: A Snapshot of the Lower Troposphere Over the Subtropical Southeast Pacific. Submitted to Bulletin of the American Meteorological Society, 2000.

30. Green, R. N. and Hinton, P. O'R.: Estimation of Angular Distribution Models from Radiance Pairs. Journal of Geophysical Research, Vol. 101, 1996, pp. 16,951-16,959.

31. Gupta, S. K.: A Parameterization for Longwave Surface Radiation from Sun-Synchronous Satellite Data. Journal of Climate, Vol. 2, No. 4, 1989, pp. 305-320.

32. Gupta, S. K., Darnell, W. L., and Wilber, A. C.: A Parameterization for Longwave Surface Radiation from Satellite Data: Recent Improvements. Journal of Applied Meteorology, Vol. 31, No. 12, 1992, pp. 1,361-1,367.

33. Hierarchical Data Format. NASA Langley Research Center, Atmospheric Sciences Data Center Web site {URL = http://eosweb/HBDOCS/hdf.html}. Accessed Feb. 2001.

34. Jefferys, W. H.: Julian Day Numbers. {URL = http://quasar.as.utexas.edu/BillInfo/JulianDatesG.html}. Accessed Feb. 2001.

35. Ignatov, A. and Stowe, L. L.: Physical Basis, Premises, and Self-Consistency Checks of Aerosol Retrievals from TRMM/VIRS. Journal of Applied Meteorology, Vol. 39, No. 12, 2000, pp. 2,259-2,277.

36. Inamdar, A. K. and Ramanathan, V.: On Monitoring the Atmospheric Greenhouse Effect from Space. Tellus, 49B, 1997, pp. 216-230.

37. Li, Z., Leighton, H. G., Masuda, K., and Takashima, T.: Estimation of SW Flux Absorbed at the Surface from TOA Reflected Flux. Journal of Climate, Vol. 6, No. 2, 1993, pp. 317-330.

38. Li, Z. and Garand, L.: Estimation of Surface Albedo from Space: A Parameterization for Global Application. Journal of Geophysical Research, Vol. 99, 1994, pp. 8,335-8,350.

39. Loeb, N. G., Green, R. N., and Hinton, P. O'R.: Top-of-Atmosphere Albedo Estimation from Angular Distribution Models: A Comparison Between Two Approaches. Journal of Geophysical Research, Vol. 104, 1999, pp. 31,255-31,260.

40. Loeb, N. G., Parol, F., Buriez, J.-C., and Vanbauce, C.: Top-of-Atmosphere Albedo Estimation from Angular Distribution Models Using Scene Identification from Satellite Cloud Property Retrievals. Journal of Climate, Vol. 13, No. 7, 2000, pp. 1,269-1,285.

41. Loeb, N. G., Priestley, K. J., Kratz, D. P., Geier, E. B., Green, R. N., Wielicki, B. A., Hinton, P. O'R., and Nolan, S. K.: Determination of Unfiltered Radiances from CERES. Submitted to Journal of Applied Meteorology, 2000.

42. Lyu, C.-H., Barnes, R. A., and Barnes, W. L.: First Results from the On-Orbit Calibrations of the Visible and Infrared Scanner for the Tropical Rainfall Measuring Mission. Journal of Atmospheric and Oceanic Technology, Vol. 17, No. 4, Apr. 2000, pp. 385-394.

43. Mace, G. G., Ackerman, T. P., Minnis, P., and Young, D. F.: Cirrus Layer Microphysical Properties Derived from Surface-based Millimeter Radar and Infrared Interferometer Data. Journal of Geophysical Research, Vol. 103, 1998, pp. 23,207-23,216.

44. Minnis, P., Garber, D. P., Young, D. F., Arduini, R. F., and Takano, Y.: Parameterizations of Reflectance and Effective Emittance for Satellite Remote Sensing of Cloud Properties. Journal of the Atmospheric Sciences, Vol. 55, No. 22, 1998, pp. 3,313-3,339.

45. Nguyen, L., Minnis, P., Ayers, J. K., Smith, W. L., Jr., and Ho, S. P.: Intercalibration of Geostationary and Polar Satellite Data Using AVHRR, VIRS, and ATSR-2 Data. Proceedings of the 10th Conference on Atmospheric Radiation, American Meteorological Society, Madison, WI, June 28 - July 2, 1999, pp. 405-408.

46. Prabhakara, C. and Dalu, G.: Remote Sensing of the Surface Emissivity at 9 μm Over the Globe. Journal of Geophysical Research, Vol. 81, 1976, pp. 3,719-3,724.

47. Release 5B SCF Toolkit Users Guide, 333-CD-510-001. Feb. 2000 {URL = http:// edhs1.gsfc.nasa.gov/waisdata/toc/cd33351oo1toc.html}. Accessed Feb. 2001.

48. Smith, G. L.: Effects of Time Response on the Point Spread Function of a Scanning Radiometer. Applied Optics, Vol. 33, No. 30, 1994, pp. 7,031-7,037.

49. Mitchum, M. V. and Fan, A.: CERES Metadata Requirements for LaTIS. CERES Software Bulletin 97-12, Rev. 1, Jan. 7, 1998 {URL = http://asd-www.larc.nasa.gov/ceres/ bulletins.html}. Accessed Feb. 2001.

50. Staylor, W. F. and Wilber, A. C.: Global Surface Albedos Estimate from ERBE Data. Proceedings of the 7th Conference on Atmospheric Radiation, American Meteorological Society, San Francisco, CA, 1990.

51. Stowe, L. L., Davis, P. A., and McClain, E. P.: Scientific Basis and Initial Evaluation of the CLAVR-1 Global Clear/Cloud Classification Algorithm for the Advanced Very High Resolution Radiometer. Journal of Atmospheric and Oceanic Technology, Vol. 16, No. 6, 1999, pp. 656-681.

52. Stowe, L. L., Ignatov, A. M., and Singh, R. R.: Development, Validation and Potential Enhancements to the Second Generation Operational Aerosol Product at NOAA/NESDIS. Journal of Geophysical Research, Vol. 102, 1997, pp. 16,923-16,934.

53. Suttles, J. T., Green, R. N., Minnis, P., Smith, G. L., Staylor, W. F., Wielicki, B. A., Walker, I. J., Young, D. F., Taylor, V. R., and Stowe, L. L.: Angular Radiation Models for Earth-Atmosphere System, Volume I—Shortwave Radiation. NASA RP 1184, July 1988.

54. Suttles, J. T., Wielicki, B. A., and Vemury, S.: Top-of-Atmosphere Radiative Fluxes: Validation of ERBE Scanner Inversion Algorithm Using Nimbus-7 ERB Data. Journal of Applied Meteorology, Vol. 31, No. 7, 1992, pp. 784-796.

55. Taylor, V. R. and Stowe, L. L.: Reflectance Characteristics of Uniform Earth and Cloud Surfaces Derived from NIMBUS 7 ERB. Journal of Geophysical Research, Vol. 89, 1984, pp. 4,987-4,996.

56. In-flight Measurement Analysis (Rev. E). TRW DRL 64, 55067.300.008E, Mar. 1997.

57. Suttles, J. T., Green, R. N., Smith, G. L., Wielicki, B. A., Walker, I. J., Taylor, V. R., and Stowe, L. L.: Angular Radiation Models for Earth-Atmosphere System, Volume II— Longwave Radiation. NASA RP 1184, Apr. 1989.

58. Wielicki, B. A. and Green, R. N.: Cloud Identification for ERBE Radiation Flux Retrieval. Journal of Applied Meteorology, Vol. 28, No. 11, 1989, pp. 1,133-1,146.

59. Zhao, X.-P. and Stowe, L. L.: Global Validation of the NOAA/NESDIS Second Generation Aerosol Retrieval Algorithm with AERONET Data. International Geoscience and Remote Sensing Symposium, Honolulu, HI, 2000.

15.0 Glossary of Terms

Term-1 Alpha

Alpha defines a version that is still at a very early stage of development and should not be used for quantitative scientific publication. Alpha versions of CERES data carry the disclaimer that they are not publishable and may be removed from the archive in the future. In cases where there are multiple Alpha versions, Alpha will be followed by an integer. When the version reaches a higher level of maturity, it is typically referred to as a Beta (See Term-5) version. CERES uses EditionX, where X is an integer, to denote versions that are ready for use in scientific publications and for which many of the uncertainties are well defined.

Term-2   Angular Bin

Term-3 Angular Distribution Model

The angular distribution model, R, is a model of anisotropy and is used to convert measured radiance, I, to flux, F, according to $F = \pi I / R$. R is normalized and a function of spectrum (SW, LW, WN), geometric angles, FOV scene type, and altitude (See Note-13).

Term-4 Area Coverage

Term-5 Beta

Beta defines a version that is still under development, should not be used for quantitative scientific publication, but is of higher quality than an Alpha (See Term-1) version. Beta versions of CERES data carry the disclaimer that they are not publishable and may be removed from the archive in the future. In cases where there are multiple Beta versions, Beta will be followed by an integer. CERES uses EditionX, where X is an integer, to denote versions that are ready for use in scientific publications and for which many of the uncertainties are well defined.

Term-6 Cookiedough

The Cloud Retrieval output is affectionately referred to as cookiedough. This temporary, intermediate product is created by Cloud Retrieval and passed to Convolution, which is affectionately referred to as Cookiecutter. Cookiedough contains hourly data at imager pixel (See Term-27) resolution; it does not contain any CERES data. Figuratively speaking, Convolution places the CERES PSF (See Term-28) over the imager pixel data and "cuts a cookie." Due to its very large size, Cookiedough is deleted immediately after Convolution finishes processing.

Term-7 Earth Equator, Greenwich Meridian System

The Earth equator, Greenwich meridian system is an Earth-fixed, geocentric, rotating coordinate system with the X-axis in the equatorial plane through the Greenwich meridian, the Y-axis lies in the equatorial plane 90° to the east of the X-axis, and the Z-axis is toward the North Pole.

Term-8 Earth Point

The viewed point on the Earth surface (See Term-9), or the point at which the PSF centroid intersects the Earth surface.

Term-9 Earth Surface

The surface of the Earth as defined by the WGS-84 Earth Model. The WGS-84 model of the Earth surface is an ellipsoid $\dfrac{x^2}{a^2} + \dfrac{y^2}{a^2} + \dfrac{z^2}{b^2} = 1$ where a = 6378.1370 km and b = 6356.7523 km (See Figure 15-2). The radius of the Earth surface is defined in Term-18.

Term-10 Elevation Angle

The elevation angle defines the position of the instrument optical axis (See Note-3) relative to the spacecraft. For nominal satellite attitude control, the elevation is near 90° for a nadir view (See Term-24), near 0° at the start of a 6.6 second scan cycle (See Figure 15-3), and near 180° at internal calibrations. Zero elevation is generally away from the Sun and 180° is generally on the sun side of the satellite.

Term-11 Field-of-View

The terms Field of View (FOV) and footprint are synonymous. The CERES FOV is determined by its PSF (See Note-3 and Term-28) which is a two-dimensional, bell-shaped function that defines the CERES instrument response to the viewed radiation field.

The resolution of the CERES radiometers is usually referenced to the optical FOV which is 1.3^o in the along-track direction and 2.6^o in the cross-track direction. For example, on TRMM with a satellite altitude of 350 km, the optical FOV at nadir (See Term-24) is 8×16 km which is frequently referred to as an equivalent circle with a 10 km diameter, or simply as 10 km resolution. On EOS-AM with a satellite altitude of 705 km, the optical FOV at nadir is 16×32 km or 20 km resolution.

The CERES FOV or footprint size is referenced to an oval area that represents approximately 95% of the PSF response (See Term-28 and Note-3 for numerical representation of FOV). Since the PSF is defined in angular space at the instrument, the CERES FOV is a constant in angular space, but grows in surface area from a minimum at nadir to a larger area at shallow viewing angles (See SSF-14). For TRMM, the length and width of this oval at nadir is 19×15 km and grows to 138×38 km at a viewing zenith angle (See SSF-20) of 70°. For EOS-AM/PM, the length and width at nadir is 38×31 km and grows to 253×70 km at a viewing zenith angle of 70°.

The ToolKit (See Term-41) routine PGS_CSC_GetFOV_Pixel (See Reference 47) returns the geodetic latitude and longitude of the intersection of the FOV centroid and the selected Model Surface. The returned longitudes are transformed from radians to degrees and then converted

from ±180° to 0° .. 360°. The returned geodetic latitudes are transformed from radians to degrees and then converted to geodetic colatitude using (90.0-latitude).

Term-12 Geocentric Latitude

Term-13 Geocentric Subsolar Point

The point on a surface where the geocentric zenith (See Term-14) vector points toward the Sun (See Figure 15-1).

Term-14 Geocentric Zenith

A vector from the center of the Earth (See Figure 15-2) to the point of interest.

Term-15 Geodetic Colatitude

Term-16 Geodetic Latitude

Term-17 Geodetic Subsolar Point

The point on a surface where the geodetic zenith (See Term-18) vector points toward the Sun (See Figure 15-1). Although the geocentric latitude θ_c and the geodetic latitude θ_d are equal, the geocentric subsolar point is different from the geodetic subsolar point.
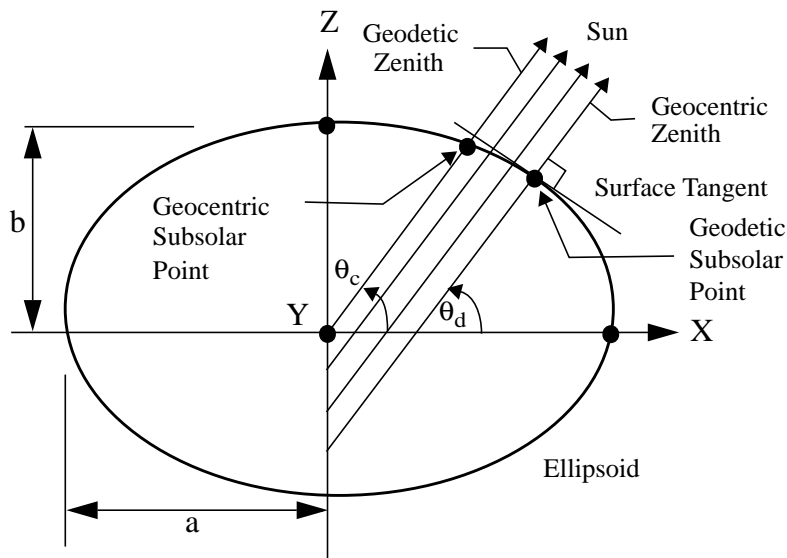
Figure 15-1. Subsolar Point

The ToolKit (See Term-41) routine PGS_CBP_Earth_CB_vector (See Reference 47) calculates the Earth-Centered Inertial (ECI) position vector from the Earth to the Sun. A second ToolKit routine, PGS_CSC_ECItoECR, transforms the position vector to the ECR or Earth equator, Greenwich meridian rectangular coordinate system. From these coordinates, the geocentric colatitude and longitude of the Sun are calculated.

Term-18 Geodetic Zenith

The vector normal to an ellipsoid (See Figure 15-2) at a point on the surface. The geodetic colatitude at the Earth surface, Θ_d , is defined as SSF-10. The relationship between latitude and colatitude is defined by $\theta_d = 90° - \Theta_d$. At a point on the surface the geocentric latitude θ_c and the geodetic latitude θ_d are related by

$$\tan\theta_c = \frac{b^2}{a^2}\tan\theta_d.$$

We can determine the radial distance r as a function of the geocentric latitude θ_c by setting
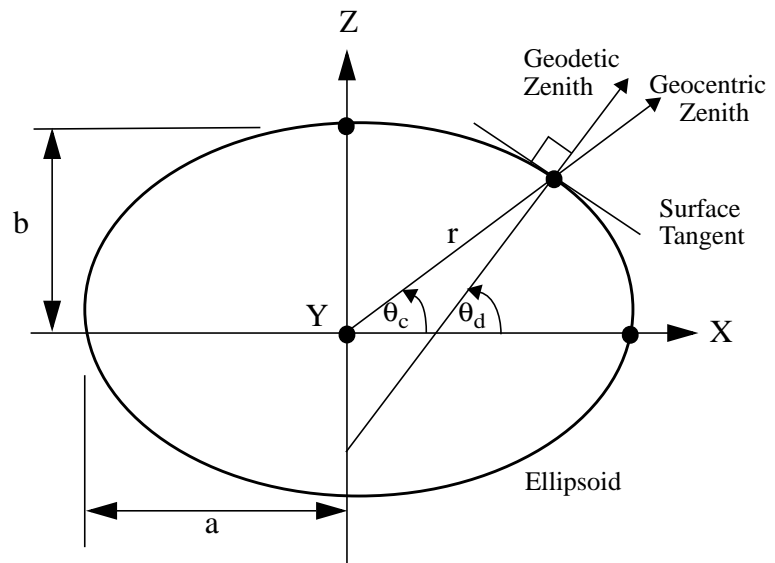
Figure 15-2. Ellipsoidal Earth Model

$x = r\cos(\theta_c), y = 0, z = r\sin(\theta_c)$ in the ellipsoidal model and solving for r or

$$r = \frac{ab}{\sqrt{a^2\sin^2\theta_c + b^2\cos^2\theta_c}}$$

The semi-major axis (a) and the semi-minor axis (b) are defined by either the Earth Surface (See Term-9) or the TOA (See Term-40).

Term-19 Granule

An SSF granule contains one hour of CERES data from a single instrument. A granule is one HDF file or an instance of a data product. Each SSF granule contains header data, metadata, and FOV parameters. The header is made up of SSF parameters recorded once per hour. The metadata is also recorded once per hour.

Term-20 Greenwich Coordinate System

Term-21 Greenwich Meridian

Term-22 Julian Date

A continuous count of time in whole and fractional days elapsed at the Greenwich meridian since noon on January 1, 4714 BCE. (See Note-4)

Term-23 Linear Interpolation

Term-24 Nadir

Nadir is the geocentric subsatellite point (See Term-38 and Figure 4-2).

Term-25 North Pole

Term-26 Optical FOV

Optical FOV appears in several places. Does it need it's own term???

Term-27 Pixel

A pixel refers to imager data. The spatial distance between pixels is its resolution. The pixel resolution for VIRS is 2 km at nadir. For MODIS the pixel resolution is 1 km at nadir.

Term-28 Point Spread Function

A Point Spread Function (PSF) is a two-dimensional bell-shaped function that defines the CERES instrument response to the viewed radiation field. Due to the response time, the radiometer responds to a larger FOV than the optical FOV and the resulting PSF centroid lags the optical FOV centroid by more than a degree of cone angle (See SSF-14) for normal scan (See Figure 15-3) rates (See Note-3).

Term-29 PSF-Weighted

Term-30 PSF-Weighted Mean

Term-31 PSF-Weighted Standard Deviation

Term-32 Rapid Retrace (or Fast Return)

Rapid retrace is defined as a much faster than nominal elevation, or cone angle, scan rate. The rapid retrace rate is currently defined as 249.69 ± 10 deg sec^{-1}. During the Short Elevation Scan cycle, there are two portions of the scan cycle where the CERES instrument sweeps across the Earth at a rate of approximately 249 deg sec $^{-1}$. These are examples of rapid retrace.

Term-33 Resolution

Term-34 Scan Cycle

Each scan cycle is 6.6 seconds in length and contains 660 measurement points so that measurements are every 0.01 seconds (See Figure 15-3). The beginning of a scan cycle is at measurement 1. The end of a cycle is 6.6 seconds later at measurement 1 of the next cycle. The last measurement in the scan cycle is 660 and is 6.59 seconds after measurement 1.

Term-35 Scientific Data Set
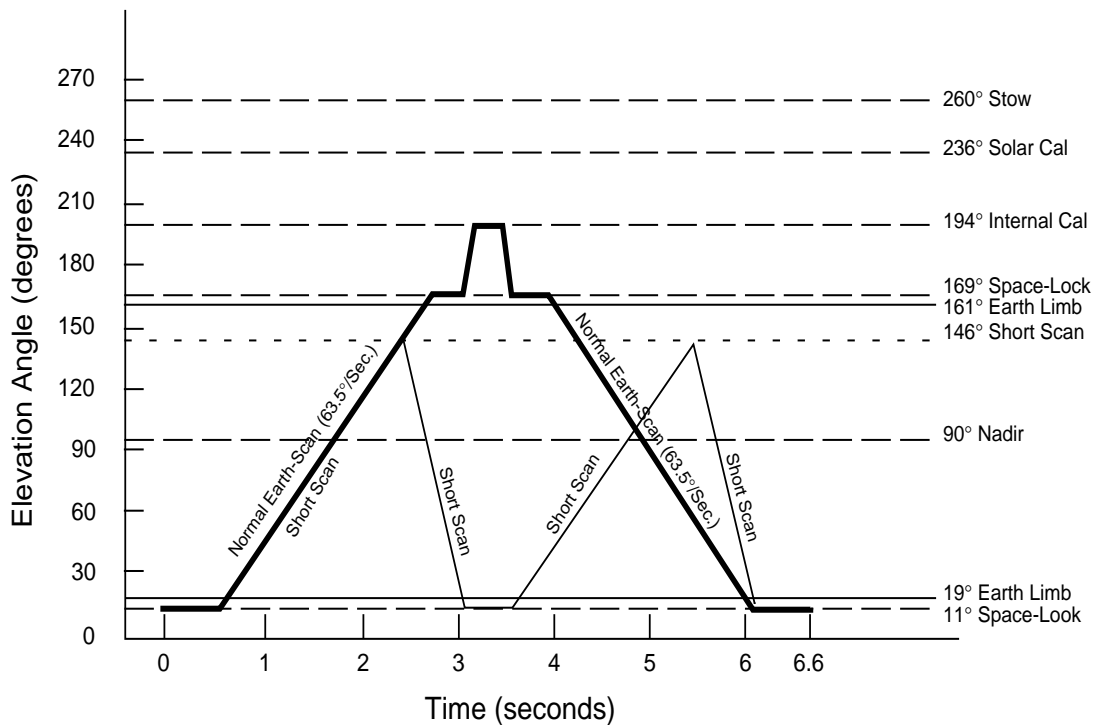
Figure 15-3. Normal and short Earth scan profiles for instrument on TRMM platform

A Scientific Data Set (SDS) is a HDF structure. It is a collection (or grouping) of parameters that have the same data type such as 8, 16, or 32-bit integers or 32, or 64-bit floating point numbers. The SSF SDS's each contain only one parameter. The SDS is an array of values and for SSF this corresponds to all values of a certain parameter for an hour. In general, an SDS is a multi-dimensional array. It has dimension records and data type which describe it. The dimensions specify the shape and size of the SDS array. Each dimension has its own attributes.

Term-36 Spectral Correction Coefficients

The Spectral Correction Coefficients (SCC) represent a regression between theoretical filtered radiances and theoretical unfiltered radiances and are used to unfilter the CERES radiances. Each CERES instrument has its own set(s) of SCC based on its spectral response. There are different SCC for land, ocean, snow, and cloud. The SCC also vary with solar zenith, viewing zenith, and relative azimuth. See Note-5 on the Spectral Correction Algorithm for details.

Beginning with the Terra Edition1A SSF data set, all Terra data sets use SCC which can vary from month to month.   The gains and spectral response functions associated with both Terra instruments are computed monthly to remove any instrument drift.

Term-37 Subpixel

A subpixel refers to imager data at a higher resolution than the pixel resolution (See Term-27). For example, at nadir MODIS has a pixel resolution of 1 km and a subpixel resolution of 250 m so that 16 subpixels are associated with each pixel. Subpixels are used to classify a pixel as clear (all

16 subpixels clear), overcast (all 16 subpixels cloudy), or broken cloud (subpixels are clear and cloudy) (See Note-2). VIRS has no data at a subpixel resolution.

Term-38 Subsatellite Point

The point on a surface below the satellite or the intersection point of a line dropped from the satellite through the surface (See Figure 15-4). The geocentric subsatellite point is on the radius vector to the center of the earth. The geodetic subsatellite point is on the geodetic zenith vector or the line dropped from the satellite is normal to the surface at the intersection point.
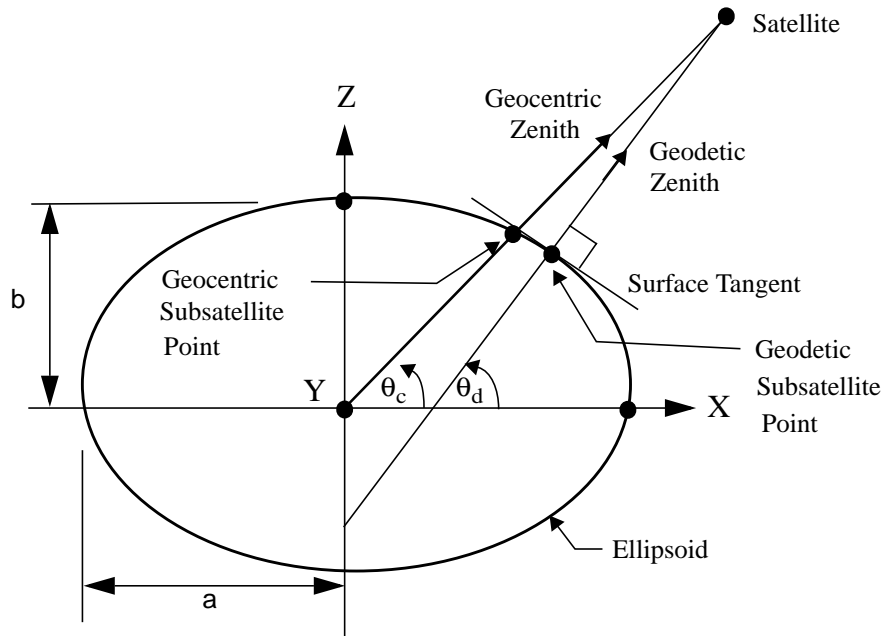
Figure 15-4. Subsatellite Point

The ToolKit (See Term-41) routine PGS_CSC_SubSatPoint (See Reference 47) returns the geodetic latitude and longitude of the geodetic subsatellite point. The returned longitudes are transformed from radians to degrees and then converted from $\pm 180°$ to $0°$ .. $360°$. The returned latitudes are transformed from radians to degrees and then converted to colatitude using (90.0 - latitude).

Term-39 Top-of-the-Atmosphere (TOA)

The TOA is a surface approximately 30 km above the Earth surface (See Term-9). Specifically, the TOA is an ellipsoid $\dfrac{x^2}{a^2} + \dfrac{y^2}{a^2} + \dfrac{z^2}{b^2} = 1$ where a = 6408.1370 km and b = 6386.6517 km (See Figure 15-2).

Term-40 TOA Point

The viewed point at the TOA, or the point at which the PSF (See Term-28) centroid intersects the TOA (See Term-39).

Term-41 ToolKit

The ToolKit (See Reference 47) is a collection of routines put together by the EOSDIS Core System Project. ToolKit routines exist for such tasks as Ancillary Data Access, Celestial Body Position, Coordinate System Conversion, Constant and Unit Conversions, Ephemeris Data Access, Geo Coordinate Transformation, Meta Data Access, and Time Date Conversion. There are also ToolKit routines for software tasks such as memory management, file I/O, process control, and error handling. Some ToolKit routines are mandatory and must be used by all EOS projects. The remaining routines are optional, but encouraged. CERES uses ToolKit routines where possible.

Term-42 Vertex data

A Vertex data (Vdata) set is an HDF structure. It is a collection (or grouping) of parameters that have different data types such as 8, 16, or 32-bit integers, floating point numbers, text, etc. The SSF Vdata SSF_Header contains 24 parameters called Header Parameters. Each parameter has only one value in a granule of one hour of data. In general, Vdata is a table of parameters of varying data type. Specifically stated, a Vdata is a customized table, comprised of a collection of similar records (rows) whose values are stored in one or more fixed length fields (columns) where individual fields can have their own data type. A Vdata is uniquely identified by a name, a class, and individual field names. The Vdata class identifies the purpose or use of its data.

Term-43 Vgroup

A Vgroup is an HDF structure. It is a collection (or grouping) of related HDF data objects. The Vgroup HDF data objects can be a combination of Vdatas, Vgroups, SDSs, or other HDF objects. The SSF Vgroups consist of related single-parameter SDSs. Each Vgroup must have a name and optionally, a class name. Vgroup class names are used to describe and classify the data objects within the Vgroup.

16.0 Acronyms and Units

16.1 CERES Acronyms

ADM	Angular Distribution Model (See Term-3)
APD	Aerosol Profile Data
Aqua	EOS Afternoon Crossing (Descending) Mission; also known as EOS-PM
ASDC	Atmospheric Sciences Data Center
ATBD	Algorithm Theoretical Basis Document
AVG	Monthly Regional Radiative Fluxes and Clouds
AVHRR	Advanced Very High Resolution Radiometer
BCE	Before Current Era
BDS	Bidirectional Scan
CC#	Configuration Code number (See Section 1.1)
CADM	CERES Angular Distribution Model
CER	CERES
CERES	Clouds and the Earth's Radiant Energy System
CID	Cloud Imager Data
CRH	Clear Reflectance History
CRS	Clouds and Radiative Swath
DAAC	Distributed Active Archive Center
DAO	Data Assimilation Office
DMS	Data Management System
ECMWF	European Centre for Medium-Range Weather Forecasts
ECR	Earth-Centered Rotating
ECS	EOS Core System
EDDB	ERBE-Like Daily Database Product
EOS	Earth Observing System
EOS-AM	EOS Morning Crossing (Ascending) Mission; also known as Terra
EOS-PM	EOS Afternoon Crossing (Descending) Mission; also known as Aqua
EOSDIS	Earth Observing System Data and Information System
ERBE	Earth Radiation Budget Experiment
ERBS	Earth Radiation Budget Satellite
ES8	ERBE-like Instantaneous Science Product
FAPS	Fixed Azimuth Plane Scan
FM	Flight Model
FOV	Field-of-View (See Term-11)
FSW	Monthly Gridded Radiative Fluxes and Clouds
GAP	Gridded Analysis Product
GB	Giga Byte
GEO	Geostationary Narrowband Radiances
GGEO	Gridded GEO Narrowband Radiances
GMS	Geostationary Meteorological Satellite
GOES	Geostationary Operational Environmental Satellite
H	High

HDF	Hierarchical Data Format
IES	Instrument Earth Scans
IGBP	International Geosphere Biosphere Programme
IMS	Information Management System
INSTR	Instrument
ISCCP	International Satellite Cloud Climatology Project
IWC	Ice Water Content
LaRC	Langley Research Center
L	Low
LM	Lower Middle
LW	Longwave
LWC	Liquid Water Content
MAM	Mirror Attenuator Mosaic
MB	Mega Byte
METEOSAT	Meteorological Satellite
MISR	Multi-angle Imaging SpectroRadiometer
MLE	Maximum Likelihood Estimator
MOA	Meteorological, Ozone, and Aerosols
MODIS	Moderate Resolution Imaging Spectrometer
MWH	Microwave Humidity
NASA	National Aeronautics and Space Administration
NCEP	National Centers for Environmental Prediction
NOAA	National Oceanic and Atmospheric Administration
OPD	Ozone Profile Data
PFM	Prototype Flight Model (on TRMM)
PSA	Product Specific Attribute
PSF	Point Spread Function (See Term-28)
QA	Quality Assessment
RAPS	Rotating Azimuth Plane Scan
RPM	Radiance Pairs Method of generating ADMs
SAB	Sorting into Angular Bins method of generating ADMs
SARB	Surface and Atmospheric Radiation Budget
SBUV-2	Solar Backscatter Ultraviolet/Version 2
SCC	Spectral Correction Coefficients (See Term-36)
SDS	Scientific Data Set (See Term-35)
SFC	Monthly Gridded TOA/Surface Fluxes and Clouds
SRB	Surface Radiation Budget
SRBAVG	Monthly TOA/Surface Averages
SS	Subsystem
SSF	Single Scanner Footprint TOA/Surface Fluxes and Clouds
SSM/I	Special Sensor Microwave/Imager
SURFMAP	Surface Map
SW	Shortwave
SWICS	Shortwave Internal Calibration Source
SYN	Synoptic Radiative Fluxes and Clouds
TBD	To be determined
Terra	EOS Morning Crossing (Ascending) Mission; also known as EOS-AM
TISA	Time Interpolation and Spatial Averaging

TMI	TRMM Microwave Imager
TOA	Top-of-the-Atmosphere (See Term-39)
TOT	Total
TRMM	Tropical Rainfall Measuring Mission
UM	Upper Middle
URL	Uniform Resource Locator
UT	Universal Time
UTC	Universal Time Code
Vdata	Vertex Data (See Term-42)
VIST	Visible and Infrared Split-window Technique
VIRS	Visible Infrared Scanner
WN	Window
ZAVG	Monthly Zonal and Global Radiative Fluxes and Clouds

16.2 CERES Units

Units	Definition
AU	Astronomical Unit
cm	centimeter
count	count, counts
day	day, Julian Date
deg	degree
deg sec^{-1}	degrees per second
du	Dobson units
fraction	fraction 0..1
g kg^{-1}	gram per kilogram
g m^{-2}	gram per square meter
hhmmss	hour, minute, second
hour	hour
hPa	hectoPascals
in-oz	inch-ounce
K	Kelvin
km	kilometer, kilometers
km sec^{-1}	kilometers per second
m	meter
mA	milliamp, milliamps
micron	micrometer, micron
msec	millisecond
mW cm^{-2}sr^{-1}μm^{-1}	milliWatts per square centimeter per steradian per micron
m sec^{-1}	meter per second
N/A	not applicable, none, unitless, dimensionless
percent	percent, percentage 0..100
rad	radian
sec	second
volt	volt, volts
W h m^{-2}	Watt hour per square meter
W^2 m^4	square Watt per meter to the 4th
W m^{-2}	Watt per square meter
W m^{-2}sr^{-1}	Watt per square meter per steradian
W m^{-2}sr^{-1}μm^{-1}	Watt per square meter per steradian per micron
°C	degrees centigrade
μm	micrometer, micron

17.0 Document Information

17.1 Document Creation Date

December 2000

17.2 Document Review Date

TBD

17.3 Document Revision Date

Month Year   Comment

17.4 Document ID:

LD_007_010_001_00_00_0_yyyymmdd(Release Date) *[get this from DAAC User Services]*

17.5 Citation

Please provide a reference to the following paper when scientific results are published using the CERES SSF data:

"Wielicki, B. A.; Barkstrom, B.R.; Harrison, E. F.; Lee III,R.B.; Smith, G.L.; and Cooper, J.E., 1996: Clouds and the Earth's Radiant Energy System (CERES): An Earth Observing System Experiment, Bull. Amer. Meteor. Soc., 77, 853-868."

When Langley Atmospheric Sciences Data Center (ASDC) data are used in a publication, the following acknowledgment is requested to be included:

"These data were obtained from the Atmospheric Sciences Data Center at NASA Langley Research Center."

The Data Center at Langley requests a reprint of any published papers or reports or a brief description of other uses (e.g., posters, oral presentations, etc.) of distributed data. This will help the Data Center determine the use of the distributed data, which is helpful in optimizing product development. It also helps the Data Center to keep its product-related references current.

17.6 Redistribution of Data

To assist the Langley Data Center in providing the best service to the scientific community, a notification is requested if these data are transmitted to other researchers.

17.7 Document Curator

The Langley ASDC Science, User & Data Services Office.

18.0 Index

B

C

D

E

F

H

I

M

N

S

T

APPENDIX A
CERES Metadata

This section describes the metadata that are written to all CERES HDF products. Table A-1 describes the CERES Baseline Header Metadata that are written on both HDF and binary direct access output science data products. The parameters are written in HDF structures for CERES HDF output products and are written as 80-byte records for binary direct access output products. Some parameters may be written in multiple records. Table A-2 describes the CERES_metadata Vdata parameters which are a subset of the CERES Baseline Header Metadata and are also written to all CERES HDF output products. For details on CERES Metadata, see the CERES Software Bulletin "CERES Metadata Requirements for LaTIS" (Reference 49).

Table A-1 lists the item number, parameter name, units, range or allowable values, the data type, and the maximum number of elements. There are two choices for parameters 22-25 and two choices for parameters 26-29. The choices depend on whether the product is described by a bounding rectangle or by a G-Ring. Abbreviations used in the Data Type field are defined as follows:

s = string	date = yyyy-mm-dd
F = float	time = hh:mm:ss.xxxxxxZ
I = integer	datetime = yyyy-mm-ddThh:mm:ss.xxxxxxZ

Table A-1. CERES Baseline Header Metadata (1 of 2)

Item	Parameter Name	Units	Range	Data Type	No. of Elements
1	ShortName	N/A	N/A	s(8)	1
2	VersionID	N/A	0 .. 255	I3	1
3	CERPGEName	N/A	N/A	s(20)	1
4	SamplingStrategy	N/A	CERES, TRMM-PFM-VIRS, AM1-FM1-MODIS, TBD	s(20)	1
5	ProductionStrategy	N/A	Edition, Campaign, Diagnostic-Case, PreFlight, TBD	s(20)	1
6	CERDataDateYear	N/A	1997 .. 2050	s(4)	1
7	CERDataDateMonth	N/A	1 .. 12	s(2)	1
8	CERDataDateDay	N/A	1 .. 31	s(2)	1
9	CERHrOfMonth	N/A	1 .. 744	s(3)	1
10	RangeBeginningDate	N/A	1997-11-19 .. 2050-12-31	date	1
11	RangeBeginningTime	N/A	00:00:00.000000Z .. 24:00:00:000000Z	time	1
12	RangeEndingDate	N/A	1997-11-19 .. 2050-12-31	date	1
13	RangeEndingTime	N/A	00:00:00.000000Z .. 24:00:00:000000Z	time	1
14	AssociatedPlatformShortName	N/A	TRMM, AM1, PM1, TBD	s(20)	1 - 4

Table A-1. CERES Baseline Header Metadata (2 of 2)

Item	Parameter Name	Units	Range	Data Type	No. of Elements
15	AssociatedInstrumentShortName	N/A	PFM, FM1, FM2, FM3, FM4, FM5, TBD	s(20)	1 - 4
16	LocalGranuleID	N/A	N/A	s(80)	1
17	PGEVersion	N/A	N/A	s(10)	1
18	CERProductionDateTime	N/A	N/A	datetime	1
19	LocalVersionID	N/A	N/A	s(60)	1
20	ProductGenerationLOC	N/A	SGI_xxx, TBD	s(255)	1
21	NumberofRecords	N/A	1 .. 9 999 999 999	I10	1
22	WestBoundingCoordinate	deg	-180.0 .. 180.0	F11.6	1
23	NorthBoundingCoordinate	deg	-90.0 .. 90.0	F11.6	1
24	EastBoundingCoordinate	deg	-180.0 .. 180.0	F11.6	1
25	SouthBoundingCoordinate	deg	-90.0 .. 90.0	F11.6	1
22	GRingPointLatitude	deg	-90.0 .. 90.0	F11.6	5
23	GRingPointLongitude	deg	-180.0 .. 180.0	F11.6	5
24	GRingPointSequenceNo	N/A	0 .. 99999	I5	5
25	ExclusionGRingFlag	N/A	Y (= YES), N (= NO)	s(1)	1
26	CERWestBoundingCoordinate	deg	0.0 .. 360.0	F11.6	1
27	CERNorthBoundingCoordinate	deg	0.0 .. 180.0	F11.6	1
28	CEREastBoundingCoordinate	deg	0.0 .. 360.0	F11.6	1
29	CERSouthBoundingCoordinate	deg	0.0 .. 180.0	F11.6	1
26	CERGRingPointLatitude	deg	0.0 .. 180.0	F11.6	5
27	CERGRingPointLongitude	deg	0.0 .. 360.0	F11.6	5
28	GRingPointSequenceNo	N/A	0 .. 99999	I5	5
29	ExclusionGRingFlag	N/A	Y (= YES), N (= NO)	s(1)	1
30	AutomaticQualityFlag	N/A	Passed, Failed, or Suspect	s(64)	1
31	AutomaticQualityFlagExplanation	N/A	N/A	s(255)	1
32	QAGranuleFilename	N/A	N/A	s(255)	1
33	ValidationFilename	N/A	N/A	s(255)	1
34	ImagerShortName	N/A	VIRS, MODIS, TBD	s(20)	1
35	InputPointer	N/A	N/A	s(255)	800
36	NumberInputFiles	N/A	1 .. 9999	I4	1

Table A-2 describes the CERES_metadata Vdata parameters which are written to all CERES HDF output science products.

Table A-2. CERES_metadata Vdata

Item	Parameter Name	Range	Data Type
1	ShortName	N/A	s(32)
2	RangeBeginningDate	1997-11-19 .. 2050-12-31	s(32)
3	RangeBeginningTime	00:00:00.000000Z .. 24:00:00:000000Z	s(32)
4	RangeEndingDate	1997-11-19 .. 2050-12-31	s(32)
5	RangeEndingTime	00:00:00.000000Z .. 24:00:00:000000Z	s(32)
6	AutomaticQualityFlag	Passed, Failed, or Suspect	s(64)
7	AutomaticQualityFlagExplanation	N/A	s(256)
8	AssociatedPlatformShortName	TRMM, EOS AM-1, EOS PM-1, TBD	s(32)
9	AssociatedInstrumentShortName	PFM, FM1, FM2, FM3, FM4, FM5, TBD	s(32)
10	LocalGranuleID	N/A	s(96)
11	LocalVersionID	N/A	s(64)
12	CERProductionDateTime	N/A	s(32)
13	NumberofRecords	1 .. 9 999 999 999	4-byte Integer
14	ProductGenerationLOC	SGI_xxx, TBD	s(256)

The SSF Product Specific Attribute (PSA) metadata are listed in Table A-3. The definitions that are nearly identical for several parameters are defined only once, even though individually distinct parameters exist as shown in the table below.

Table A-3. SSF Product Specific Metadata Parameters

Item	Parameter Name	Range	Data Type
1	PercentCrosstrackFOV	0.0 .. 100.0	32 bit real
2	PercentRapsFOV	0.0 .. 100.0	32 bit real
3	PercentOtherFOV	0.0 .. 100.0	32 bit real
4		Record Size (bytes) =nnn	

APPENDIX B
SSF Parameter Origination

The following table specifies the origination of each parameter in the SSF product. The Subsystem column lists the Subsystem number and Product according to the following code:

Table B-1. Subsystem Product Code

Subsystem Name	Number	Product Code
Geolocate and Calibrate Earth Radiances	SS 1.0	IES
Cloud Retrieval	SS 4.1-4.3	cookiedough
Convolution	SS 4.4	Int-SSF
Inversion	SS 4.5	SSF
Surface Estimation	SS 4.6	SSF
Regrid Humidity and Temperature Fields	SS 12.0	MOA

Table B-2. SSF_Header

Item: Name	Subsystem responsible for writing	CERES Product where parameter originates
SSF-H1: SSF ID	4.4	Int-SSF
SSF-H2: Character name of CERES instrument	4.4	IES
SSF-H3: Day and Time at hour start	4.4	IES/Int-SSF
SSF-H4: Character name of satellite	4.4	IES
SSF-H5: Character name of high resolution imager instrument	4.4	cookiedough
SSF-H6: Number of imager channels	4.4	cookiedough
SSF-H7: Central wavelengths of imager channels	4.4	cookiedough
SSF-H8: Earth-Sun distance at hour start	4.4	IES
SSF-H9: Beta Angle	4.4	Int-SSF
SSF-H10: Colatitude of subsatellite point at surface at hour start	4.4	IES
SSF-H11: Longitude of subsatellite point at surface at hour start	4.4	IES
SSF-H12: Colatitude of subsatellite point at surface at hour end	4.4	IES
SSF-H13: Longitude of subsatellite point at surface at hour end	4.4	IES
SSF-H14: Along-track angle of satellite at hour end	4.4	IES
SSF-H15: Number of Footprints in SSF product	4.4	Int-SSF/SSF
SSF-H16: Subsystem 4.1 identification string	4.4	cookiedough
SSF-H17: Subsystem 4.2 identification string	4.4	cookiedough
SSF-H18: Subsystem 4.3 identification string	4.4	cookiedough
SSF-H19: Subsystem 4.4 identification string	4.4	Int-SSF
SSF-H20: Subsystem 4.5 identification string	4.5	SSF
SSF-H21: Subsystem 4.6 identification string	4.6	SSF
SSF-H22: IES production date and time	4.4	IES
SSF-H23: MOA production date and time	4.4	MOA via cookiedough
SSF-H24: SSF production date and time	4.5/4.6	SSF

Table B-3. SSF SDS Summary (1 of 6)

Item: SDS Name	Subsystem responsible for writing	Product where parameter originates
SSF-1: Time of Observation	4.4	IES
SSF-2: Radius of satellite from center of Earth at observation	4.4	IES
SSF-3: X component of satellite inertial velocity	4.4	IES
SSF-4: Y component of satellite inertial velocity	4.4	IES
SSF-5: Z component of satellite inertial velocity	4.4	IES
SSF-6: Colatitude of subsatellite point at surface at observation	4.4	IES
SSF-7: Longitude of subsatellite point at surface at observation	4.4	IES
SSF-8: Colatitude of subsolar point at surface at observation	4.4	IES
SSF-9: Longitude of subsolar point at surface at observation	4.4	IES
SSF-10: Colatitude of CERES FOV at surface	4.4	IES
SSF-11: Longitude of CERES FOV at surface	4.4	IES
SSF-12: Scan sample number	4.4	IES
SSF-13: Packet number	4.4	IES
SSF-14: Cone angle of CERES FOV at satellite	4.4	IES
SSF-15: Clock angle of CERES FOV at satellite wrt inertial velocity	4.4	IES
SSF-16: Rate of change of cone angle	4.4	IES
SSF-17: Rate of change of clock angle	4.4	IES
SSF-18: Along-track angle of CERES FOV at surface	4.4	IES
SSF-19: Cross-track angle of CERES FOV at surface	4.4	IES
SSF-20: CERES viewing zenith at surface	4.4	IES
SSF-21: CERES solar zenith at surface	4.4	IES
SSF-22: CERES relative azimuth at surface	4.4	IES
SSF-23: CERES viewing azimuth at surface wrt North	4.4	IES
SSF-24: Altitude of surface above sea level	4.4	cookiedough/Int-SSF
SSF-25: Surface type index	4.4	cookiedough/Int-SSF
SSF-26: Surface type percent coverage	4.4	cookiedough/Int-SSF
SSF-27: CERES SW ADM type for inversion process	4.5	SSF
SSF-28: CERES LW ADM type for inversion process	4.5	SSF
SSF-29: CERES WN ADM type for inversion process	4.5	SSF
SSF-30: ADM geo	4.5	SSF
SSF-31: CERES TOT filtered radiance - upwards	4.4	IES
SSF-32: CERES SW filtered radiance - upwards	4.4	IES

Table B-3. SSF SDS Summary (2 of 6)

Item: SDS Name	Subsystem responsible for writing	Product where parameter originates
SSF-33: CERES WN filtered radiance - upwards	4.4	IES
SSF-34: Radiance and Mode flags	4.4	IES
SSF-35: CERES SW radiance - upwards	4.5	SSF
SSF-36: CERES LW radiance - upwards	4.5	SSF
SSF-37: CERES WN radiance - upwards	4.5	SSF
SSF-38: CERES SW TOA flux - upwards	4.5	SSF
SSF-39: CERES LW TOA flux - upwards	4.5	SSF
SSF-40: CERES WN TOA flux - upwards	4.5	SSF
SSF-41: CERES downward SW surface flux - Model A	4.6	SSF
SSF-42: CERES downward LW surface flux - Model A	4.6	SSF
SSF-43: CERES downward WN surface flux - Model A	4.6	SSF
SSF-44: CERES net SW surface flux - Model A	4.6	SSF
SSF-45: CERES net LW surface flux - Model A	4.6	SSF
SSF-46: CERES downward SW surface flux - Model B	4.6	SSF
SSF-47: CERES downward LW surface flux - Model B	4.6	SSF
SSF-48: CERES net SW surface flux - Model B	4.6	SSF
SSF-49: CERES net LW surface flux - Model B	4.6	SSF
SSF-50: CERES broadband surface albedo	4.4	Int-SSF
SSF-51: CERES LW surface emissivity	4.4	Int-SSF
SSF-52: CERES WN surface emissivity	4.4	Int-SSF
SSF-53: Number of imager pixels in CERES FOV	4.4	Int-SSF
SSF-54: Imager percent coverage	4.4	Int-SSF
SSF-55: Imager viewing zenith over CERES FOV	4.4	cookiedough/Int-SSF
SSF-56: Imager relative azimuth angle over CERES FOV	4.4	cookiedough/Int-SSF
SSF-57: Surface wind - U-vector	4.5	MOA
SSF-58: Surface wind - V-vector	4.5	MOA
SSF-59: Surface skin temperature	4.5	MOA
SSF-60: Column averaged relative humidity	4.5	MOA
SSF-61: Precipitable water	4.5	MOA
SSF-62: Flag - Source of precipitable water	4.5	MOA/SSF
SSF-63: Cloud property extrapolation over cloudy area	4.4	Int-SSF
SSF-64: Notes on general procedures	4.4	Int-SSF
SSF-65: Notes on cloud algorithms	4.4	cookiedough/Int-SSF
SSF-66: Clear area percent coverage at subpixel resolution	4.4	cookiedough/Int-SSF

Table B-3. SSF SDS Summary (3 of 6)

Item: SDS Name	Subsystem responsible for writing	Product where parameter originates
SSF-67: Cloud-mask clear-strong percent coverage	4.4	cookiedough/Int-SSF
SSF-68: Cloud-mask clear-weak percent coverage	4.4	cookiedough/Int-SSF
SSF-69: Cloud-mask snow/ice percent coverage	4.4	cookiedough/Int-SSF
SSF-70: Cloud-mask aerosol B percent coverage	4.4	cookiedough/Int-SSF
SSF-71: Flag - Type of aerosol B	4.4	cookiedough/Int-SSF
SSF-72: Cloud-mask percent coverage supplement	4.4	cookiedough/Int-SSF
SSF-73: Total aerosol A optical depth - visible	4.4	cookiedough/Int-SSF
SSF-74: Total aerosol A optical depth - near IR	4.4	cookiedough/Int-SSF
SSF-75: Aerosol A supplement 1	4.4	cookiedough/Int-SSF
SSF-76: Aerosol A supplement 2	4.4	cookiedough/Int-SSF
SSF-77: Aerosol A supplement 3	4.4	cookiedough/Int-SSF
SSF-78: Aerosol A supplement 4	4.4	cookiedough/Int-SSF
SSF-79: Imager-based surface skin temperature	4.4	cookiedough/Int-SSF
SSF-80: Vertical temperature change	4.5	SSF
SSF-81: Clear/layer/overlap condition percent coverages	4.4	cookiedough/Int-SSF
SSF-82: Note for cloud layer	4.4	cookiedough/Int-SSF
SSF-83: Mean visible optical depth for cloud layer	4.4	cookiedough/Int-SSF
SSF-84: Stddev of visible optical depth for cloud layer	4.4	Int-SSF
SSF-85: Mean logarithm of visible optical depth for cloud layer	4.4	cookiedough/Int-SSF
SSF-86: Stddev of logarithm of visible optical depth for cloud layer	4.4	Int-SSF
SSF-87: Mean cloud infrared emissivity for cloud layer	4.4	cookiedough/Int-SSF
SSF-88: Stddev of cloud infrared emissivity for cloud layer	4.4	Int-SSF
SSF-89: Mean liquid water path for cloud layer (3.7)	4.4	cookiedough/Int-SSF
SSF-90: Stddev of liquid water path for cloud layer (3.7)	4.4	Int-SSF
SSF-91: Mean ice water path for cloud layer (3.7)	4.4	cookiedough/Int-SSF
SSF-92: Stddev of ice water path for cloud layer (3.7)	4.4	Int-SSF
SSF-93: Mean cloud top pressure for cloud layer	4.4	cookiedough/Int-SSF
SSF-94: Stddev of cloud top pressure for cloud layer	4.4	Int-SSF
SSF-95: Mean cloud effective pressure for cloud layer	4.4	cookiedough/Int-SSF
SSF-96: Stddev of cloud effective pressure for cloud layer	4.4	Int-SSF
SSF-97: Mean cloud effective temperature for cloud layer	4.4	cookiedough/Int-SSF
SSF-98: Stddev of cloud effective temperature for cloud layer	4.4	Int-SSF
SSF-99: Mean cloud effective height for cloud layer	4.4	cookiedough/Int-SSF
SSF-100: Stddev of cloud effective height for cloud layer	4.4	Int-SSF

Table B-3. SSF SDS Summary (4 of 6)

Item: SDS Name	Subsystem responsible for writing	Product where parameter originates
SSF-101: Mean cloud base pressure for cloud layer	4.4	cookiedough/Int-SSF
SSF-102: Stddev of cloud base pressure for cloud layer	4.4	Int-SSF
SSF-103: Mean water particle radius for cloud layer (3.7)	4.4	cookiedough/Int-SSF
SSF-104: Stddev of water particle radius for cloud layer (3.7)	4.4	Int-SSF
SSF-105: Mean ice particle effective diameter for cloud layer (3.7)	4.4	cookiedough/Int-SSF
SSF-106: Stddev of ice particle effective diameter for cloud layer (3.7)	4.4	Int-SSF
SSF-107: Mean cloud particle phase for cloud layer (3.7)	4.4	cookiedough/Int-SSF
SSF-108: Mean water particle radius for cloud layer (1.6)	4.4	cookiedough/Int-SSF
SSF-109: Mean ice particle effective diameter for cloud layer (1.6)	4.4	cookiedough/Int-SSF
SSF-110: Mean cloud particle phase for cloud layer (1.6)	4.4	cookiedough/Int-SSF
SSF-111: Mean vertical aspect ratio for cloud layer	4.4	cookiedough/Int-SSF
SSF-112: Stddev of vertical aspect ratio for cloud layer	4.4	Int-SSF
SSF-113: Percentiles of visible optical depth for cloud layer (13)	4.4	cookiedough/Int-SSF
SSF-114: Percentiles of IR emissivity for cloud layer (13)	4.4	cookiedough/Int-SSF
SSF-115: Imager channel central wavelength	4.4	cookiedough/Int-SSF
SSF-116: All subpixel clear area percent coverage	4.4	cookiedough/Int-SSF
SSF-117: All subpixel overcast cloud area percent coverage	4.4	cookiedough/Int-SSF
SSF-118: Mean imager radiances over clear area	4.4	cookiedough/Int-SSF
SSF-119: Stddev of imager radiances over clear area	4.4	Int-SSF
SSF-120: Mean imager radiances over overcast cloud area	4.4	cookiedough/Int-SSF
SSF-121: Stddev of imager radiances over overcast cloud area	4.4	Int-SSF
SSF-122: Mean imager radiances over full CERES FOV	4.4	cookiedough/Int-SSF
SSF-123: Stddev of imager radiances over full CERES FOV	4.4	Int-SSF
SSF-124: 5th percentile of imager radiances over full CERES FOV	4.4	cookiedough/Int-SSF
SSF-125: 95th percentile of imager radiances over full CERES FOV	4.4	Int-SSF
SSF-126: Mean imager radiances over cloud layer 1 (no overlap)	4.4	cookiedough/Int-SSF
SSF-127: Stddev of imager radiances over cloud layer 1 (no overlap)	4.4	Int-SSF
SSF-128: Mean imager radiances over cloud layer 2 (no overlap)	4.4	cookiedough/Int-SSF
SSF-129: Stddev of imager radiances over cloud layer 2 (no overlap)	4.4	Int-SSF
SSF-130: Mean imager radiances over cloud layer 1 and 2 overlap	4.4	cookiedough/Int-SSF

Table B-3. SSF SDS Summary (5 of 6)

Item: SDS Name	Subsystem responsible for writing	Product where parameter originates
SSF-131: Stddev of imager radiances over cloud layer 1 and 2 over-lap	4.4	Int-SSF
SSF-132: Percentage of CERES FOV with MODIS land aerosol	4.4	cookiedough/Int-SSF
SSF-133: PSF-wtd MOD04 cloud fraction land	4.4	cookiedough/Int-SSF
SSF-134: PSF-wtd MOD04 aerosol types land	4.4	cookiedough/Int-SSF
SSF-135: PSF-wtd MOD04 dust weighting factor land	4.4	cookiedough/Int-SSF
SSF-136: PSF-wtd MOD04 corrected optical depth land (0.470)	4.4	cookiedough/Int-SSF
SSF-137: PSF-wtd MOD04 corrected optical depth land (0.550)	4.4	cookiedough/Int-SSF
SSF-138: PSF-wtd MOD04 corrected optical depth land (0.659)	4.4	cookiedough/Int-SSF
SSF-139: MOD04 number pixels percentile land (0.659) in CERES FOV	4.4	cookiedough/Int-SSF
SSF-140: PSF-wtd MOD04 mean reflectance land (0.470)	4.4	cookiedough/Int-SSF
SSF-141: PSF-wtd MOD04 mean reflectance land (0.659)	4.4	cookiedough/Int-SSF
SSF-142: PSF-wtd MOD04 mean reflectance land (0.865)	4.4	cookiedough/Int-SSF
SSF-143: PSF-wtd MOD04 mean reflectance land (2.130)	4.4	cookiedough/Int-SSF
SSF-144: PSF-wtd MOD04 mean reflectance land (3.750)	4.4	cookiedough/Int-SSF
SSF-145: PSF-wtd MOD04 std reflectance land (0.470)	4.4	cookiedough/Int-SSF
SSF-146: Percentage of CERES FOV with MODIS ocean aerosol	4.4	cookiedough/Int-SSF
SSF-147: PSF-wtd MOD04 cloud fraction ocean	4.4	cookiedough/Int-SSF
SSF-148: PSF-wtd MOD04 solution indices ocean small, average	4.4	cookiedough/Int-SSF
SSF-149: PSF-wtd MOD04 solution indices ocean large, average	4.4	cookiedough/Int-SSF
SSF-150: PSF-wtd MOD04 effective optical depth average ocean (0.470)	4.4	cookiedough/Int-SSF
SSF-151: PSF-wtd MOD04 effective optical depth average ocean (0.550)	4.4	cookiedough/Int-SSF
SSF-152: PSF-wtd MOD04 effective optical depth average ocean (0.659)	4.4	cookiedough/Int-SSF
SSF-153: PSF-wtd MOD04 effective optical depth average ocean (0.865)	4.4	cookiedough/Int-SSF
SSF-154: PSF-wtd MOD04 effective optical depth average ocean (1.240)	4.4	cookiedough/Int-SSF
SSF-155: PSF-wtd MOD04 effective optical depth average ocean (1.640)	4.4	cookiedough/Int-SSF
SSF-156: PSF-wtd MOD04 effective optical depth average ocean (2.130)	4.4	cookiedough/Int-SSF

Table B-3. SSF SDS Summary (6 of 6)

Item: SDS Name	Subsystem responsible for writing	Product where parameter originates
SSF-157: PSF-wtd MOD04 optical depth small average ocean (0.550)	4.4	cookiedough/Int-SSF
SSF-158: PSF-wtd MOD04 optical depth small average ocean (0.865)	4.4	cookiedough/Int-SSF
SSF-159: PSF-wtd MOD04 optical depth small average ocean (2.130)	4.4	cookiedough/Int-SSF
SSF-160: PSF-wtd MOD04 cloud condensation nuclei ocean, average	4.4	cookiedough/Int-SSF

APPENDIX C
Programmer Notes

C.1 General Programmer Notes

MOA data product

The MOA data product is thought to be partially geocentric and partially geodetic. The meteorological data from DAO is assumed to be geocentric, and the microwave precipitable water data (SSM/I) is known to be geodetic. As per 3/15/99 conversation with Tom Charlock, the ECMWF data is geolocated geographically (center of gravity).

SSF and ES-8 specific differences

The following list expands upon the SSF and ES-8 difference discussed in Section 1.6.
- SSF FOVs are geolocated at the surface using a geodetic model. ES-8 FOVs are geolocated at TOA using a geocentric model.
- SSF radiances are inverted to flux at the surface. ES-8 radiances are also inverted to flux at surface but flux geolocated at TOA.
- SSF ADM surface types are based upon a 10 minute IGBP map and current snow map. ES-8 Scene ID surface types come from a 2.5 degree geomap and monthly averaged snow.
- SSF cloud amount is determined from imager data. ES-8 cloud amount is determined by MLE.

Other items of secondary interest

There is no PSF defined for FOVs which are sampled at very rapid elevation scan rates. For this reason, FOVs collected during rapid retrace portion of short scan, where elevation scan rate is approximately 249 deg/sec, are never included on an SSF.

The SSF data product must have restart capability. The Inversion and Surface Estimation portion of SS 4.0 must be able to reprocess existing SSF granules.

Upwelling fluxes are defined to be positive. Downwelling fluxes are also defined to be positive. A net flux is defined as downwelling flux minus upwelling flux.

For Edition1 of the TRMM-PFM data, the SSF will only contain valid TOA flux values (See SSF-38 to SSF-40) for FOVs which have a "clear area percent coverage at subpixel resolution"(See SSF-66) greater than 99.9%. The remaining TOA flux values will be set to CERES default (See Table 4-5). When the TOA flux values contains CERES default, the surface flux values derived from them (See SSF-41 to SSF-46, and SSF-48) will also be set to CERES default. Surface fluxes which are independent of TOA flux (See SSF-47 and SSF-49) are not impacted.

C.2 List of Parameters which are never set to CERES Default

Most SSF parameters are set to a CERES default (See Table 4-5) when data is unavailable or considered to be suspect. However, there is a handful of parameters which, by definition, must be

available and cannot be suspect if the FOV is to be included on the SSF. These parameters can never contain a CERES default value. What follows is a list of such parameters.

Most SSF_Header parameters (SSF-H1 to SSF-H24, except SSF-H7)
All Time and Position parameters (SSF-1 to SSF-19)
All Viewing Angle parameters (SSF-20 to SSF-23)
Radiance and Mode flags (SSF-34)
Imager percent coverage (SSF-54)

C.3   Programmer Notes on SSF Header Parameters

SSF-H1: SSF ID

SSFs produced as ValidationR4 had an SSF ID of 113.

The SSF ID should be verified by all software intending to read an SSF granule to guard against reading the data incorrectly.

SSF-H2: Character name of CERES instrument

The character name of CERES instrument is assigned based on the numerical code provided on the level 0 file.

SSF-H3: Day and Time at hour start

This parameter is in 28 character CCSDS ASCII Time Code A format. It should always be exactly on the hour, with minutes and seconds set to 0.

IES contains a Julian day which Cookiecutter, SS 4.4, reads and converts to ASCII. For TRMM, SS 1.0, receives a 64 bit encoded mission elapsed spacecraft time. For EOS, the spacecraft time has a 1/1/1958 epoch.

For more information about different types of time, see Brooks Childers' CERES software bulletin 95-10, dated August 25, 1995. The SDP Toolkit Users Guide for the ECS Project section on Time and Date Conversion Tools discusses time formats and toolkit calls.

SSF-H4: Character name of satellite

The full satellite acronym is contained in the metadata.

SSF-H5: Character name of high resolution imager instrument

The imager pixels from this high resolution imager are convolved with the CERES FOV to determine cloud properties for the FOV. There is a one to one correspondence between the imager and the satellite. For example, VIRS is on TRMM, MODISam1 is on AM-1, and MODISpm1 is on PM-1.

SSF-H6: Number of imager channels

These imager channels are available to Cloud Retrieval for determining cloud and clear-sky properties. For TRMM, all 5 VIRS channels are available. For EOS-AM, 19 MODIS channels

are expected to be available. Cookiedough provides a table with all of the possible 20 imager channels and denotes which of these were available.

All the MODIS channels are provided to cloud retrieval at 1 kilometer resolution. The 0.645 spectral band is provided at the observed 250 meter resolution in addition to the aggregated one kilometer resolution data. The 1.64 and 2.13 μm bands are observed at 500 meter resolution and aggregated into a one kilometer pixel, however the observed data is not provided. The remaining channels are all observed at 1 kilometer resolution.

SSF-H7: Central wavelengths of imager channels

The central wavelengths of the available channels are copied, by Cookiecutter, from a Cookiedough table that contains all of the possible 20 imager channels but denotes those which were actually available.

SSF-H10: Colatitude of subsatellite point at surface at hour start

It is the same as the colatitude of subsatellite point at surface at hour end written on the previous hour's SSF.

All colatitudes and longitudes at hour start and end are computed from the satellite ephemeris data. Therefore, missing CERES data does not impact these parameters.

SSF-H11: Longitude of subsatellite point at surface at hour start

It is the same as the longitude of subsatellite point at surface at hour end written on the previous hour's SSF.

SSF-H14: Along-track angle of satellite at hour end

The position of the satellite at hour end always corresponds to an along-track angle of 0.0 degrees in the next hour.

SSF-H17: Subsystem 4.2 identification string

When MODIS imager input is used, additional emittance maps will be added. An emittance map is needed for every thermal (LW) channel.

SSF-H20: Subsystem 4.5 identification string

For SSF ID = 112, cc in CADM_cc_YYYYMMDD identifies the model as SW or LW seasonal. Valid values are SW (shortwave, all seasons), WN (LW winter), SP (LW spring), SM (LW summer), and AT (LW autumn). For SSF ID >= 113 (See SSF-H1), "cc" identifies the model coefficients as SW (shortwave), LW (longwave), or WN (window). "YYYYMMDD" identifies the date that these coefficients were assembled into a file.

SSF-H22: IES production date and time

IES production date and time uniquely identifies that IES.

SSF-H23: MOA production date and time

The production date and time is of the MOA used by subsystems 4.1 - 4.3. If Subsystem 4.5 - 4.6 has run, this same MOA was also used by it. This string uniquely identifies the MOA file used.

SSF-H24: SSF production date and time

The SSF production date and time is a system time. Date and time are determined and written by the creating subsystem, either Subsystem 4.4 or Subsystem 4.5-4.6. This will not be the same date and time found the metadata of the HDF SSF file.

C.4 Programmer Notes on SSF FOV Parameters

SSF-1: Time of Observation

CERES software bulletin 96-07 states that the SSF will contain all the data accumulated during that hour, regardless of along-track angle. For TRMM, Subsystem 1.0, Instrument, receives a 64 bit encoded mission elapsed spacecraft time. For EOS, the spacecraft time has a 1/1/1958 epoch. For more information about time, see CERES software bulletin 95-10, dated August 25, 1995.

SSF-6: Colatitude of subsatellite point at surface at observation

Toolkit User's Guide defines subsatellite point as the point at the foot of a normal dropped from the satellite to the (WGS-84) Earth model. The North Pole colatitude is 0° and the South Pole colatitude is 180°.

SSF-8: Colatitude of subsolar point at surface at observation

The subsolar point is at the foot of a normal dropped from the Sun to the WGS-84 Earth model. Due to the very large Sun distance, the geodetic colatitude and longitude of the subsolar point are the same as the geocentric colatitude and longitude of the Sun. The North Pole colatitude is 0° and the South Pole colatitude is 180°.

SSF-13: Packet number

The packet number is the relative number of packets received by Subsystem 1.0 for a given day. Every packet sent by the instrument contains 6.6 seconds of data, or 660 contiguous CERES FOVs.

Packet number 0 corresponds to the last packet from the previous day. Depending on where midnight falls within the packet, FOV from this last packet of the previous day may exist in the previous day's IES, the current day's IES, or both. If midnight occurs before the first Earth view (full or partial) FOV within the packet, all the IES FOVs associated with this packet will have a relative packet number of 0 and exist on the IES for the current day. If midnight occurs after the first Earth view FOV but before the last, the packet will be split between two days and have 2 relative packet numbers assigned to it. If midnight occurs after the last Earth view FOV, all the IES FOVs associated with that packet will fall in the previous day. The packet number should never reset during the day.

Missing packets at the beginning of a day will not be accounted for in the packet number. After that, missing packets will be accounted for. Restated, only after the first packet number of the day, either 0 or 1, has been established will packet number increase by the number of missing packets. A packet number can be established even if there are no Earth view FOVs associated with it.

Relative packet number is not expected to exceed 13091 for any given day and it should not be impacted by any instrument resets which might occur. (NOTE: The instrument packet number will be reset to zero whenever the instrument resets. However, the next instrument packet number containing science data after a reset will be much higher because the ground intervention required to return to Earth viewing scans can not be instantaneous. The relative packet number will attempt to reflect the number of missing packets should such an event occur.)

SSF-14: Cone angle of CERES FOV at satellite

The maximum cone angle value for a given CERES instrument is dependent upon satellite altitude.

SSF-15: Clock angle of CERES FOV at satellite wrt inertial velocity

In RAPS mode the clock angle will range from 0 to 360 degrees. However, if the sun is in the orbit plane, the azimuth range is restricted to avoid scanning the sun. For more information about the restricted azimuth range due to the Sun's Beta angle, see the TRMM Operations Agreement.

When operating in a crosstrack scan, the clock angle will approach 0/360 degrees or 180 degrees at very small cone angles. This occurs because the scan is slightly off nadir. Therefore, at small cone angles, the clock angle should never be used to determine the type of scan.

SSF-16: Rate of change of cone angle

The rate of change of the cone angle is calculated as a two point difference between consecutive scan angle positions. A one count change in scan angle is equal to 0.0055 degrees. CERES FOVs are spaced 0.01 seconds apart. Thus, an increase of one count results in a cone rate change of 0.55 degrees/second. Cone angle rate changes of 0.55 between CERES FOVs and cone angle rate changes of 1.1 over several CERES FOVs are not uncommon. The expected cone angle rate of change for the normal scan, moving portion of the nadir scan, and slow segment of the short scan is approximately ±63 deg/sec. The stationary portion of the nadir scan is expected to have a cone angle rate of approximately 0 deg/sec. The expected cone angle rate of change for the rapid-retrace portion of the short scan is approximately ±250 deg/sec. However, the current Subsystem 4.4 algorithm does not process CERES FOVs from the rapid-retrace portion of the short scan, so these FOVs will not be placed on the SSF.

SSF-17: Rate of change of clock angle

Like the cone angle rate, the clock angle rate is also expected to vary between CERES FOVs. It is based on instrument azimuth position count. A one count difference in position accounts for a .549 deg/sec change in clock rate.

SSF-18: Along-track angle of CERES FOV at surface

For a more complete discussion of the CERES FOV ordering on the SSF, refer to CERES Software Bulletin 96-07.

SSF-23: CERES viewing azimuth at surface wrt North

The angle is based on a right handed coordinate system with the origin at the Earth point, the Z axis pointing along the positive radius vector, and the X axis pointing North.

SSF-24: Altitude of surface above sea level

Sea ice height is not included in altitude.

The surface altitude map will be replaced with a static map based on the USGS 1 km elevation map. The Earth model used to create the USGS elevation map is unknown. It is likewise unknown whether the USGS elevation map is geocentric, geodetic, or other.

Clouds treats the altitude map as though it is the same as the imager, namely geodetic and based on the WGS-84 Earth model.

SSF-25: Surface type index

Every imager pixel identifies the surface as one of surface types 1 - 18 and indicates whether snow or ice is present. Subsystem 4.4 combines this information to generate one of the above 20 surface types for each pixel before computing a PSF-weighted average of each of the surface types.

The Olson vegetation map, used together with the IGBP surface map to identify tundra, is a 0.5 degree map containing 72 vegetation types.

CERES uses a set of surface maps. All of these maps are on a 10 minute, equal angle grid. The Earth Models; whether the maps are geocentric, geodetic, or other; and whether the maps are consistent with each other is unknown. These maps include:

- 17 IGBP + Tundra surface scene types
- Fresh snow data (comes in as polar projected data with ~ 47 km resolution; spread to 10 minute)
- Sea Ice (comes in as polar projected data with ~ 47 km resolution; spread to 10 minute)
- Broadband and Window Emissivity
- Land Percentage
- Elevation

SSF-26: Surface type percent coverage

As the surface type percent coverage is calculated, round-off error is compensated for those instances where there are eight or less surface types. The potential surface area round off is defined as twice the total of the surface percent coverage minus 100. If the absolute value of the potential surface area round off exceeds the number of surface types, surface types and percent coverage are set to CERES defaults. If the potential surface area round off is less than the number of surface types, but not equal to 0, the surface area of the most prevalent types are adjusted upward or downward so they percent coverage sums to 100 percent. This is done for sums of 103 to 97. Only the first surface type percent coverage is adjusted up or down by 1 for totals one away from 100. The first three surface type percent coverage is adjusted up or down by 1 for totals three away from 100. If the total surface percent coverage exceeds 103 or is below 97, all surface types and surface type percent coverage are set to CERES defaults.

SSF-27: CERES SW ADM type for inversion process

For VIRS12 ADMS, if all surface type indices are set to CERES default or if the total surface area sums to zero percent, then the ADM surface type and, consequently, the ADM type are set to CERES default. If the non-default sum of the surface type percent coverages exceeds 101 or is

less than or equal to 90, then the geotype and, consequently, the ADM type are set to unknown or 0.

If by some quirk, the clear percent coverage at subpixel resolution is set to CERES default, the ADM type is also set to CERES default.

VIRS12 ADMs use the value of 0 to denote an unknown scene.

Users of ValidationR2, ValR2-NL, ValidationR1, and AtLaunch SSF granules should be aware that the full set of RPM ADMs (11/1/97; constructed by Hinton and Fletcher using RPM method and Nimbus-7 data) were used to invert radiances. These granules are older versions of the SSF and were created when the ADM type was defined as being independent of ADM construction. RPM ADMs use the same 12 ERBE Scene types as the VIRS12A.

The ADM version number in the Subsystem 4.5 identification string indicates which set of ADMs was used.

SSF-28: CERES LW ADM type for inversion process

See "SSF-27: CERES SW ADM type for inversion process" programmer notes directly before this parameter.

SSF-29: CERES WN ADM type for inversion process

See "SSF-27: CERES SW ADM type for inversion process" programmer notes.

For ValidationR2 and earlier SSFs, the window channel ADMs are identical to the longwave ADMs (generated using the RPM method). Beginning with ValidationR3 and VIRS12A, a set of 12 WN ADMs has been developed using CERES data.

SSF-30: ADM geo

The ADM geo's exact definition will be determined later.

SSF-33: CERES WN filtered radiance - upwards

Actual bandpass is estimated to be from 8.15 to 11.85 µm.

SSF-35: CERES SW radiance - upwards

The filtered measurements are multiplied by regression coefficients which are a function of scene type, directional angles, and geocentric colatitude of the Earth point. If the 3 channel intercomparison of the filtered radiances fails or if the CERES SW flux at TOA, upwards (SSF-38), which is calculated from this radiance, is determined to be unacceptable, this variable is still produced and it is not set to CERES default. During the day, the ERBE-like unfiltered SW measurements are estimated from "good" filtered SW (SSF-32) and TOT (SSF-31) measurements. Daytime ERBE-like SW unfiltered radiance values will also differ from CERES SW unfiltered radiance values because the thermal SW radiance adjustments differ.

Prior to ValidationR4, Fred Rose's theoretical coefficients were used to compute the thermal SW radiance adjustments. If the filtered window radiance was not "good" (See SSF-34), then the

constant $SW^{thermal} = 0.35 \, W m^{-2} sr^{-1}$ was used for all scenes. Under normal conditions the thermal shortwave was derived from the filtered window radiance and was given by

$$SW^{thermal} = A_0 + A_1 x + A_2 x^2 + A_3 x^3$$

$$x = m_f^{WN} * \text{WNchan\_width}$$

$$A_0 = 0.180000$$

$$A_1 = 0.001620$$

$$A_2 = 0.000133$$

$$A_3 = 0.000016$$

SSF-36: CERES LW radiance - upwards

The filtered measurements are multiplied by regression coefficients which are a function of scene type, directional angles, and geocentric colatitude of the Earth point. If this computation can not be made, the CERES LW unfiltered radiance, upward is set to the corresponding CERES default. Even if the 3 channel intercomparison of the filtered radiances fails or if the CERES LW flux at TOA, upwards, which is calculated from this radiance, is determined to be unacceptable, this variable is still produced and it is not set to CERES default. Daytime CERES LW unfiltered radiance values may vary from the ERBE-like LW unfiltered radiance because the mean nighttime filtered SW radiance adjustment may differ.

SSF-37: CERES WN radiance - upwards

The filtered measurements are multiplied by a regression coefficient which is a function of scene type, directional angles, and geocentric colatitude of the Earth point. Even if the 3 channel intercomparison of the filtered radiances fails or if the CERES WN flux at TOA, upwards (SSF-40), which is calculated from this radiance, is determined to be unacceptable, this variable is still produced and it is not set to CERES default. For ValidationR3, a new, corrected set of WN spectral correction coefficients are used.

SSF-38: CERES SW TOA flux - upwards

r_{earth} is the radius of the WGS-84 Earth model ellipsoid at the Earth point. r_{TOA} is the radius of the CERES-TOA model at the same geodetic colatitude and longitude as the Earth point. SSFs through ValidationR2_005000 use the SW RPM ADMs (NIISW03.971101) to invert the SW flux. SSFs produced after that use the SW VIRS12A ADMs.

The VIRS12A ADMS are actually a mixture of new SW ADMS from Norman Loeb and old RPM ADMS. The new SW ADMS from Norman Loeb do not contain good ADM values for ERBE Scene types 3, 5, 8 and 11, so the old RPM ADM values are used for those cases. The RPM ADM normalization constants are used for VIRS12A.

SSF-39: CERES LW TOA flux - upwards

See SSF-40 for notes on r_{earth} and r_{TOA}. SSFs through ValidationR2_005000 use the LW RPM ADMs (NIILWss.971101 where ss is SP, SM, AT, or WN) to invert the LW flux. SSFs produced after that use the LW VIRS12A ADMs.

When using the RPM ADMs, R^i (or the ADM) is determined at the geocentric colatitude of the Earth point, however, the viewing zenith remains based on the geodetic zenith at the Earth point.

The VIRS12A LW ADMS are broken down into day and night. Unlike the VIRS12A SW ADMS, the VIRS12A LW ADMS have a set of normalization constants. For the VIRS12A LW ADMs, R^i is determined at the geodetic colatitude of the Earth point. When using VIRS12LW ADMs, fluxes which are greater than 450 W m^{-2} or less than 50 W m^{-2} are set to CERES default.

SSF-40: CERES WN TOA flux - upwards

WN channel estimate of 8.15 to 11.85 µm is more accurate. Kory is putting together the information to send to Ramanathan/Inamdar. See SSF-38 for notes on r_{earth} and r_{TOA}. SSFs through ValidationR2_005000 use the LW RPM ADMs (NIILWss.971101 where ss is SP, SM, AT, or WN) to invert the WN channel. SSFs produced after that use the WN VIRS12A ADMs.

When using the LW RPM ADMs, R^i (or the ADM) is determined at the geocentric colatitude of the Earth point, however, the viewing zenith remains based on the geodetic zenith at the Earth point.

The WN VIRS12A ADMs are broken down into day and night and have a corresponding set of normalization constants. For the VIRS12A WN ADMs, R^i is determined at the geodetic colatitude of the Earth point.

SSF-50: CERES broadband surface albedo

To compute this value, Subsystem 4.4 does a table lookup of the broadband surface albedo for each surface type within the CERES FOV and then computes a weighted average based on surface type percent coverage.

SSF-51: CERES LW surface emissivity

Subsystem 4.4 does a table lookup of the LW surface emissivity for each surface type within the FOV and then computes a weighted average based on surface type percent coverage.

SSF-52: CERES WN surface emissivity

It is computed in the same manner as the LW surface emissivity (SSF-51).

SSF-59: Surface skin temperature

If ECMWF MOA is used as input, then over land regions this parameter comes from an ECMWF energy balance surface model that is based on latent heat and sensible heat.

SSF-60: Column averaged relative humidity

This parameter was added when the SSF ID increased from 113 to 114 and the production strategy was set to ValidationR4. The request to add this parameter came from Dave Young. For ValidationR4 SSFs, this parameter is hidden in SSF-106 (Mean vertical aspect ratio) lower layer.

SSF-61: Precipitable water

This parameter is not based on imager pixel data. When accessing MOA, both SSM/I flag and value are checked. If flag indicates SSM/I available and value is not default, then SSF-61 and SSF-62 are set to microwave values. In all other cases, SSF-61 and SSF-62 are set to the meteorological values.

SSF-63: Cloud property extrapolation over cloudy area

Computer round-off error and very small areas with no layer coverage can not be distinguished from one another. If the amount of cloud area without cloud properties (no layer) is smaller than 0.0002 percent, then it is completely ignored. Extrapolation is set to 0 (nothing was extrapolated), no adjustments are made to layer and overlap coverages, but overcast narrowband imager parameters may include information from otherwise ignored pixel(s). While not expected to occur often, such scenarios are possible.

SSF-65: Notes on cloud algorithms

SSF-65-A: Saturated 3.7 mm note: Default imager radiances are never included in SSF mean imager radiances (See SSF-118 through SSF-131), and the percentage of default imager pixel radiances is not recorded anywhere.

SSF-65-B: Potential overlap note: There are 2 overlap algorithms. As of December 2000, overlap computed from 0.63μm channel (old Baum algorithm modified by Young) is what's getting passed (incorrectly) in cookiedough. Other algorithm uses 1.6μm channel (Baum algorithm). Both algorithms produce 8 possible outputs:

- clear_sky   =   0
- single_cloud   =   1
- highr_cloud   =   2
- lower_cloud   =   3
- ovrlp_cloud   =   4
- shadow   =   5
- unknown   =   6
- MaskTBD_BadData =   7

(Cookiecutter is expecting only 0 - no overlap or 1 - overlap. Cookiedough passing all numbers. Therefore, cookiecutter interpreting single cloud as overlap.)

This paragraph applies to overlap computed using 1.6μm channel. As of August 2000, potential overlap results uncertain if snow, sea ice, smoke, or fires exist within tile. Potential overlap could be computed only if the following conditions were met:
- all pixels in tile have same ecosystem type
- surface elevation < 3 km
- solar zenith angle < 70 deg

- viewing zenith angle < 50 deg
- tile has moderate or high probability of sunglint
- cloud cover within tile > 20%

If < 90% of tile cloudy, use clear pixels to calculate mean and stddev of 1.6μm reflectance and 11μm brightness temperatures. Otherwise, use values from clear-sky map.

SSF-69: Cloud-mask snow/ice percent coverage

May 2000: Snow/ice determination is limited to daytime, land pixels. Microwave based, daily, dynamic snow map and ice map used, but not heavily depended upon, to make snow decision.

SSF-70: Cloud-mask aerosol B percent coverage

December, 2000: The following aerosol detection algorithms are implemented:
- smoke (limited to daytime pixels over all land and ocean IGBP types)
- aerosol (limited to daytime pixels over all land and ocean IGBP types)

There is also a MOA total column aerosol optical depth which is different than aerosol A and B. For Terra, MOA will most likely contain aerosol parameters from the MODIS aerosol data product.

SSF-72: Cloud-mask percent coverage supplement

December, 2000: Fire detection is limited to daytime pixels over forest (IGBP types 1-5).

August, 2000: Shadow added for first time.

SSF-82: Note for cloud layer

The first attempt at grouping imager pixels into cloud layer uses water phase. However, the effective pressure between these two layers must be greater than 50 hPa and they have to be statistically different at the 95 percentile level. If these conditions are not satisfied, the largest gap in the effective pressure of a sorted list is used to divide the clouds into two layers. The same test as given before must be past. If there are less than three imager pixels for a layer or neither method produces statistically different layers, all cloud properties are averaged into one layer.

SSF-85: Mean logarithm of visible optical depth for cloud layer

For granules with an SSF ID of 112, this parameter was identified as the mean logarithmically averaged visible optical depth for cloud layer and defined as EXP(mean logarithm of visible optical depth for cloud layer).

SSF-86: Stddev of logarithm of visible optical depth for cloud layer

For granules with an SSF ID of 112, this parameter was identified as the stddev of logarithmically averaged visible optical depth for cloud layer and defined as CERES default.

SSF-115: Imager channel central wavelength

For VIRS there are only 5 imager channels. Therefore, the imager channel selection and order is fixed for all TRMM SSF data sets.

MODIS has many more channels. For Terra-Beta1 processing, the MODIS channels selected are as shown in the following table. Note that odd refers to odd days in the calendar month and even refers to even days within the calendar month.

Index	Day (solar zenith < 90)	Night (solar zenith > 90)
1	0.64 µm	8.5 µm
2	0.47 µm (odd) 1.6 µm (even)	13.3 µm
3	3.7 µm	3.7 µm
4	11.0 µm	11.0 µm
5	0.86 µm	12.0 µm

SSF-118: Mean imager radiances over clear area

Note from 8/13/98 discussion with Richard Green (applies to all narrowband imager radiance parameters): Cookiecutter should average only those imager radiances which the Clouds subsystem determined to be good values and usable in determining cloud properties. Alternately stated, if Subsystems 4.1 - 4.3 determines that a pixel radiance is bad or suspect, for any reason, then the radiance value on Cookiedough should be set to the CERES default. The mean imager radiance should be computed based only on actual radiances passed into Cookiecutter.

Note based on 9/22/98 e-mail from Walter Miller: the original VIRS channel 1 (0.63 µm) and channel 2 (1.6 µm) data prior to June 1998 did not have solar gains from flight cals properly analyzed. Later versions of nighttime channel 2 VIRS radiances are useable. Later versions of nighttime channel 1 VIRS radiances are dominated by bit noise within 6 hours of local midnight.

Version 4 VIRS data does not seem to contain any negative radiances. In January and February 1998, VIRS was still operating in "night" mode at night, so radiances for channels 1 and 2 were never sent down. Later VIRS data was run in perpetual "day" mode, so channel 1 & 2 radiances were sent down at all times. It is unknown whether version 5 VIRS data will contain any negative radiances.

The following applies to TRMM SSF granules processed before 2000. VIRS channel 2 (1.6 µm) has a thermal leak. Clouds adjusts the 1.6 µm channel radiance internally, but the radiance passed through Cookiedough is not adjusted - it is the actual VIRS radiance. Therefore, the thermal leak adjustment is not part of any VIRS channel 2 radiance values stored on the SSF. Discussions with Walt indicate that 0.63 µm channel radiance is also adjusted, and that adjustment does not propagate it's way onto the SSF either. Reflectances are computed from radiances, but cloud retrieval does not allow negative reflectances. Therefore, Cloud Retrieval always uses the absolute value of the computed reflectance. There is no differentiation between day and night for any imager radiances written to the SSF.

The following applies to TRMM SSF granules processed after March 2000 and is based on a March 6, 2000 e-mail and telephone conversation with Walt Miller. The general policy is that any imager radiance adjustments made by Clouds are passed on to the SSF via cookiedough. In

particular, this includes the VIRS calibration changes which clouds can make by using a slope/intercept table. Other adjusts are not as simple. The VIRS channel 2 (1.6 μm) thermal leak adjustment made in Clouds is always passed into the aerosol optical thickness algorithm and on to the SSF through Cookiedough. However, negative reflectances which result from the thermal leak adjustment are never used by cloud retrieval. If the negative value is sufficiently close to zero, its absolute value is used by cloud retrieval. Otherwise, the VIRS channel 2 value is ignored by cloud retrieval. Likewise, if VIRS channel 1 (0.63 μm) is negative, it is ignored by cloud retrieval but used by the aerosol optical thickness algorithm and passed on through Cookiedough. Saturated VIRS channel 3 (3.75 μm) radiances are not passed on through Cookiedough; they are set to default. However, to minimize the number of imager pixels classified as missing, a maximum 3.75 μm reflectance value is used for cloud retrieval. Although VIRS channels 4 and 5 (10.8 μm and 11.9 μm) can also saturate, no adjustments are made. When these channels saturate, default values are passed to Cookiedough and the channels are not used for cloud retrieval.

SSF-134 MOD04 number pixels percentile land (0.659) in CERES FOV.

Note from Walter Miller 2/13/03. When processing MODIS aerosols, they only use the darkest 10 to 40 percentile of available pixels. For each 10x10 km grid box, the actual number of imager quarter-kilometer pixels are reported. This number can range between 0 and 400. During processing, we assign this number to all 25 pixels within the grid box. Once these pixels are assigned to a CERES FOV, the value on individual pixels are summed. Over the CERES FOV, the magnitude of this number is a factor both of how many pixels could be used by MODIS and the number of imager pixels within a CERES FOV.